CANADIAN THESES ON MICROFICHE

I.S.B.N.

THESES CANADIENNES SUR MICROFICHE

NOTICE·

The quality of this microfiche is heavily dependent upon the quality of the original thesis submitted for microfilming. Every effort has been made to ensure the highest quality of reproduction possible.

If pages are missing, contact the university which granted the degree.

Some pages may have indistinct print especially if the original pages were typed with a poor typewriter ribbon or if the university sent us a poor photocopy.

Previously copyrighted materials (journal articles, published tests, etc.) are not filmed.

Reproduction in full or in part of this film is governed by the Canadian Copyright Act, R.S.C. 1970, c. C-30. Please read the authorization forms which accompany this thesis.

AVIS

La qualité de cette microfiche dépend grandement de la qualité de la thèse soumise au microfilmage. Nous avons tout fait pour assurer une qualité supérieure de réproduction.

S'il manque des pages, veuillez communiquer avec l'université qui a conféré le grade.

La qualité d'impression de certaines pages peut laisser à désirer, surtout si les pages originales ont été dactylographiées à l'aide d'un ruban usé ou si l'université nous a fait parvenir une photocopie de mauvaise qualité.

Les documents qui font déjà l'objet d'un droit d'auteur (articles de revue, examens publiés, etc.) ne sont pas microfilmés.

La reproduction, même partielle, de ce microfilm est soumise à la Loi canadienne sur le droit d'auteur, SRC 1970, c. C-30. Veuillez prendre connaissance des formules d'autorisation qui accompagnent cette thèse.

Canada

PERMISSION TO MICROFILM — AUTORISATION DE MICROFILMER

• Please print or type — Écrire en lettres moulées ou dactylographier

Full Name of Author — Nom complet de l'auteur

BÉLA VERKÓCZY

Date of Birth — Date de naissance
15 April 1936

Country of Birth — Lieu de naissance
HUNGARY

Permanent Address — Résidence fixe
441 MICHENER PARK Edmonton Alberta

Title of Thesis — Titre de la thèse
Sulfur atom reactions with selected alkenes and alkynes

University — Université
University of Alberta

Degree for which thesis was presented — Grade pour lequel cette thèse fut présentée
PhD.

Year this degree conferred — Année d'obtention de ce grade
1981

Name of Supervisor — Nom du directeur de thèse
Professor O. P. Strausz

Date
8th of May 1981

Signature
B. Verkóczy

NL 91 (4 77)

THE UNIVERSITY OF ALBERTA

SULFUR ATOM REACTIONS WITH SELECTED ALKENES AND ALKYNES

by

Ⓒ Béla Verkóczy

A THESIS

SUBMITTED TO THE FACULTY OF GRADUATE STUDIES AND RESEARCH

IN PARTIAL FULFILMENT OF THE REQUIREMENTS FOR THE DEGREE

OF DOCTOR OF PHILOSOPHY

DEPARTMENT OF CHEMISTRY

EDMONTON, ALBERTA

SPRING, 1981

THE UNIVERSITY OF ALBERTA

RELEASE FORM

NAME OF AUTHOR ..... Béla Verkóczy ....

TITLE OF THESIS .. Sulfur atom reactions with selected ......
.... alkenes and alkynes ....
....

.DEGREE FOR WHICH THESIS WAS PRESENTED ..... Ph.D. ......

.YEAR THIS DEGREE GRANTED .... 1981 ......
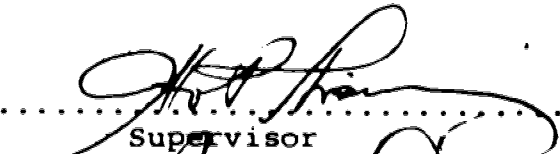
(Signed) _B. Verkóczy_
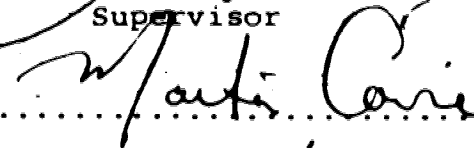
PERMANENT ADDRESS:

441 MICHENER PARK
Edmonton, Alberta T6H 4M5
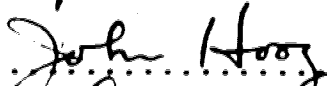
Dated .4th of May...........1981

THE UNIVERSITY OF ALBERTA

FACULTY OF GRADUATE STUDIES AND RESEARCH
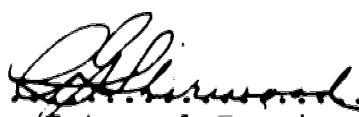
The undersigned certify that they have read,
and recommend to the Faculty of Graduate Studies and
Research, for acceptance, a thesis entitled SULFUR ATOM
REACTIONS WITH SELECTED ALKENES AND ALKYNES submitted by
Béla Verkóczy in partial fulfilment of the requirements
for the degree of Doctor of Philosophy in chemistry.

....
Supervisor

....

....

....

....
External Examiner

Date ....May 4...................1981

ABSTRACT

$S(^1D_2)$ atoms, generated by the gas phase photolysis ($\lambda > 240$ nm) of COS, react with C_2H_4 to yield vinylthiol (VT) and thiirane (Th). From the dependence of the VT/Th ratio upon total pressure, relative concentrations and wavelength of irradiation, it is concluded that VT forms by a dual mechanism, direct insertion of the $S(^1D_2)$ atom into the C-H bond, and unimolecular isomerization of the initially formed "hot" thiirane. The rate constant for the latter reaction, derived from the experimental data is in good agreement with that calculated from RRKM methods by I. Safarik.

Both (^3P) and $(^1D_2)$ sulfur atoms react with allene to yield methylenethiirane in quantitative yields and the S+ cummulene reactions in general constitute an exceptionally convenient method for the synthesis of the novel family of unsaturated thiiranes. The non-occurrence of the insertion reaction is attributed to hyperconjugative effects.

The reactions with C_2H_2, $HC{\equiv}CCF_3$ and $CF_3C{\equiv}CCF_3$ are characterized by poor product recoveries and extensive polymerizations at room temperature. For the case of $S(^1D_2)$ atoms the primary adduct is likely the corresponding thiirene and for (^3P) atoms, the thioketocarbene. Both adducts undergo further reactions with the alkyne to

produce thiophenes and, in the cases of C_2H_2 and $HC{\equiv}CCF_3$, benzenes. The product yields increase markedly along the series C_2H_2, C_3HF_3, C_4F_6 and in all cases approach 100% at elevated temperature. The $S+C_4F_6$ and $S+C_4F_6+C_2H_2$ systems have been examined in detail under varying conditions of pressure, concentration and temperature, from which rate parameters for the addition of $S(^1D_2)$ and (^3P) atoms to C_4F_6 could be estimated. The latter reaction is extremely slow, in keeping with the electrophilic character of ground state sulfur atoms.

Thiirene, formed from the $S(^1D_2) + C_2H_2$ reaction, is highly reactive in the gas phase and undergoes rapid isomerization in preference to addition to an alkyne. The introduction of CF_3 groups however confers an enhanced degree of stability on the molecule and the bis(trifluoromethyl)thiirene + C_4F_6 reaction is quantitative under optimal conditions. The reactivity of C_4F_6S toward C_2H_2, C_3HF_3 and C_4F_6 is about the same, in agreement with the predicted nucleophilic character of this species.

Of the many complex secondary reactions occurring in the $S + C_4F_6$ system, the most important are photoinduced isomerization of the thiophene to Dewar structure and addition of S atoms to thiophene. The latter adduct is the precursor of a variety of hitherto unknown products.

ACKNOWLEDGMENTS

For the neat and conscientious typing of the manuscript, I express my sincere appreciation to Mrs. J. Jorgensen.

I wish to thank the University of Alberta for financial assistance throughout the entire course of this investigation.

As a token of recognition for the sacrifice and hardship my absence and presence caused in the home, I dedicate this dissertation to my family who, inspite of the difficulties, faithfully remained my moral support and inspiration to the finish.

TABLE OF CONTENTS

LIST OF TABLES

LIST OF FIGURES

CHAPTER I

INTRODUCTION

The chemistry of bivalent radicals has been the
subject of extensive investigations. The best known
example is methylene, the history of which dates from
forty years ago.[1,2] The group VI A elements, oxygen,
sulfur, selenium and tellurium are the simplest divalent
reagents and hence knowledge of their chemistry is vital
to our understanding of the periodic system of the
elements. This was not realized for quite some time
however, mainly because suitable precursor molecules
were not recognized.

In 1955 Cvetanovic[3,4] showed that nitrous oxide
was a good source for the generation of ground and
excited state oxygen atoms,[5] and soon afterwards sources
for sulfur, selenium and tellurium atoms were
reported.[6-12] Within the two subsequent decades a large
number of mechanistic and kinetic data were generated
and numerous theoretical studies concerning mechanistic
details of oxygen and sulfur atom reactions with organic
molecules have been published. In spite of these
achievements, however, some aspects of the chemistry of
these species remain uncertain.

The spectroscopic states, sources, and the general
chemistry of group VI A atoms will now be reviewed.

A. Spectroscopic states and photochemical sources for group VI A atoms.

In the ns^2p^4 ground electron configuration of these atoms the outer four electrons are distributed over the three p orbitals and, according to strict selection rules, this gives rise to five spectroscopic states designated as $^3P_{0,1,2}$, $^1D_2$ and $^1S_0$. The energies of these states are given in Table I-1. Radiative transitions from the metastable $^1D_2$ and $^1S_0$ states to the ^3P_J ground states are forbidden by spin selection rules. Consequently, the excited singlet states have long natural lifetimes with respect to radiative decay to the triplet state, and they can undergo chemical reactions as well as collisional relaxation to the ground state. The large amount of data available concerning the reactions of these atoms show that both the reactivity and the types of chemical reactions are markedly affected by their spin states which, in many cases, have been well characterized. For all the ground state group VI A atom reactions investigated to date the reactive entity is the $^3P_2$ species (henceforth denoted as ^3P) which is rapidly produced via thermal equilibration. To date, no data are available on the reactivities of $^3P_1$ and $^3P_2$ atoms although only for the cases of selenium and of tellurium, where the

TABLE I-1

Energy levels of the first four atoms of the Group VI A elements[a]

Term	Energy, kcal mol^{-1}			
	O	S	Se	Te
	[He]^{2}2s^{2}p^4	[Ne]^{10}3s^{2}p^4	[Ar]^{18}4s^{2}3d^{10}4p^4	[Kr]^{36}5s^{2}4d^{10}5p^4
$^3P_2$	0	0	0	0
$^3P_1$	0.45	1.14	5.69	13.5
$^3P_0$	0.65	1.64	7.25	13.6
$^1D_2$	45.4	26.4	27.4	30.2
$^1S_0$	96.6	63.4	64.2	66.3

[a]Reference 13.

spin-orbit splitting is relatively large, are some differences possible.

A good source compound must satisfy the following criteria:

a) absorb in an accessible and suitable range of the electromagnetic spectrum;

b) be readily available in stable form at various temperatures;

c) be usable in the gas phase;

d) produce atoms in clearly defined spectroscopic states; and

e) produce inert photofragment(s).

The most commonly used gas phase photochemical sources of O, S, Se and Te atoms are summarized in Table I-2.

B. Oxygen atom reactions.

1. Reactions of $O(^1D_2)$ atoms

i) Reactions with alkanes

The reactions of $O(^1D_2)$ atoms, generated from the $\lambda = 214$ nm photolysis of N_2O, with a series of representative alkanes have been investigated by Cvetanovic and coworkers,[15-20] by Lin and De More,[21] De More and Raper,[22] and recently by Kajimoto *et al.*[23]

TABLE I-2

Best sources of O, S, Se and Te atoms

Process	Quantum yield	λ,nm	Reference
$N_2O + h\nu \rightarrow N_2 + O(^1D_2)$	1.4	184.9	5
$N_2O + Hg(^3P_1) \rightarrow N_2 + Hg(^1S_0) + O(^3P_{0,1,2})$	.8	253.7	3
$COS + h\nu \rightarrow CO + S(^1D_2)$	0.9	240	7,8,9
$COS + CO_2 + h\nu + CO + S(^3P_{0,1,2})$	0.9	240	7
$COS + Hg(^3P_1) \rightarrow CO + Hg(^1S_0) + S(^3P_{0,1,2})$	0.9	253.7	7
$COSe + h\nu \rightarrow CO + Se(^1D_2)$	0.1	193	14
$\rightarrow CO + Se(^3P_0)$	0.05	193.	14
$\rightarrow CO + Se(^3P_1)$	0.25	193	14
$\rightarrow CO + Se(^3P_2)$	0.35	193	14
$CSe_2 + h\nu \rightarrow CSe + Se(^3P_{0,1,2})$	-	<230	11
$(CH_3)_2Te + h\nu \rightarrow 2CH_3 + Te(^3P_J)$	-	<270	12

in the condensed and gas phases. It was concluded that the interaction of $O(^1D_2)$ atoms with alkanes can proceed in three distinct ways:

a) insertion into C-H bonds to form vibrationally excited alcohols

$$O(^1D) + RH \longrightarrow ROH^* \qquad [1]$$

which can undergo fragmentation:

$$ROH^* \longrightarrow R + OH \qquad [2]$$

or collisional stabilization (this is readily achieved in an argon matrix):

$$ROH^* + M \longrightarrow ROH \qquad [3]$$

b) Abstraction of H atoms to form OH and alkyl radicals:

$$O(^1D) + RH \longrightarrow R + OH \quad \text{and} \qquad [4]$$

c) a third, as yet unidentified primary process, which leads to molecular elimination of H_2.[15-21]

The gas phase reactions of $O(^1D)$ with CH_4 and C_2H_6 were studied in detail by Lin and DeMore,[21] employing the 185 nm photolysis of N_2O as a source of $O(^1D)$ atoms. On the basis of pressure effects and the results of chemical scavenging experiments the following primary steps were proposed:

$$N_2O + h\nu \longrightarrow N_2 + O(^1D) \qquad\qquad [5]$$

$$O(^1D) + CH_4 \longrightarrow CH_3OH* \qquad\qquad [6]$$

$$\longrightarrow CH_3 + OH \qquad\qquad [7]$$

$$\longrightarrow (CH_4O)* \longrightarrow H_2 + CH_2O \qquad\qquad [8]$$
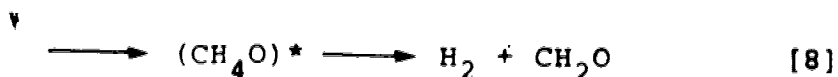
The estimated rate constant for insertion is $k_6 = 1 \times 10^{11}$ ℓ mol^{-1} s^{-1} and the measured value for hydrogen abstraction is $k_7 = 1.3 \times 10^{11}$ ℓ mol^{-1} s^{-1}. By assuming unit collision efficiency for the deactivation step [9] $(2 \times 10^{11}$ ℓ mol^{-1} $s^{-1})$,

$$CH_3OH* + M \longrightarrow CH_3OH \qquad\qquad [9]$$

and from kinetic analysis of the data, the lifetime of CH_3OH* was estimated to be about 8×10^{-13} s. In the case of ethane the lifetime of the adduct was at least five times longer, but nevertheless stabilization was not complete even in the presence of 100 atm He. In the presence of 33 atm SF_6, however, a far more efficient moderating gas, increased stabilization was observed by Kajimoto et al.,[23] and an extrapolated value of 0.67 was reported for the branching ratio, i.e., $k_6/(k_6 + k_7 + k_8)$.

Yamasaki and Cvetanovic[15] have established that the lifetimes of the "hot" alcohols produced from

insertion increase with ████ number of carbon atoms in the alkane substrates, for example, $\sim 10^{-11}$ s for hot propyl alcohol and 4×10^{-9} s for hot neopentyl alcohol.

The mode of molecular H_2 formation is uncertain since H_2 constitutes only about 2-9% of the total products formed. However, it is generally recognized that not all of the reaction paths can be described in terms of the unimolecular decomposition of a chemically activated ROH* intermediate. Thus, the contribution of step [8] is essentially the same both in the gas phase and in liquid argon,[21] which is inconsistent with a CH_3OH* intermediate having an appreciable lifetime. Furthermore, Cvetanovic and coworkers[17,19,20] have shown that the abstraction of H atoms by $O(^1D)$ atoms does not proceed *via* ROH* intermediates.

Further insights into the $O(^1D)$ + alkane reactions can be deduced from the recent elegant study of Luntz[24] who employed laser photolysis in combination with laser induced fluorescence to measure the nascent OH internal state distributions from the $O(^1D)$ + CH_4, C_2H_6, C_3H_8 and $(CH_3)_4C$ reactions. The overall results can be summarized as follows:

1. The OH rotational states are bimodal, hence OH is produced by two mechanisms:

   a) insertion, characterized by a broad distribution of high rotational states, and

b) Abstraction, leading to low rotational OH states.

2. The insertion complex undergoes rapid decay to OH + R and a slower, RRKM-type decay *via* C-C cleavage.

3. Insertion predominates for the cases of CH_4 and C_2H_6 but is less competitive with regard to abstraction for C_3H_8 and $(CH_3)_4C$.[21]

4. The rotational state distribution for the abstraction component is very similar to that observed for $O(^3P)$ + alkane reactions (*vide infra*) but does not lead to any marked selectivity in the OH spin doublets as was observed for the case of $O(^3P)$ atoms.

On this basis, and because physical quenching of $O(^1D)$ atoms by alkanes does not appear to take place,[19] it was concluded that the abstraction component arises from a singlet-triplet surface crossing in the entrance channel of the insertion surface.

ii) <u>Reactions with alkenes</u>

In spite of their importance very few results are available on these reaction in the gas phase.

Sato and Cvetanovic[25,26] and later, Preston and Cvetanovic[27] studied the photolysis of NO_2 in the presence of 1-butene and examined the effects of photolysis wavelength, pressure (SF_6 or CO_2 up to 300 torr), and inert gases. Below ~230 nm production of

$O(^1D)$ atoms becomes energetically feasible but even in this region it appears that $O(^3P)$ atoms are still produced. The major addition products were ethyloxirane, 1-butanal and methyl ethyl ketone and a large number of fragmentation products were also observed. Overall, however, the data were inconclusive and it was suggested that all the observed addition products arise from $O(^3P)$ atom precursors, the $O(^1D)$ reactions proceeding entirely to fragmentation. The initial adduct for the 1-butene reaction, for example, was postulated to be a hot oxirane:

$$O(^1D) + CH_3CH_2CH=CH_2 \longrightarrow [C_2H_5 \overset{O}{\triangle}]^* \qquad [10]$$
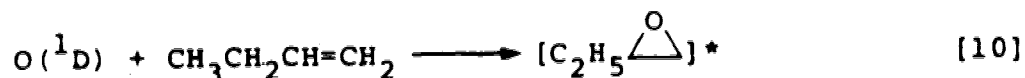
which then fragments immediately:

$$[C_2H_5 \overset{O}{\triangle}]^* \longrightarrow \text{fragmentation} \qquad [11]$$

The above observations indicate that $O(^1D)$ atoms are extremely reactive with alkenes.

The reactions of $O(^1D)$ atoms with propylene have been recently studied by Kajimoto et al.,[28] who employed the 206.2 nm photolysis of N_2O as a source of $O(^1D)$ atoms and up to 150 atm He pressure to stabilize the hot adducts. The major addition reactions, along with their high pressure extrapolated fractional yields, can be summarized as follows:

$$O(^1D) + CH_3CH=CH_2 \longrightarrow [CH_3\overset{O}{\overset{/\backslash}{CH-CH_2}}]^* \xrightarrow{M} CH_3\overset{O}{\overset{/\backslash}{CH-CH_2}} \quad [12]$$

22%

$$\longrightarrow [CH_3CH=CHOH]^* \xrightarrow{M} CH_3CH_2CHO \quad [13]$$

22%

$$\longrightarrow [CH_3\overset{OH}{\underset{|}{C}}=CH_2]^* \xrightarrow{M} CH_3COCH_3 \quad [14]$$

11%

$$\longrightarrow [HOCH_2CH=CH_2]^* \xrightarrow{M} HOCH_2CH=CH_2$$

20% [15]
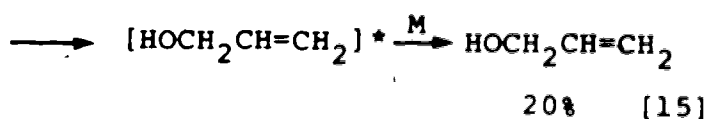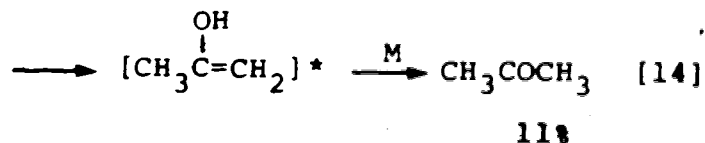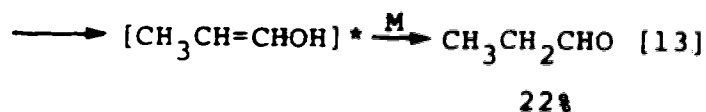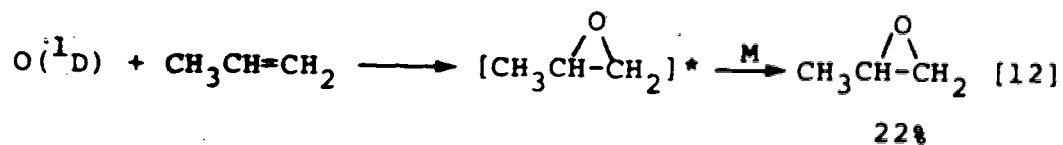
Minor amounts of fragmentation products (acrolein, 2%, and acetaldehyde, 6%) were also observed. The detection of allylalcohol as a major product, together with the observation that the overall product distribution is different from that obtained from the $O(^3P) + C_3H_6$ reaction, strongly suggest that the reactive species are $O(^1D)$ atoms.

The above results show that $O(^1D)$ atoms manifest little discrimination, not only in their insertion reactions but also with regard to the relative rates of insertion and addition, *viz.*, addition constitutes 22% of the product-forming reactions, as compared to 48% for $S(^1D)$ atoms (*vide infra*). This was ascribed to the higher energy content of $O(^1D)$ atoms.

About 25% of the overall reaction with propylene proceeds *via* abstraction,

$$O(^1D) + C_3H_6 \longrightarrow OH + C_3H_5 \qquad\qquad [16]$$
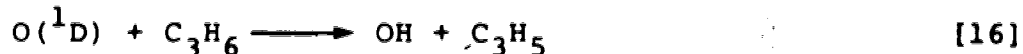
or collisional deactivation,

$$O(^1D) + C_3H_6 \longrightarrow O(^3P) + C_3H_6 \qquad\qquad [17]$$
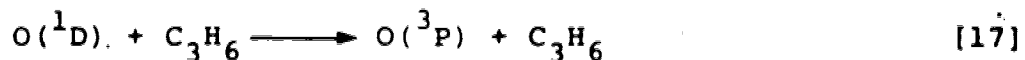
but it was not possible to reach any conclusion regarding the occurrence of either of these steps.

Recently Kajimoto and Fuemo,[29] employing the direct photolysis of N_2O at $\lambda = 214$ nm for the generation of $O(^1D)$ atoms, have examined the reactivity of $O(^1D)$ atoms with a number of representative alkenes in the gas phase, and reported rate constant measurements, relative to the $O(^1D) + N_2O$ reaction. In absolute terms the values range from 1.3×10^{11} ℓ mol^{-1} s^{-1} for ethylene to 6.4×10^{11} ℓ mol^{-1} s^{-1} for 2-methyl-2-butene, confirming Cvetanovic's earlier suggestion that $O(^1D)$ atoms are extremely reactive toward alkenes and consequently relatively indiscriminate with regard to the nature of the substrate.

iii) Reactions with alkynes

The gas phase reactions of $O(^1D)$ atoms with 2-butyne have been briefly investigated in a static system.[30] A large variety of non-condensable products were formed but the oxygen-containing products could not be characterized. Significantly, no methyl vinyl ketone

was detected, indicating that the primary adduct formed must have a very short lifetime with respect to fragmentation.

The possible primary steps in the $O(^1D)$ + alkyne reaction, postulated by analogy with the alkane and alkene systems are given below for the case of acetylene.

$$O(^1D) + \equiv \longrightarrow \overset{O}{\triangle} (S_0)* \qquad [18]$$

$$\longrightarrow \equiv-OH(S_0)* \qquad [19]$$

$$\longrightarrow \equiv \cdot + OH \qquad [20]$$

where * designates vibrational excitation.

Oxirenes have been postulated as intermediates in the peroxyacid oxidations of alkynes[31] and according to (*ab initio*) MO calculations[32,33] step [18] is a spin, and energetically allowed process. To date, all attempts to isolate antiaromatic oxirene, even under low temperature matrix conditions, have been unsuccessful, but indirect and compelling evidence for its transient existence as an intermediate in the photochemical Wolff rearrangement of α-diazoketones and esters for example, has been reported.[34-38] The reactions of interest in the present context are:

$$\underset{R-C-C-R}{\overset{O \ N_2}{\| \ \|}} \xrightarrow{h\nu} N_2 + \underset{R-C-C-R'}{\overset{O}{\|}} (S_2) \qquad [21]$$

$$R-\overset{\overset{\textstyle O}{\|}}{C}-\overset{..}{C}-R' \ (S_2) \longrightarrow R-\overset{\overset{\textstyle O}{\|}}{C}-\overset{..}{C}-R' \ (S_1)* \qquad\qquad [22]$$

$$R-\overset{\overset{\textstyle O}{\|}}{C}-\overset{..}{C}-R' \ (S_1)* \begin{array}{c} \longrightarrow R\ R'C=C=O \qquad [23] \\ \xrightarrow{[24]} \ RC\overset{\textstyle O}{\underset{\diagdown}{\diagup}}CR' \xrightarrow{[25]} R\overset{\overset{\textstyle O}{\|}}{C}-\overset{..}{C}R'(S_1) \\ \xrightarrow[{[26]}]{M} R\overset{\overset{\textstyle O}{\|}}{C}CR'(S_1) \xrightarrow[{[27]}]{} RR'C=C=O \end{array}$$
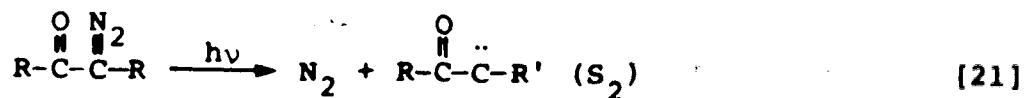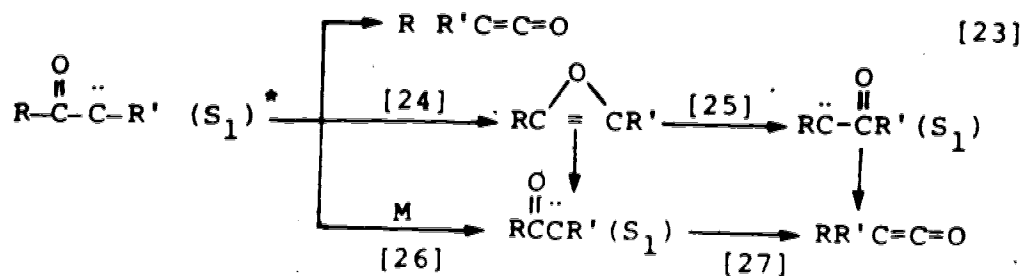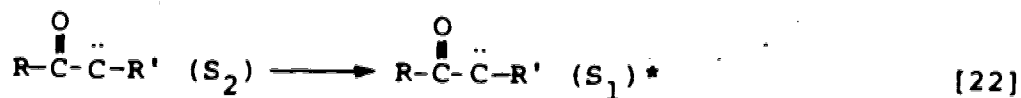
Ab initio MO calculations on the relative stabilities
of five C_2H_2O isomers and the activation energies for
some of their interconversions are illustrated in
Figure I-1 where it is seen that although oxirene is
thermodynamically unstable it is relatively kinetically
stable with respect to ring opening for which an
activation energy of ~7.3 kcal mol^{-1} is predicted.[32,33]

Reaction [19], C-H insertion to form ethynol, is
postulated by analogy with the $O(^1D)$ + alkene reaction.
Ethynol has not been synthesized to date but theoretical
calculations (Figure I-1) indicate that it is an
energetically accessible species.

H-atom abstraction, reaction [20] is also
postulated by analogy with the $O(^1D)$ + alkane reaction.
The exothermicity of this reaction is -136.2 kcal mol^{-1}
and hence energetically feasible.

It should be noted that the energy levels shown
in Figure I-1 refer to ground state species: it is
probable that the initial $O(^1D)$ + alkyne adduct contains
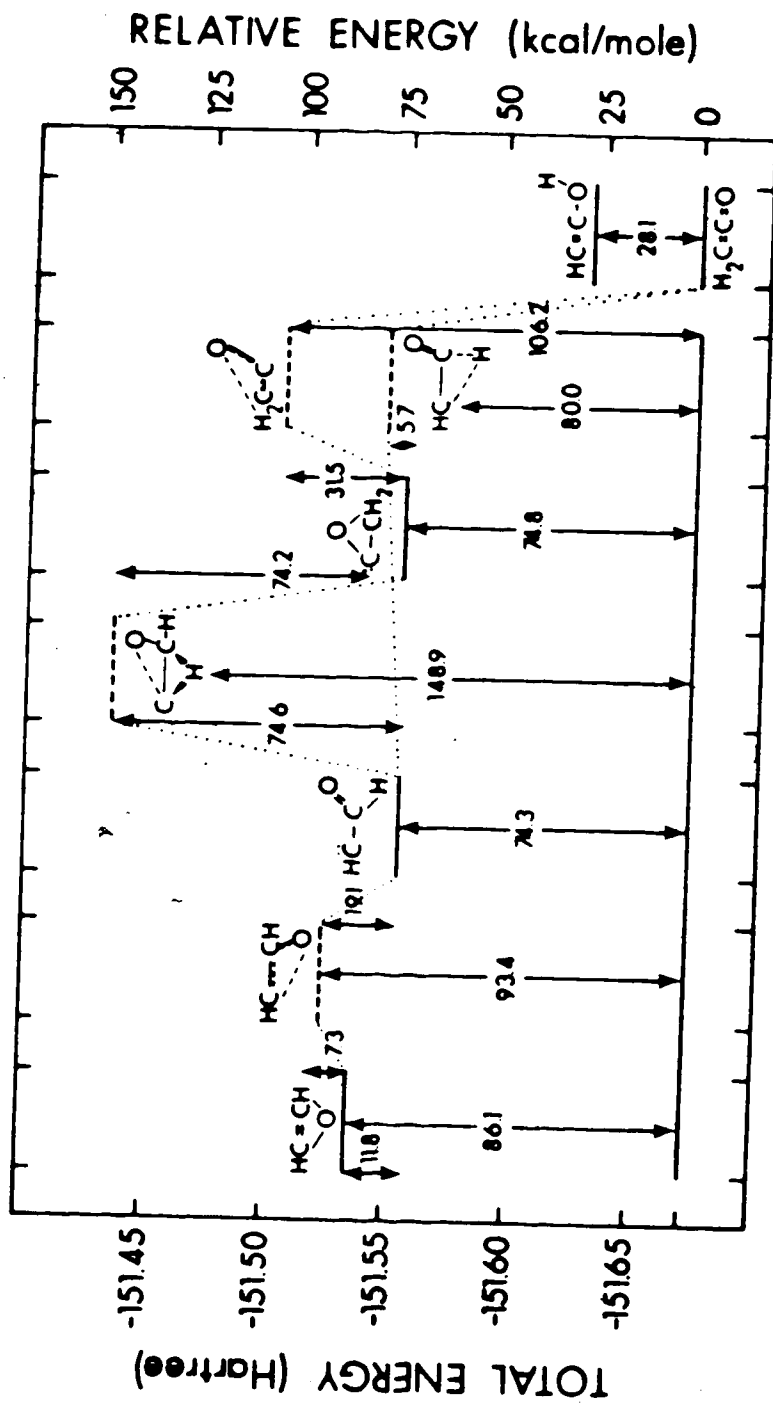
FIGURE I-1. Relative energies of the C_2H_2O isomers and activated complexes. [32,33]

sufficient excess energy to fragment within the period of a vibration.

2. Reactions of $O(^3P)$ atoms

In most of the studies to be considered in this section, triplet oxygen atoms were generated in the gas phase by the mercury sensitization of N_2O:

$$N_2O + Hg(^3P_1) \longrightarrow N_2 + Hg(^1S_0) + O(^3P) \qquad [28]$$
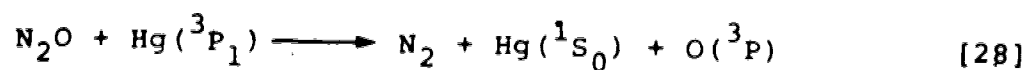
This is a particularly convenient source, since N_2 serves as an internal actinometer for the amount of $O(^3P)$ atoms formed.[4,5]

i) Reactions with alkanes

The reactions of $O(^3P)$ atoms with alkanes have been investigated by Cvetanovic and coworkers[39] who proposed that the sole primary process is hydrogen abstraction, i.e.,

$$O(^3P) + RH \longrightarrow OH + R \qquad [29]$$

The chemical dynamics of reaction [29] for a number of saturated hydrocarbons have been examined by Anderson and Luntz,[40] employing the molecular beam-laser induced fluorescence technique to measure the nascent internal state distributions and excitation functions of the OH radicals formed in step [29]. It was found

that the vibrational state distribution of OH depended markedly on the type of hydrogen abstracted, with vibrational excitation increasing dramatically along the series primary, secondary, and tertiary bonds. Furthermore, it was found that the dynamic thresholds for OH formation were in good agreement with experimentally derived activation energies. These results thus confirm the identity of OH as the primary product.

Absolute rate constants for a number of $O(^3P)$ + alkane systems have been measured by a variety of techniques.[41] For example, Atkinson and Pitts,[42] employing the modulation phase shift technique, measured the rate value for the reaction:

$$O(^3P) + C_4H_{10} \longrightarrow C_4H_9 + OH \qquad [30]$$
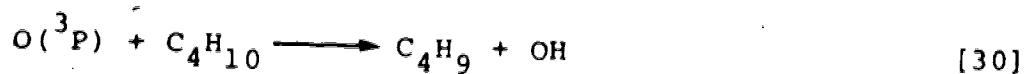
$k_{30} = 1.88 \times 10^7$ l mol^{-1} s^{-1} and $E_a \sim 5.8$ kcal mol^{-1}. In general the rate constants for the $O(^3P)$ + higher alkane reactions range from 10^6 to 10^8 l mol^{-1} s^{-1}. For methane[41] and ethane[41] however, $k \sim 1 \times 10^4$ and 5.5×10^5 l mol^{-1} s^{-1}, respectively, as a consequence of the high activation energies for these reactions, 9 and 6.4 kcal mol^{-1}, respectively.

The effect of alkyl substitution on the rate of hydrogen atom abstraction may be seen for the case of substituted butanes. Thus, the rate constant values

obtained for 2,2,3,3-tetramethylbutane[41] (8×10^6 ℓ mol^{-1} s^{-1}), 2-methylbutane[41] (8×10^7 ℓ mol^{-1} s^{-1}) and 2,3-dimethylbutane[41] (1.2×10^8 ℓ mol^{-1} s^{-1}) clearly indicate a marked trend in the order $1° < 2° < 3°$ C-H, as would be expected on the basis of the known bond strengths,[43] i.e., ~100, ~95, and ~92 kcal mol^{-1}, respectively.

ii) Reactions with alkenes

O(^{3}P) atom reactions with alkenes are characterized by extensive rearrangement and fragmentation of the primary adduct. The O atom preferentially adds to the least substituted carbon atom and the end products are oxiranes, aldehydes and ketones, the yields of which strongly depend on the experimental conditions as well as on the nature of the alkene.

The nature of the transition state of these reactions remains the subject of some controversy.[44-46] On the basis of the observation that the room temperature reaction of O(^{3}P) atoms with either cis- or trans-2-butene affords equal amounts of cis and trans dimethyloxiranes, and from spin conservation principles, Cvetanovic[4] proposed that the initial adduct is a triplet biradical intermediate in which there is no barrier to rotation and which can either cyclize to oxirane

or undergo intramolecular H-atom alkyl radical shift
to form carbonyl compounds, for example,

$$O(^3P) + \qquad \longrightarrow \qquad \qquad [31]$$

$$\longrightarrow \qquad [32]$$

$$\longrightarrow \qquad [33]$$

$$\longrightarrow \qquad [34]$$
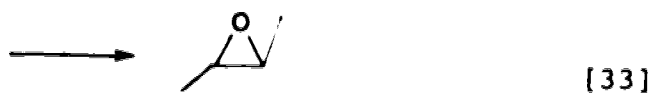
The driving force behind carbonyl formation is attributed
to the high strength of the C=O bond.

However, Klein and Scheer[45,47,48] later showed that
the relative isomer yields were temperature dependent
in the range 77-300°K, and proposed a hydrogen bridged
intermediate in which hydrogen bonding restricts rotation
about the C-C bond, giving rise to a planar structure
as shown below:

(T_1) and (T_1) etc.
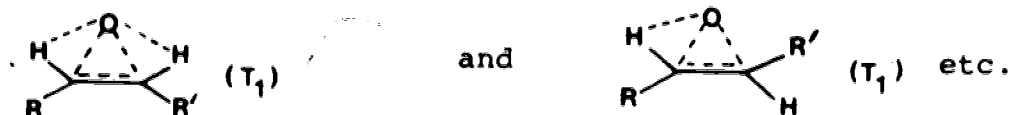
The reaction then presumably follows a concerted path
without the participation of a triplet biradical. The
temperature dependence of the stereoselectivity would
then be a consequence of decreased hydrogen bonding

with increasing temperature.

Neither of the above discussed mechanisms are, however, fully satisfactory and in fact *ab initio* MO· calculations[49-51] on the $O(^3P)$ + C_2H_4 reaction path and on the ground and lowest triplet excited states of oxirane indicate that, in the first excited triplet state oxirane, the rotational barrier is prohibitively high. Hence isomerization and H and/or alkyl shifts are more likely to take place on a lower lying surface reached by intersystem crossing, which could be the ground singlet (vibrationally excited) or, alternatively, a low-lying excited singlet state, having ionic character.

A great deal of absolute rate data are now available for $O(^3P)$ + alkene reactions and some of these are summarized in Table I-3. In general the activation energy decreases with increasing alkyl substitution on the double bond, eventually becoming negative, and varies linearly with the ionization potential of the alkene, clearly pointing to the electrophilic character of $O(^3P)$ atoms.

iii) Reactions with alkynes

Triplet oxygen atom reactions with alkynes also lead to extensive fragmentation of the primary adduct. The products in general are polymer, CO, alkenes and

TABLE I-3

Rate constants[a] and Arrhenius parameters for the Group VI A triplet state atom reactions with selected alkenes

Alkenes	$O(^3P_J)$			$S(^3P_J)$[f]			$Se(^3P_J)$[g,h]			$Te(^3P_J)$[f]		
	$kx10^{-9}$ ℓmol^{-1} s^{-1}	E_a kcal mol^{-1}	$Ax10^{-9}$ ℓmol^{-1} s^{-1}	$kx10^{-9}$ ℓmol^{-1} s^{-1}	E_a kcal mol^{-1}	$Ax10^{-9}$ ℓmol^{-1} s^{-1}	$kx10^{-9}$ ℓmol^{-1} s^{-1}	E_a kcal mol^{-1}	$Ax10^{-9}$ ℓmol^{-1} s^{-1}	$kx10^{-8}$ ℓmol^{-1} s^{-1}	E_a kcal mol^{-1}	$Ax10^{-9}$ ℓmol^{-1} s^{-1}
Ethylene	0.42[b]	1.7	7.0	0.82	1.5	10.0	0.82	2.8	11.0	0.13	2.5	1.0
Propylene	2.29[b]	0.72	7.6	5.58	0.36	10.0	2.9	2.4	13.0	1.2	0.6	0.32
1-Butene	2.38[b]	0.66	7.2	9.03	-0.22	7.5	5.8	2.3	31.0	1.5	-	-
cis-2-Butene	10.8[b]	-0.27	6.7	15.0	-0.51	5.3	19.7	1.2	20.0	6.3	-	-
iso-Butene	10.4[b]	-0.10	8.7	44.3	-0.86	9.7	36.9	1.0	24.0	-	-	-
TME[c]	39.8	-0.92	8.6	107.4	-1.84	5.0	-	-	-	38.5	-1.6	0.25
Allene	0.71[d]	1.9	18.7	-	-	-	-	-	-	-	-	-
PFE[e]	-	-	-	0.11	2.9	14.0	-	-	-	-	-	-
trans-1,2-di-fluoroethylene	-	-	-	0.035	4.12	34.0	-	-	-	-	-	-

[a]298°K. [b]Reference 52. [c]TME = tetramethylethylene; data from reference 53,54. [d]Reference 55.
[e]PFE = perfluoroethylene; data from reference 56. [f]Reference 57. [g]Reference 58. [h]Reference 59.

unsaturated ketones, and the distribution strongly

depends on experimental conditions such as temperature,

phase, pressure and nature of the alkyne.

The $O(^3P)$ + C_2H_2 reaction has been investigated

in considerable detail under a variety of experimental

conditions.[61,62] In the gas phase the major products

are CO, H_2, propadiene, propyne and polymer but under

solid matrix conditions (20°K) ketene was detected.

This observation prompted Haller and Pimentel[63] to

propose that the primary adduct,

$$O(^3P) + C_2H_2 \longrightarrow (C_2H_2O)* \qquad [35]$$
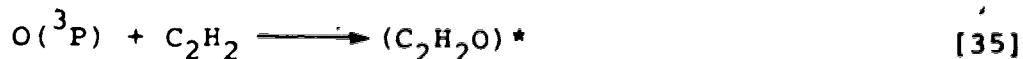
has a lifetime sufficiently long under matrix isolation

conditions to allow isomerization to excited triplet

state ketene:

$$(C_2H_2O)* \longrightarrow (CH_2{=}C{=}O)* \qquad [36]$$

Attempts to detect ketene in gas phase experiments have

been unsuccessful and it has been shown that the hot

adduct fragments in several different ways, e.g.,

$$(C_2H_2O)* \longrightarrow CH_2* + CO \qquad [37]$$

$$\longrightarrow H + C_2HO \qquad [38]$$

$$\longrightarrow H_2 + C_2O \qquad [39]$$

Reactions [37] - [39] were estimated to account for 25, 0.3 and 42 (± 10)%, respectively, of the oxygen atoms formed.[64,65] The remaining fraction of oxygen atoms presumably ends up as polymer.

Reaction [35] is extremely efficient, and the rate parameters are:[66] $k_{35} = 1.7 \times 10^{10} \exp(-\frac{1600}{RT}) \ell \ mol^{-1} \ s^{-1}$.

Haller and Pimentel proposed the following structures for the C_2H_2O adduct:

O·
|
HC=ĊH   and
A
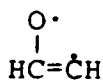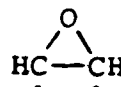
$$\overset{O}{\overset{/\backslash}{HC\!\!-\!\!CH}}$$

B

Structure B would correspond to triplet state oxirene and structure A may be identical to the formylmethylene structure $H\overset{O}{\overset{\|}{C}}$-CH. With regard to the former possibility, as yet unpublished *ab initio* MO calculations from this laboratory[67] indicate that triplet state oxirene lies 68 kcal mol^{-1} above the triplet state ketocarbene, and thus is probably not energetically accessible. Even if the C_2H_2O adduct possesses a diradical structure as in A, any possible change in this energy separation should be minimal. In general, theoretical calculations on the reaction paths involved in the addition of divalent species to unsaturated bonds concordantly predict an unsymmetrical approach to one of the carbon atoms. For these reasons it is suggested that the

diradical A (or its formylmethylene isomer) is the primary adduct formed in the $O(^3P) + C_2H_2$ reaction.

The $O(^3P)$ + propyne reaction at low pressure was investigated by Brown and Thrush[62] in a discharge flow system, in which oxygen atoms were monitored using ESR spectroscopy. Since no propyne-oxygen complex was detected, they concluded that the overall initial step of the reaction is

$$O(^3P) + CH_3C\equiv CH \longrightarrow CH_3\ddot{C}H + CO \qquad [40]$$
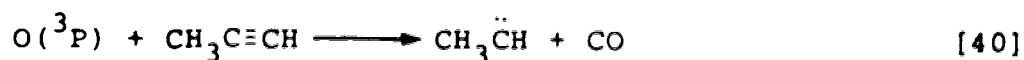
and reported $k_{40} = (3.2 \pm 0.4) \times 10^8$ ℓ mol^{-1} s^{-1} at 298°K.

The propyne system was later reinvestigated under static conditions and at moderate pressures by Ogi and Strausz.[68] The major products were CO, H_2, C_2H_2, C_2H_4 and acrolein (CH_2=CHCHO). On this basis and from the pressure dependence of the relative product yields, the following reaction mechanism was proposed (where * signifies vibrational excitation):

$$O(^3P) + CH_3C\equiv CH \longrightarrow (CH_3\overset{\overset{\displaystyle O}{\|}}{\ddot{C}}-CH)* \qquad [41]$$
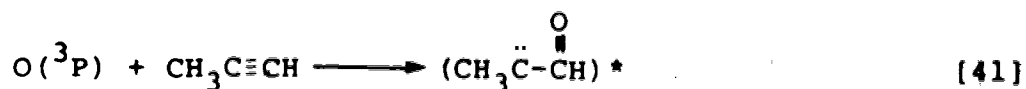
The vibrationally excited ketocarbenes may then isomerize to ketene,

$$CH_3\overset{\overset{\displaystyle O}{\|}}{\ddot{C}}-CH* \longrightarrow \overset{CH_3}{\underset{H}{>}}C=C=O* \qquad [42]$$

be thermalized

$$CH_3\overset{O}{\overset{\|}{\underset{..}{C}}}-CH* + M \longrightarrow CH_3\overset{O}{\overset{\|}{\underset{..}{C}}}-CH \qquad [43]$$
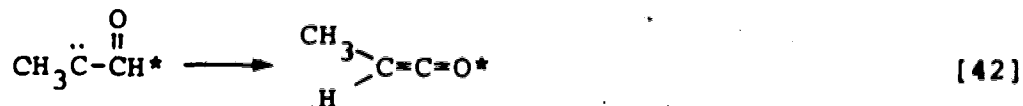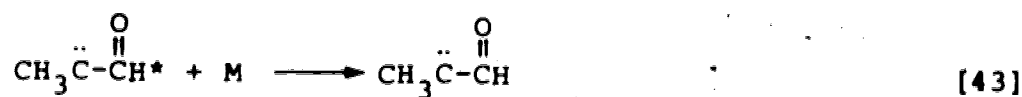
or undergo 1,2 hydrogen shift to yield acrolein:

$$CH_3\overset{O}{\overset{\|}{\underset{..}{C}}}-CH* \longrightarrow CH_2=CH-\overset{O}{\overset{\|}{C}}H \qquad [44]$$

The major products observed arise from the decomposition of the methyl ketene formed in [42]

$$\underset{H}{\overset{CH_3}{>}}C=C=O* \xrightarrow[\text{or } \Delta]{h\nu} CO + :C\underset{CH_3}{\overset{H}{<}}* \qquad [45]$$

$$:C\underset{CH_3}{\overset{H*}{<}} \longrightarrow CH_2=CH_2* \qquad [46]$$

$$CH_2=CH_2* \overset{M}{\nearrow} \overset{CH_2=CH_2}{\underset{CH\equiv CH + H_2}{\searrow}} \qquad \begin{array}{l}[47a]\\ \\ {[47b]}\end{array}$$
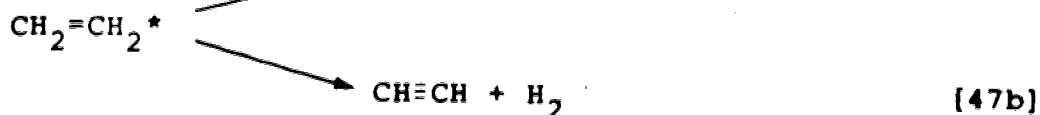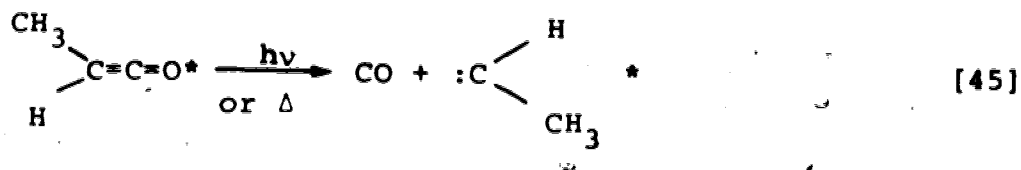
Steady state treatment of the above mechanism predicts the following relation:

$$\frac{R_{CH_2=CHCHO}}{R_{CO.}} = \frac{k_{43}[M]}{k_{42}}$$

from which k_{42} was estimated to be *ca.* 4.4×10^{10} s^{-1}.

The dimethylacetylene reaction was investigated by Ogi and Strausz[68] and by Avery and Heath,[69] who reported basically the same results but differed slightly in some mechanistic aspects. The principal products of the reaction are CO and C_3H_6 in nearly equal yields, and methyl vinyl ketone (MVK). Ogi and Strausz noted that while the MVK yield is enhanced and the CO yield is suppressed by increasing pressure, the sum of the CO and MVK yields is pressure independent. These trends were explained in terms of the following mechanism,[68]

$$O(^3P) + CH_3C{\equiv}CCH_3 \longrightarrow CH_3{-}\overset{\overset{\displaystyle O}{\|}}{C}{-}\ddot{C}CH_3 \,(T_0)* \qquad [48]$$

$$CH_3\overset{\overset{\displaystyle O}{\cdot\!\|}}{C}CH_3\,(T_0)* \longrightarrow (CH_3)_2C{=}C{=}O\,(T_1) \qquad [49]$$

$$\xrightarrow{+M} CH_3\overset{\overset{\displaystyle O}{\cdot\!\|}}{C}CH_3\,(T_0) \qquad [50]$$

$$CH_3\overset{\overset{\displaystyle O}{\cdot\!\|}}{C}CH_3\,(T_0) \longrightarrow CH_2{=}CH{-}\overset{\overset{\displaystyle O}{\|}}{C}CH_3 \qquad [51]$$

$$(CH_3)_2C{=}C{=}O\,(T_1) \longrightarrow CO + (CH_3)_2\ddot{C} \qquad [52]$$

$$(CH_3)_2\dot{\ddot{C}} \longrightarrow CH_3CH{=}CH_2 \qquad [53]$$
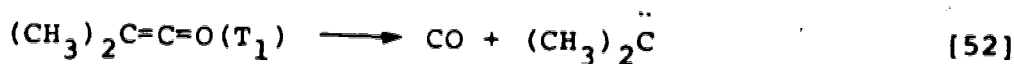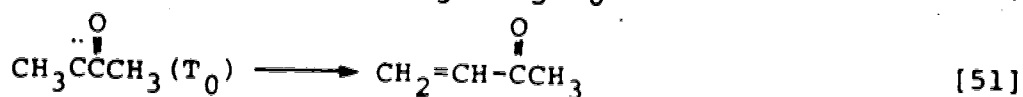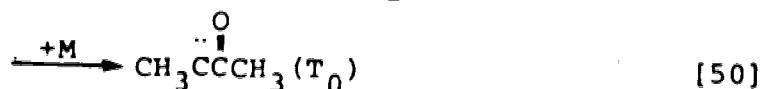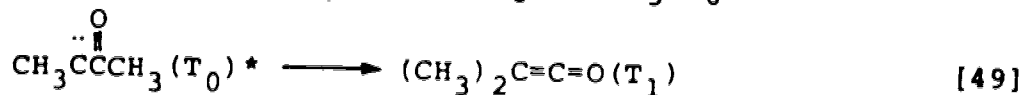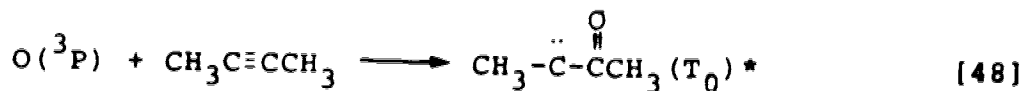
which predicts that at very high pressures the only major product should be MVK. Avery and Heath[69] proposed that MVK is formed *via* a carbene-enol-ketone rearrangement

$$CH_3\overset{\overset{\displaystyle O}{\cdot\!\|}}{C}CH_3 \longrightarrow CH_3\overset{\overset{\displaystyle OH}{|}}{\underset{\cdot\cdot}{C}}{-}\dot{C}{=}CH_2 \qquad [54]$$

$$CH_3\overset{\overset{\textstyle OH}{|}}{\underset{\cdot}{C}}-\overset{\cdot}{C}=CH_2 \longrightarrow CH_3-\overset{\overset{\textstyle OH}{|}}{C}=C=CH_2* \qquad [55]$$

$$CH_3-\overset{\overset{\textstyle OH}{|}}{C}=C=CH_2* \rightleftharpoons CH_3-\overset{\overset{\textstyle O}{||}}{C}-CH=CH_2* \qquad [56]$$
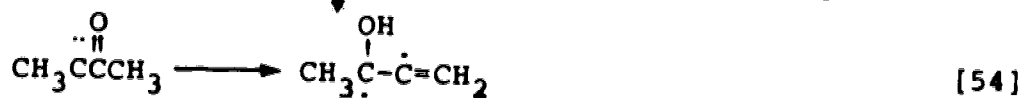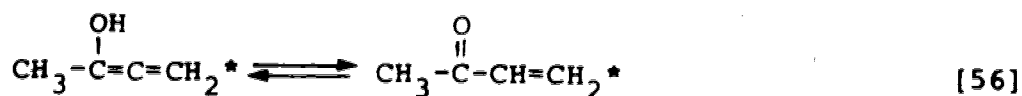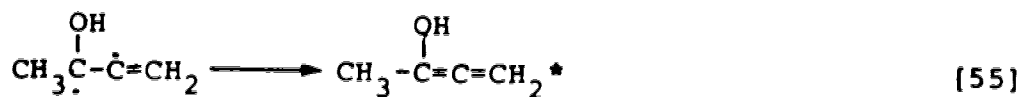
but there is no experimental evidence for the intermediacy of an enol and inclusion of this complicated sequence in the mechanism appears to be unwarranted.

Recently Shaub et al.[70] studied the gas phase reactions of $O(^3P)$ atoms with a series of 1-alkynes, employing the flash photolysis-CO laser resonance technique, and used the vibrational energy distribution of the CO product to elucidate the mechanism of $O(^3P)$ + alkyne reactions. Their results are entirely consistent with the mechanism proposed earlier by Ogi and Strausz.[68]

Some selected rate parameters for the reactions of $O(^3P)$ atoms with selected alkynes, determined by a variety of techniques, are given in Table I-4. The observed trends in the rate constants and activation energies are similar to those observed for the case of alkenes.

C. Reactions of Sulfur Atoms

1. Sources of sulfur atoms

The photodissociation of CS_2 has been shown[74] to yield $S(^3P)$ atoms in the 190-210 nm region,

TABLE I-4

Rate constants (298°K) and Arrhenius parameters for $O(^3P)$ and $S(^3P)$ atom reactions with selected alkynes

Alkyne	$O(^3P)$			$S(^3P)$[f]		
	$k \times 10^{-8}$ $\ell \text{mol}^{-1} \text{ s}^{-1}$	E_a kcal mol^{-1}	$A \times 10^{-10}$ $\ell \text{mol}^{-1} \text{ s}^{-1}$	$k \times 10^{-9}$ $\ell \text{mol}^{-1} \text{ s}^{-1}$	E_a kcal mol^{-1}	$A \times 10^{-10}$ $\ell \text{mol}^{-1} \text{ s}^{-1}$
Acetylene	0.94[a]	3.0	1.41	0.23	3.0	3.39
Propyne	5.4[b]	1.95	1.41	4.8	0.9	2.00
1-Butyne	11.5[c]	1.6	1.70	3.3	0.6	0.91
2-Butyne	29.5[d]	1.8	6.0	16.0	-0.6	0.58
1-Pentyne	4.9±0.6[e]	-	-	-	-	-
2-Pentyne	-	-	-	18.0	-0.85	0.43
1-Hexyne	3.6±0.4[e]	-	-	-	-	-
Perfluoro-2-butyne	-	-	-	0.21	-	-

[a]Reference 41.   [b]Reference 71.   [c]Reference 66.   [d]Reference 72.   [e]Reference 70.   [f]Reference 73.

$$CS_2 + h\nu \longrightarrow CS + S(^3P) \qquad\qquad [57]$$

and this source has been employed in some flash photolysis studies.[75] For continuous photolysis experiments, however, CS_2 is not suitable because reaction [57] is a spin forbidden process and leads to a low $S(^3P)$ yield as well as to polymerization of the CS radicals.

The photochemical decomposition of SPF_3 was studied briefly[76] in the wavelength region 190-210 nm, and apparently produces $S(^1D_2)$ atoms:

$$SPF_3 + h\nu \longrightarrow S(^1D_2) + PF_3 \qquad\qquad [58]$$
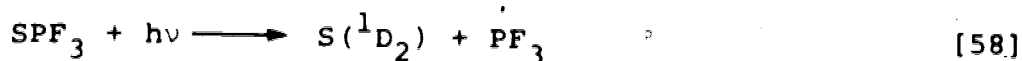
However, PF_3 almost certainly undergoes reaction with substrates and no further studies using this source have been attempted.

The most useful source of sulfur atoms to date is the photolysis of carbonyl sulfide.[6] It is a gas, readily available and soluble in most organic solvents.

The spin allowed photodissociation process

$$COS(^1\Sigma^+) + h\nu \longrightarrow CO(^1\Sigma^+) + S(^1D_2) \qquad\qquad [59]$$
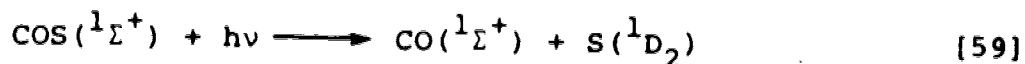
requires 98.8 kcal mol^{-1},[77] corresponding to $\lambda < 290$ nm. According to MO calculations[7] the lowest lying electronic state corresponds to a $\pi \rightarrow \pi^*$ transition ($3\pi \rightarrow 3\pi^*$), with an energy requirement $\Delta E = 4.8$ eV or

110.7 kcal mol^{-1}.

The first UV absorption band of COS, which shows vibrational structure, extends from *ca.* 260 nm to the vacuum UV.[7,78] The shorter wavelength region of the band is independent of temperature but the longer wavelength portion has a positive temperature coefficient. The mean radiative lifetime of the excited state of COS is ~3 x 10^{-7} s. The quantum yield (ϕ) of CO formation in the gas phase photolysis is 1.8 at 240 nm[7] for P_{COS} > 100 torr, and therefore the primary step [59] must be followed by an abstraction reaction:

$$S(^1D_2) + COS(^1\Sigma^+) \longrightarrow CO(^1\Sigma^+) + S_2(^1\Delta_g) \qquad [60]$$
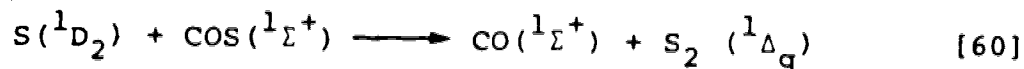
The quantum yield efficiency of primary step [59] is 0.9 in the gas[7] and solution[9] phases.

The earlier suggestion[46] that S(^{3}P) atoms may also be produced in the spin forbidden primary process,

$$COS(^1\Sigma^+) + h\nu \longrightarrow CO(^1\Sigma^+) + S(^3P) \qquad [61]$$
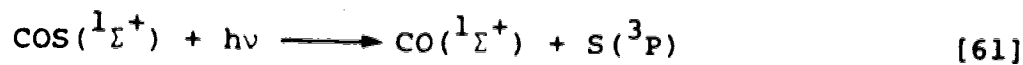
has recently been confirmed experimentally[79] from the kinetics of the 240 nm photolysis of 300 torr COS in the presence of very low pressures (1-30 torr) propylene. Thus the observed variations in the CO and C_3H_6S yields with increasing propylene pressure can best be explained if it is assumed that only 67-74% of the sulfur atoms

produced initially are in the $^1D_2$ state.

The complete mechanism should comprise the following additional reactions:

$$S(^1D_2) + COS(^1\Sigma^+) \longrightarrow COS(^1\Sigma^+) + S(^3P) \qquad [62]$$

$$S(^3P) + COS(^1\Sigma^+) \longrightarrow CO(^1\Sigma^+) + S_2(^3\Sigma_g^-) \qquad [63]$$

$$S_2(^1\Delta_g) + M \longrightarrow S_2(^3\Sigma_g^-) \qquad [64]$$

$$S(^3P) + S_2(^3\Sigma_g^-) \longrightarrow S_3, \text{ etc...} \qquad [65]$$
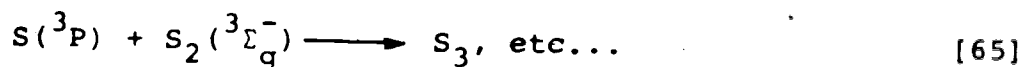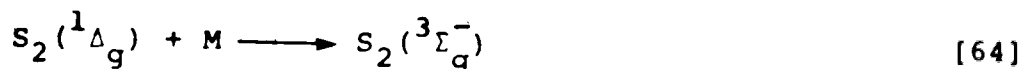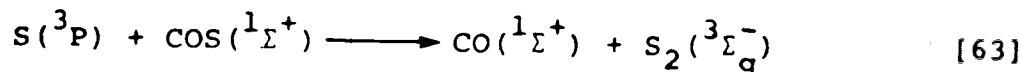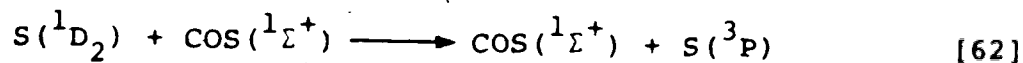
To date there is no direct evidence for the deactivation step [62] although kinetic analysis of COS-alkane and COS-alkene systems[80,108] strongly suggests that this step is operative.

Absolute rate constants for two of the above reactions have been measured. Using the flash photolysis-kinetic spectrocopy technique. Donovan et $al.$[81] monitored the growth and decay of the $S_2(^1\Delta_g)$ state and reported a lower limit of 4×10^{10} ℓ mol^{-1} s^{-1} for the rate of abstraction by $S(^1D_2)$ atoms, i.e., step [60]. More recently, Donovan and coworkers[82] were able to monitor the $S(^1D_2)$ atom concentration directly by time resolved atomic absorption photometry of the 167 nm resonance transition $(3p^3 4s^1 (^1D_2) \rightarrow 3p^4 (^1D_2))$ and reported a value of 7.23×10^{10} ℓ mol^{-1} s^{-1} for the total rate of decay of $S(^1D_2)$ atoms, i.e., steps [60] and [62].

Klemm and Davis,[83] employing the flash photolysis-resonance fluorescence kinetic technique to monitor $S(^3P)$ atoms, reported a value of 2×10^6 ℓ mol^{-1} s^{-1} for the abstraction reaction [63] and measured an activation energy of 3.63 ± 0.12 kcal mol^{-1}.

In the presence of a reactive substrate, additional reactions such as

$$S(^1D_2) + substrate \longrightarrow product \qquad [66]$$

$$\longrightarrow S(^3P) \qquad [67]$$

$$S(^3P) + substrate \longrightarrow product \qquad [68]$$
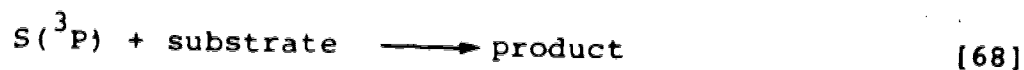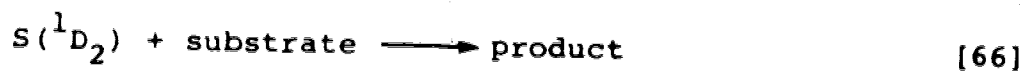
must be considered in competition with steps [60], [62] and [63]. This mechanism may be evaluated in the following manner. If the rate of CO formation in the absence of substrate is defined as R_{CO}^0, then the rate of total S atom formation is $R_{CO}^0/2$. Where the rate of CO formation in the presence of substrates R_{CO}, the total rate of sulfur abstraction, step [60] and [63], is given by

$$R_{abst.} = (R_{CO} - R_{CO}^0/2) \qquad [I]$$

and the rate of sulfur atom reactions other than abstraction is

$$R_{reaction} = (R_{CO}^0 - R_{CO})$$ [II]

Thus, the total rate of sulfur atoms produced is

$$R_{abst.} + R_{reaction} = R_{CO}^0/2$$ [III]

These relations therefore allow product yield analysis in.terms of sulfur atoms produced in the photolysis, provided that complete product recovery is possible. Moreover, the availability of the absolute rate constants for steps [60] and [63] permits the evaluation of the rate constants for reaction with the substrate, i.e., steps [66] and [68].

For the study of $S(^3P)$ atom reactions the mercury sensitization of COS has been employed,[7]

$$Hg(^3P_1) + COS \longrightarrow Hg(^1S_0) + S(^3P) + CO$$ [69]
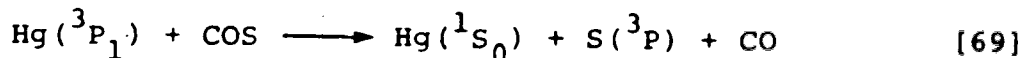
with $\phi_{(CO)} = 1.8$ and $\phi_{[69]} = 0.9$. Alternatively, it has been demonstrated[84,85] that CO_2 deactivates $S(^1D_2)$ atoms to the ground state very effectively:

$$S(^1D_2) + CO_2 \longrightarrow S(^3P) + CO_2*$$ [70]
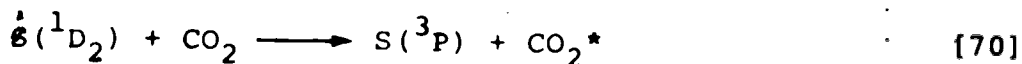
Since the presence of a large excess of CO_2 ($CO_2/COS \approx 6$) has no detectable effect on the CO yield[6,84,86] the following reaction

$$COS* + COS \longrightarrow 2CO + S_2$$ [71]

can be ruled out.

The production of $S(^1S_0)$ atoms

$$COS(^1\Sigma^+) + h\nu \longrightarrow CO(^1\Sigma^+) + S(^1S_0) \qquad [72]$$
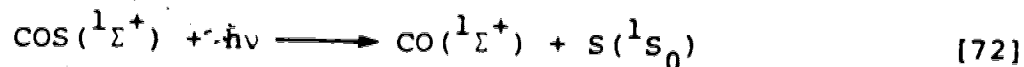
requires a minimum energy of 136 kcal mol^{-1}, corresponding to $\lambda < 210.5$ nm. This step is predicted[7] to originate from a n-π* transition ($9\sigma \rightarrow 4\pi*$), with a calculated energy requirement of $\Delta E = 5.9$ eV or 136 kcal mol^{-1}.

The reactivities of $S(^1S_0)$ atoms have only been studied recently.[87-89] Since product analysis has not been performed, only absolute rates of quenching and/or reaction with various substrate are available. Because of the forbidden nature of the transition to the ground state the $S(^1S_0)$ state is relatively long lived and decays over 100 μs, and can be monitored either by absorption at 178.2 nm ($^1P_1 \leftarrow {}^1S_0$) or by the emissions at 772.5 nm ($^1S_0 \rightarrow {}^1D_2$) and at 458.9 nm ($^1S_0 \rightarrow {}^3P_1$).

The absolute rate constants for the decay this species, as reported by Donovan,[87] strongly vary with the nature of the substrate and the type of interaction. For example, in the cases of Ar, H_2, CO_2, CO, the decay values are low, in the range 10^4 to 4×10^5 ℓ mol^{-1} s^{-1}, corresponding to quenching, while for H_2S, CS_2, NO, and NO_2 the measured rate values are $(2-5) \times 10^{11}$ ℓ mol^{-1} s^{-1}, suggesting a chemical reaction.

2. Reactions of S($^1D_2$) atoms

i) Reactions with alkanes

S($^1D_2$) atoms react with ethane, propane, etc., *via* concerted C-H bond insertion to yield the corresponding isomeric thiols in approximately statistical ratios;[84,85,90] in terms of sulfur atoms produced, approximately 74% are scavenged by the alkane. With increasing alkane pressure the thiol yields increase but never reach 100% in terms of sulfur atoms produced, and the limiting CO yield remains about 20% higher than $R_{CO}^0/2$. These results are illustrated for the S($^1D_2$) + ethane reaction in Figure I-2 and clearly indicate that the only fate of the S(^3P) atoms present in this system is abstraction from COS, i.e., step [63].

As mentioned above, the reactions with higher alkanes afforded only the corresponding thiols in good yields and since products that could have been formed from radical precursors were demonstrably absent it was concluded that thiols are formed by concerted S($^1D_2$) atom insertion into the C-H bond:[46,84,85,90]

$$S(^1D_2) + RH \longrightarrow RSH \tag{73}$$

Kinetic analysis of the COS-alkane systems[84,85,90] indicates that deactivation also takes place in parallel
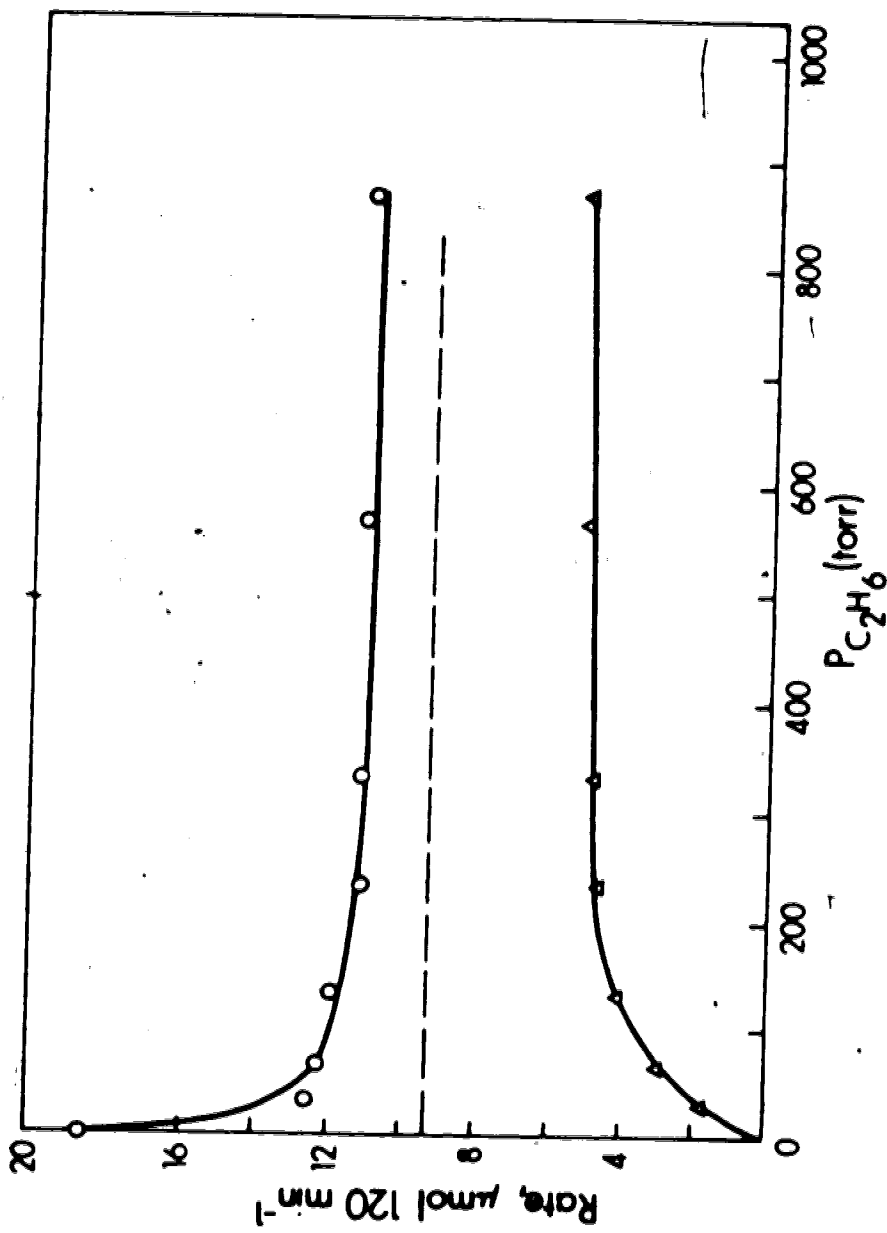
FIGURE I-2. The effect of pressure on the rates of product formation.[85] $P_{COS} = 100$ torr; O, CO rate; Δ, ethane thiol rate; $--- R^0_{CO}/2$.

with insertion,

$$S(^1D_2) + RH \longrightarrow S(^3P) + RH^* \qquad [74]$$

and the rate constant for step [74] lies in the range $(1.2-0.3) \times 10^{10}$ ℓ mol^{-1} s^{-1}.

The statistical distribution of the thiol products indicates that the rate of insertion in the gas phase is indiscriminate with respect to bond order.[84,85,90]

The estimated gas phase rate constants for insertion are all close to the collision frequency values and lie in the range $(1.2-0.7) \times 10^{10}$ ℓ mol^{-1} s^{-1}. The activation energy is estimated to have an upper value of ~ 3 $kcal$ mol^{-1}. The nature of the transition state of the insertion reaction has not been elucidated at the present time.

The reaction with methane leads to extensive fragmentation owing to the short lifetime of the adduct as a consequence of the small number of internal degrees of freedom in the molecule. The final products are CH_3SH, H_2S, CH_3SSCH_3, CH_3SCH_3, CS_2, C_2H_6, and H_2, and the fragmentation process is envisaged by the following mechanism:

$$S(^1D_2) + CH_4 \longrightarrow CH_3SH^* \qquad [75]$$

$$\longrightarrow CH_3 + SH \qquad [76]$$

$$\longrightarrow CH_3S + H \qquad [77]$$

$$CH_3SH^* \longrightarrow CH_2 + H_2S \qquad [78]$$

$$\overset{\bullet}{\longrightarrow} CS + 2H_2 \qquad [79]$$

$$+ M \longrightarrow CH_3SH + M^* \qquad [80]$$
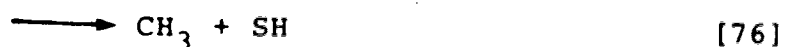
only at extremely high pressures (beyond 2 atm) is the hot thiol formed in reaction [75] expected to be stabilized.

With the exception of CH_4, the reactions of $S(^1D_2)$ atoms with alkanes afford the corresponding thiols in nearly quantitative yields. This is in sharp contrast with the $O(^1D_2)$ + alkane systems (section I-1, i) where fragmentation cannot be suppressed even by several atmospheres of a moderator gas. This is undoubtedly a consequence of the high exothermicity of step [1], e.g., for the reaction $O(^1D)$ + C_2H_6 → $C_2H_5OH(g)^*$ $\Delta H = -140$ kcal mol^{-1}, whereas the $S(^1D)$ + C_2H_6 → $C_2H_5-SH^*$ reaction the exothermicity is only -82.8 kcal mol^{-1}.

A similar argument may be used for the reaction of $O(^1D)$ + C_2H_6 → C_2H_5· + OH·, $\Delta H = -48.9$ kcal mol^{-1}, as compared to $S(^1D)$ + C_2H_6 ⇸ C_2H_5· + ·SH with $\Delta H = -11.6$ kcal mol^{-1}. Thus, the small exothermicity of the last reaction offers a satisfactory explanation for the absence of H atom abstraction by the $S(^1D)$ atom from alkanes.

ii) Reactions with alkenes

$S(^1D_2)$ atoms react with ethylene to yield two products, thiirane (Th) and vinyl thiol (VT), in about equal amounts[77,91] for $C_2H_4/COS > 3$. With higher alkenes all the possible alkenyl thiols are produced, but only for the case of propylene was vinylic thiol detected. Alkenyl thiols are presumably formed *via* insertion into the C-H bond, by analogy with the $S(^1D_2)$ + alkane reaction (*vide supra*), in competition with cycloaddition to the double bond to yield the corresponding thiiranes.. The rate of insertion into the primary, secondary and tertiary C-H bonds of alkenes is also nearly statistical.[77,92] For example, the following steps are involved in the reaction with 1-butene:

$$S(^1D_2) + CH_3CH_2CH=CH_2 \longrightarrow CH_3-CH_2\overset{\overset{\displaystyle S}{\diagup\diagdown}}{CH-CH_2} \quad (70\%) \qquad [81]$$

$$\longrightarrow CH_2\overset{\overset{\displaystyle SH}{|}}{CH}CH=CH_2 \quad (20\%) \qquad [82]$$

$$\longrightarrow CH_2=CHCH_2CH_2-SH \qquad\qquad [83]$$
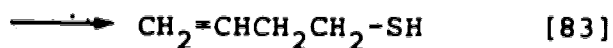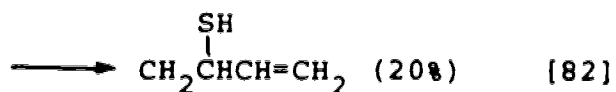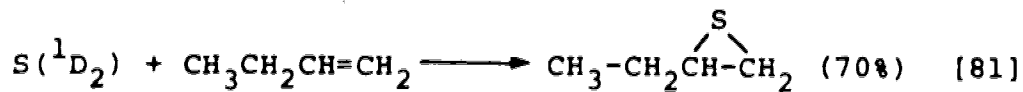
In general, the $S(^1D_2)$ *cyclo*addition and insertion reactions proceed with rates close to 1/20 of the gas kinetic collision frequency, i.e., $\sim 10^{10}$ ℓ mol^{-1} s^{-1}, and upper values of the activation energies are estimated to be 1-2 kcal mol^{-1}.

The product yields in the $S(^1D_2)$ + alkene reactions[86,91] are close to 100% in terms of sulfur atoms produced and as the alkene pressure increases the CO yield decreases and becomes very close to the $R_{CO}^0/2$ value, suggesting that all the sulfur atoms can be scavenged by the alkene. The above results are best illustrated by Figure I-3 for the case of ethylene.

The effect of halogen substitution on the reactions of $S(^1D)$ atoms with alkenes was investigated by Wiebe[91] who observed that vinylic type thiols were formed only for the case of those alkenes where a terminal $=CH_2$ group was present, i.e.,

$$S(^1D_2) + \begin{array}{c} R_1 \\ R_2 \end{array}\!\!\!\!>\!\!=\!\!<\!\!\!\!\begin{array}{c} H \\ X \end{array} \;\;\xrightarrow{\;\;\times\;\;}\;\; \begin{array}{c} R_1 \\ R_2 \end{array}\!\!\!\!>\!\!=\!\!<\!\!\!\!\begin{array}{c} SH \\ X \end{array} \qquad [84]$$
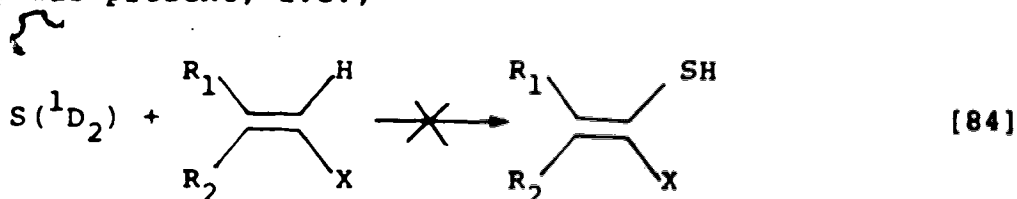
where X = F, Cl. *Cyclo*addition and insertion into the C-H bonds of the R groups were not affected but product recoveries were not quantitative.

To summarize, the $S(^1D_2)$ + alkene reactions lead to the vibrationally excited addition or insertion products, thiiranes and thiols respectively in quantitative yield. This is in sharp contrast to the $O(^1D)$ + alkene reactions (section I-1, ii), where fragmentation predominates in the gas phase and H abstraction takes place in competition with addition. The reason for the
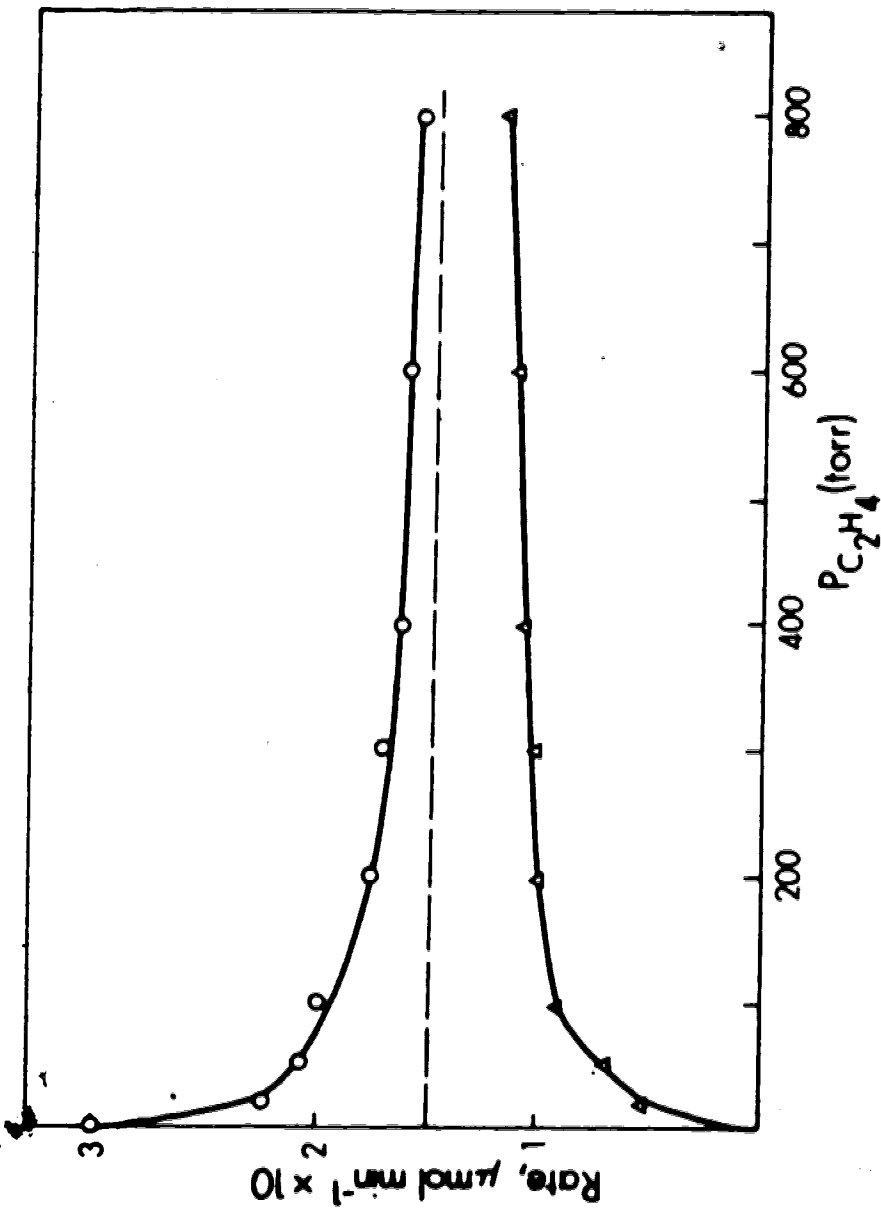
FIGURE I-3. The effect of ethylene pressure on the rates of product formation P_{COS} = 100 forr; $\circ$, CO rate; $\triangle$, Thiirane + Vinylthiol rates; --- $R_{CO}^0/2.91$.

apparent difference in the chemistry of $O(^1D)$ and $S(^1D)$ atoms with alkenes is again related to the large difference in exothermicities of the corresponding reactions. For example, $\Delta H = -144$ kcal mol^{-1} for the $O(^1D) + C_2H_4 \rightarrow C_2H_4O^*$ reaction but only -91.2 kcal mol^{-1} for the $S(^1D) + C_2H_4 \rightarrow C_2H_4S$ reaction.

iii) Reactions with alkynes

The reactions of $S(^1D_2)$ atoms with alkynes have only been briefly examined and are characterized by low product recoveries and extensive polymerization.

The gas phase photolysis of acetylene-COS mixtures[93] afforded CO, CS_2, benzene and thiophene in a combined yield of 5% and large amounts of solid polymer. Unlike the $S(^1D_2)$ + alkane or alkene systems, where the product yield increased with substrate pressure then remained constant, some unusual pressure variations, illustrated in Figure I-4, were reported.

It was suggested that the initial C_2H_2S adduct could be thiirene and/or a biradical isomer which could be formed either in the primary process or by ring cleavage in thiirene:

$$S + C_2H_2 \longrightarrow \overset{S}{\triangle} \qquad [85]$$

$$\longrightarrow \dot{C}_2H_2\dot{S} \qquad [86]$$
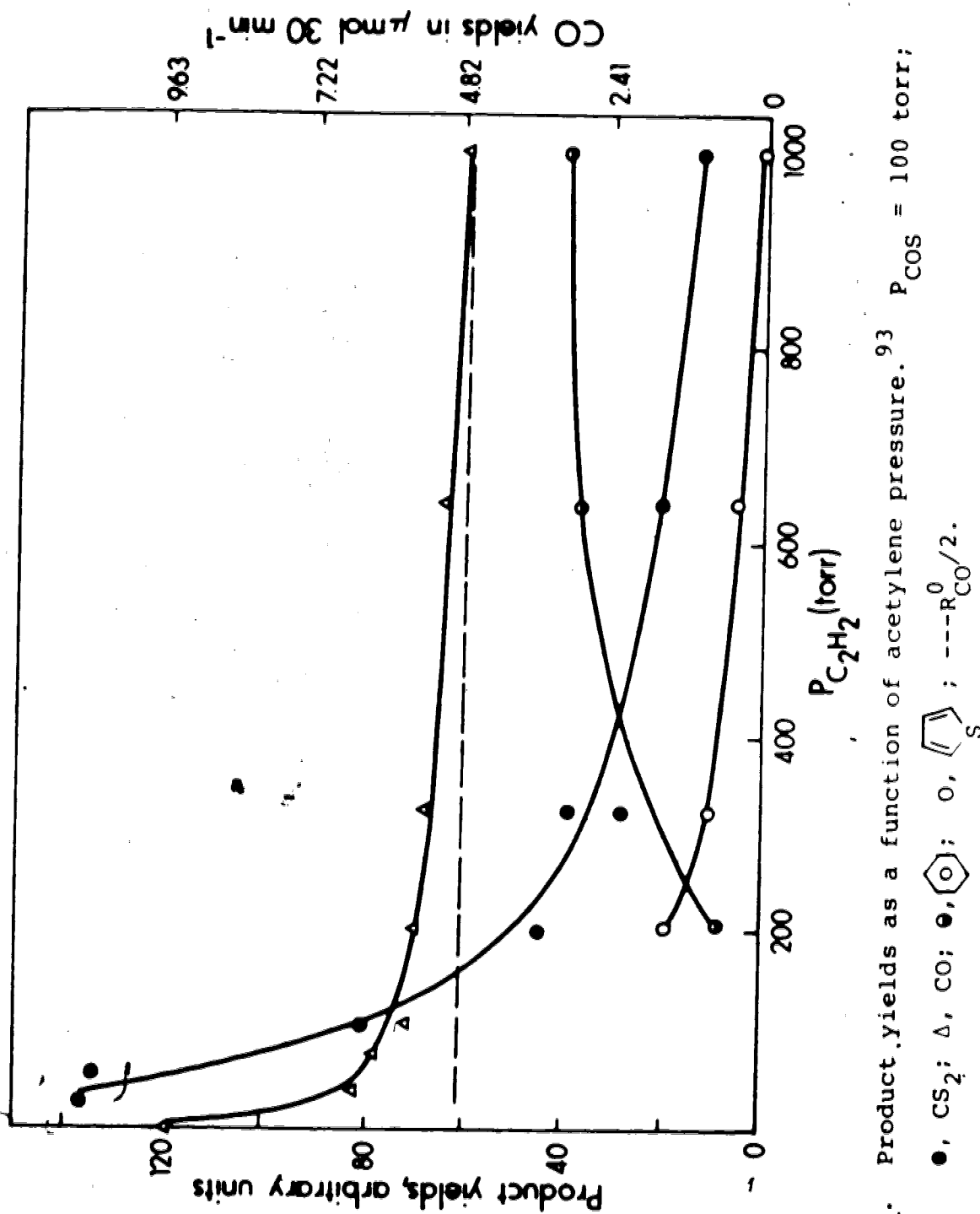
FIGURE I-4. Product yields as a function of acetylene pressure.[93] $P_{COS} = 100$ torr;

●, CS_2; Δ, CO; ◓, ⬡; ○, ⬠$_S$; $---R_{CO}^0/2$.

$$\overset{\cdot}{\underset{\text{S}}{\triangle}} \longrightarrow \overset{\cdot}{C_2}H_2\overset{\cdot}{S} \qquad\qquad [87]$$

Benzene was thought to form *via* the following sequence:

$$\overset{\cdot}{C_2}H_2\overset{\cdot}{S} + C_2H_2 \longrightarrow \overset{\cdot}{C_4}H_4\overset{\cdot}{S} \qquad\qquad [88]$$

$$\overset{\cdot}{C_4}H_4\overset{\cdot}{S} + C_2H_2 \longrightarrow \overset{\cdot}{C_6}H_6\overset{\cdot}{S} \qquad\qquad [89]$$

$$\overset{\cdot}{C_6}H_6\overset{\cdot}{S} \longrightarrow C_6H_6 + S \qquad\qquad [90]$$

It was proposed that thiophene forms *via* cyclization of the $\overset{\cdot}{C_4}H_4\overset{\cdot}{S}$ species formed in step [88]:

$$\overset{\cdot}{C_4}H_4\overset{\cdot}{S} \longrightarrow \underset{\text{S}}{\langle\!\langle\;\rangle\!\rangle} \qquad\qquad [91]$$

No detailed mechanistic interpretation was offered for CS_2 formation.

The gas phase photolysis of methylacetylene-COS mixtures[93] led to the formation of CO, dimethyl thiophene (3%) and trimethylbenzene(~2%); the balance was solid polymer. CS_2 was not formed.

In the dimethylacetylene-COS reaction,[93] studied under similar experimental conditions, the only condensable product of the photolysis was tetramethyl-thiophene(~5%). Hexamethylbenzene and CS_2 were demonstrably absent.

The photolysis of perfluoro-2-butyne-COS mixtures has been examined[93] at $\lambda = 228.8$ nm. The only condensable

product observed was perfluorotetramethylthiophene (PFTMT), the yield of which increased with C_4F_6 pressure to ~50% while the CO yield decreased very gradually and did not reach its half value even at butyne pressures greater than 1000 torr.

The initial $S(^1D_2)$ + C_2H_2 adduct could be antiaromatic thiirene, $\triangle$, or a biradical species $HC=CH$ which has been shown[32,33] to be isoenergetic with thioformyl-methylene, $HC-CH$. Other possible intermediates are,

$:\triangle$, $HC\equiv C-SH$, $H_2C=C=S$
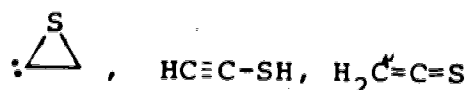
but the following results militate against their intervention.

In flash photolysis-kinetic mass spectrometric studies[94] of $COS-C_2H_2$ mixtures a transient species corresponding to mass C_2H_2S, was detected, of mean lifetime ~1s. Similar experiments with other alkynes led to the detection and lifetime measurements of the corresponding sulfur adducts, e.g., with methylacetylene, 5s; dimethylacetylene, 7s; and perfluoro-2-butyne, 0.1s. These long lifetimes negate the possibility of electronically excited or radical-like carriers. Also, thioketenes were ruled out as alternative structures because their formation would require an intramolecular hydrogen, methyl or trifluoromethyl group migration, a

shift which must somehow be reversed to form the thio-
phenes observed in the static photolysis experiments.
Moreover, this migration should be least likely for the
case of perfluoro-2-butyne and yet the thiophene yield
in this system was the highest.[93]

On the basis of these considerations it was
concluded that the primary adduct of the $S(^1D_2)$ + alkyne
reaction is the corresponding thiirene.[94]

In order to obtain more substantiative evidence
for the transient existence of thiirene, alternative
C_2H_2S precursors were considered. It was anticipated,
for example, that the photodecomposition of 1,2,3-
thiadiazoles would proceed *via* N_2 extrusion and genera-
tion of a C_2H_2S biradical species which could then
rearrange to thiirene:

$$+ h\nu \longrightarrow R\overset{\cdot}{C}=\overset{\cdot}{C}R + N_2 \qquad [92]$$

$$R\overset{\cdot}{C}=\overset{\cdot}{C}R \longrightarrow R\text{---}\overset{S}{\triangle}\text{---}R \qquad [93]$$
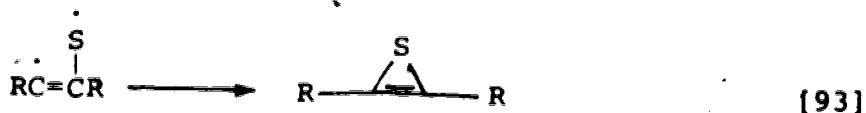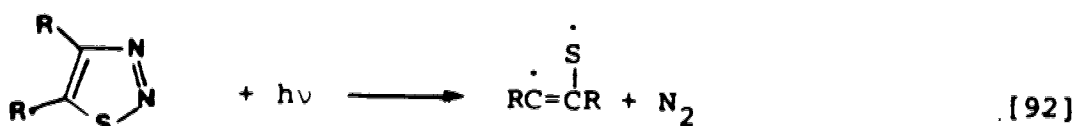
The gas phase photolysis (λ = 250 nm) of a number of
thiadiazoles (R = H, CH$_3$) was examined[94,95] and the
major products were found to be N_2 and polymers; small
amounts of CS_2 and the corresponding alkyne were also
produced. In the presence of hexafluoro-2-butyne,
however, 2,3-bis(trifluoromethyl)thiophenes were formed

in pressure dependent yields, as in the $S(^1D_2) + 2\text{-}C_4F_6$
system. Moreover, photolysis of either 4-methyl or
5-methyl-1,2,3-thiadiazole in the presence of
perfluoro-2-butyne led to the formation of 5-methyl-2,3-
bis(trifluoromethyl)thiophene as the sole product,
indicating that both thiadiazoles generate the same
indistinguishable intermediate. Of all the possible
C_3H_4S isomers only thiirene and methylthioketene can
be considered as viable structures. However, if methyl-
thioketene were the reacting intermediate, two
rearrangements would be required: one for the thio-
formylmethylene → thioketene transformation and the other,
in the $(C_3H_4S + C_4F_6)$ adduct. Moreover, the expected
product would be the 4-methyl isomer on account of the
different migratory aptitudes of H and CH_3. Hence, it
was concluded that the reactive intermediate in the
thiophene-forming reaction is thiirene,

[94]
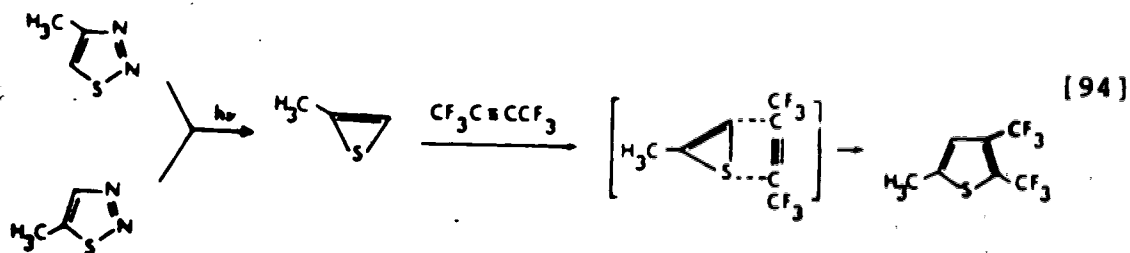
and that the same mechanism applies to the thiophene-forming step in the $S(^1D_2)$ + alkyne systems.

Subsequently, a number of thiirenes were isolated and characterized[97-102] from the low temperature photolysis of matrix isolated 1,2,3-thiadiazoles and vinylene thiocarbonates and their chemical properties were shown[102] to be consistent with the results of *ab initio* MO calculations[32,33] on the relative thermodynamic stabilities of the lowest singlet and triplet states of the six possible C_2H_2S isomers, Figure I-5.

Of all the possible isomers only thioformylmethylene is predicted to have a triplet ground state, although the T_0-S_1 energy separation is small (~8 kcal mol^{-1}). The thioformylmethylene-thiirene rearrangement, step [93] (R = H), would appear to require vibrational excitation, in agreement with the observation that the thiirene yields from matrix isolated 1,2,3-thiadiazoles increase with increasing photonic energy.

The shorter C=C bond distance[32] in thiirene as compared to ethylene and cyclopropene, suggests a more efficient C=C overlap and the chemical properties of thiirenes, by analogy to those of allenes, should be intermediate between those of double and triple bonds. At the same time the weaker C-S bonds become more reactive, leading to rearrangement, self and cross

FIGURE I-5. Calculated energy differences of the C_2H_2S isomers.[32,33]

dimerization *via* ring opening.

In general the reactivities of thiirenes depend upon the number and type of substituents[102] and the experimental conditions. It has been shown, for example, that electron-withdrawing substituents markedly enhance the stability of thiirene.[96]

The most predominant photolytic reaction of thiirenes is rearrangement to thioketenes. This probably takes place *via* the Wolff Rearrangement of S_1 thioketocarbene formed as a result of C-S cleavage,

$$R\text{---}\overset{S}{\triangle}\text{---}R + h\nu \longrightarrow R\overset{S}{\overset{\|}{C}}CR(S_1) \longrightarrow R_2C\text{=}C\text{=}S \qquad [95]$$
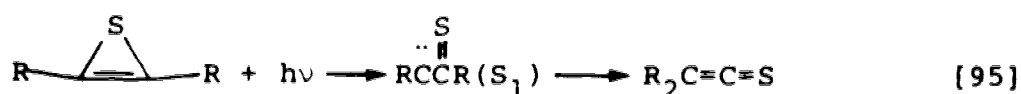
although the occurrence of the following minor pathway cannot be excluded:

$$R\text{---}\overset{S}{\triangle}\text{---}R + h\nu \longrightarrow :\overset{S}{\triangle}\overset{R}{\underset{R}{\diagdown}} \longrightarrow R_2C\text{=}C\text{=}S \qquad [96]$$
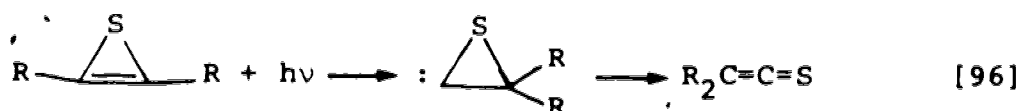
For the particular case of bis(trifluoromethyl)thiirene where CF_3 group migration cannot take place, it appears that S atoms and C_4F_6 are the photodecomposition products:

$$F_3CC\overset{S}{\triangle}CCF_3 + h\nu \longrightarrow C_4F_6 + S \qquad [97]$$
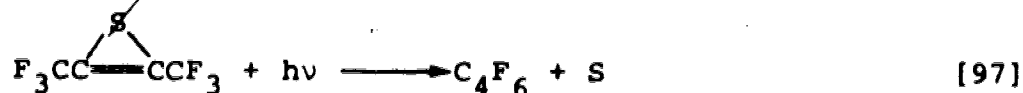
For thiirene and trifluoromethylthiirene a second competing decomposition pathway leads to ethynylthiols:

$$R-\triangle S + h\nu \longrightarrow R-\triangle \overset{H}{\underset{S^+}{}} {}_{-} \longrightarrow RC\equiv C-SH \qquad [98]$$

The intervention of the zwitter ion in the rearrangement is plausible in view of the predicted[93,103] basicity of thiirenes, as manifested by the fact that only the asymmetrical 2,3-bis(trifluoromethyl)thiophene was formed in the $S(^1D_2) + C_2H_2 + C_4F_6$ system.[93]

3. Reactions of $S(^3P)$ atoms

Unlike $O(^3P)$ atoms, $S(^3P)$ atoms are inert towards alkanes, as expected, since H atom abstraction by the latter is an endothermic reaction.

i) Reactions with alkenes

$S(^3P)$ atom reactions with alkenes afford a single product, the corresponding thiirane, in nearly quantitative yields[46]

$$S(^3P) + {=\!=\!=} \longrightarrow \triangle S \qquad [99]$$

The unique feature of the $S(^3P)$ atom *cyclo*addition reaction with alkenes is its high stereospecificity, which has been demonstrated for the following alkenes:[84,86,91] *cis* and *trans*-2-butene, *cis* and

trans-1,2-difluoroethylene, and *cis* and *trans*-1,2-di-
chloroethylene. In each case the predominant geometrical
isomer of the thiirane product is that which corresponds
to the parent alkene, e.g.,

$$S(^3P) + \quad \longrightarrow \quad \underset{90\%}{} + \underset{10\%}{} \qquad [100]$$

$$S(^3P) + \quad \longrightarrow \quad \underset{98\%}{} + \underset{2\%}{} \qquad [101]$$
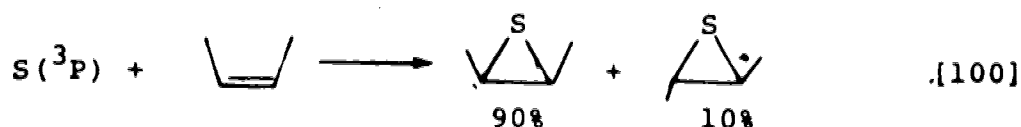
This was the first known case of a triplet state reagent
undergoing a stereospecific reaction with a substrate
and in order to shed light on the mechanism involved,
EHMO calculations were carried out[104,105] on the
reaction path of the $S(^3P) + C_2H_4$ reaction and on the
ground singlet and excited triplet and singlet states
of thiirane. The calculations predict that the lowest
lying triplet (T_1) state of thiirane lies ~40 kcal mol^{-1}
above the ground state, has a ring distorted equilibrium
geometry, and features a rotational energy barrier of
23 kcal mol^{-1}. This high value provides an adequate
rationale for the observed high stereospecificity of
the $S(^3P)$ + alkene reactions. T_1 thiirane is thus the
primary adduct in reaction [99] and has been shown to
be extremely resistant towards collisional deactivation.[106]

Selected rate parameters determined by flash
photolysis kinetic spectroscopy in the gas phase for
$S(^3P)$ atom reactions with representative alkenes are
given in Table I-3. The activation energies decrease
as the number of alkyl substituents on the double bonded
carbons increase, and decrease with halogen substitution,
a clear manifestation of the electrophilic nature of
$S(^3P)$ atoms.[46] These variations in E_a can be correlated
with molecular properties such as ionization potentials,
excitation energies and bond orders.[56-59] As with the
case of $O(^3P)$ atoms, the reactions with highly substituted
alkenes feature negative activation energies.

ii) Reaction with alkynes

Very little work has been done on the reactions
of $S(^3P)$ atoms with alkynes. With acetylene[93] the
products are unchanged quantities of benzene and thio-
phene but a drastically reduced CS_2 yield as compared
to the $S(^1D_2)$ + C_2H_2 reaction.

In the $S(^3P)$ + $CH_3C\equiv CH$ and $S(^3P)$ + $CF_3-C\equiv C-CF_3$
systems[93] the nature and yields of the products were
the same as for the case of $S(^1D_2)$ atom reactions (*vide
supra*). Thus, it appears that unlike $S(^1D_2, ^3P)$ atom
reactions with alkanes and alkenes, the nature of the
products with alkynes is not affected by the spin state

of the S atom.

On the basis of spin conservation and the results of MO calculations[32,33] (Figure I-5),[32] the primary product of the $S(^3P) + C_2H_2$ reaction should be ground triplet state thioformylmethylene:

$$S(^3P) + HC\equiv CH \longrightarrow HC\overset{\overset{\displaystyle S}{\|}}{-}CH \quad (T_0)$$ [102]
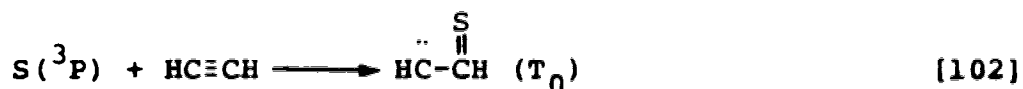
This is analogous to the $O(^3P)$ atom + alkyne case.[36,68,70]

Absolute rate constants have been measured for a number of $S(^3P)$ + alkyne reactions, some of which are listed in Table I-4. Unfortunately, Arrhenius parameters have only been measured for acetylene and methyl acetylene, where it is seen that the activation energies and A factors are considerably higher than for the $S(^3P)$ + ethylene and propylene reactions. As in the $S(^3P)$ + alkene series, the rate constants increase with increasing alkyl substitution.

D. Reactions of Selenium Atoms

Recently, Shaw et al.,[14] determined the absolute quantum yields of Se $^1S_0$, $^1D_2$ and $^3P_{0,1,2}$ atom production from atomic absorption measurements following the photodissociation of COSe with an ArF laser at 193 nm. The measured lifetimes of $^1S_0$ and $^1D_0$ show that they rapidly react with the parent molecule. The quenching

rates of $^3P_1$ atoms by CO_2 and CO gases were also determined.

The measured quantum yields for the formation, monitored at the indicated transition wavelengths, are as follows:

$\phi(^1S_0) = 0.25$ (199.5 mm); $\phi(^1D_2) = 0.10$ (185.5 nm); $\phi(^3P_0) = 0.05$ (206.3 nm); $\phi(^3P_1) = 0.25$ (204.0 nm); and $\phi(^3P_2) = 0.35$ (196.0 nm).

Rate constants for the abstraction reactions

$$Se(^1S_0) + COSe \longrightarrow Se_2{}^* + CO \qquad [103]$$

$$Se(^1D_2) + COSe \longrightarrow Se_2{}^* + CO \qquad [104]$$
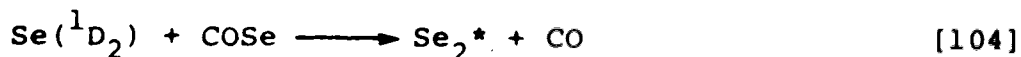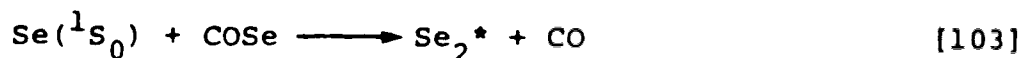
are $k_{103} = (9.0 \pm 0.2) \times 10^{10}$, and $k_{104} = (9.0 \pm 0.5 \times 10^{10}$ ℓ mol^{-1} s^{-1}, respectively, in good agreement with earlier reported values.[107]

For the quenching reactions,

$$Se(^3P_0) + CO \longrightarrow Se(^3P_2) + CO{}^* \qquad [105]$$

$$Se(^3P_1) + CO \longrightarrow Se(^3P_2) + CO{}^* \qquad [106]$$
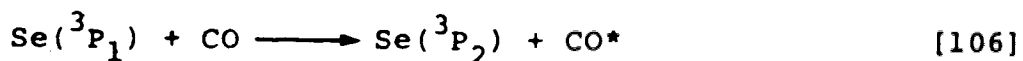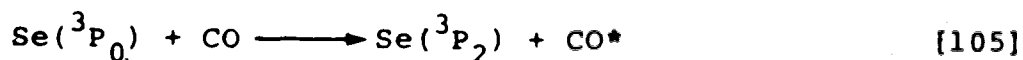
the following rate constants were reported: $k_{105} = (6.0 \pm 0.5) \times 10^9$, and $k_{106} = (9.6 \pm 0.5) \times 10^9$ ℓ mol^{-1} s^{-1}.

1. Reactions of $Se(^1D_2)$ atoms

The gas-phase photolysis of COSe has been found[10] to be a good source of $Se(^1D_2)$ atoms:

$$CoSe + h\nu \ (\lambda = 230-270 \ nm) \longrightarrow CO + Se(^1D_2) \qquad [107]$$
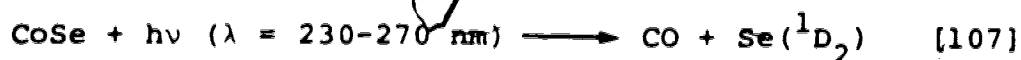
Unfortunately, conventional photolysis of COSe in the presence of either alkanes or alkenes, leads to extensive polymerization and no lower molecular weight products could be detected. However, in experiments employing flash-photolysis kinetic absorption spectroscopy in combination with mass spectrometric detection techniques,[10] the photolysis of COSe in the presence of various alkenes led to the detection of transient intermediates which were identified as unstable episelenides:

$$Se(^1D_2) + RC=CR \longrightarrow \overset{\displaystyle Se}{RC \underset{}{-\!\!-}CR} \qquad [108]$$
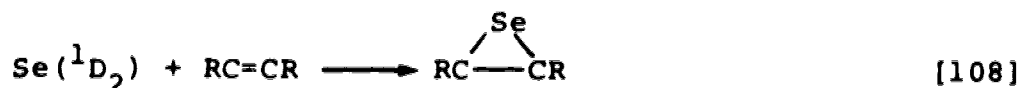
Significantly, it appears that $Se(^1D_2)$ atoms, unlike $S(^1D_2)$ and $O(^1D_2)$ atoms, do not insert into the C-H bonds of alkenes.

The latter method was also used to monitor the reactions of $Se(^1D_2)$ atoms with C_3H_8, $cyclo\text{-}C_3H_6$, $cyclo\text{-}C_4H_8$, C_2H_6, $iso\text{-}C_4H_{10}$. In each case, mass fragmentation patterns consistent with selenomercaptans were observed, indicating that $Se(^1D_2)$ atoms insert

into the C-H bonds of alkanes:

$$Se(^1D_2) + RH \longrightarrow RSeH \qquad [109]$$

The insertion reaction, as expected, is indiscriminate.

2. Reactions of Se(^{3}P) atoms

Absolute rate constants for the addition reactions of Se(^{3}P) atoms to alkenes have been measured using flash-photolysis kinetic absorption spectroscopy and are listed in Table I-3. In these studies, CSe_2 was used as a source[11] of Se(^{3}P) atoms:

$$CSe_2 + h\nu \ (\lambda < 230 \ nm) \longrightarrow CSe + Se(^3P) \qquad [110]$$

The activation energies for cycloaddition are somewhat larger than for the case of S(^{3}P) atoms but nevertheless follow the same trend.

E. Reactions of Tellurium Atoms

The reactions of Te(^{3}P) atoms, produced from the flash-photolysis of dimethyltelluride,

$$CH_3TeCH_3 + h\nu \ (\lambda < 270 \ nm) \longrightarrow 2CH_3 + Te(^3P) \qquad [111]$$
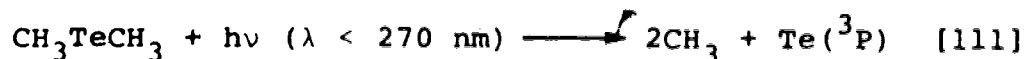
have been examined[12,57] with a limited number of alkenes. The unstable epitelluride products were detected by kinetic absorption spectroscopy and kinetic mass

spectrometry. The rate constants, listed in Table I-3, are the lowest in the series O, S, Se, Te and it would appear that the reason for this is the very small A factors.

F. Aim of the Present Investigation

It was decided to examine three different aspects of sulfur atom chemistry.

1. The thiirane-vinylthiol isomerization

As noted above, $S(^1D_2)$ atoms react with ethylene to yield thiirane and vinylthiol in approximately equal amounts under the following conditions:[84] $P_{(COS)} = $ 100 torr, $P_{(C_2H_4)} \geqslant$ 200 torr, λ = 240 nm. Yet under similar conditions the reaction with propylene afforded 68.3% methylthiirane, 15% methylvinylthiol, and 16.7% allylthiol.[84] On the basis of these observations it was suggested[84] that vinyl thiol forms *via* a dual mechanism, direct insertion,

$$S(^1D_2) + H_2C=CH_2 \longrightarrow H_2C=CHSH \qquad [112]$$
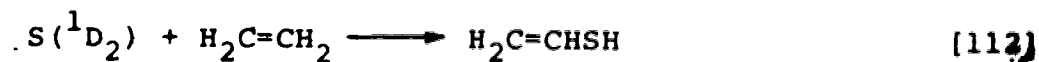
and unimolecular isomerization of "hot" thiirane:

$$S(^1D) + H_2C=CH_2 \longrightarrow \left(H_2C\overset{S}{\underset{}{\diagup\!\!\diagdown}}CH_2 \right)^* \qquad [113]$$

$$\left(\underset{CH_2——CH_2}{\overset{S}{\triangle}} \right)^* \longrightarrow H_2C=CHSH \qquad [114]$$
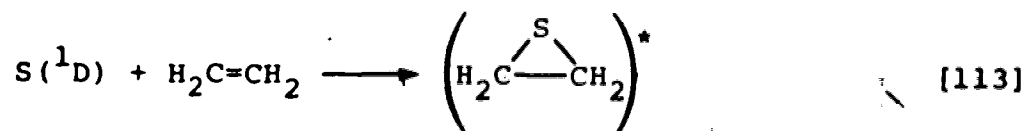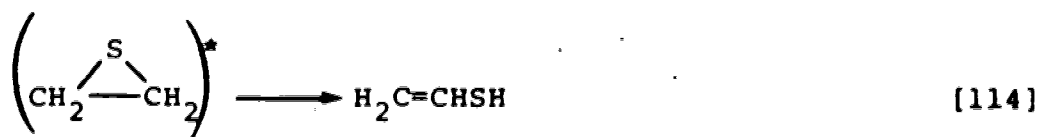
Chemically activated thiirane formed in step [113] has an energy content of ~ 85 kcal mol^{-1}, which should be sufficient to promote this isomerization.

Subsequently, it was shown that the vinylthiol/ thiirane ratio from the $S(^1D_2) + C_2H_4$ reaction decreases to 0.4 and 0.2 in the liquid and solid phases,[77] respectively. On the other hand, under the same conditions, the relative thiol yields from the $S(^1D_2) + C_3H_6$ reaction were only slightly suppressed,[77,108] suggesting that in this case thiols are formed almost exclusively via the insertive route.

It was, therefore, decided to carry out a more detailed investigation of the $S(^1D_2) + C_2H_4$ reaction in order to elucidate the mechanistic details of the novel, hypothetical thiirane-vinyl thiol isomerization.

2. Reactions of S atoms with allene

At the time this project was initiated the only multifunctional alkene substrate investigated was 1,4-butadiene. Both $S(^1D_2)$ and $S(^3P)$ atoms react with this molecule to yield vinylthiirane[92]

$$S(^1D_2, {}^3P) + H_2C=CH-CH=CH_2 \longrightarrow H_2C=CH-\underset{CH-CH_2}{\overset{S}{\triangle}} \qquad [115]$$
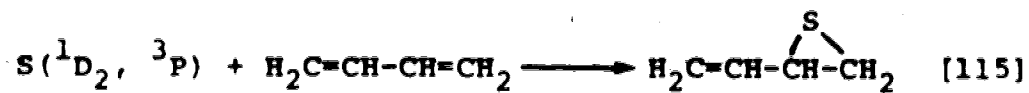
and no insertion products were observed when $S(^1D_2)$ atoms were the reactive species.

It was, therefore, decided to examine the reactions of S atoms with cummulenes, beginning with the parent compound allene. Moreover, the expected major product, methylene thiirane, had not been synthesized and it was therefore of interest to characterize the properties and chemical reactivity of this novel compound.

3. Reactions of S atoms with alkynes

The exploratory work carried out many years ago on the S + alkyne systems[93] showed that thiophenes, benzenes and CS_2 are formed in very small yields (~5% total), regardless of the spin state of the sulfur atom. The lifetimes of the initial adducts were shown to increase with increasing substitution, and this effect is particularly pronounced upon perfluoroalkyl substitution. Mechanistic details however could not be deduced from the data and it was therefore decided to reinvestigate the reactions of $S(^1D_2, {}^3P)$ atoms with alkynes in more detail. 3,3,3-Trifluoropropyne and perfluoro-2-butyne were initially chosen as substrates in the hope that higher product yields could be achieved. In order to shed light on the mechanistic details of the reaction and the nature of the intermediates involved, the effects

of total pressure, COS concentration, temperature and
added gases would be studied. In the light of these
results it was subsequently decided to reexamine some
aspects of the S + C_2H_2 reaction and to carry out
competetive experiments with C_2H_2 and C_4F_6 to assess
the relative reactivities of the transient intermediates.

CHAPTER II

EXPERIMENTAL

1) The high vacuum system

The static high vacuum apparatus employed (Figures II-1 and 2) was constructed of Pyrex glass and the system was evacuated to 10^{-6} torr pressure with the aid of a two stage mercury diffusion pump, backed by a Welch Duo-Seal Model 1405 oil rotary pump. Hoke teflon seated valves (TY 440), glass stopcocks, lubricated with high vacuum N and L grease, Delmar mercury float valves, ace teflon valves, and springham valves were used, depending on the operation. When ethylene and allene were the substrates the valves leading to the photolytic cell were made of teflon, while in the case of alkynes, stainless steel high temperature Hoke valves (number 421 306Y-316-SS) were employed. A McLeod gauge was used to measure pressures less than 0.5 torr, and to check the Pirani gauges (Consolidated Electrodynamics Cat. No. GP-001), which were used to monitor distillations and gas transfers.

With the aid of a one stage mercury diffusion pump and a Toepler pump, non-condensable gases such as carbon monoxide were collected and measured in a calibrated gas buret. Using a mercury manometer (for pressures greater than 1 torr) or a Baratron gauge (for pressures less than 1 torr).

Figure II-1. The high vacuum system (front view) - P - Pirani tube; ● - Hoke valve; ◐ - glass stopcock; ◑ - springham valve; ◐ - mercury floatvalve; A - air inlet; B - to g.c. injection; D - distillation train; G - small gas buret; H.V. - high vacuum; L - low vacuum; L.D. - calibrated sampler; M - mercury manometer; Mc - McLeod gauge; S - storage bulb; T - solid N₂ trap; U - u trap.
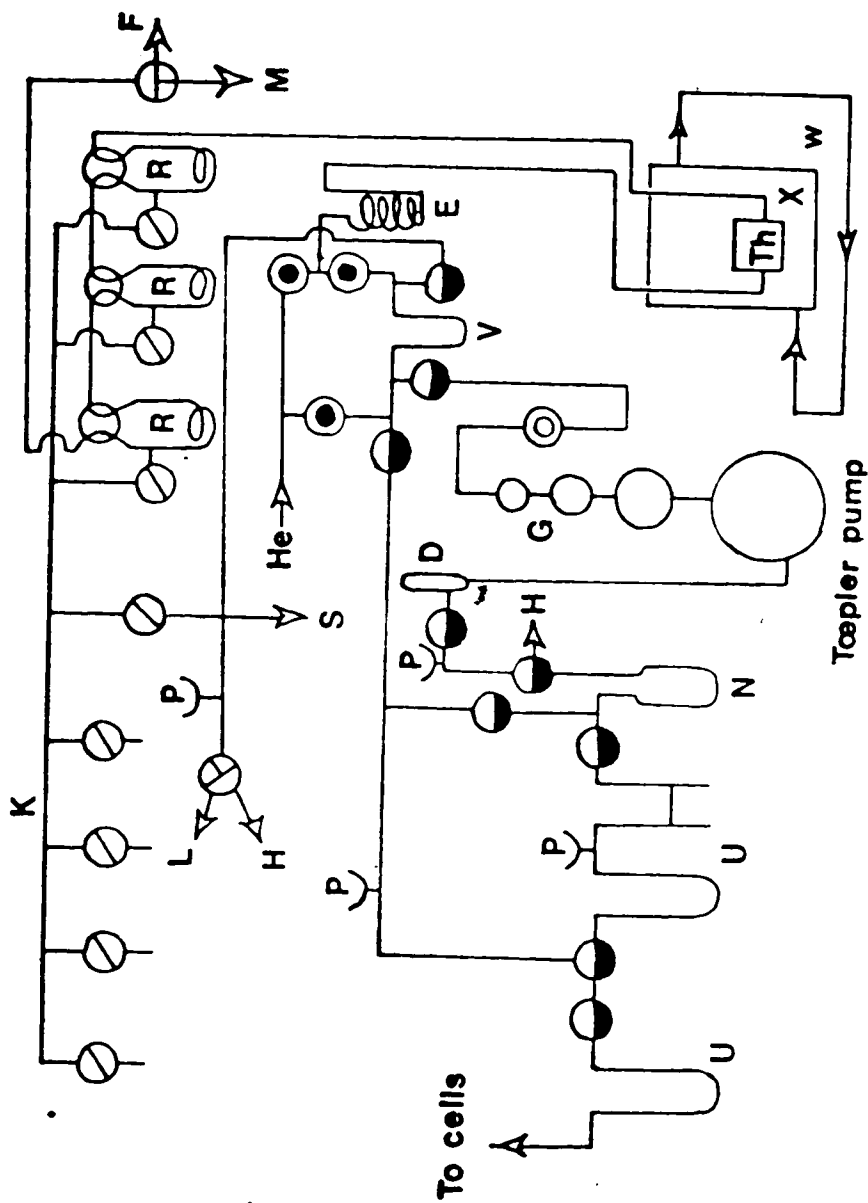
Figure II-2. The high vacuum system (rear view) – D – one stage mercury diffusions pump; E – g.c. column; F – effluents; G. gas buret; H – high vacuum; K – sampling manifold for spectroscopic analysis; L – low vacuum; M – oil manometer for Helium flow; P – Pirani tubes; R – samples trapping coil; S – to storage manifold; N – solid N_2 trap; U – distillation train; Th – thermistor; X – heat exchanger; W – circulating water bath; ⊘ – glass stopcock; ⊘ – 3-way glass stopcock; ⦿ – mercury float valve; ● – 4-way glass stopcock; ◉ – Ace teflon valve; V – g.c. sample loop; ⊖ – springham valve.

2) Photolysis assembly

Photolyses were performed in cylindrical quartz cells, (ℓ x diam.) 10.0 x 5.0 cm, connected through ace teflon valves or Hoke valves to a conventional grease-free vacuum system. The light sources employed were a) a Hanovia medium pressure mercury arc equipped with a 6 mm Vycor 7910 filter to limit the effective radiation to > 220 nm. b) An Osram cadmium lamp (unfiltered) emitting resonance lines at 288.8 and 326.1 nm. c) A Philips zinc lamp (83106 E) with an effective emission resonance line at 213.9 nm. The output of the lamps was reproducible to *ca* 3% except for the zinc lamp whose intensity was extremely variable and thus could not be used for quantitative work. One of the quartz cells was placed in an aluminum block furnace (2.5 cm thick) equipped with four 500 watt pencil heaters, powered and regulated by an API 2-Mode proportional electronic controller, for temperature studies. Temperatures, accurate to ±0.5°C, were measured with an iron-constant thermocouple.

For high pressure studies a cylindrical stainless steel cell (ℓ x diameter) 7.5 x 3.5 cm directly attached to a high temperature Hoke valve was employed. The windows were constructed of 0.8 cm thick quartz and secured onto the cell body by screw actions on a pair of external steel rings.

3) Analytical methods

a) Gas chromatography was used for qualitative identification and analysis, and for checking the purity of materials. Components of the system consisted of the sample loop, column, sample trapping system (locations are shown on Figure II-2), microthermistor cell fitted with Gow-Mac 13-502 thermistors and placed in a constant temperature bath kept at 26°C for the ethylene and allene systems, and 30°C for the alkynes. The bridge current was monitored at 8.0 mA. Helium was used as the carrier gas at a flow rate of 25.0 cm^3 min^{-1}. The helium (Matheson) was dried by passage through a 100 x 2 cm column of molecular sieve and checked on a 30 x 2 cm drierite column. An Edwards needle valve was employed to control the flow rate, which was measured on an Octoil-s manometer calibrated by a bubble flow meter. All parts of the chromatographic assembly through which products passed were constructed of glass or Teflon, except for the detector block itself, in order to minimize decomposition of unstable sulfur products.

The sample unit consisted of a U shaped sample loop into which the products were frozen at -196°C. The helium flow through the by-pass and the sample loop was controlled by three Ace teflon valves. Other inlets to the sampler unit were sealed by raising the mercury

level fully to eliminate all dead space. The products
were allowed to thaw and, by closing the by-pass and
opening the through flow valves, were swept onto the g.c.
column. Product elution times, column packings, lengths,
and operating conditions are given in Tables II-1
and II-2. Adequate resolution was obtained in all
cases.

The detector (molar) response was calibrated for
each compound either using the calibrated gas buret for
gaseous materials or by injecting known quantities of
liquids with a micro-syringe. Linear responses were
observed for 0.1 - 10.0 μmole sample amounts, within the
range of experimental product yields. Chromatographic
peak areas were measured with an Ott planimeter. The
overall reproducibility was *ca* 5%.

Product samples were collected downstream from
the g.c. effluent for spectroscopic identification. The
sample holders were made of quartz in order to reduce
surface decomposition.

b) Mass spectra were obtained on an AEI MS-12
instrument with the ion source operating at 70 eV and
the ionization chamber kept at *ca* 50°C. Samples were
analyzed either individually *via* a "probe" or a g.c.
column adapted to the MS-12 chromatograph, Varian
Aerograph series 1400. The resulting data were interpreted

TABLE II-1

G.C. operating conditions and elution times[a]
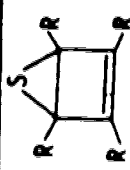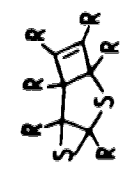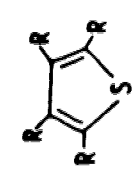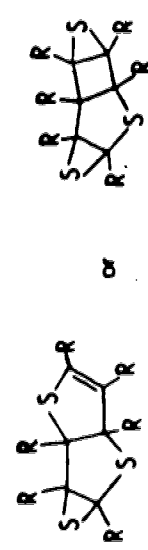
Compound	Structure	Column	Elution time min.
Vinyl thiol (VT)	$H_2C=CH-SH$	I	2.5
Thiirane (Th)	S (triangle)	I	5.0
Methylenethiirane (MeTh)	S (triangle)	II	42.2
Methylthiirane (MTh)	S (triangle)	II	37.5
Carbondisulfide	CS_2	II	10.0
Carbondisulfide	CS_2	III	4.0

(continued...)

(a) He flow rate 25 ml min^{-1}; column temperature 23°C; (I) = 2 mm ID x 122 mm glass column containing 60/80 mesh Diatoport S coated with 10% tricresylphosphate (TCP); (II) = 3.2 mm ID x 305 cm teflon column, 60/80 mesh Chromosorb W.A. coated with 10% TCP; (III) = 2 mm ID x 122 mm glass column containing 60/80 mesh Chromosorb W.A. coated with 10% TCP.
(b) Where R = CF₃.   (c) Compound number from Table V-5.   (d) Compound number from Table V-4.
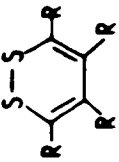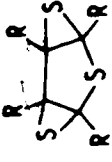
69.

TABLE II-1 (continued)

Compound	Structure	Column	Elution time min.
Perfluorotetramethyl Dewar thiophene (PFTMDT)			
14c		III	2.7
		III	5.6
Perfluorotetramethyl thiophene (PFTMT)			
15c		III	19.0
16c	$(C_4F_6S)_2$	III	33.0
17c	$(C_4F_6)_3S_2$	III	45.0
		III	56.0
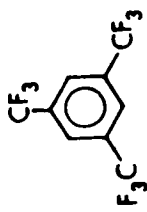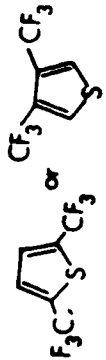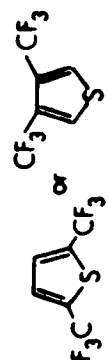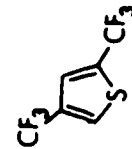
(continued....)

TABLE II-1 (continued)

Compound	Structure	Column	Elution time min.
3,4,5,6-perfluoromethyl-1,2-dithiin 19[c]	(dithiin ring structure with R groups)	III	77.0
20[c*]	$(C_4F_6S)_3$	III	98.0
21[c]	$(C_4F_6S)_3$	III	124.0
	(ring structure with S and R groups)	III	156.0
3,3,3-trifluoromethyl thioketene	$CF_3-CH=C=S$ (or isomers)	III	1.0
Unknown (MW 288)		III	9.0

(continued...)

TABLE II-1 (continued)

Compound	Structure	Column	Elution time min.
1,3,5-tris(trifluoromethyl)benzene		III	9.5
2,5 or 3,4-bis(trifluoromethyl)-thiophene		III	15.0
2 or 3-trifluoromethyl-thiophene		III	36.0
2,5 or 3,4-bis(trifluoromethyl)-thiophene		III	31.0
2,4-bis(trifluoromethyl)thiophene		III	30.0

(continued...)

TABLE II-1 (continued)

Compound	Structure	Column	Elution time min.
2,3,4 or 2,3,5-tris(trifluoromethyl)-thiophene		III	9.0
1,3,5-tris(trifluoromethyl) dewar benzene		III	63.0
12^d		III	83.0
11^d		III	41.0
Benzene		III	14.5
Thiophene		III	18.5
3,4-(bistrifluoromethyl)-1,2-dithietene		III	42.0

73.

TABLE II-2

Materials Used

Material	Supplier	Purification
Helium	Canadian Liquid Air Linde	Passed through molecular sieve
Ethylene	Matheson research grade	Degassed at -186°C Distilled at -160°C
Carbonylsulfide	Matheson	Bubbled through sat. solns. of NaOH and Pb(OAc)₂. Distilled at -130°C.
Carbon dioxide	Airco	None
Allene	Teaching grade	Distilled at -132°C
Acetylene	Matheson	Distilled at -139°C
3,3,3-Trifluoropropyne	Columbia Organic Chemicals Company	Distilled at -115°C
Perfluoro-2-butyne	Columbia Organic Chemicals Company	Distilled at -98°C
Perfluorotetramethylthiophene (PFTMT)	Prepared[a]	Distilled at 131°C Crystallized at -20°C

[a]Ref. 109.

using a computer model Data General Nova 3, employing a
DS-50 programme.

ç) U.V. spectra were recorded on a Unicam 1800
spectrometer employing a 10.0 x 1.6 cm quartz cell equipped
with cold finger.

d) **Infrared spectra were obtained in the gas phase**
on either a Perkin Elmer Infracord instrument in a 7.5 cm
micro gas cell or a Nicolet 7199 FTIR instrument employ-
ing a 10.0 x 1.9 cm cylindrical quartz cell to eliminate
all metal surfaces. The windows of this cell were made
of Kodak ZnS polycrystals and were attached to the
quartz cylinder with epoxy glue. In each case the
spectrum of the empty cell was recorded and the final
product spectrum was corrected for interference fringes
and other extraneous contributions.

e) Three N.M.R. spectrometers were employed for
structural determinations; Bruker WP-60, Bruker 200 and
400 MHz instruments, equipped with proton (^{1}H) or
fluorine (^{19}F) probes. Gas samples were condensed into
medium walled NMR sample tubes containing degassed,
solidified CCl_3D as solvent and as an internal standard.
In case of ^{19}F NMR, trifluoroacetic acid was employed
as an external standard. All NMR samples were purified
by repeated passes through the g.c. system. NMR samples

were run either at room temperature (24°C) or -30°C depending on the stability of the material.

4. Operational procedures

In the preparation of reaction mixtures, components partial pressures were determined either by the mercury manometer or the Baratron pressure gauge and the mixtures transferred to storage bulbs located close to each cell. When required, the mixture was distilled into the cell through a vertical U trap at the lowest temperature possible dictated by the vapour pressures of the substrates. This procedure ensured a mercury free environment, thus preventing the occurrence of photosensitization reactions or the formation of solid HgS. The purified mixture was equilibrated at a predetermined temperature for at least one hour before irradiation. The medium pressure mercury arc was equilibrated one hour before irradition and the cadmium and zinc resonance lamps, for 30 minutes.

For each series of experiments actinometry was performed frequently to check the stability of the radiation source and the transmittance of the cell.

Actinometric measurements were done using 50-150 torr COS, for which $\phi_{(CO)} = 1.8$[7] at $\lambda = 240$ nm.

After photolysis carbon monoxide was quantitatively collected and measured in a gas buret with the aid of a Toepler pump backed up by a one stage mercury diffusion pump. To ensure complete CO recovery the reactants and products were warmed and frozen several times to free any CO trapped in solid matrix. Substrates and products were then separated by trap to trap distillations at 1-3 torr pressure. In the presence of ethylene product separation was achieved by passing the photolyzed mixture through three traps at -196°C and a solid N_2 (-210°C), then, through three traps at -139°C (chloroethane). A similar technique was employed for the allene and alkyne systems except for the last three traps which were kept at -132°C (n-pentane) for allene and -98°C (methanol) for the alkynes. Repeated checks for carryover were performed by redistilling the reaction mixtures. The separated products then were transferred quantitatively to the g.c. sample loop for analysis.

After each experiment, air was allowed into the cell and subsequent heating to ca 500°C with an oxygen flame oxidized and volatilized any sulfur or polymer which deposited on the cell walls.

5. Materials and purification (Table 2-5)

a) Helium (Canadian Liquid Air, Linde) was passed through a 100 x 2 cm molecular sieve.

b) Ethylene (Matheson research grade) was degassed at -186°C and distilled through two steps at -160°C (*iso*pentane).

c) Carbonyl sulfide (Matheson) was purified to remove H_2S and CO_2 by passage through four washing bottles containing concentrated sodium hydroxide and saturated lead acetate solutions in an alternating fashion, collected in a cold trap at -196°C, distilled *in vacuo* at -132°C and degassed at -161°C. G.c. analysis of the purified sample confirmed the absence of any foreign material.

d) Carbondioxide (Airco >99.9% pure) was used as such.

e) Allene (Matheson, teaching grade, 99%) was degassed at -186°C and distilled at -132°C. The purified sample contained less than 0.5% propylene as impurity.

f) Acetylene (Matheson, purity *ca* 99%) was degassed at -186°C.

g) 3,3,3-Trifluoropropyne (Columbia Organic Chemicals, purity 99.0%) was distilled repeatedly at -115°C and the purity checked on a 6 ft g.c. porapak N column, and by g.c.-MS.

h) Perfluoro-2-butyne (Columbia Organic Chemicals Co., 99.0% purity) was distilled at -98°C several times. The remaining impurities, as analyzed by g.c. were less than 0.2%.

i) Perfluorotetramethylthiophene (PFTMT) was prepared according to Krespan[109] for calibration purposes.

Sulfur (6.4 g), hexafluoro-2-butyne (30 g) and iodine (12.7 g) were heated in a sealed vessel at 200°C for 6-10 hours and the liquid product consisted of some unreacted iodine 3,4-(bistrifluoromethyl)-1,2-dithietene and PFTMT. The iodine was removed by shaking with mercury and decanting the liquid. The dithietene b.p. 93-94°C was distilled out of the mixture and the fraction collected at 134°C was 99.4% PFTMT. This fraction was reheated to about 50°C and then allowed to cool to -20°C and kept there for 24 hours. The supernatant liquid was then decanted and the large transparent crystals were heated again completely melted. The cooling was then repeated and the resulting crystals, when melted at room temperature, became a clear liquid. G.c. analysis of 0.1 μℓ of this liquid did not reveal any trace impurities and hence this sample was used to calibrate the g.c. for quantitative work.

CHAPTER III

THE UNIMOLECULAR ISOMERIZATION OF CHEMICALLY ACTIVATED
THIIRANE TO VINYL THIOL

A. Results

A detailed kinetic-mechanistic study of the $S(^1D_2)$ + ethylene reaction was performed under static conditions. The effects of exposure time, relative concentrations and total pressures on the products distribution were examined in order to determine whether vinyl thiol (VT) can be formed *via* two independent reaction paths, direct insertion of $S(^1D_2)$ atoms into the C-H bond, and structural isomerization of chemically activated thiirane (Th).

1. Reaction products and their properties

Photolysis ($\lambda \approx 240$ nm) of COS-ethylene mixtures led to the formation of CO, VT, Th, and, at longer exposure times, elemental sulfur and a solid organosulfur polymer.

In the initial stages of this work it was observed that the yields of Th and VT were not very reproducible and were quite sensitive to exposure time. For this reason it was decided to investigate the thermal stabilities and surface properties of these compounds as

well as their spectral characteristics.

i) Properties of thiirane

The UV spectrum was obtained as shown in Figure III-1
for "low" and "high" concentrations of thiirane in the
gas phase. The high pressure extinction coefficients
for the two maxima at λ = 259.2 and 243 nm are 1.2. x 10^{-3}
$torr^{-1}$ cm^{-1} and 1.80 x 10^{-3} $torr^{-1}$ cm^{-1}, respectively
and are in excellent agreement with the values reported
by Davis[110] in 1957.

For the "low" concentration Th spectrum the
extinction coefficient for the most intense maximum at
λ = 218 nm calculated to be 2.1 x 10^{-2} $torr^{-1}$ cm^{-1}.
The vapor phase infra red spectrum of Th and some
thermodynamic properties are described in reference 111.

At room temperature and in the gas phase Th is very
stable and undergoes thermal decomposition only above
150°C.[85,90,112] In contact with fresh pyrex surfaces,
however, it undergoes slow polymerization even at room
temperature. Hence, the entire vacuum system was
"treated" with gaseous Th (1 torr) for 48 hours, after
which good reproducibility was achieved.

ii) Properties of vinylthiol

Prior to the discovery that VT is a major product
of the $S(^1D_2)$ + C_2H_4 reaction[84,91] it was believed that

81.
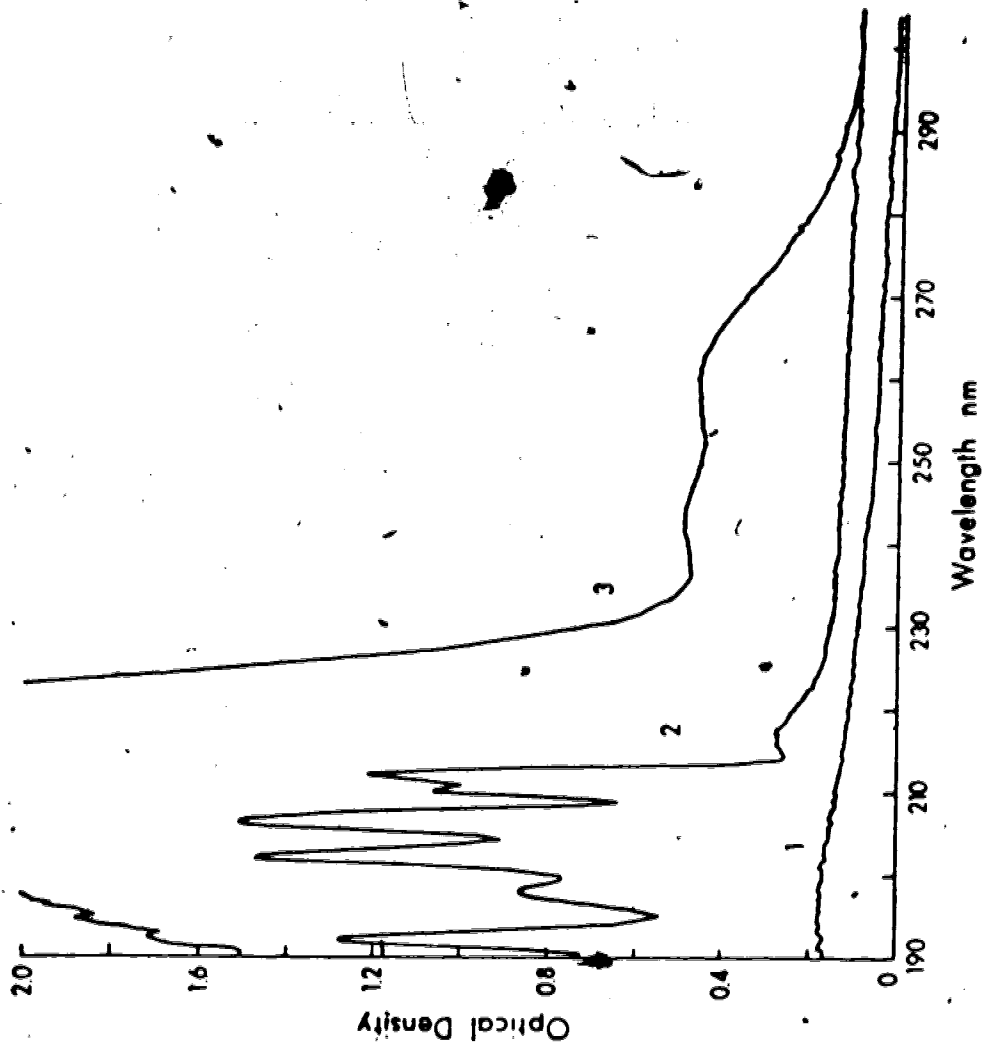
Figure III-1. UV spectra of "low" and "high" concentration thiirane (Th) gas samples. 1: base line of 32.4 ml quartz cell (10 cm path length); 2: "low" concentration Th. P = 1.02 torr; 3: "high" concentration Th. P = 32.33 torr.

VT, like vinyl alcohol, was non-existent. Subsequently, VT and a number of substituted vinyl thiols were synthesized by the photochemically induced chain addition of H_2S to the corresponding acetylene.[113,114] Although VT is a moderately reactive molecule it is sufficiently stable, under controlled conditions, to allow spectral characterizations.

In the present study it was observed that VT readily reacts with metal surfaces. Thus a 3.0 mm i.d x 10 cm long glass column packed with clean copper filings and placed between the sample loop and the chromatographic column, quantitatively removed VT from a sample containing VT, Th and CS_2. Stainless steel was less reactive and could be significantly deactivated by repeated passes of VT over the surface. In neither case could any volatile products be observed, which suggests that polymeric products are formed.

The reactivity of VT on quartz and Pyrex surfaces was also investigated. Experimentally significant amounts of VT were lost from a sample exposed to clean Pyrex surfaces for less than one hour. The rate of loss decreased if the surface was cooled to liquid nitrogen temperature. "Curing" of the surfaces greatly reduced the surface activity.

Quartz surfaces, freshly flamed in the presence of air, caused only slight losses in the VT samples. "Cured" or unflamed quartz exhibited negligible activity.

The U.V. spectrum obtained in the gas phase is shown in Figure III-2. VT begins to absorb at 300 nm and the absorption intensity gradually increases to a maximum at 218 nm, with $\epsilon = 0.253$ $torr^{-1}$ cm^{-1}, then again decreases gradually.

2. The effects of exposure time and pressure on the product yields

The extinction coefficients and optical densities for VT (0.020 torr), Th (0.018 torr) and COS (41.20 torr) are summarized in Table III-1 for $\lambda = 253.7$, 228.8 and 213.9 nm. It is seen that absorption by VT and Th can effectively compete with that by COS and thus, secondary photolysis can be expected.

Preliminary experiments indeed showed that the ratios of the two principal products, VT and Th, were exposure time-dependent and moreover, the absolute rates of formation of both VT and Th tended to decrease with increasing exposure time, the former more rapidly than the latter. Therefore, in order to obtain kinetically useful results which correctly reflect the primary product yields, a series of exposure time studies were
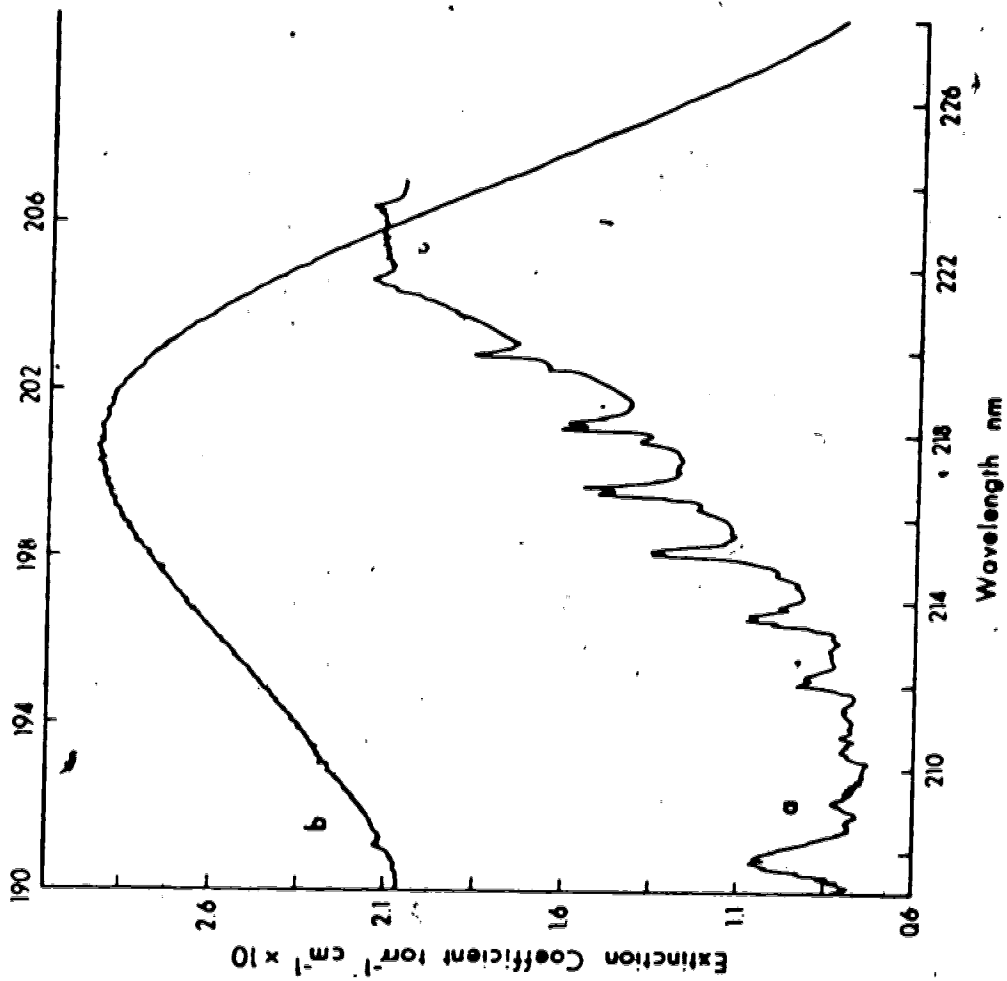
Figure III-2. UV spectrum of vinyl thiol. Upper scale refers to spectrum a, lower scale to spectrum b.

84.

TABLE III-1

Light Absorption by the Reaction Components

	λ (nm)	ε ($torr^{-1}cm^{-1}$)	Pressure (torr)	O.D.
VT	253.7	1.56×10^{-2}	0.020	3.1×10^{-4}
	228.8	8.6×10^{-2}		1.7×10^{-3}
	213.9	2.36×10^{-1}		4.7×10^{-3}
Th	253.7	1.18×10^{-3}	0.018	2.2×10^{-5}
	228.8	2.37×10^{-3}		4.3×10^{-5}
	213.9	1.95×10^{-2}		3.5×10^{-4}
COS	253.7	2.3×10^{-4}	41.20	9.0×10^{-3}
	228.8	3.42×10^{-3}		1.4×10^{-1}
	213.9	3.42×10^{-3}		1.4×10^{-1}

performed at various COS/C_2H_4 ratios and total pressures.

The results, using $\lambda = 254$ nm radiation and $COS/C_2H_4 = 0.2$ mixtures, are summarized in Tables III-2 to III-5 and those for $COS/C_2H_4 = 0.7$ mixtures, in Tables III-6 to III-14. Some representative plots of VT/Th *versus* exposure time are illustrated in Figure III-3. In all cases curvature was obtained to varying extent but each plot could be fitted by the standard least square method to a second degree polynomial. The calculated polynomials are listed in Appendix A. The zero time extrapolated values of VT/Th obtained from these calculations are listed in Table III-15.

In some experiments the CO yields were also measured in addition to those of VT and Th, and these data are listed in Tables III-8, -10, and -12. From these results it can be seen that at low conversions the scavenging of sulfur atoms by COS and C_2H_4 is complete and the combined yield of VT, Th and CO is 100% within experimental error.

From the results summarized in Table III-15, it is seen that the $(VT/Th)_0$ ratio for $COS/C_2H_4 = 0.20$ is considerably higher than for $COS/C_2H_4 = 0.70$ at comparable pressures. The $(VT/Th)_0$ ratios for both COS/C_2H_4 mixture ratios decrease as the total pressure increases.

TABLE III-2

Time dependence of the product yields at 253 torr total pressure and $COS/C_2H_4 = 0.2$.[a]

Time, min.	VT	Th	VT/Th
	arbitrary units		
5	85.3	63.7	$1.34^{b} \pm 0.12$
10	146	126	$1.16^{c} \pm 0.05$
20	264	266	0.99
30	315	376	0.84
60	375	720	0.52

[a] $\lambda = 254$ nm.

[b] Average of three determinations.

[c] Average of two determinations.

TABLE III-3

Time dependence of the product yields at 852 torr total
pressure and $COS/C_2H_4 = 0.2.$[a]

Time, min.	VT	Th	VT/Th
			arbitrary units	
1	59	44.5	1.33
2.5	142	106	1.34
5	294	237	1.24
10	501	447	1.12
15	595	573	1.04[b]±0.02
22.5	870	900	0.97
30	905	1280	0.71
45	1047	1680	0.64
60	1100	2055	0.54

[a] $\lambda = 254$ nm.

[b] Average of two determinations.

TABLE III-4

Time dependence of the product yields at 1196 torr total pressure and $COS/C_2H_4 = 0.2.$[a]

Time, min.	VT	Th	VT/Th
	arbitrary units		
5	210	176	1.19
10	387	351	1.10
20	606	669	0.91
30	765	1000	0.77
40	905	1320	0.69

[a] $\lambda = 254$ nm.

TABLE III-5

Time dependence of the product yields at 1680 torr total
pressure and $COS/C_2H_4 = 0.2.$ [a]

Time, min.	VT	Th	VT/Th
	arbitrary units		
5	347	311	1.12
10	693	729	0.95
20	1100	1320	0.83
30	1440	1940	0.74
40	1510	2550	0.59

[a] $\lambda = 254$ nm.

TABLE III-6

Time dependence of the product yields at 100 torr total pressure and $COS/C_2H_4 = 0.7$.[a]

Time, min.	VT	Th	VT/Th
	arbitrary units		
2.0	0.21	0.21	$1.04^{b} \pm 0.10$
3.0	0.30	0.29	$1.02^{b} \pm 0.02$
4.0	0.39	0.37	$1.04^{b} \pm 0.04$
6.0	0.63	0.60	1.05
7.0	0.60	0.61	0.97
8.0	0.73	0.74	0.99
10.0	0.79	0.83	0.93
11.0	0.88	0.91	0.95
12.0	0.91	1.01	0.89
16.0	0.91	1.21	0.75

[a] $\lambda = 254$ nm.

[b] Average of three determinations.

TABLE III-7

Time dependence of the product yields at 162 torr total pressure and $COS/C_2H_4 = 0.7$.[a]

Time,	VT	Th	
min.	arbitrary units		VT/Th
5	154	144	1.07
10	263	258	1.02
20	432	471	0.92
30	525	648	0.81
60	615	1025	0.60

[a] $\lambda = 254$ nm.

TABLE III-8

Product yields of the photolysis at 220 torr total pressure and COS/C_2H_4 = 0.7.[a]

Time, min.	CO	VT	Th	VT,Th	Product[b] Recovery, %
	Yield, μmoles				
3.0	2.46	0.80	0.81	0.99	97.6
5.0	4.23	1.24	1.30	0.96	97.4
7.0	5.79	1.43	1.66	0.86	91.3
9.0	7.49	1.77	2.06	0.86	90.5
12.0	9.82	2.08	2.57	0.81	86.8
15.0	12.32	2.28	2.99	0.76	84.4

[a] λ = 254 nm.

[b] Product recovery = $\left[\dfrac{CO + VT + Th}{R^0_{CO} \times Time} \right] \times 100$; R^0_{CO} = 1.39 μmoles/min.

TABLE III-9

Time dependence of the product yields at 336 torr total pressure and $COS/C_2H_4 = 0.7$.[a]

Time, min.	VT	Th	VT/Th
	arbitrary units		
1.0	36	36	1.00
2.5	122	119	1.03
5	203	206	0.99
10	372	396	0.94
20	621	732	0.85
30	795	999	0.80
60	1035	1635	0.63
120	1030	2080	0.50

[a] $\lambda = 254$ nm.

TABLE III-10

Product yields of the photolysis at 440 torr total pressure and $COS/C_2H_4 = 0.7$.[a]

Time, min.	CO	VT	Th	VT/Th	Product[b] Recovery, %
	Yield, μmoles				
4.0	4.26	1.35	1.43	0.95	94.5
6.0	6.48	1.90	2.08	0.92	93.7
8.0	8.42	2.30	2.63	0.88	89.7
15.0	15.32	3.27	4.28	0.76	82.0
19.9	21.69	3.43	5.20	0.66	81.9

[a] $\lambda = 254$ nm.

[b] Product Recovery $= \left[\dfrac{CO + VT + Th}{R_{CO}^0 \times Time} \right] \times 100$; $R_{CO}^0 = 1.86$ μmoles/min.

TABLE III-11

Time dependence of the product yields at 600 torr total pressures and $COS/C_2H_4 = 0.7$.[a]

Time, min.	VT	Th	VT/Th
	arbitrary units		
5	182	181	1.00
10	327	351	0.93
20	588	696	0.85
30	723	963	0.75
40	939	1350	0.70

[a] λ = 254 nm.

TABLE III-12

Product yields of the photolysis at 660 torr total pressure and $COS/C_2H_4 = 0.7$.[a]

Time, min.	CO	VT	Th	VT/Th	Product[b] Recovery, %
		Yield, μmoles			
2.0	2.43	0.84	0.86	0.97	99.3
3.0	3.80	1.22	1.34	0.91	101.1
4.0	5.06	1.65	1.74	0.95	101.6
5.1	6.46	2.05	2.22	0.92	101.2
8.0	9.78	2.85	3.28	0.87	95.6
9.1	11.10	2.90	3.63	0.80	93.1
10.0	12.40	3.19	3.96	0.81	94.0
12.0	14.60	3.50	4.56	0.77	90.8
15.0	17.74	3.98	5.31	0.75	86.6

[a] $\lambda = 254$ nm.

[b] Product Recovery $= \left[\dfrac{CO + VT + Th}{R_{CO}^0 \times Time} \right] \times 100$; $R_{CO}^0 = 2.08$ μmoles/min.

TABLE III-13

Time dependence of the product yields at 880 torr total pressure and $COS/C_2H_4 = 0.7$.[a]

Time, min.	VT	Th	VT/Th
	Yield, μmoles		
2.0	1.15	1.30	$0.88^b \pm 0.02$
4.0	2.33	2.53	$0.92^b \pm 0.01$
6.0	3.15	3.71	0.85
8.0	3.83	4.82	0.80
12.0	4.91	6.37	0.77
14.5	5.10	7.34	0.70
20.0	5.79	9.04	0.64

[a] $\lambda = 254$ nm.

[b] Average of two determinations.

TABLE III-14

Time dependence of the product yields at 1272 torr total
pressure and $COS/C_2H_4 = 0.7$.[a]

Time, min.	VT	Th	VT/Th
	arbitrary units		
5	.339	420	0.81
10	723	906	0.80
20	1190	1600	0.74
30	1645	2290	0.72
40	1875	2905	0.65

[a] $\lambda = 254$ nm.
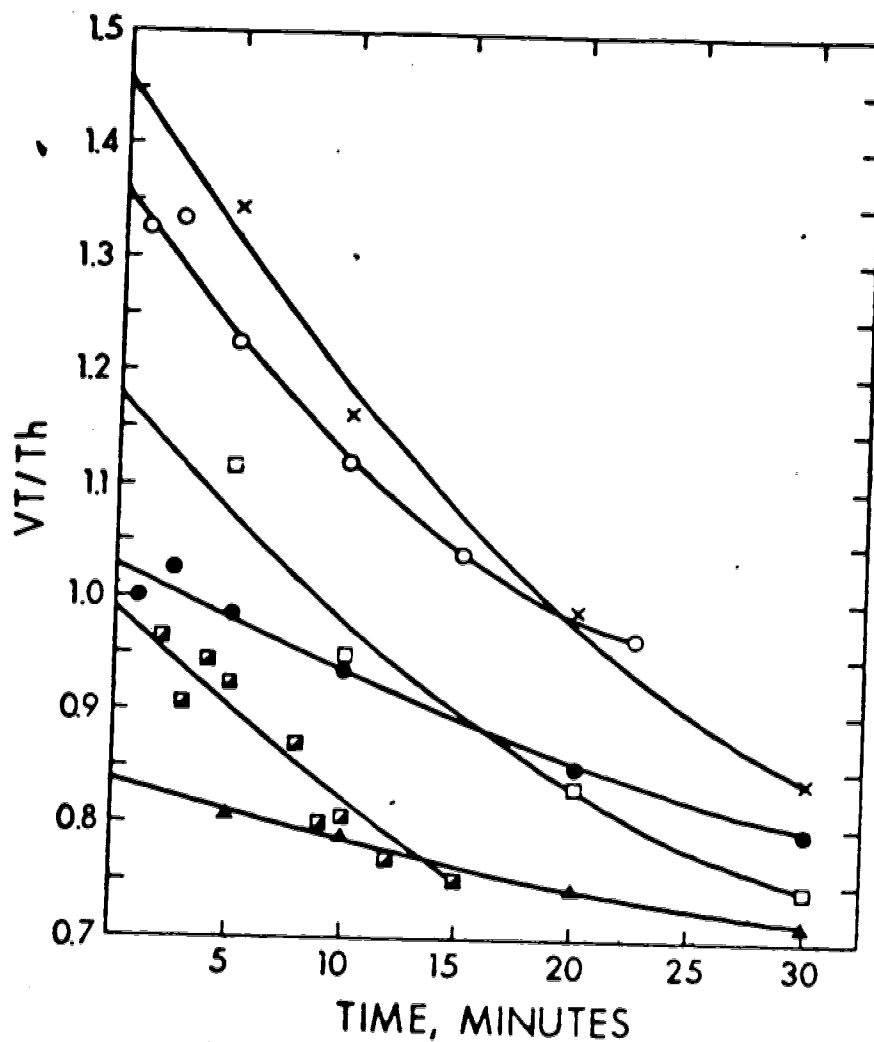
Figure III-3. The dependence of VT/Th on exposure time for COS/C_2H_4 = 0.2 at total pressures of X : 253 torr; ○: 852 torr; □: 1680 torr; and for COS/C_2H_4 = 0.7, at total pressures of ● : 336 torr; ◪ : 660 torr; ▲ : 1272 torr.

TABLE III-15

Variation in the zero exposure time extrapolated value of VT/Th as a function of total pressure and COS/C_2H_4 ratio.[a]

Pressure, torr	COS/C_2H_4	$(VT/Th)_{t=0}$
253	0.20	1.46
852	0.20	1.36
1196	0.20	1.32
1680	0.20	1.18
100	0.7	1.14
162	0.7	1.13
220	0.7	1.04
336	0.7	1.03
440	0.7	1.02
600	0.7	1.06
660	0.7	0.99
880	0.7	0.94
1272	0.7	0.84

[a] $\lambda = {\sim}254$ nm.

A few experiments were performed employing shorter wavelength radiation. The results using the cadmium resonance lamp (λ = 229 nm) are listed in Table III-16, and those using the zinc lamp (λ = 214 nm), in Tables III-17 to III-20.

The experiments at λ 214 and 229 nm were not very reproducible and the zero time extrapolation became quite troublesome. This was particularly difficult for low COS concentrations, where smaller quantities of VT were produced and thus surface effects were more pronounced. Nevertheless, the results show that the values of (VT/Th)$_{t=0}$ from either the 229 or 214 nm photolyses are higher than those in the 254 nm photolysis.

B. Discussion

The λ = 254 nm photolytic decomposition of COS proceeds *via* two pathways: spin allowed dissociation to CO and $S(^1D_2)$ atoms in 67% yield,

$$COS + h\nu \longrightarrow CO + S(^1D_2) \qquad [1a]$$
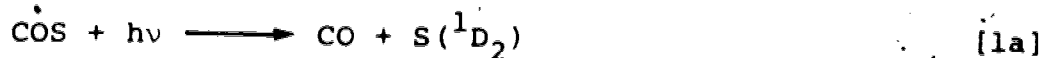
and a spin forbidden process

$$COS + h\nu \longrightarrow CO + S(^3P) \qquad [1b]$$

to give CO and $S(^3P)$ atoms in 33% yield.

TABLE III-16

Time dependence of the product yields at 843 torr total pressure and $COS/C_2H_4 = 0.2$.[a]

Time, min.	VT	Th	VT/Th
	arbitrary units		
2.5	243	158	1.55
3	565	369	1.53
10	940	650	1.45
20	1480	1140	1.30
30	1835	1565	1.17
60	2280	2635	0.87

[a] $\lambda = 229$ nm.

TABLE III-17

Time dependence of the product yields at 100 torr total pressure and COS/C_2H_4 = 0.67.[a]

Time, min.	VT	Th	VT/Th
	Yield, μmoles		
2	0.45	0.40	1.09^{b}±0.05
3	0.61	0.56	1.09
4	0.70	0.68	1.03^{c}±0.03
5	0.85	0.81	1.05
6	0.88	0.87	1.01^{c}±0.01
8	0.92	0.93	0.99
10	1.02	1.10	0.93
12	1.03	1.25	0.82^{d}±0.02
15	0.95	1.21	0.79

[a] λ = 214 nm.

[b] Average of four measurements.

[c] Average of three measurements.

[d] Average of two measurements.

TABLE III-18

Time dependence of the product yields at 200 torr total

pressure and $COS/C_2H_4 = 0.67$.[a]

Time, min.	VT	Th	VT/Th
	Yield, μmoles		
2.5	0.81	0.69	1.17
6	1.36	1.32	1.03
8	1.56	1.58	0.99
10	1.68	1.84	0.91
12	1.79	2.03	0.88

[a] $\lambda = 214$ nm.

TABLE III-19

Time dependence of the product yields at 400 torr total pressure and $COS/C_2H_4 = 0.67.$[a]

Time, min.	VT	Th	VT/Th
	Yield, μmoles		
1.5	0.82	0.69	1.18
2	1.06	0.87	1.21
2.5	1.20	1.02	1.18
3.5	1.51	1.31	1.15
5	1.89	1.72	1.10
7	2.36	2.22	1.06
8.5	2.44	2.29	1.06
10	2.54	2.50	1.01

[a] λ = 214 nm.

TABLE III-20

Time dependence of the product yields at 800 torr total pressure and $COS/C_2H_4 = 0.67$.[a]

Time min.	VT	Th	VT/Th
	Yield, μmoles		
4	1.90	1.71	1.11
5	2.14	1.87	1.15
6	2.36	2.18	1.08
8	3.15	2.96	1.07
11.1	3.59	3.39	1.06
14	3.74	3.70	1.01

[a] $\lambda = 214$ nm.

$S(^1D_2)$ atoms may abstract a sulfur atom from COS,

$$COS + S(^1D_2) \longrightarrow CO + S_2 \qquad [2a]$$

or be quenched to the triplet state:

$$COS + S(^1D_2) \longrightarrow COS* + S(^3P) \qquad [2b]$$
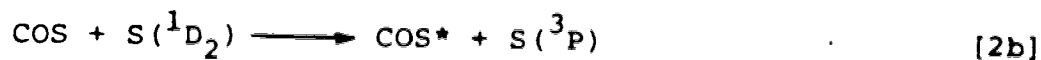
In competition with reactions [2a] and [2b], the singlet sulfur atom may insert directly into the vinylic C-H bonds of C_2H_4 to yield VT,

$$C_2H_4 + S(^1D_2) \longrightarrow CH_2CHSH \qquad [3a]$$

or add to the double bond to yield a vibrationally excited singlet ground state thiirane molecule, having an excess vibrational energy content of 91.2 kcal mol^{-1}:

$$C_2H_4 + S(^1D_2) \longrightarrow (\text{△S})^{*} \qquad [3b]$$
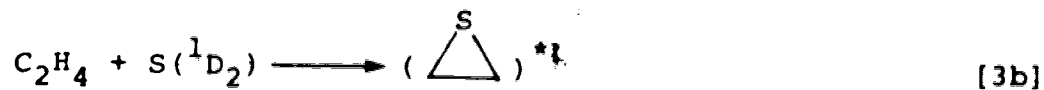
This energy corresponds to the enthalpy change of the reaction (85.2 kcal mol^{-1}) plus the excess translational energy of the $S(^1D_2)$ atom (6 kcal mol^{-1}) produced in the mercury lamp photolysis. The hot thiirane molecule then may undergo unimolecular rearrangement to VT,

$$(\text{△S})^{*} \longrightarrow CH_2CHSH \qquad [4]$$

or suffer collisional deactivation to the thermalized

ground state,

$$\left(\triangle^{S} \right)^{*} + M \longrightarrow \triangle^{S} + M^{*} \qquad [5]$$
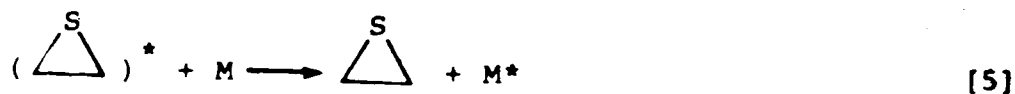
where M stands for the quenching gases COS and C_2H_4.

The only other reaction of consequence in this system is the stereospecific[115] cycloaddition reaction involving $S(^3P)$ atoms to form triplet state thiirane,

$$C_2H_4 + S(^3P) \longrightarrow \triangle^{S} (T_1) \qquad [6]$$
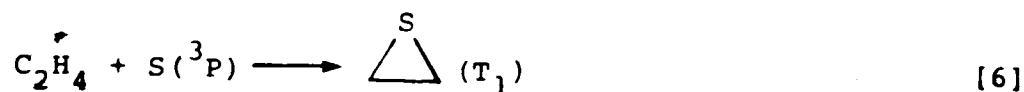
which is slowly deactivated to the ground singlet state.[112]

If the chemically activated thiirane molecule truly undergoes isomerization in this system, as postulated from earlier experimental[84,91,112] and theoretical studies[104,105,116] then the product yield ratio VT/Th should be dependent on total pressure for a given ratio of reactant concentrations. The values of $(VT/Th)_{t=0}$ (Tables III-15, -21 and Figure III-3) for the two COS/C_2H_4 ratios examined, 0.2 and 0.7, are plotted as a function of total pressure in Figure III-4 where it is seen that $(VT/Th)_{t=0}$ is indeed pressure dependent and gradually decreases with increasing pressure. The COS/C_2H_4 ratio also affects the magnitude of $(VT/Th)_{t=0}$: the higher the ratio, the higher the value of $(VT/Th)_{t=0}$
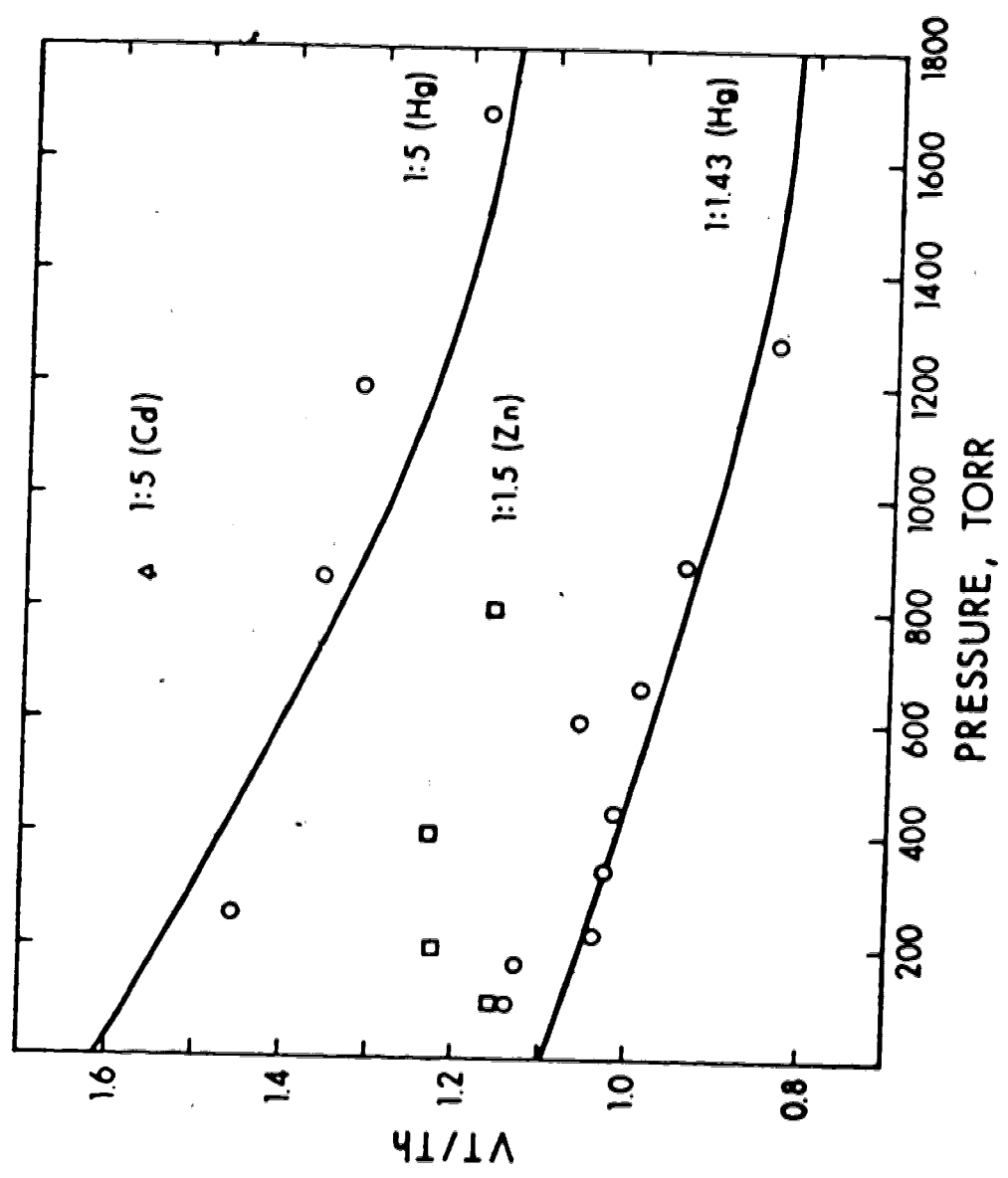
Figure III-4. The dependence of $(VT/Th)_{t=0}$ on total pressure using Zn, Cd and Hg resonance lamps. The COS/C_2H_4 ratios are indicated.

at a given total pressure. It will now be shown that
the pressure dependence of (VT/Th) can be used to
calculate the rate constant for the Th → VT rearrangement.

Steady-state treatment of steps [1] - [6] (derived
in Appendix A) gives the following expression for VT/Th:

$$\frac{R_{VT}}{R_{Th}} = \frac{k_3 k_4 + k_{3a} k_5 [M]}{\frac{1}{2} k_3 k_4 + \alpha k_4 \frac{[COS]}{[C_2 H_4]} + (\alpha \frac{[COS]}{[C_2 H_4]} + \beta) k_5 [M]} \qquad [I]$$

where $k_3 = k_{3a} + k_{3b}$, $\alpha = \frac{1}{2} k_{2a} + \frac{3}{2} k_{2b}$, $\beta = \frac{1}{2} k_{3a} + \frac{3}{2} k_{3b}$,
and $[M] = [COS] + [C_2 H_4]$.

At [M] = 0 equation [I] reduces to

$$\left[\frac{R_{VT}}{R_{Th}}\right]_{p=0} = \frac{k_3}{\frac{1}{2} k_3 + \alpha \frac{[COS]}{[C_2 H_4]}} \qquad [II]$$

and, for [M] = ∞, to

$$\left[\frac{R_{VT}}{R_{Th}}\right]_{p=\infty} = \frac{k_{3a}}{\alpha \frac{[COS]}{[C_2 H_4]} + \beta} \qquad [III]$$

In addition to equations I-III, the following
relationship should also hold:

$$\frac{VT(\text{from rearrangement}) + VT(\text{from insertion})}{Th} = \left[\frac{VT}{Th}\right]_{p=0} \qquad [IV]$$

Since at zero pressure all the hot Th molecules undergo isomerization to VT.

Similarly, at infinite pressure,

$$\frac{VT\ (from\ insertion)}{VT\ (from\ rearrangement)\ +\ Th} = \left[\frac{VT}{Th}\right]_{p\ =\ \infty} \qquad [V]$$

since under this condition all the hot Th* molecules are stabilized to Th.

The experimental values of equations [IV] and [V] for $[COS]/[C_2H_4] = 0.20$ are 1.62 and 0.48, and for $[COS]/[C_2H_4] = 0.70$, 1.10 and 0.38, respectively. The last value is in agreement with $VT/Th = 0.44$ obtained in a liquid phase mixture of ethylene and carbonyl sulfide at room temperature.[46]

The rate constant k_{2a} has been estimated by Donovan *et al.*[117] as having a minimum value of 4.0×10^{10} ℓ mol^{-1} s^{-1}. Accepting this value and recalling that the primary step [1b] produces $S(^3P)$ atoms in 33% yield, it is possible to evaluate the rate constant values k_{2b}, k_{3a}, k_4 from the present data.

With the aid of the equations below and the data from Table III-12 it is possible to calculate the fraction of $S(^1D_2)$ atoms consumed in reactions [2a] and [2b], and that consumed in reactions [3a] and [3b]:

Thus,

$$100 \times \frac{R_{CO} - R^0_{CO/2}}{R^0_{CO/2}} =$$

$$\frac{\text{Rate of sulfur atom abstraction by } S(^1D_2) \times 100}{\text{Rate of total sulfur atoms formed}} =$$

$$\frac{(1.22 - 1.04) \times 100}{1.04} = 17\%, \text{ step 2a} \qquad [VI]$$

From Figure III-5 the zero pressure extrapolated value of VT/Th for $COS/C_2H_4 = 0.7$ is 1.10, i.e.,

$$\frac{VT}{Th}_{p=0} = \frac{\text{step [3a] + step [3b]}}{\text{step [6]}} = \frac{1.1}{1.0}$$

Taking $[VT]_{p=0} + [Th]_{p=0} = 2.10$, the fraction of $S(^1D_2)$ atoms reacting, excluding abstraction, will be given by

$$\frac{[VT]_{p=0}}{[VT]_{p=0} + [Th]_{p=0}} = \frac{1.10}{2.10} \qquad [VII]$$

To obtain the percentage of $S(^1D_2)$ atoms used up in step [3], equation [VII] is multiplied by the factor

$$\frac{([VT]_{p=0} + [Th]_{p=0}) \times 100}{R^0_{CO/2}}$$

Thus, from the data in Table III-12,

$$\text{Step [3]} = \frac{[VT]_{p=0} \times 100}{R^0_{CO/2}} = \qquad [VIII]$$

$$\frac{1.10}{2.10} \frac{(0.84 + 0.86) \times 1/2 \times 100}{2.08/2} = 43\%$$

Now since

$$\text{step [2b]} = \text{step [1a]} - (\text{step [2a]} + \text{step [3]}) \qquad [IX]$$

$$= 67 - (17 + 43) = 7\%$$

the relative rate constants are

$$k_{2a}/k_{2b} = 17/7 = 2.4 \text{ and}$$

$$k_{2a}/k_3 = (17/43) \cdot ([C_2H_4]/[COS]) = 0.4 \times 1.43$$

$$= 0.57$$

assuming a gas collision frequency for the deactivation of hot thiirane, step [5], and the following collisional diameters, $\sigma(COS) = 4.13$ Å, $\sigma(C_2H_4) = 4.23$ Å, and $\sigma(C_2H_4S) = 5.2$ Å, $k_5 = 2.3 \times 10^{14}$ cm^3 mol^{-1} s^{-1}.

The above relative rate constant ratios and the calculated value of k_5 were used for iteration and curve fitting from equations [I]-[V], from which the following absolute rate constants were derived by I. Safarik:[118]

$$k_{2b} = 1.8 \times 10^{13} \ cm^3 \ mol^{-1} \ s^{-1}$$

$$k_{3a} = 4.2 \times 10^{13} \ cm^3 \ mol^{-1} \ s^{-1}$$

$$k_{3b} = 3.8 \times 10^{13} \ cm^3 \ mol^{-1} \ s^{-1}$$

$$k_4 = 5.0 \times 10^{10} \ s^{-1}$$

The solid curves shown in Figure III-4 were calculated by equation [I] and are in good agreement with experimental results. It should be noted that if step [1b] is excluded from the mechanism, steady state treatment yield at the intercept when [M] = 0,

$$\left[\frac{R_{VT}}{R_{Th}}\right]_{p=0} = \frac{k_{3a}+k_{3b}}{k_{2b}}\frac{[COS]}{[C_2H_4]}$$ [X]

and for different COS/C_2H_4 ratios predicts at zero pressure that

$$\frac{(VT/Th)_{p=0}\ (1)}{(VT/Th)_{p=0}\ (2)} = \frac{[COS]/[C_2H_4]\ (2)}{[COS]/[C_2H_4]\ (1)}$$

where (1) and (2) refer to the two different COS/C_2H_4 ratios. Inspection of Figure III-4 shows that this, far from being the case and therefore the above kinetic arguments provide the most compelling evidence to date for the occurrence of step [1b].

In order to check the validity of the kinetically derived value of k_4, the rate of unimolecular isomerization of chemically activated thiirane was calculated from RRKM theory by I. Safarik in the following manner.[118] The expression employed was

$$k_4 = k(E^*) = \frac{\lambda}{h}\frac{\Sigma P(E^\dagger)}{N(E^*)}$$ [XI]

where $\Sigma P(E^\dagger)$ and $N(E^*)$ represent the sum of states and the density of states, respectively, λ is the degeneracy of the reaction path and h is the Planck's constant. The sum of states and the density of states have been computed by direct count, with the aid of an algorithm developed by Rabinovitch.[119]

The energy $<E^*>$ of the chemically activated thiirane molecule can be obtained from the equation

$$<E^*> = \Delta H_f^o(C_2H_4) + \Delta H_f^o(S(^1D_2)) - \Delta H_f^o(C_2H_4S) + \Delta E_{tr} \qquad [XII]$$

where ΔE_{tr} is the translational energy of $S(^1D_2)$ atoms. On substitution of the values[120,121] $\Delta H_f^o(C_2H_4) = 12.5$ kcal mol^{-1}, $\Delta H_f^o(S(^1D_2)) = 92.0$ kcal mol^{-1}, $\Delta H_f^o(C_2H_4S) = 19.3$ kcal mol^{-1} and $\Delta E_{tr} = 6.0$ kcal mol^{-1}, $<E^*> = 91.2$ kcal mol^{-1}.

For the RRKM calculation it is necessary to adopt a set of vibrational frequencies for the activated complex in order to calculate the sum of states. It was assumed that the intramolecular hydrogen shift proceeds through a bicyclic structure which is depicted in Figure III-5. The vibrational frequencies[122] assigned to the stable thiirane and the activated complex are listed in Table III-21.

The experimental A factor is not available and the set of vibrational frequencies assigned to the activated complex corresponds to an estimated A factor of 1×10^{14} s^{-1}, or an activation entropy of $\Delta S^{\dagger} = 3.5$ e.u. The low value of the adapted A factor reflects the rigid structure of the activated complex.

From preliminary investigations on the thermal rearrangement of thiirane to vinyl thiol it has been
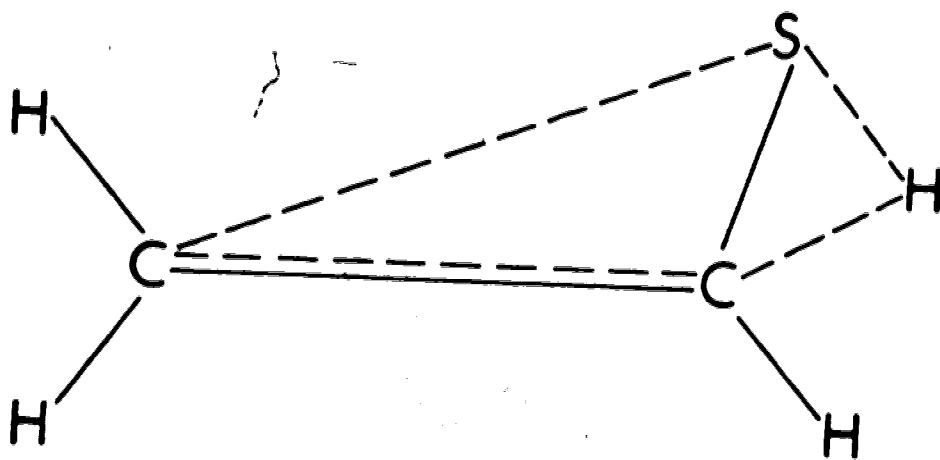
Figure III-5. Assumed structure of the activated complex.

TABLE III-21

Vibrational frequencies of the thiirane molecule and the activated complex.[122]

ν_1	3018.5 cm^{-1}	ν_8	890.2 cm^{-1}
ν_2	1466.0 cm^{-1}	ν_9	3010.4 cm^{-1}
ν_3	1107.1 cm^{-1}	ν_{10}	1431.9 cm^{-1}
ν_4	1023.5 cm^{-1}	ν_{11}	1060.2 cm^{-1}
ν_5	633.3 cm^{-1}	ν_{12}	645.9 cm^{-1}
ν_6	3109.2 cm^{-1}	ν_{13}	3100.6 cm^{-1}
ν_7	1160.3 cm^{-1}	ν_{14}	947.1 cm^{-1}
		ν_{15}	820.5 cm^{-1}

3000 cm^{-1}	(3)	700 cm^{-1}	(1)
1500 cm^{-1}	(1)	600 cm^{-1}	(2)
1000 cm^{-1}	(3)	500 cm^{-1}	(1)
900 cm^{-1}	(2)	150 cm^{-1}	(1)

estimated[112] that the activation energy for this step lies in the range 55-65 kcal mol^{-1}.

According to *ab initio* MO calculations[104,105,116] on the ring distortion potential of thiirane, the 62 kcal mol^{-1} value for E_a can bring about an increase in the C-C-S bond angle from 65°, the equilibrium value, to about 120° in the activated complex. This geometry would greatly enhance the unimolecular hydrogen shift.

The computed RRKM rate constant has a value of 7.6 x 10^{10} s^{-1}, in reasonably good agreement with the kinetically derived value of 5.0 x 10^{10} s^{-1}.

The lifetime of the hot thiirane molecule is rather short, of the order of ~1.3 x 10^{-11} s, however, deactivation with COS or C_2H_4 is very efficient and could occur with collision frequency.

Detailed studies of S($^1D_2$) atom reactions with higher alkene homologs[46] have shown that no isomerization takes place, with the possible exception of the propylene reaction. In the higher substituted alkene reactions, the absence of alkene-2-thiols is explained by steric effects which would hinder insertion into the C-H bond, and the non-occurrence of the Th-VT rearrangement process. The reason for the absence of isomerization in the higher alkenes is due to the increased number of internal degrees of freedom in the

substrate: thus, the vibrationally excited substituted thiiranes have considerably longer lifetimes than the parent hot thiirane molecule, and collisional deactivation is 100% efficient. Unfortunately, experiments in the fall-off region, where variations in product distribution as a function of total pressures would allow detection of the isomerization process, would be extremely difficult owing to secondary photolysis and other losses.

It is probable that the analogous unimolecular rearrangement reaction also occurs in the case of $O(^1D_2)$ atom reactions with ethylene and even higher alkenes, but could not be detected because of the instability of the resulting vinyl alcohols. Selenium thiols could also be formed *via* isomerization, however, their thermal instability also precludes kinetic studies.

Experiments performed at shorter wavelengths did not yield reliable quantitative results. However, the values of (VT/Th) obtained in either the 229 or 214 nm photolyses are definitely higher than those in the 254 nm photolysis (Figure III-4). The apparent fall-off at low pressure in the 214 nm photolysis is due partly to analytical product loss and partly to fluctuations in the zinc lamp intensity.

The increase in the relative yield of VT at shorter wavelengths can be due to either/or any combination of three factors:

a) The relative yields of primary steps [1a] and [1b] are wavelength dependent. In earlier studies on the reactions of $S(^1D_2)$ atoms with alkanes it has been shown[85,90] that at λ 229 nm step [1a] comprises 74% of step [1], *viz.* 67% at λ 254 nm.

b) The excess translational energy content of the $S(^1D_2)$ atom increases with increasing photonic energy, with approximate values of 6, 12, and 16 kcal mol^{-1} at λ 254, 229, and 214 nm, respectively. Therefore, the energy content of the hot Th should increase proportionally, thus shortening the lifetime of the hot *cyclo-adduct.*

c) The reactive rates of insertion and addition, steps [3a] and [3b] may depend on the excess translational energy carried by the $S(^1D_2)$ atoms. However, the activation energies for these two steps must be very small and any effect on rate would probably be negligible.

From the calculated RRKM unimolecular isomerization rate constants as a function of total energy (at 229 nm

$k_{4a} = 1.9 \times 10^{11} \text{ s}^{-1}$; at 214 nm, $k_{4b} = 3.4 \times 10^{11} \text{ s}^{-1}$), and assuming that the relative rate constants for other reactions remain unaltered, a few percent decrease in the initial amount of $S(^3P)$ formation can be estimated from the experimental data.

Finally it should be noted that two rotomeric structures of VT have recently been studied by Raman spectroscopy.[123,124]
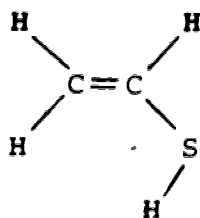
planar *syn*
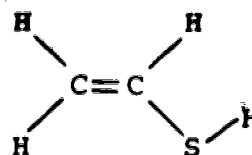
planar *anti*

However, the energy difference between the rotomers is very small, the *syn*-VT lying only ~8 cal below the *anti*-VT.

CHAPTER IV

SULFUR ATOM REACTIONS WITH ALLENE

1. Reaction products

The direct photolysis at $\lambda = 240$ nm of a mixture of 100 torr COS and 300 torr allene led to the formation of ten products, the elution times of which are summarized in Table IV-1. Empirical formulae were assigned on the basis of MS, and structural assignments were deduced from MS, NMR, UV and IR data, depending on the compound.

Allene begins to absorb at $\lambda \approx 260$ nm and at 250 nm, $\varepsilon \approx 1.3 \times 10^{-5}$ torr^{-1} cm^{-1}. Hence, it appeared likely that the hydrocarbon products detected arise from the direct photolysis of allene. As expected, a 15 minute photolysis of 400 torr allene led to the formation of all these products, the distributions of which were very similar to those obtained from a 10 minute photolysis of 25 torr COS + 225 torr C_3H_4. Subsequently, experiments at various COS/C_3H_4 ratios were carried out and it was found that for COS/$C_3H_4 \geqslant 10$ the only retrievable products were the sulfur-containing products IV, VII and VIII.

Products IV and VII were identified as CS_2 and methylthiirane (MTh), by comparison of their gc elution

123

TABLE IV-1

Photolysis products of the allene-carbonyl sulfide system.[a]

Peak number	Elution time (minutes)	Molecular weight	Empirical formula	Compound	Identified by
I	3.6	54	C_4H_6		MS
II	5.3	78	C_6H_6[b]		MS
III	8.3	82	C_6H_{10}		MS
IV	8.8	76	CS_2	carbon disulfide	MS, elution time
V	19.3	80	C_6H_8		MS
VI	21.6	78	C_6H_6[b]		MS
VII	36.0	74	C_3H_6S	methylthiirane	MS, NMR, elution time
VIII	39.8	72	C_3H_4S	methylenethiirane	MS, NMR, IR, UV
IX	47.9	78	C_6H_6[b]		MS
X	55.0	78	C_6H_6[b]		MS

[a] $\lambda > 240$ nm; $P_{COS} = 100$ torr; $P_{C_3H_4} = 300$ torr. [b] The elution time of benzene is 40 min.

times and mass spectra with those of authentic samples. MTh appeared 'to be a primary product and since propylene was a detectable impurity in the allene substrate and could not be readily removed by conventional means, it would appear that this product arises from the reaction

$$S(^1D_2, \; ^3P) + C_3H_6 \longrightarrow CH_3\text{-}\overset{\displaystyle S}{\overset{\displaystyle \diagup\diagdown}{CH}\text{-}CH_2} \qquad\qquad [1]$$
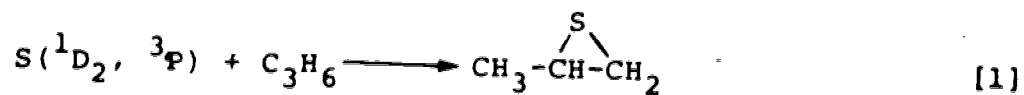
On the basis of the well established chemical reactivity of sulfur atoms product VIII could be

$$CH_2=C\overset{\displaystyle S}{\overset{\displaystyle \diagup\diagdown}{\rule{1.2cm}{0.4pt}}}CH_2 \qquad\qquad or \qquad\qquad CH_2=C=CHSH$$

i.e., resulting from addition or insertion, respectively.

The major fragments observed in the mass spectrum of product VIII, together with their relative intensities and tentative assignments are:

m/e	relative intensities	fragment
72	60.9	$C_3H_4S^{+\cdot}$
71	100.0	$C_3H_3S^{+\cdot}$
46	16.2	$H_2CS^{+\cdot}$
45	37.8	$HCS^{\cdot +}$
39	34.4	$H_2C=C=CH^{+\cdot}$

The gas phase IR spectrum of product VIII is shown in Figure IV-1. The most prominent peak occurs at
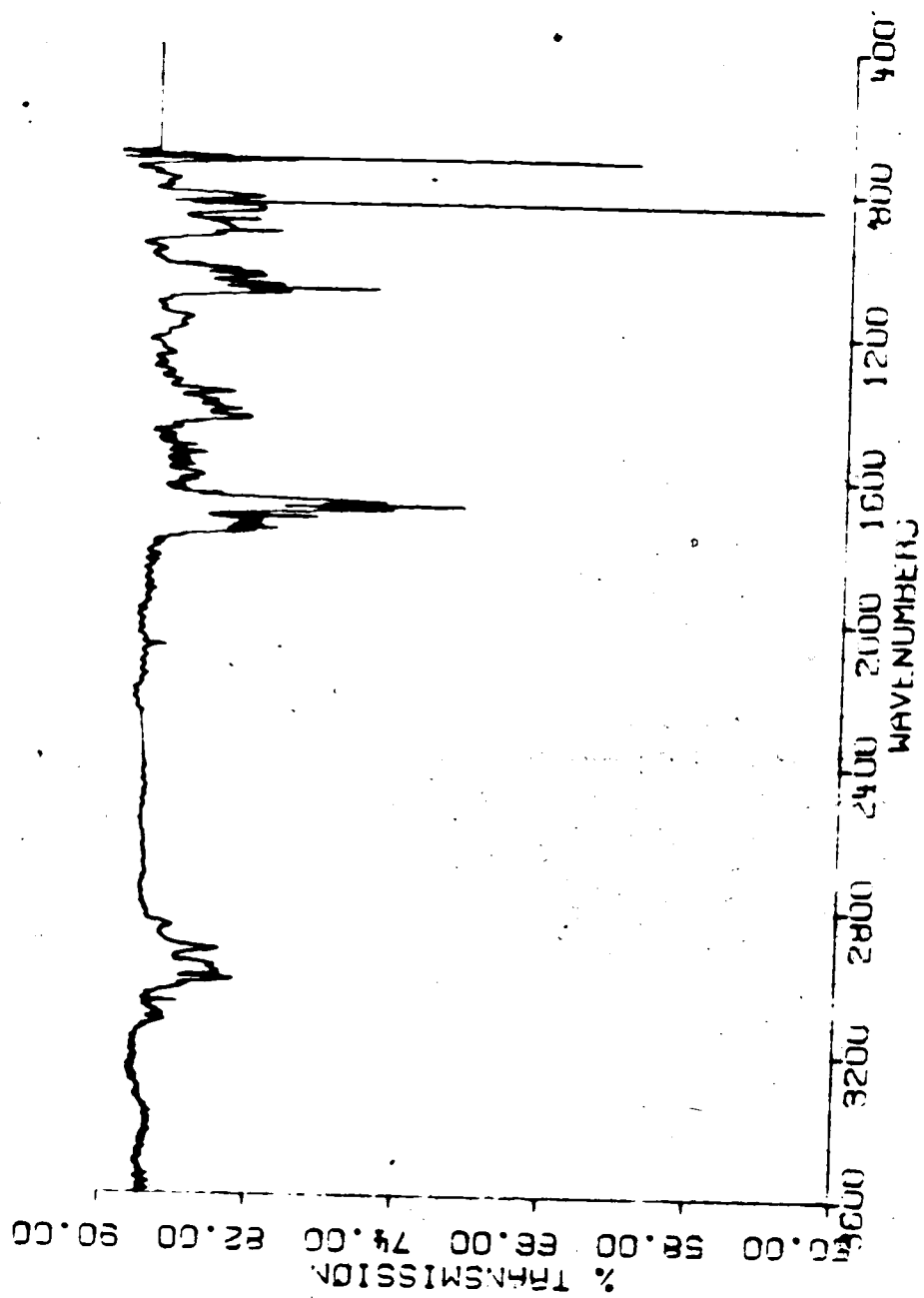
FIGURE IV-1. The gas phase FTIR spectrum of methylenethiirane

850 cm^{-1}. It is well recognized that the hydrogen out of plane deformation frequency of disubstituted ethylenes of the type $R_1R_2C=CH_2$ is around 890-880 cm^{-1} and the presence of an adjacent oxygen or chlorine atom causes a shift to lower frequencies. In allene and asymmetrically di-substituted allenes this band is observed at *ca.* 850 cm^{-1}.[125] Significantly, the medium intensity band in the 1915-1980 cm^{-1} region characteristic of the asymmetric double bond stretching frequency in cummulenes is absent in the spectrum: therefore, the carrier of the spectrum cannot be allene-thiol. The overtone of the 850 cm^{-1} band should occur around 1700 cm^{-1}, which is in the $C=C_{st}$ region. Because of this it is difficult to assign the expected $C=C_{st}$ frequency for MeTh.

The ^1H NMR spectrum of product VIII in $CDCl_3$ at -30°C is shown in Figure IV-2. The observed 2.7 ppm position of the methylenic protons is not consistent with the expected chemical shift of the $=CH_2$ (4.5-5.5 ppm) moiety in allene thiol but on the other hand, is in agreement with the $-CH_2-$ shift (2.3 ppm) in thiirane.[91] Moreover, this ABX_2 type of spectrum is only consistent with that expected from MeTh.

It should be noted that several other isomeric structures can be formulated for the C_2H_4S adduct but none of these can be reconciled with above spectral data
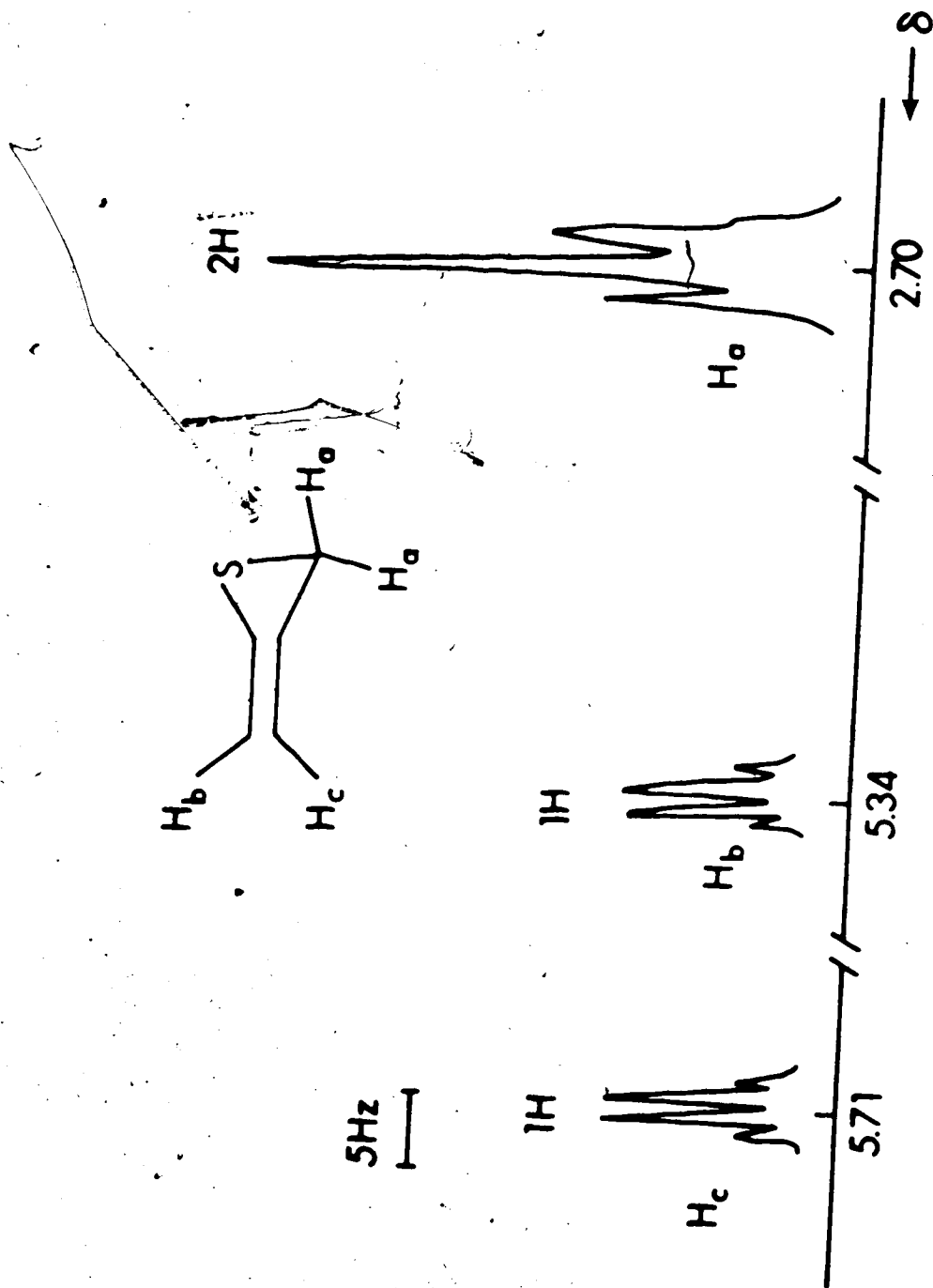
FIGURE IV-2. ^{1}H NMR spectrum of methylenethiirane.

which concordantly point to the methylene thiirane
structure. The correctness of this assignment is
further substantiated by the fact that $S(^3P)$ atoms,
which can only undergo *cyclo* addition to above bonds,
react with allene to yield the same major product (*vide
infra*).

2. Properties of methylenethiirane

The U.V. spectrum of MeTh is shown in Figure IV-3
and features three absorption maxima. The first is
fairly broad and is centered at λ_1 = 275 nm with
ε_1 = 6.2 x 10^{-3} $torr^{-1}$ cm^{-1}. The second, extending
from 250 nm to 210 nm with a maximum at λ_2 = 231 nm,
is very intense and ε_2 = 0.21 $torr^{-1}$ cm^{-1}. The third
absorption at λ_3 ≃ 202 nm is relatively weak but is
nevertheless well defined. The second and third
electronic transitions exhibit some vibrational struc-
ture, and in this respect the spectrum is similar to
that of thiirane (*vide supra*, Figure III-1) although
the spectrum of MeTh, as expected, is shifted to longer
wavelengths.

In the present investigation it was noted that
MeTh is very sensitive to surfaces, especially to pyrex
glass and metals. However, no gas phase decomposition
products were detected, suggesting that surface polymer-
ization is predominant. Decomposition takes place on

130.
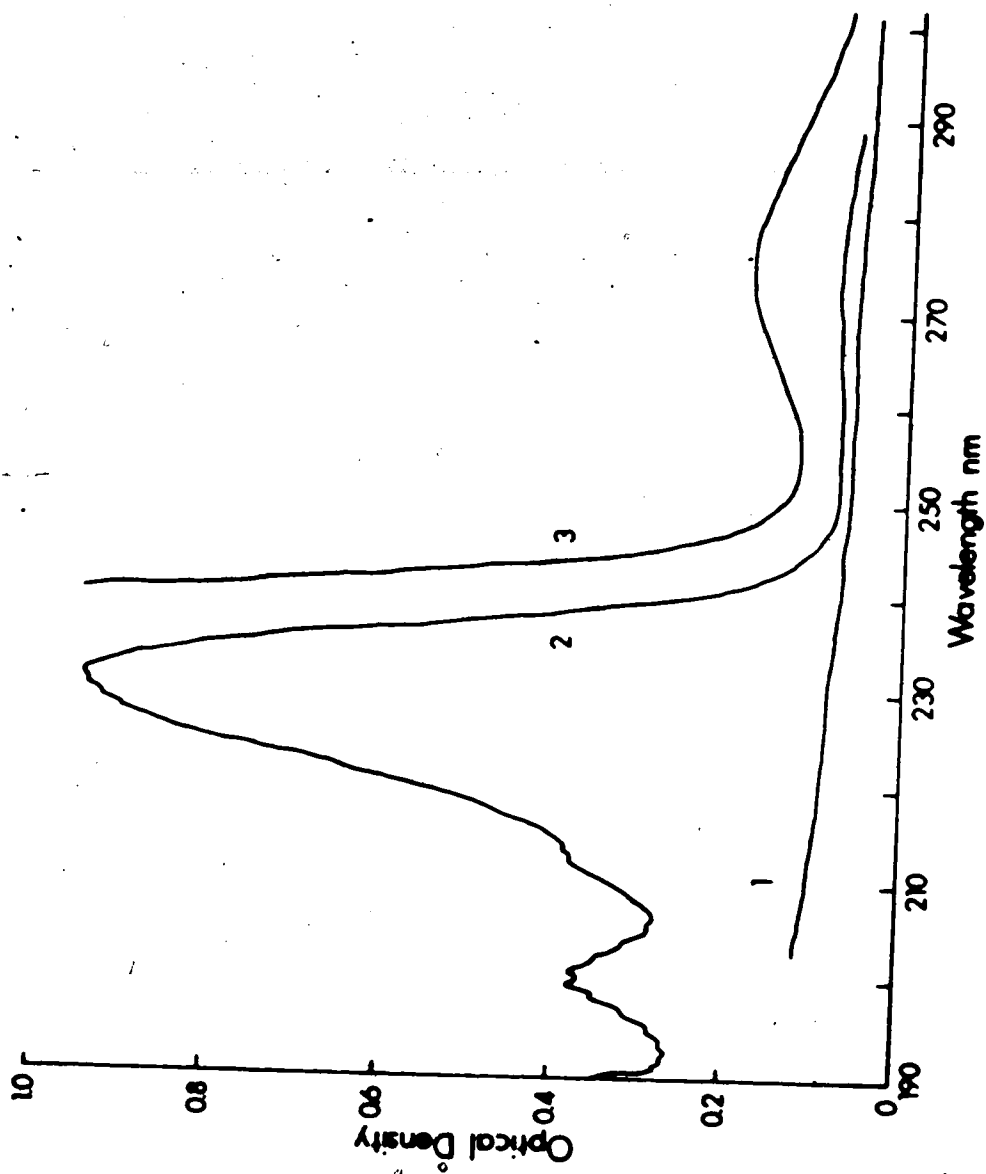
FIGURE IV-3. U.V. spectra of "low" and "high" concentration methylenethiirane (MeTh) gas samples. 1: base line of the 32.4 ml quartz cell (10 cm. path length); 2: "low" concentration MeTh, P = 0.88 torr; 3: "high" concentration MeTh, P = 1.80 torr.

prolonged storage (in excess of 20 hours) even at -196°C.

In order to determine the half-life of MeTh, the rate of disappearance of the large band at 231 nm was monitored at room temperature for a few μmoles of sample. The decay results are given in Table IV-2. The rate of decay of MeTh appears to be a second order process with respect to MeTh, as indicated by the plot in Figure IV-4, with a half-life of ~12 hours. One possible decomposition product, CS_2, which features a strong absorption at λ = 197.5 nm, was not detected.

3. Effects of exposure time and added CO_2 pressure on the product yields.

As noted above, direct photolysis of allene can be minimized for $COS/C_3H_4 \geqslant 10$. Such a mixture at 600 and 1200 torr total pressure was photolyzed for various periods of time and the results are summarized in Tables IV-3 and IV-4. At low conversions the yields of the minor products, CS_2 and MTh (methylthiirane), were small and difficult to measure quantitatively, hence are not amenable to kinetic analysis. Their combined yield amounted to 9-17% of the total condensables. The time dependence of the rate of formation of MeTh is illustrated in Figure IV-5. The extrapolated rates at zero exposure time at the two pressures examined are

TABLE IV-2

Decay of methylenethiirane[a]

Time (minute)	O.D.[b]	c[c]	c^{-1}[d]
0	1.84	4.78	2.09
5	1.76	4.58	2.19
30	1.61	4.18	2.39
50	1.54	4.00	2.50
81	1.50	3.89	2.57
105	1.44	3.74	2.68
125	1.42	3.68	2.71
175	1.37	3.55	2.81
250	1.28	3.32	3.01
1170	0.70	1.83	5.48
1597	0.56	1.45	6.88

[a] $T = 25°C$; cell path length = 10.0 cm; P = 0.88 torr; $[MeTh]_{t=0}$ = 1.55 μmol.

[b] Optical density.

[c] Molar concentration of MeTh $\times 10^{-5}$.

[d] $\times 10^4$ ℓ mol^{-1}.
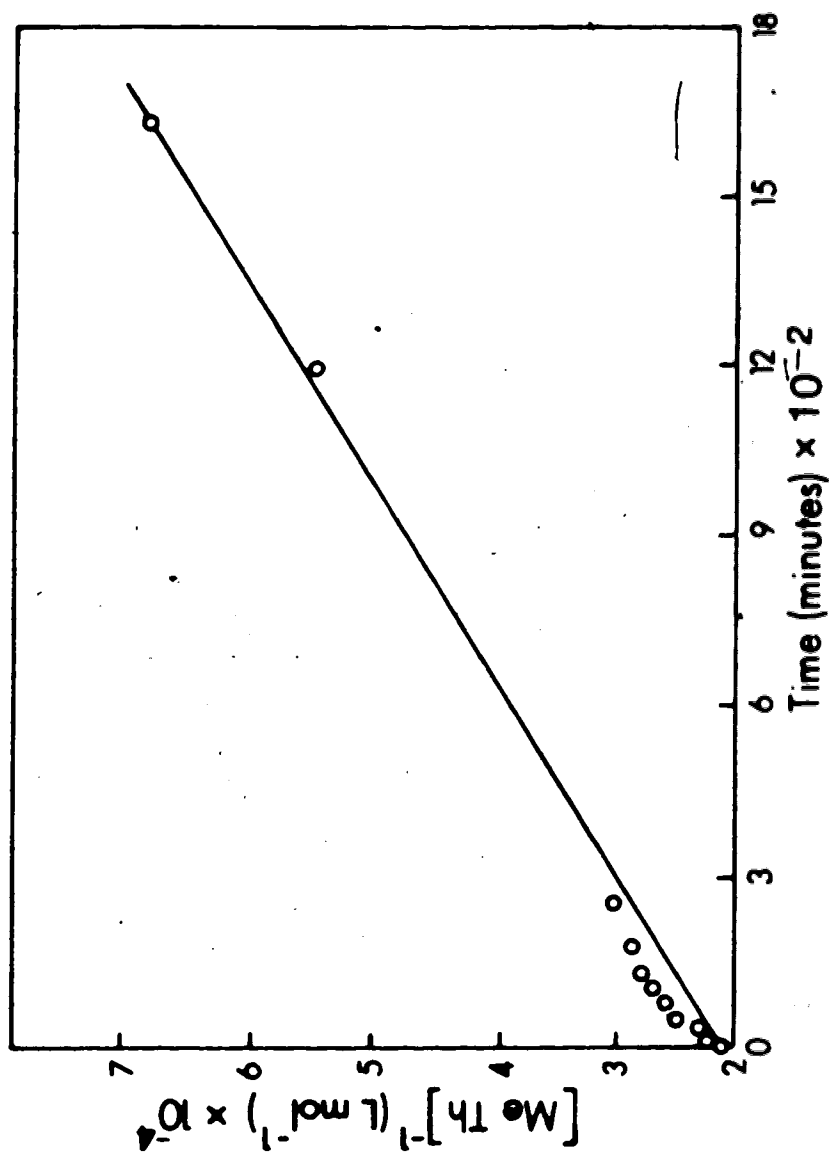
FIGURE IV-4. Rate of decay of MeTII at 25°C.

TABLE IV-3

Effects of exposure time on the product yields from the $S + C_3H_4$ reaction[a] for $P(COS)$ = 545 torr and $P_{(C_3H_4)}$ = 55 torr.

Time (min)	Yields in μmoles					% Product recovery[c]
	CO	MeTh	CS_2	MTh[b]	Σ products	
1	2.19	0.59	0.06	0.02	2.86	91.1
1[d]	2.17[d]	0.57[d]	0.03[d]	0.02[d]	2.78[d]	88.9[d]
3	6.23	1.55	0.02	0.07	7.87	83.5
5	10.44	1.86	0.12	0.07	12.49	79.6
7	14.37	2.01	0.26	0.12	16.71	76.0

[a] λ > 240 nm; R^0_{CO} = 3.14 μmol min^{-1}. [b] The yields of MTh must be taken into account in order to calculate the % product recovery. [c] % Product recovery = $\frac{\Sigma \text{ products}}{CO^0} \times 100$

[d] In the presence of 600 torr CO_2.

TABLE IV-4

Effects of exposure time on the product yields from the $S + C_3H_4$ reaction[a] for $P(COS) = 1090$ torr and $P(C_3H_4) = 109$ torr.

Time (minute)	Yields in μmoles					% Product recovery[c]
	CO	MeTh	CS_2	MTh[b]	Σ products	
1	2.73	1.19	0.10	0.04	4.06	97.8
3	7.99	2.81	0.49	0.11	11.40	91.6
5	13.20	3.37	0.30	0.10	16.97	81.7
7	18.32	3.94	0.43	0.11	22.80	80.6

[a] $\lambda > 240$ nm; $R^0_{CO} = 4.15$ μmol min⁻¹ for the first 4 minutes, then $R^0_{CO} = 3.90$ μmol min⁻¹.

[b] The yields of MTh must be taken into account in order to calculate the % product recovery.

[c] % product recovery $= \dfrac{\Sigma \text{ products}}{CO^0} \times 100.$
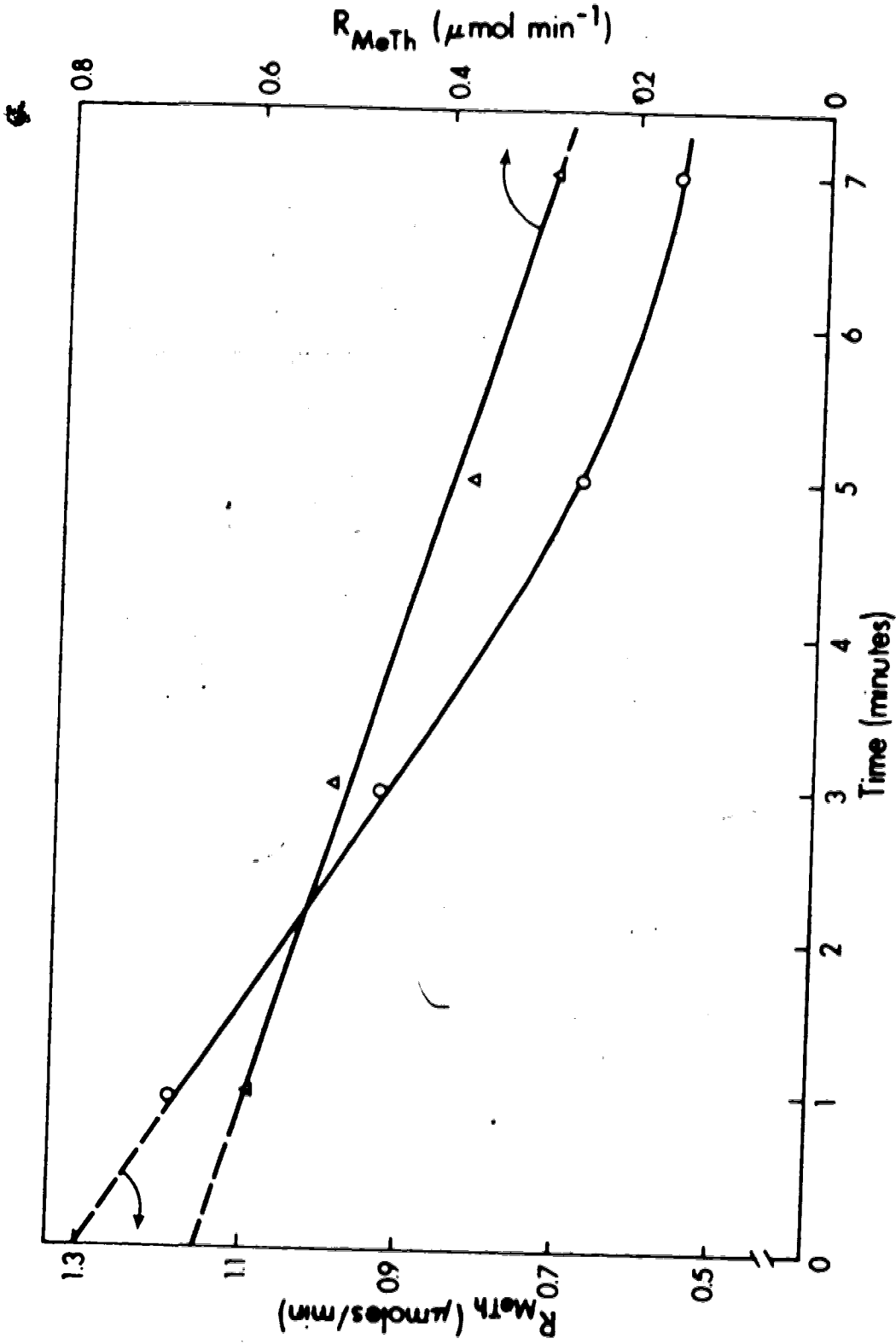
FIGURE IV-5. Exposure time dependence of MeTh. Δ, $P_{(COS)}$ = 545 torr; $P_{(C_3H_4)}$ = 55 torr.

O, $P_{(COS)}$ = 1090 torr; $P_{(C_3H_4)}$ = 109 torr.

plotted as a function of pressure in Figure IV-6.

The results listed in Table IV-3 also show that added CO_2 has no effect on the product yields or their distribution.

4. Discussion

Both ($^1D_2$) and (^3P) sulfur atoms react with allene to yield a single product, methylenethiirane:

$$S(^1D_2, \; ^3P) + H_2C=C=CH_2 \longrightarrow H_2C=C\overset{\displaystyle S}{\underset{\textstyle }{\diagup\diagdown}}CH_2 \qquad [2]$$
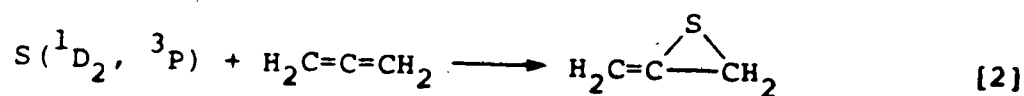
The expected insertion product

$$S(^1D_2) + H_2C=C=CH_2 \longrightarrow H_2C=C=CHSH \qquad [3]$$
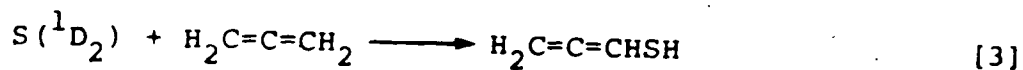
has not been synthesized and is probably unstable, both thermally and photochemically. If this is the case, however, the high product yields obtained at 1100 torr and at low conversion (Table IV-4) strongly suggest that insertion, if it occurs, is a minor reaction pathway.

This result is in contrast to the $S(^1D_2) + C_3H_6$ reaction where insertion into the terminal $=CH_2$ moiety accounts for 19% of the overall reaction, but parallels the $S(^1D_2) + 1,3\text{-}C_4H_6$ system, where cycloaddition is the only observable reaction.[92]

In the case of allene the longer C-H and shorter C-C bonds, as compared to ethylene, indicate the

138.
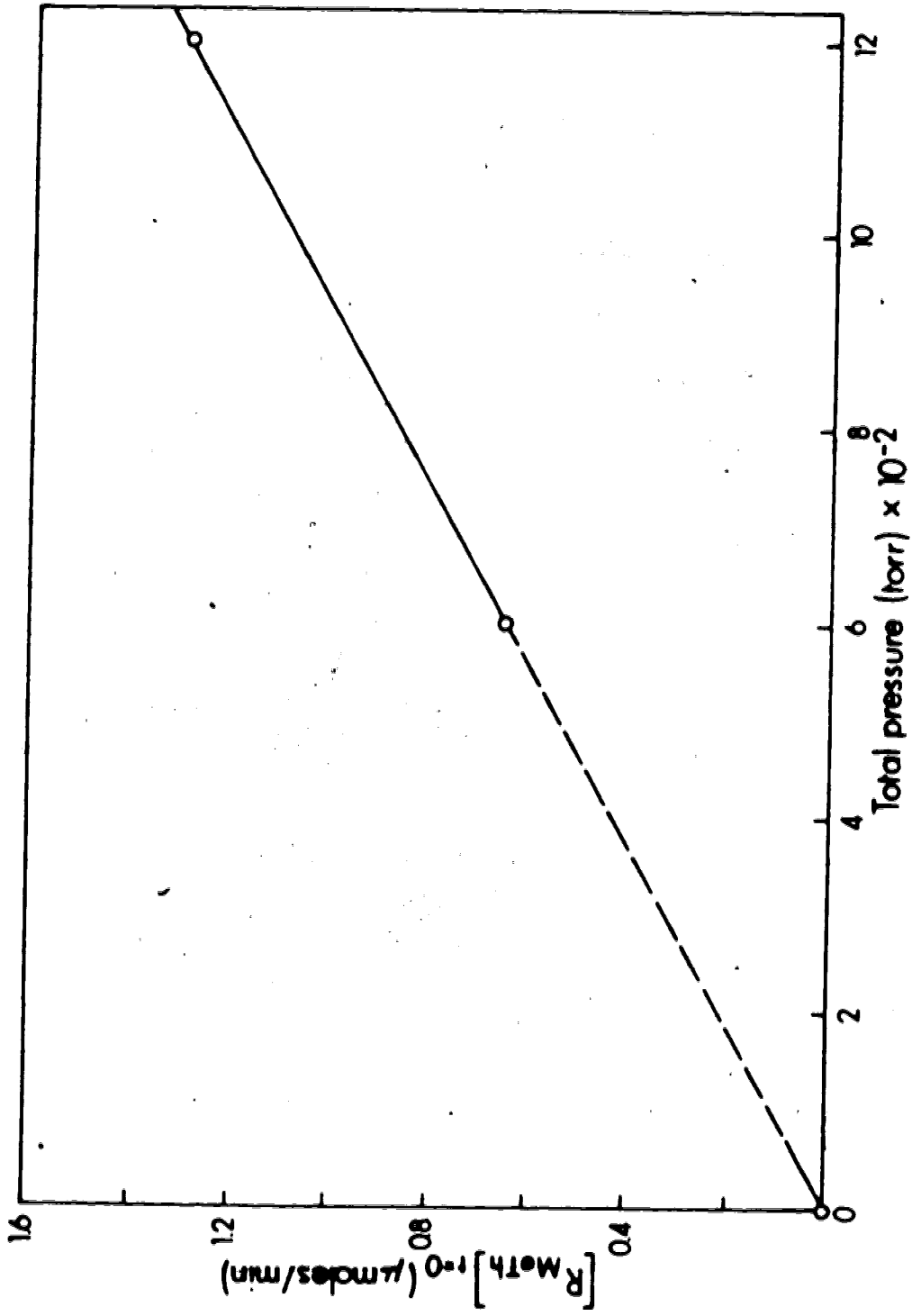
FIGURE IV-6. Effect of pressure on MeTh rates.

occurrence of hyperconjugation, which confers partial triple bond character to the molecule:[126]
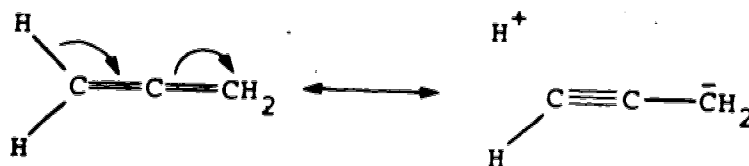
Hence, it would appear that the greater availability of the π orbitals, as in the case of 1,3-butadiene, favours the *cyclo*addition reaction. Because of the geometry and polarizability of the π bonds, the orientation of ionic and free radical additions is strongly affected by the nature of the groups already attached to the cummulene bond. Thus, in allene the central carbon is electrophilic, whereas in tetramethylallene the same carbon is nucleophilic.[126]

At the time this project was carried out, methylene-thiirane had not been synthesized. Since then however, two papers appeared on this topic.

Block *et al.*,[127] employing the flash vacuum pyrolysis-microwave spectroscopic approach, synthesized and characterized MeTh from two different precursors. Pyrolysis of either ^{13}C or d_2 labelled source compounds afforded randomly labelled (between the thiirane ring and the exocyclic methylene groups) MeTh, suggesting a common, symmetrical intermediate:

$$\Delta \longrightarrow \left[\triangleright = S \right] \longrightarrow C_2H_4 + [CS]$$

[4]

$$\xrightarrow[-C_5H_6]{\Delta} \quad \rightleftharpoons \quad \left[\right] \quad \rightleftharpoons \quad$$
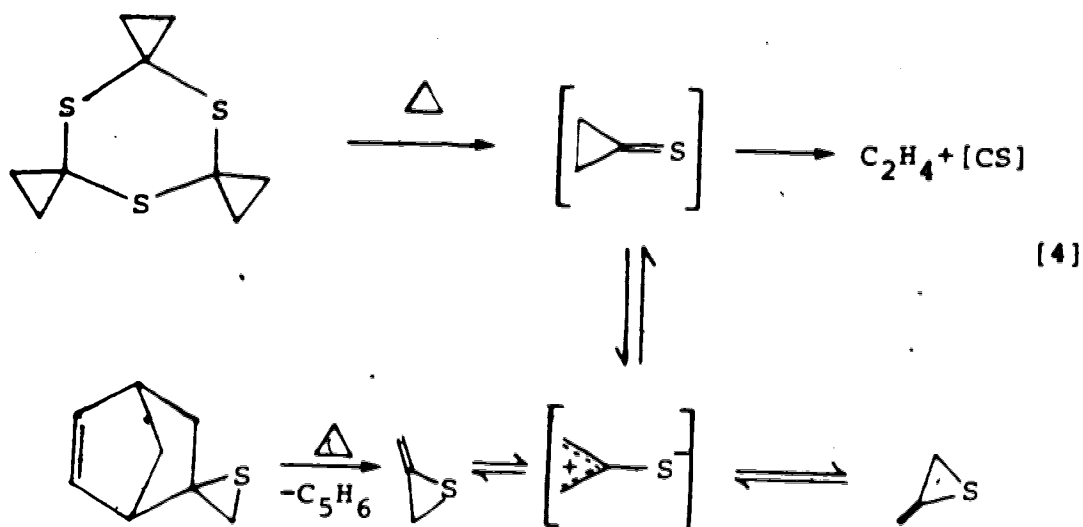
About the same time de Boer and coworkers[128] observed that MeTh is formed upon pyrolysis of a cyclic carbonate:

$$\xrightarrow[0.5 \text{ mm}]{495°} \quad H_2C = \overset{S}{\underset{CH_2}{\triangle}}$$

[5]
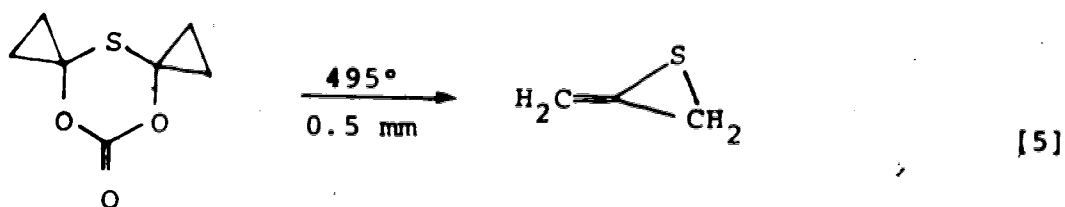
and reported the mass, ultraviolet, infrared and proton NMR spectra of MeTh. Their data are in excellent agreement with those obtained in the present work.

The chemistry of thiiranes containing unsaturated substituents is interesting from both the experimental and theoretical point of view. As noted above, MeTh decomposes slowly in the gas phase and at room temperature to yield exclusively polymer whereas at elevated

temperatures allene, C_2H_4 and CS_2 are formed. This observation, together with Block *et al.*'s labelling experiments, points to the occurrence of the tautomeric equilibrium,

[6]
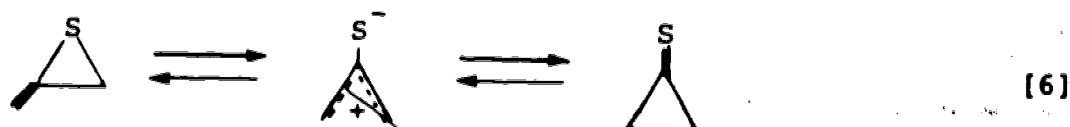
C_2H_4 and CS presumably arise *via* decomposition of cyclopropanethione,

CS + C_2H_4 [7]
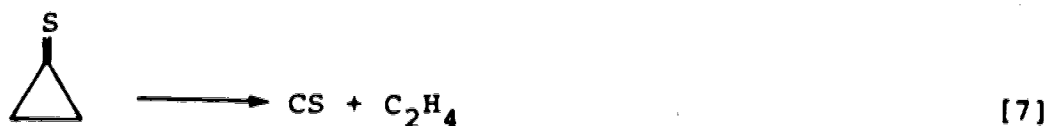
which is thermodynamically less stable (by 7 kcal mol^{-1})[127] than the MeTh tautomer. The tendency to thermal poly-merization at moderate temperatures parallels the reactivity of allenethiirane.[115]

The energy content of the initially formed hot MeTh can be calculated from the relation:

$$\langle E^* \rangle = \Delta H_f^\circ(C_3H_4) + \Delta H_f^\circ(S(^1D_2)) - \Delta H_f^\circ(C_3H_4S) + \Delta E_{tr} \quad [I]$$

Using the following thermochemical data[46,129]

$\Delta H_f^\circ(C_3H_4) = 46.1$ kcal mol^{-1}; $\Delta H_f^\circ(S(^1D_2)) = 92.0$ kcal mol^{-1}; $\Delta H_f^\circ(C_3H_4S) = 42.1$ kcal mol^{-1}; $\Delta E_{tr} = 6.0$ kcal mol^{-1} (where ΔE_{tr} is the translational energy of the singlet sulfur atom) $\langle E^* \rangle = 102$ kcal mol^{-1}. This energy is more than

sufficient to bring about isomerization or bond cleavage but these reactions do not appear to be significant in the pressure regime studied here, most likely as a result of the increased number of vibrational degrees of freedom (as compared to the C_2H_4S case) which confer a certain degree of stability to the excited MeTh molecule. Thus, on the one hand, the CS_2 yields, although erratic in some cases, do not appear to be of primary origin, and on the other, the MeTh yields appear to be pressure dependent (Figure IV-6). It is suggested that most, if not all, of the CS_2 arises as a consequence of secondary photolysis of MeTh, in a manner analogous to the high temperature thermal decomposition:

$$\text{(structure)} + h\nu \rightleftharpoons \text{(structure)} \rightleftharpoons \text{(structure)} \longrightarrow CS + C_2H_4 \qquad [8]$$

De Boer and coworkers have suggested that, since the reactivity of CS is similar to that of carbenes,[130] CS_2 could form from the reaction

$$CS + \text{(structure)} \longrightarrow CS_2 + C_3H_4 \qquad [9]$$
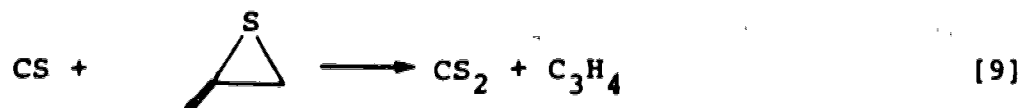
by analogy to the general carbene + heterocyclopropane reactions.[130]

Unfortunately, a specific search for C_2H_4 was not carried out in the present investigation.

The photochemical behaviour of MeTh is similar to that of allenethiirane[115] in that both feature CS bond cleavage; the end product of the latter decomposition is thiophene and hydrogen:

$$CH_2=CH-CH-CH_2 + h\nu \longrightarrow CH=CH-\overset{\bullet}{C}H-CH_2\overset{\bullet}{S} \qquad [10]$$

$$\overset{\bullet}{C}H=CH-\overset{\bullet}{C}H-CH_2\overset{\bullet}{S} \longrightarrow \left[\underset{S}{\bigcirc}\right]^* \longrightarrow \underset{S}{\bigcirc} + H_2 \qquad [11]$$
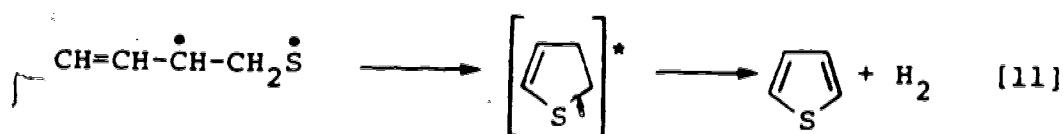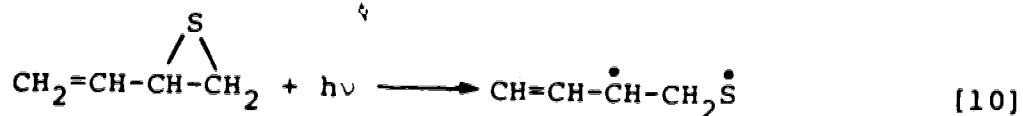
In both cases however polymerization is dominant process.

As noted above, allene is also a product of the thermal decomposition of MeTh. Although it is possible that step [9] contributes to some extent, a more plausible pathway for the formation of allene would be *via* bimolecular desulfurization. This suggestion is based by analogy with the thermal decomposition of thiirane,[112] and its simple alkyl substituted derivatives, which have been shown to afford the corresponding alkene and elemental sulfur through the intermediacy of the triplet state. Thus,

$$MeTh \overset{\triangle}{\longrightarrow} MeTh\ (T_1) \qquad [12]$$

$$MeTh\ (T_1) + MeTh \longrightarrow 2C_3H_4 + S_2 \qquad [13]$$
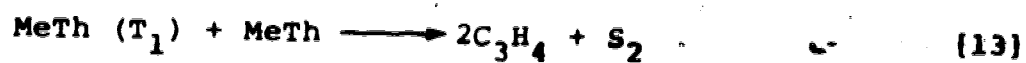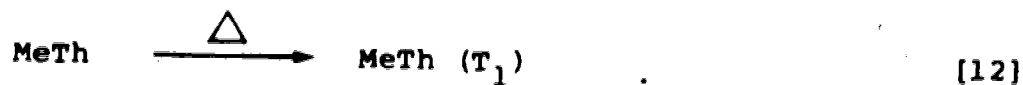
This competing pathway very likely takes place in photolysis as well.

It is interesting to note that the photochemical[106] and thermal decomposition of thiirane and its various CH_3, C_2H_5 and C_3H_7 substituted derivatives all proceed via the intermediacy of the triplet state to yield the corresponding alkene and sulfur, yet the presence of an unsaturated substituent leads to the occurrence of competing pathways involving isomerization, C-C and C-S cleavage. More detailed studies on the latter systems would be interesting from both the experimental and theoretical point of view.

In contrast, methyleneoxirane has not been isolated from the $O(^3P)$ + C_3H_4 reaction;[131] the reaction products are CO (57%), C_2H_4 (38%) and acrolein (1%) and the following scheme was proposed:

$$H_2C=C=CH_2 + O(^3P) \longrightarrow H_2C=\overset{\overset{\displaystyle O^\bullet}{|}}{\underset{\bullet}{C}}CH_2 \qquad [14]$$

$$\longrightarrow \bullet O-\overset{}{C}\underset{\diagdown CH_2}{\overset{\diagup CH_2}{}} \qquad [15]$$

$$H_2C=\overset{\overset{\displaystyle O^\bullet}{|}}{\underset{\bullet}{C}}CH_2 \longrightarrow [H_2C=\overset{\overset{\displaystyle O}{\diagup\diagdown}}{C-CH_2}]^* \qquad [16]$$

$$\longrightarrow H_2C=CHCHO \qquad [17]$$

$$\bullet O-C \overset{CH_2}{\underset{CH_2}{<}} \bullet \longrightarrow \left[\overset{\overset{O}{\parallel}}{\underset{CH_2-CH_2}{C}} \right]^* \qquad [18]$$

$$[H_2C=\overset{\overset{O}{\triangle}}{C}-CH_2]^* \longrightarrow \left[\overset{\overset{O}{\parallel}}{\underset{CH_2-CH_2}{C}} \right]^* \qquad [19]$$

$$\left[\overset{\overset{\overset{\bullet}{O}}{\parallel}}{\underset{H_2C-CH_2}{C}} \right]^* \longrightarrow H_2\overset{\bullet}{C}-CH_2-\overset{\bullet}{C}=O \qquad [20]$$

$$\longrightarrow CO + C_2H_4 \qquad [21]$$

$$H_2\overset{\bullet}{C}-CH_2-\overset{\bullet}{C}=O \longrightarrow H_2C=CHCHO \qquad [22]$$
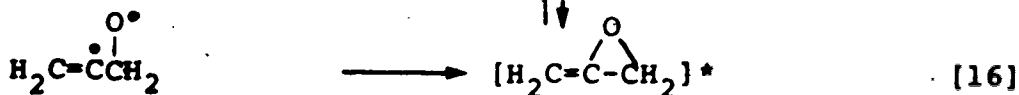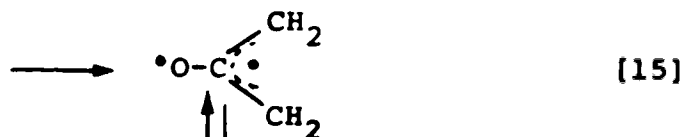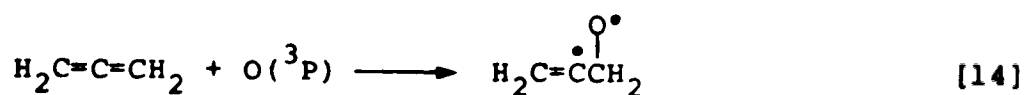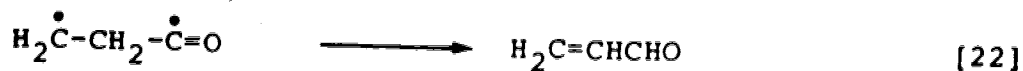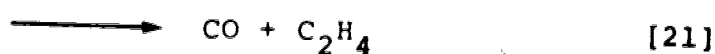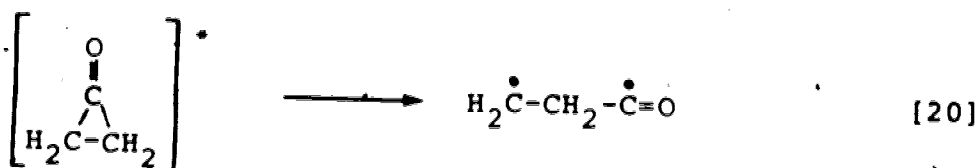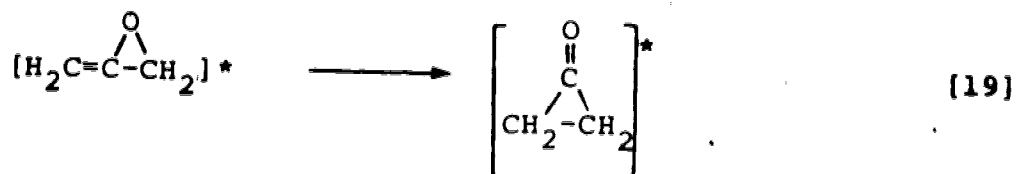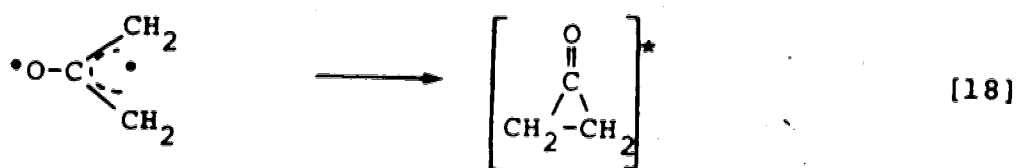
The later experimental results of Lin et $al.$[132] are consistent with the above mechanism. This scheme is completely analogous to the case of the S + C_3H_4 reaction, but because the relative stabilities of the isomers are reversed the final products are different. Thus, simple thermodynamical calculations predict that cyclopropanone is 21 kcal mol^{-1} more stable[131] than methyleneoxirane ($cyclo$propanone polymerizes readily at room temperature[131]) whereas cyclopropanethione is less stable than MeTh by 7 kcal mol^{-1}.[127]

The relative rate constant for the allene + $O(^3P)$ reaction was reported by Havel[131] and absolute rate parameters were determined recently by Cvetanovic *et al.*;[55] k_{14} = (1.8 ± 0.41) x 10^{10} exp $[\frac{-1872 \pm 54\ cal}{RT}]$ ℓ mol^{-1} s^{-1}. At room temperature (298°K) k_{14} = 7.7 x 10^8 ℓ mol^{-1} s^{-1}. The analogous rate constant for the $S(^3P)$ + C_3H_4 reaction has not been measured, but considering the well established general trends[46] of the $S(^3P)$ atom reactions with alkenes, it is possible to estimate the rate parameters for this reaction. Thus, the rate constant value should be in the range (2-4) x 10^9 ℓ mol^{-1} s^{-1}, and the activation energy should lie between 0 and 1 kcal mol^{-1}.

The *cyclo*addition reaction of sulfur atoms with C_3H_4 to form MeTh appears to be characteristic of cummulene systems in general. Thus, $S(^1D_2)$ atoms react with methylallene to yield the two possible thiiranes as major products,[133]

$$CH_3-CH\overset{S}{\underset{\triangle}{\frown}}C=CH_2 \qquad CH_3-CH=C\overset{S}{\underset{\triangle}{\frown}}CH_2$$
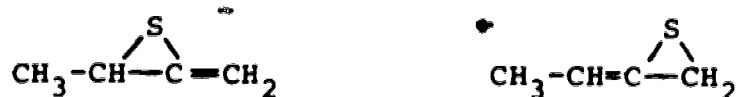
in comparable yields. Insertion into the CH_3 moiety also takes place, but to a much lesser extent. Thus, the reactions of $S(^1D_2)$ atoms with cummulenes constitute a convenient and nearly quantitative method of synthesizing the novel series of unsaturated thiiranes.

It should be noted that the first substituted allenethiirane was synthesized by Middleton[134] in 1969 from the following sequence,

$$\begin{array}{c} CF_3 \\ \diagdown \\ \diagup \\ CF_3 \end{array} C=C=S + (CF_3)_2CN_2 \longrightarrow (CF_3)_2C=C \begin{array}{c} N=N \\ | \quad | \\ \diagdown \quad \diagup \\ S \end{array} C(CF_3)_2 \quad \xrightarrow[\text{atm press.}]{\dfrac{\text{Reflux}}{\text{3-4 hours}}}$$

$$(CF_3)_2C=C\overset{\displaystyle S}{\overbrace{\qquad}}C(CF_3)_2 \; + \; N_2$$
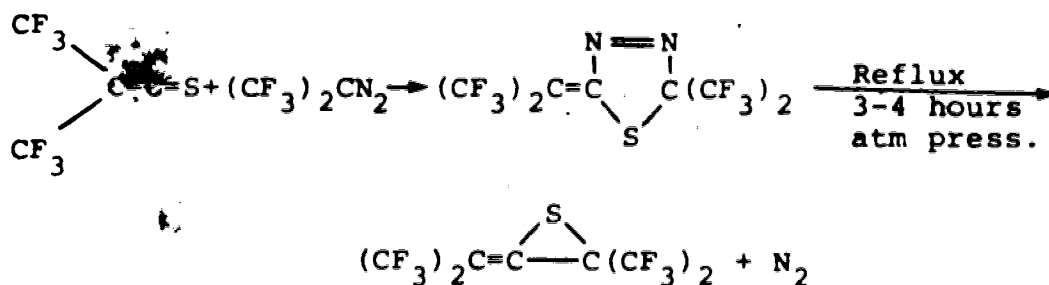
and in 1976 Hortman and Bhattacharjya described[135] a general synthetic route for the preparation of a number of substituted allenes involving the pyrolysis of alkali metal salts of thietanone tosyl hydrazones:

$$\begin{array}{c} N\text{-}\bar{N}\text{-}TS \; (Na^+, \; Li^+) \\ R \diagup\!\!\!\diagdown R \\ R \diagdown\!\!\!\diagup R \\ S \end{array} \quad \xrightarrow{\;\triangle\;} \quad \left[\begin{array}{c} R \quad \cdot\cdot \quad R \\ \diagup\!\!\!\!\diagdown\!\!\!\!\diagup \\ R \quad \quad R \\ S \end{array} \right] \quad \longrightarrow \quad \begin{array}{c} R \quad\quad R \\ R\diagup\!\!\!\diagdown\diagup\!\!\!\diagdown R \\ S \end{array}$$
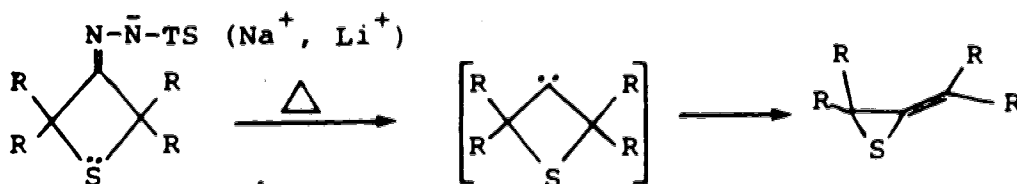
where R = CH_3, C_2H_5. These substituted methylene thiiranes are stable compounds. Neither of these methods however, led to the synthesis of parent MeTh.

CHAPTER V

REACTIONS OF SULFUR ATOMS WITH ALKYNES

Results

A. Reactions of sulfur atoms with acetylene

1. Reactions of $S(^1D_2)$ atoms with C_2H_2 at 160°C

The products were the same as those reported previously,[93] i.e., benzene, thiophene and CS_2. The product yield and distribution under the present conditions is given in Table V-1. The effect of temperature on the product yield is significant when compared to the exploratory room temperature study;[93] the product recovery, 5% at 25°C, increased to nearly 100% at 160°C in terms of total sulfur atoms formed.

2. Reactions of $S(^3P)$ atoms with C_2H_2 at 144°C

The total product yield in this system where all S atoms are deactivated to the $S(^3P)$ state amounted to only 4.7%, Table V-2, in terms of total sulfur atoms formed, which is comparable to that obtained in a previous room temperature study.[93] It appears that both $S(^1D_2)$ and $S(^3P)$ atoms lead to the same products.

TABLE V-1

Product yields from the $S(^1D_2, {}^3P) + C_2H_2$

reaction at 160°C.[a]

Product	Yield (μ moles)	% Yield[b]
Carbon disulfide	0.426	81.5
Benzene	0.124	11.9[c]
Thiophene	0.041	3.9
Total		97.3

[a] $\lambda > 240$ nm; Photolysis time = 4.0 minutes; R^0_{CO} = 0.726 μmol min^{-1}; $P(C_2H_2)$ = 240 torr; $P(COS)$ = 80 torr;

[b] in terms of total sulfur atoms produced; R_{CO}=0.465 μmol min^{-1};

[c] assuming that one S atom leads to the formation of one benzene molecule.

TABLE V-2

Product yield from the $S(^3P) + C_2H_2$ reaction at 144°C.[a]

Product	Yield (μ moles)	% Yield[b]
Carbon disulfide	0.040	3.4
Benzene	0.0182	0.8[c]
Thiophene	0.0118	0.5
Total		4.7

[a] $\lambda > 240$ nm; Photolysis time = 20.0 minutes; P(COS) = 40 torr; $P(C_2H_2)$ = 120 torr; P_{CO_2} = 1400 torr; R_{CO}^0 = 0.325 μmol min^{-1}; R_{CO} = 0.208 μmol min^{-1}.

[b] in terms of total sulfur atoms produced;

[c] assuming that one S atom leads to the formation of one benzene molecule.

B. Sulfur atom reactions with 3,3,3-trifluoropropyne

1. Products of the reaction

Photolysis of a mixture of 480 torr C_3HF_3 and 80 torr COS at 150°C led to the formation of eight products, the structure, relative yields and modes of identification of which are presented in Table V-3. With the exception of 2 none of these products have been reported in the literature. Their mass spectra, together with the ^{19}F NMR spectra of the major products 4, 6 and 8 are given in Appendix B.

a) Product 4.
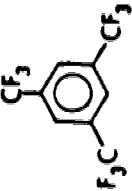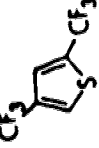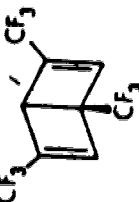
The mass spectrum featured the parent ion (M^+ = 282) at a relative intensity of 87.6. The ^{19}F NMR spectrum consists of a single peak at 99.35 ppm, which resolves into a complex quartet under high resolution.

The U.V. spectrum of 4 consists of an absorption maximum at 201 nm and a less intense one at 272 nm. These features are similar to those of the U.V. spectrum reported by Barlow et al.[137] for hexakis(trifluoromethyl)-benzene in n-pentane, which has an absorption maximum at 212 nm.

The proposed structure (Table V-3) of 4 is consistent with the above spectral properties; moreover, by analogy

TABLE V-3

Product yields from the reactions of sulfur atoms with 3,3,3-trifluoropropyne at 150°C.[a]

Compound number	Relative g.l.c. peak area	Products	MW	Elution Time (minutes)	Identified by
1	trace	$S=C=CH-CF_3$	126	1.0	MS
2	0.01	CS_2	76	4.0	MS, elution time
3	0.14	?	288	9.0	MS
4	1.00	(benzene ring, CF_3 substituents)	282	9.5	MS, NMR
5	0.17	(thiophene ring, CF_3 substituents)	220	31.0	MS, UV
6	0.90	(thiophene ring, CF_3 substituents)	220	30.0	MS, NMR, UV
7	0.18	(thiophene ring, CF_3 substituent)	152	36.0	MS, UV, NMR
8	0.50	(bicyclic structure, CF_3 substituents)	282	63.0	MS, NMR, UV

[a] $\lambda > 240$ nm; Photolysis time = 130 minutes; $P(C_3HF_3) = 480$ torr; $P(COS) = 80$ torr.

with the S + C_2H_2 reaction,[93] 1,3,5-tris(trifluoromethyl)-benzene was expected to be a product of the $S+C_3F_3H$ system.

b) Product 8.

The relative intensity of the parent ion (M^+ = 282) is 98.1. The ^{19}F NMR spectrum featured two peaks integrating into 2:1 at 99.81 and 96.06 ppm, respectively indicating that two equivalent and one nonequivalent CF_3 groups are present in the molecule. High resolution of the first peak at 99.81 ppm led to a very complex pattern but the other one remained a broad single peak.

The UV spectrum features three absorption maxima, a strong one at 203 nm and two weak ones of equal intensity at 263 and 269 nm. The first absorption is in agreement with the value λ_1 = 202.5 nm reported by Barlow *et al.*,[137] for hexakis(trifluoromethyl)dewar benzene. Moreover, exposure time studies have shown that 8 is a photolysis product of 4 and thus the assigned Dewar benzene structure is the most reasonable one.

c) Product 6.

The mass spectrum features the parent ion (M^+ = 220) as the second most intense peak, with relative intensity of 98.0. The UV spectrum of this product features an absorption maximum at λ = 226 nm. This absorption is

common to all CF_3 substituted thiophenes[93,109] examined to date and may vary by ±2 nm depending on the degree and type of substitution.

The ^{19}F NMR spectrum yields two single peaks of equal intensity at 99.66 and 103.65 ppm. Under high resolution both peaks give rise to complex doublets. Since the ^{19}F NMR and UV spectra of 2,3-bis(trifluoromethyl)thiophene, which has been synthesized,[93,109] differ from the ones described above, therefore the only remaining reasonable structure for 6 is 2,4-bis(trifluoromethyl)thiophene.

d) Product 7.

The parent ion (M^+ = 152) is the most intense peak in the mass spectrum. In the UV spectrum a strong absorption occurs at λ = 224 nm and a weak one at λ = 272 nm, in good agreement with the UV spectrum obtained for 2,3,4-tris(trifluoromethyl)thiophene (*vide infra*). The ^{19}F NMR spectrum of 7 yields a single peak at 100.29 ppm. This chemical shift is consistent with that observed for 6 (99.66 ppm). A careful study of all the available ^{19}F-NMR spectra of various CF_3-substituted thiophenes strongly suggests that the high field shifted positions, (i.e., 99.66 ppm as compared to 103.65 ppm in 6) correspond to a CF_3 group adjacent to the sulfur atom. On this

basis 7 is tentatively identified as 2-trifluoromethyl-thiophene.

e) Product 5.

The mass spectrum again yielded the parent ion (M^+ = 220) as the most intense peak. The UV spectrum shows one maximum λ = 226 nm, suggesting a substituted thiophene. Since the 2,3- and 2,4-isomers can be discounted, this product is therefore either 2,5- or 3,4-bis(trifluoromethyl)thiophene.

f) Product 1.

Product 1 was only obtained in trace amounts, but its MS fragmentation pattern (Appendix B) is consistent with the 3,3,3-trifluorothioketene structure. The molecular ion (M^+ = 126) signal has a relative intensity of 74.4. The $(M-32)^+$ signal, of relative intensity 37.2, likely corresponds to the loss of a sulfur atom. The most intense peak $(M-51)^+$ may be associated with the loss of S and F atoms. This type of fragmentation pattern strongly militates against the $CF_3-C\equiv C-SH$ isomeric structure.

2. Effects of added C_4F_6

A 1:1 mixture of PFB-2 and 3,3,3-trifluoropropyne and COS at a total pressure of 680 torr was photolyzed

at 150°C for 60 min. The observed products, together
with their relative distribution, are given in Table V-4.
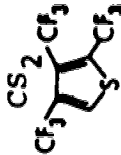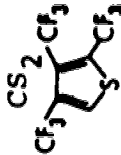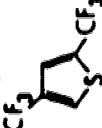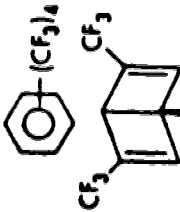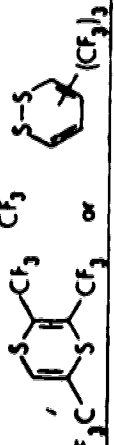
One of the major products, $\underset{\sim}{9}$, has not been reported
in the literature. Its mass spectrum yields the parent
ion (M^+ = 288) as the most intense peak. The UV spectrum
features a strong absorption maximum at 226 nm and a
weak one at 272 nm, in close resemblance to the UV
spectrum of 2-trifluoromethylthiophene, described above.
Its ^{19}F NMR spectrum consists of three peaks of equal
intensity, indicating that three chemically distinct
CF_3 groups are present in the molecule. Under high
resolution the peak at 105.02 ppm yields a complex
quartet, the peak at 103.26 ppm a quartet, and the third
peak at 101.57 ppm also resolves into a set of quartets.
On the basis of the above spectral data and those of
similar systems[93,109] it is reasonable to assign the
2,3,4-tris(trifluoromethyl)thiophene structure to $\underset{\sim}{9}$.

The other major product of this system is PFTMT,
$\underset{\sim}{10}$, and its properties will be described later. Products
$\underset{\sim}{11}$ and $\underset{\sim}{12}$ were only formed in trace amounts and hence
could not be characterized. The tentative structures
given in Table V-4 are based partly on their MS and
partly on kinetic considerations (vide infra).

The yields of $\underset{\sim}{6}$ and of $\underset{\sim}{8}$ were very small. The
trisubstituted benzene $\underset{\sim}{4}$, the monosubstituted thiophene $\underset{\sim}{7}$,

TABLE V-4

Product yields from the reaction of sulfur atoms with a 1:1 mixture of CF_3-C≡CH and CF_3-C≡C-CF_3 at 150°C.[a]

Compound number	Relative g.l.c. peak area	Products	MW	Elution Time min	Identified by
1	unresolved	S=C=CH-CF_3	126	1.0	MS
2	0.01	CS_2	76	4.0	MS, elution time
9	1.00		288	9.0	MS, NMR, UV
10	1.00		356	19.0	MS, NMR, UV elution time
6	0.06		220	30.0	MS, NMR, UV
11	0.03		350	41.0	MS
8	0.05		282	63.0	MS, NMR, UV
12	<0.01		320	83.0	MS

[a] λ > 240 nm; Photolysis time 60 min; P(C_3HF_3) = 300 torr; P(C_3HF_3) = 300 torr; P(C_4F_6) = 300 torr; P(COS) = 80 torr.

and the unknown compound $\underset{\sim}{3}$ were demonstrably absent.

3. Effect of added C_2H_2

Photolysis (60 min) of a mixture of 510 torr C_3HF_3,
170 torr C_2H_2 and 80 torr COS at 150°C yielded no
additional products, but it was observed that the product
yields were considerably lower than those obtained in the
absence of C_2H_2.

4. Effect of temperature

The yields of all the major products were higher
at 150°C than at 25°C but their relative distribution
was unchanged, indicating that all the observed products
are thermally stable.

C. Sulfur atom reactions with perfluoro-2-butyne (PFB-2)

In order to assess the absorption characteristics
of the substrate at room temperature, the gas phase UV
spectrum of 422 torr PFB-2 was obtained. Absorption begins
about $\lambda < 250$ nm, becoming quite strong below 235 nm.
$\varepsilon \simeq 5 \times 10^{-6}$ at 240 nm and 1.7×10^{-4} torr^{-1} cm^{-1} at 228 nm.

G.c. analysis of a photolyzed sample (60 min) of
500 torr C_4F_6 showed no sign of products, as expected,
owing to the very small extinction coefficient at the
effective photolyzing wavelength (>240 nm).

I. High conversion experiments

Photolysis of 480 torr C_4F_6 and 280 torr COS for 192 min. at 25°C led to the formation of ten products, the elution times and tentative structure assignments of which are listed in Table V-5. All pertinent MS, ^{19}F NMR spectra are given in Appendix B.

1. Spectral and thermal characteristics of the products

a) Perfluorotetramethylthiophene 10 (PFTMT)

The preparation, spectral and thermal properties of 10 have been described by Krespan.[109] It absorbs from 180 to 258 nm, with two unresolved maxima of approximately equal intensity, at $\lambda = 226$ and 239 nm. At 240 nm $\varepsilon \approx$ 0.36 torr^{-1} cm^{-1}. It should be noted that the absorption maximum at 226 nm is characteristic of all trifluoro-methyl-substituted thiophenes and therefore is useful for identification purposes. PFTMT is thermally stable[109] and can be handled at higher temperatures without observable loss.

b) Perfluorotetramethyldewar-thiophene 13 (PFTMDT)

PFTMDT (13) was first reported by Heicklen et al.[138] Its UV, MS and ^{19}F NMR spectra have been described in detail and the former two are identical to those of

TABLE V-5

Products detected from reactions of sulfur atoms with PFB-2

Compound number	Compound name	Structure[a]	MW	Elution time (minutes)	Identified by
13	Perfluorotetramethyl Devar-thiophene (PFTMDT)		356	2.7	MS,UV
14			550	5.6	MS,NMR
10	Perfluorotetramethyl thiophene (PFTMT)		356	19.0	MS,UV,NMR
15	Dimer	$(C_4F_6S)_2$	388	33.0	MS
16		$(C_4F_6)_3S_2$	550	45.0	MS
17	Trimer	(a) or (b)	582	56.0	MS,NMR
18	3,4,5,6-trifluoromethyl 1,2-dithiin		388	77.0	MS,NMR
19	Trimer	$(C_4F_6S)_3$	582	98.0	MS
20	Trimer	$(C_4F_6S)_3$	582	124.0	MS
21			420	156	MS,NMR

$\lambda > 240$ nm; $P(C_4F_6) = 480$ torr; $P(COS) = 280$ torr; Photolysis time = 192 min.

[a] $R = CF_3$.

160.

product $\underline{13}$. The MS gives the parent ion ($M^+ = 356$) as the second most intense peak at 99.0 on the relative scale. The gas phase UV spectrum of PFTMDT features two maxima at 247.5 and 336.5 nm, with corresponding extinction coefficients of 1.3 x 10^{-2} and 2.7 x 10^{-3} torr^{-1} cm^{-1}, respectively.

At room temperature $\underline{13}$ is stable; its conversion to PFTMT at higher temperature was described by Kobayashi $et\ al.$,[139] but the uncatalyzed reaction rate is very slow even at 160°C ($\tau_{1/2} \approx 5$ h in benzene).

c) Compound $\underline{14}$

The structural assignment (Table V-5) for this compound was made partly on the basis of kinetic considerations and partly on the basis of its MS and ^{19}F NMR spectra, listed in Appendix B. The MS gives only a low intensity peak (7.5) for the parent ion ($M^+ = 550$). The ^{19}F NMR spectrum consists of four single peaks which integrate in the ratio 2:2:1:1. The high resolution spectrum leaves the low field peak at 109.70 ppm unresolved (integration 2), resolves the second peak at 103.19 into two similar complex structures (integration 2), the third peak at 99.74 ppm leads to a very complex structure (integration 1) and the high field peak at 87.00 ppm is again resolved into a very complex structure. This

product appears to be unstable in the gas phase at room temperature, and disappears after several hours without forming any recoverable products.

d) Perfluoro 3,4,5,6-tetramethyl 1,2-dithiin (18).

This compound is thermally unstable and sensitive to surfaces. When a gaseous sample of the dimer 18 was stored in a quartz cell at room temperature for about 16 hours it has decomposed completely. Gc analysis of the decomposition products showed the presence of PFTMT, PFB-2 and a very broad trailing peak having variable elution times (7 to 15 min). Storage at -196°C in a quartz tube for about 14 hours effected 50% decomposition. Only very small amounts of PFTMT and PFB-2 were detected, and the broad peak was absent.

The relative intensity of the parent ion (M^+ = 388) is only 39.5. The UV spectrum of 18 is ill defined; the weak absorption range is between ~280 to 190 nm, but features at least one maximum at 250 nm. The ^{19}F NMR spectrum of 18 (Appendix B) shows the presence of two equivalent pairs of CF_3 groups at 108.47 and 99.45 ppm. Under high resolution both peaks yield complex spectra. The FT-IR spectrum (in Argon matrix at 10°K) features a weak absorption at 1600-1650 cm^{-1}, suggesting the presence of a double bond in this molecule.

Only 1,4-dithiins have been reported in the literature but in the photolysis studies by Zeller *et al.*[140,141] on substituted thiadiazoles the transient existence of 1,2-dithiins was postulated in order to explain the mode of formation of some of the products. The 1,2-dithiin structure for product 18 is consistent with the above spectral data and also with kinetic mechanistic considerations (*vide infra*).

e) Trimer 17

The mass spectrum features only a low intensity signal 9.3 for the parent ion (M^+ = 582). The ^{19}F NMR spectrum consists of six lines of equal intensities at 106.38, 106.04, 101.93, 98.61, 97.88, 89.21 ppm. The high resolution spectrum is described in Appendix B.

The UV spectrum of 17 shows continuous absorption from 190 to about 320 nm, with several maxima of comparable intensities at λ = 208, 225, 244, 256, 288 nm.

The FT-IR spectrum was obtained in an Argon matrix at 10°K and a weak absorption was observed in the region 1600-1650 cm^{-1}, which may correspond to the $\diagup C = C \diagdown$ stretching frequency.

On the basis of the molecular weight and the ^{19}F NMR spectrum which shows the presence of six unequivalent CF_3 groups, the most reasonable structures for this

product are 17a and 17b (Table V-5). Although a more

definitive structural assignment cannot be elucidated

at this time, mechanistic considerations (*vide infra*)

tend to support the unsaturated isomer, 17a.

Gc analysis of a gaseous sample of 17, stored in a

quartz cell for about 16 hours at room temperature, showed

the presence of PFTMT, and traces of undecomposed trimer.

No products could be detected after storage in a quartz

tube at -196°C for 48 hours, however the original peak

size decreased by about 30%. Therefore, the trimer is a

fairly stable compound at low temperature.

f) Compound 21

The parent ion ($M^+ = 420$) is a medium intensity

signal (37.9) in the mass spectrum of 21.

The ^{19}F NMR spectrum featured two signals of 1:1

integration, hence two sets of equivalent pairs of CF_3

groups are present in the molecule. High resolution

yields two sets of very complex spectra at 103.50 and

101.00 ppm respectively.

Additional support for the structure assigned to 21,

given in Table V-5 on the basis of molecular weight and

the ^{19}F NMR spectrum comes from kinetic mechanistic

considerations (*vide infra*).

Storage of product $\underset{\sim}{21}$ for several days at 25°C in a quartz tube effected no appreciable loss, therefore, it appears to be thermally stable. Its thermal stability at higher temperature was not investigated.

The remaining products of the high conversion experiments, $\underset{\sim}{15}$, $\underset{\sim}{16}$, $\underset{\sim}{19}$ and $\underset{\sim}{20}$ were detected only in very small amounts and because of their thermal and surface instabilities it was not possible to characterize them further.

2. Effects of exposure time on the product yields

The dependence of the product yields on exposure time is listed in Table V-6, and illustrated in Figure V-1, from which it may be seen that the PFTMT yield gradually decreases with time while that of PFTMDT and the trimer $\underset{\sim}{17}$ gradually increase. The other products, $\underset{\sim}{14}$, $\underset{\sim}{15}$, $\underset{\sim}{19}$, $\underset{\sim}{20}$ and $\underset{\sim}{21}$, were not detected in the first 15 min, and formed only in traces at 30 min photolysis time.

At longer exposure times (192 min, see Table V-5) the following general trends were observed:

    a) A near correspondence between the rate of increase of $\underset{\sim}{13}$ and the rate of decrease of $\underset{\sim}{10}$, suggesting that the former arises from photo-conversion of the major product PFTMT, $\underset{\sim}{10}$.

TABLE V-6

Exposure time dependence of the product yields in the S + C$_4$F$_6$ reaction[a]

Time (min)	yield, μmoles				peak area in planimeter units				
	CO	CO°-CO	10	% 10	10	13	18	16	17
5	7.69	2.76	0.71	25.7	21100	5	240	365	700
10	13.71	7.19	1.05	14.6	31500	54	346	387	1802
20	26.04	15.76	1.77	11.2	53300	385	430	750	6005
30	41.51	21.19	2.37	11.2	71100	893	690	775	11110

[a] λ > 240 nm; T = 23°C; P(C$_4$F$_6$) = P(COS) = 300 torr; R$_{CO}^0$ = 2.09 μmol min^{-1}.
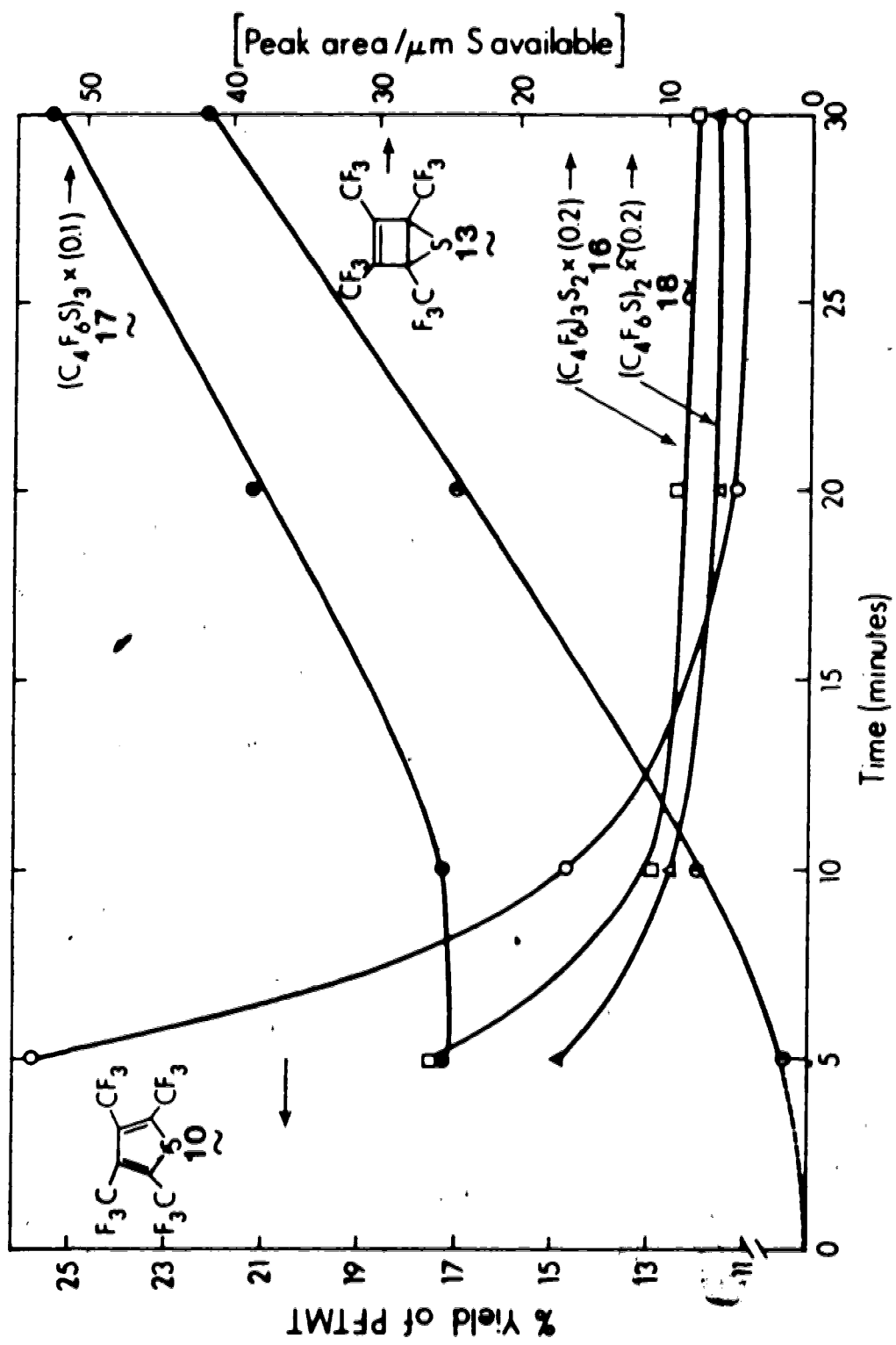
FIGURE V-1. Exposure time dependence of the product yields in the photolysis of 300 torr C_4F_6 and 300 torr COS.

b.) The yield of compound 14 increased slightly.

c) Several large and unresolved peaks appeared at elution times corresponding to those of the trimer 17 and dimer 18.

d) Trimers 19 and 20 were detected at elution times 98.0 and 124 min, respectively. The trimer 19 yield remained unchanged as compared to the 60 min experiment.

e) Traces of compound 21 were detected, eluting at 156 min. Its yield is strongly time dependent.

The effect of exposure time is negligible for the case of products 14, 15, 16, 18, 19, 20.

3. Effect of C_4F_6 pressure on the product yields

A mixture consisting of 480 torr C_4F_6 and 280 torr COS was photolyzed for 46 min and the yield of the trimer 17 increased approximately two-fold as compared to that from a mixture of 240 torr C_4F_6 and 280 torr COS (46 min photolysis time). Thus, the yield 17 is not only a function of exposure time but also of PFB-2 concentration. Assuming equal detector responses the major products were formed in the ratio 13:17:18 = 1:1:1.

4. Effect of COS pressure on the product yields

Photolysis of 80 torr COS and 240 torr C_4F_6 for 36 min

led to the formation of $\underset{\sim}{10}$, $\underset{\sim}{13}$, $\underset{\sim}{16}$, $\underset{\sim}{17}$ and $\underset{\sim}{18}$. $\underset{\sim}{17}$ and $\underset{\sim}{18}$ were formed in a 1:1 ratio but $\underset{\sim}{13}$ was formed in only small amounts. When 200 torr COS was added to this mixture and photolyzed for 16 min the dimer yield doubled, and remained unchanged at longer exposure time (46 min). Only small amounts of trimer $\underset{\sim}{17}$ were detected for the 16 min photolysis, but longer exposure time (46 min) greatly enhanced its yield (approximately six-fold increase).

5. Effect of added PFTMT on the product yields

Photolysis of a mixture consisting of 480 torr C_4F_6 and 280 torr COS in the presence of 26 μmol PFTMT led to the following results:

a) A dramatic, 25-fold increase in the yield of PFTMDT, a clear indication that this product arises from secondary photolysis of PFTMT.

b) A substantial increase in the yield of compound $\underset{\sim}{14}$.

c) A 35-40% decrease in the yield of trimer $\underset{\sim}{17}$ and a slight decrease in the yield of dimer $\underset{\sim}{18}$.

6. Secondary reactions of PFTMT (10)

a) Reactions with S atoms

In order to more clearly define the possible secondary reactions of $\underset{\sim}{10}$, 300 torr COS was photolyzed (40 min) in

the presence of 35 µmol PFTMT. The major reaction
product was identified as compound 21 (Table V-5).
Small amounts of 13 and traces of an unidentified
compound (possibly an isomer of $(C_4F_6S)_2$) were also
detected.

b) Reactions with C_4F_6

Photolysis (40 min) of a mixture of 300 torr C_4F_6
and 35 µmol PFTMT led to the exclusive formation of 13.
The original concentration of 10 was depleted by half.

7. Effect of temperature on the product yields

In order to examine the thermal stabilities of the
products the photolysis (30 min) of 80 torr COS and 240
torr C_4F_6 was carried out at 160°C. Only 10 and 13
were detected in increased yields as compared to room
temperature experiments.

II. Low conversion experiments

Under conditions of low conversion (cf. Figure V-2)
the only sulfur-containing product is PFTMT (10). The
following series of experiments were carried out in
order to shed light on the nature of the primary processes
leading to the formation of this compound.

TABLE V-7

Effect of PFB-2 pressure on the PFTMT yield[a]

$P_{C_4F_6}$ (torr)	Rates μmol min⁻¹				% PFTMT	k_{12}/k_{13}[d]
	CO	$S_{abstr.}$[b]	$S_{addn.}$[c]	PFTMT		
1	1.760	0.880	-	-	-	-
5	1.707	0.827	0.053	0.008	12.9	0.30
10	1.632	0.752	0.130	0.008	6.1	0.21
20	1.652	0.772	0.115	0.016	11.5	0.41
40	1.627	0.747	0.133	0.031	23.2	1.23
80	1.481	0.601	0.280	0.062	22.1	0.84
160	1.430	0.550	0.330	0.096	25.7	1.15
320	1.255	0.375	0.505	0.135	26.7	0.93
520	1.168	0.288	0.593	0.163	27.5	1.03
720	1.155	0.275	0.607	0.166	27.4	1.44
1020	1.070	0.190	0.690	0.195	28.2	1.17
1320	0.965	0.085	0.795	0.205	25.8	0.44

Ave= 1.12

[a] $\lambda > 240$ nm; $P_{COS} = 300$ torr; Photolysis time = 2.0 min.; $R_{CO}^0 = 1.76$ μmol min⁻¹; T = 23°C.

[b] $S_{abstr.}$ = rate of sulfur abstraction = $R_{CO}-R_{CO}^0/2$. [c] $S_{addn.}$ = rate of sulfur additon = $R_{CO}^0-R_{CO}$. [d] Calculated from experimental rates by correcting for contributions by S(³P) atoms (vide infra).
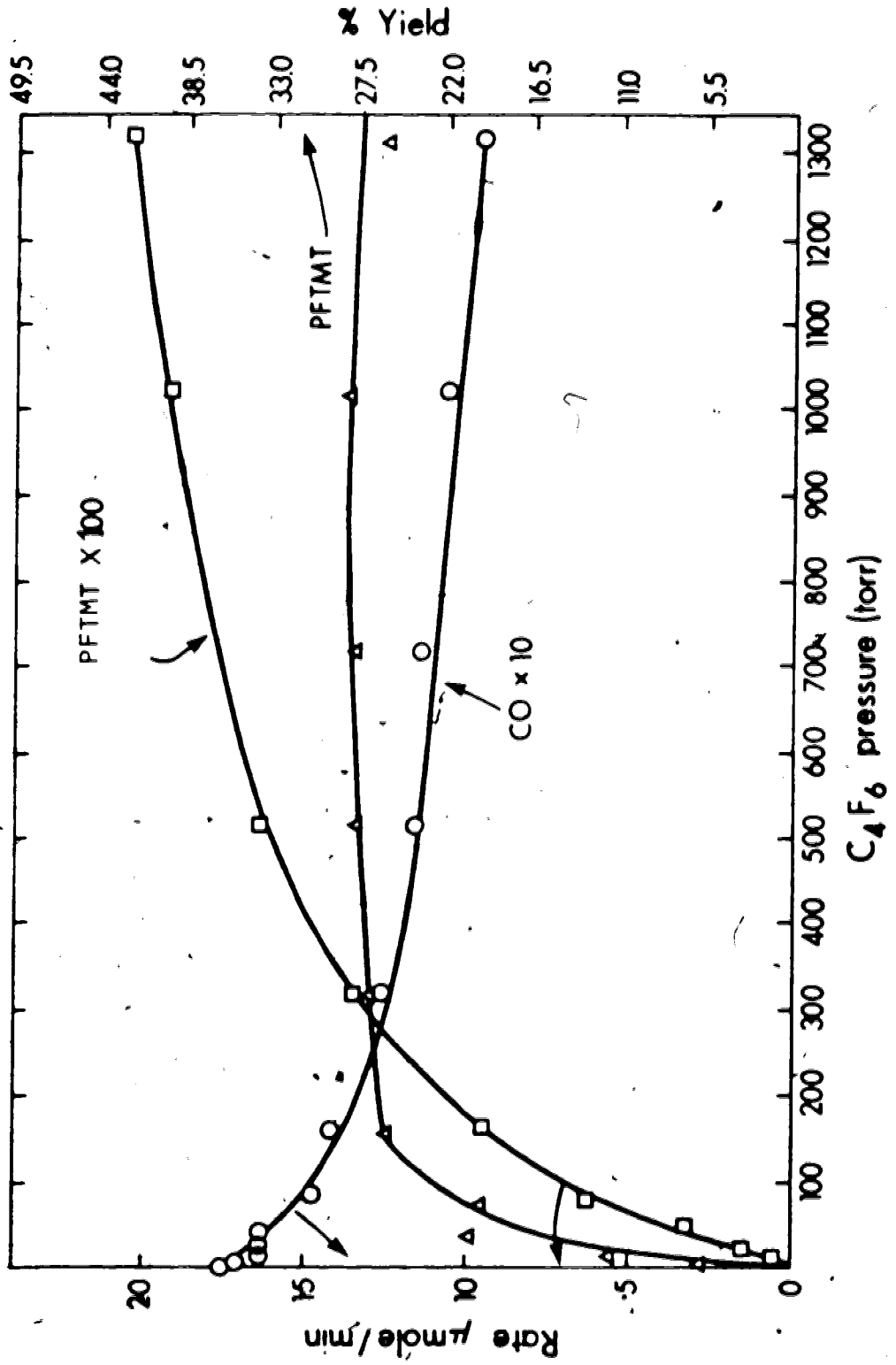
FIGURE V-2. The effect of PFB-2 pressure on the yields of PFTMT and CO. P(COS) = 300 torr.

1. Effect of PFB-2 pressure

The data are listed in Table V-7 and illustrated in Figure V-2, the most striking feature of which is the very shallow decline in the CO yields, which do not approach $CO°/2$ even at 1300 torr pressure. This is in marked contrast to the sulfur + alkene systems, where the CO yields initially decline very rapidly with increasing alkene pressure.

2. Effect of the COS/C_4F_6 ratio

As may be seen in Table V-8 and Figure V-3 the PFTMT yield is sensitive to the butyne/carbonylsulfide ratio. The observed linear relationship with increasing relative concentration of C_4F_6, however, is expected to curve and eventually level off at higher butyne pressures.

3. Effect of total pressure

The results of this investigation are shown in Table V-9 and Figure V-4, where it is seen that increasing the total pressure from 200 to 1200 torr effects a small but definite enhancement in the PFTMT yield.

4. Effect of added CO_2

In the presence of increasing pressures of CO_2, which has been shown to deactivate $S(^1D)$ atoms to the

TABLE V-8

Effect of the COS/C_4F_6 ratio on the PFTMT yield[a]

$P_{C_4F_6}/P_{COS}$	P_{total} (torr)	% PFTMT yield
1	600[b]	26.1
6.25	580[c]	32.6
19	1600[d]	46.2

[a] λ > 240 nm. [b] R_{CO}^0 = 1.517 μmol min^{-1}; Photolysis time = 2.0 min.

[c] R_{CO}^0 = 0.639 μmol min^{-1}; Photolysis time = 3.0 min., [d] R_{CO}^0 = 0.611 μmol min^{-1};
Photolysis time = 3.0 min.
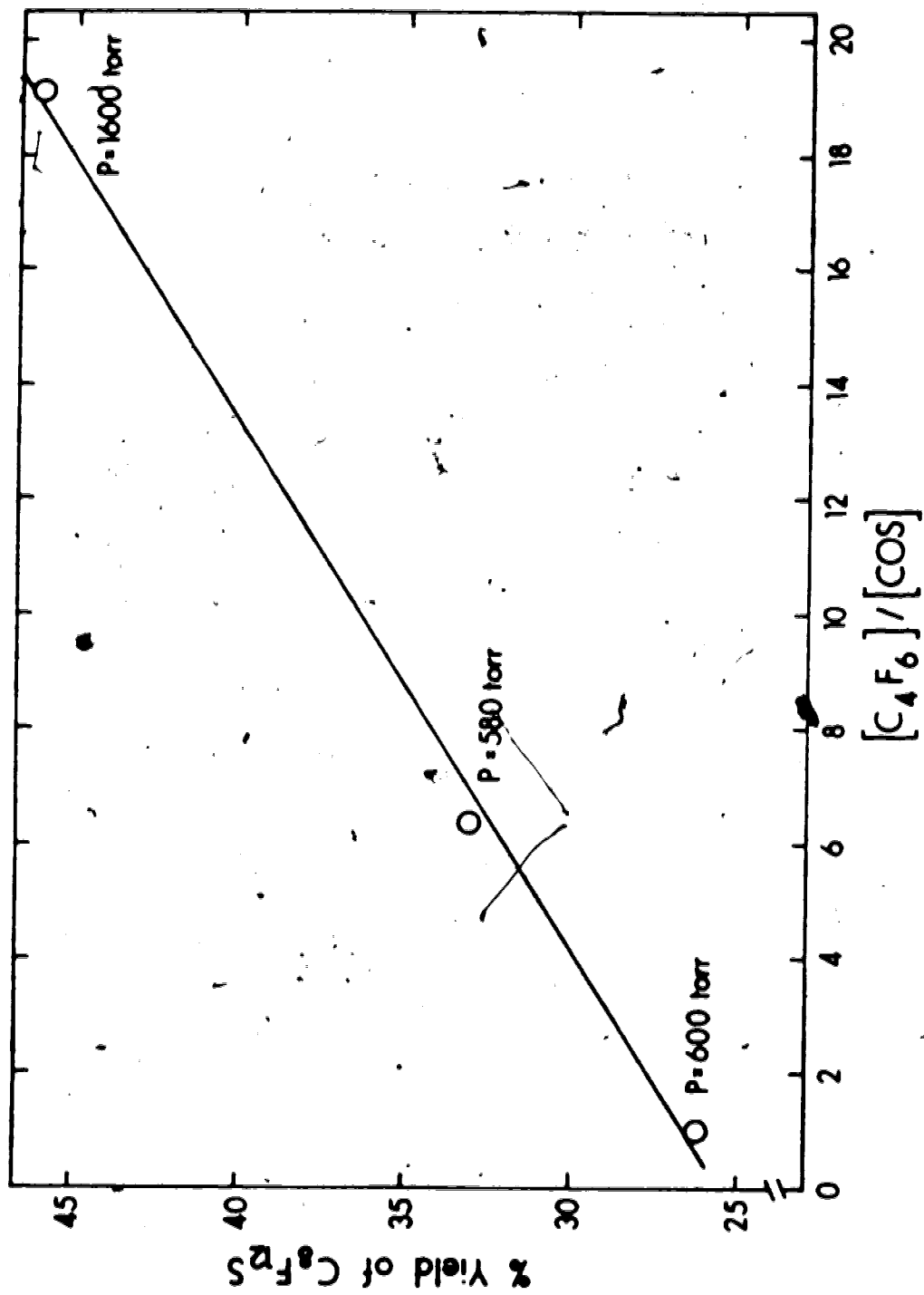
FIGURE V-3. Effect of relative substrate concentrations on the PFTMT yield.

TABLE V-9

Effect of total pressure on the PFTMT yield[a]

P_{total} (torr)	% PFTMT yield
200	25.0[b]
600	26.1[c]
1200	29.4[d]

[a] λ > 240 nm; C_4F_6/COS = 1.0.; [b] R_{CO}^0 = 0.749 μmol min⁻¹; Photolysis time = 3.0 min.

[c] R_{CO}^0 = 1.517 μmol min⁻¹; Photolysis time = 2.0 min. [d] R_{CO}^0 = 2.241 μmol min⁻¹;

Photolysis time = 1.0 min.
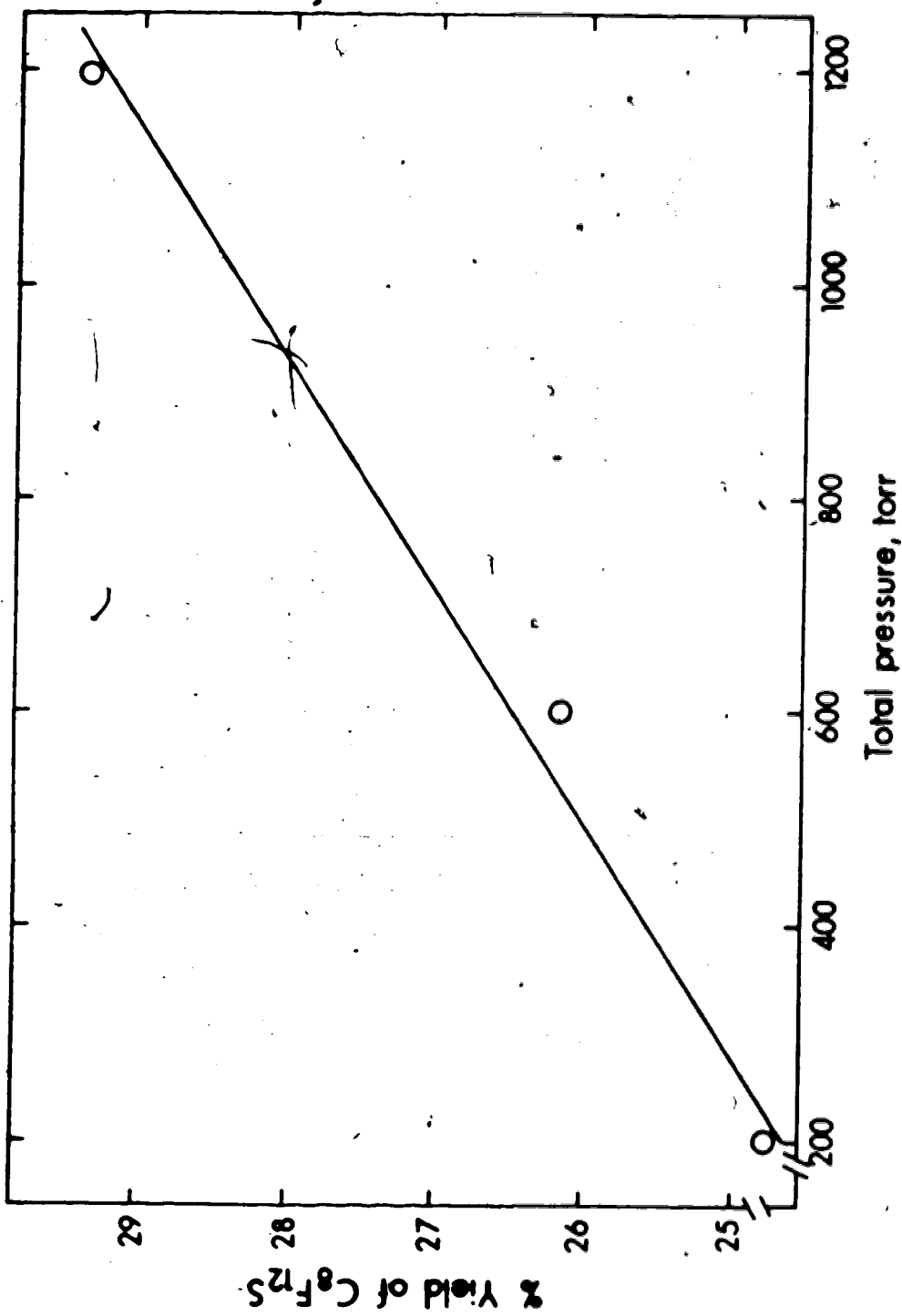
FIGURE V-4. Effect 6f total pressure on the PFTMT yield. $C_4F_6/COS \xi$ 1.0.

ground (^{3}P) state, the PFTMT yield gradually decreased to a limiting value of about 14% at 3400 torr, as shown in Figure V-5. No new products were detected. At this point C_4F_6 was gradually added to the mixture in order to see whether the PFTMT yield was sensitive to the COS/C_4F_6 ratio: under these conditions the PFTMT yield has only marginally increased to 18%, in sharp contrast to the case where ($^1D_2$) sulfur atoms were the reactive species. The pertinent data are given in Table V-11 and illustrated in Figure V-6.

5. Effect of temperature

Blank experiments showed that PFB-2 and PFTMT are stable at 160°C and moreover, allowing the photolyzate to remain standing for 3 hours at room temperature, did not affect the product yields.

The effect of temperature is shown in Table V-12 and illustrated in Figure V-7 where it is seen that the PFTMT yield increases with increasing temperature and at 120°C reaches 100%, in terms of sulfur atoms produced. Beyond this temperature the yield is 100% regardless of pressure and relative $COS-C_4F_6$ concentrations. Upon prolonged photolysis at this temperature the PFTMT yield is drastically reduced and a small amount of PFTMDT was detected.

TABLE V-10

Effect of CO_2 on the yield of PFTMT[a],

$P(CO_2)$ (torr)	% PFTMT yield
0	25.4[b]
800	18.0[c]
1400	13.6[b]
3400	14.8[b]

[a] λ > 240 nm. [b] R_{CO}^0 = 0.149 μmol min^{-1}; photolysis time = 20.0 min. [c] R_{CO}^0 = 0.348 μmol min^{-1};

photolysis time = 4.0 min.; T = 23°C; $P(C_4F_6)$ = 120 torr; $P(COS)$ = 40 torr.
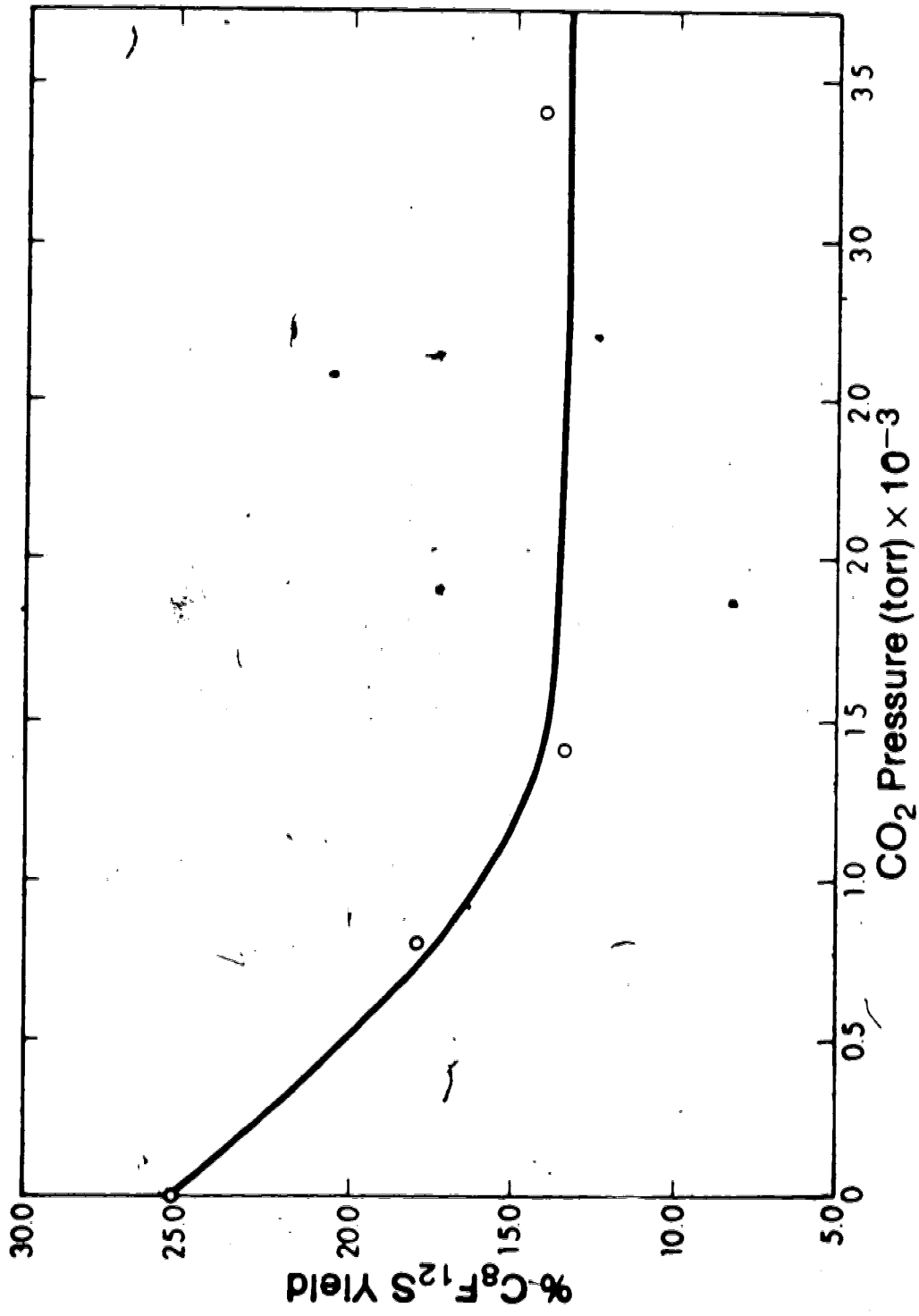
FIGURE V-5. Effect of CO_2 pressure on the PFTMT yield. $P(COS) = 40$ torr; $P(C_4F_6) = 120$ torr.

TABLE V-11

Effect of PFB-2 pressure on the yield of PFTMT[a]

$P_{C_4F_6}$ (torr)	Rates, μmol min^{-1}			% PFTMT yield
	CO°	CO	PFTMT	
120	2.98	1.67	0.185	14.8
240	2.55	1.45	0.221	20.4
360	2.55	1.33	0.222	18.8
600	2.28	1.19	0.211	19.4

[a] $\lambda > 240$ nm; P(COS) = 40 torr; P(CO$_2$) = 3400 torr; Photolysis time = 20.0 min.; T = 23°C.
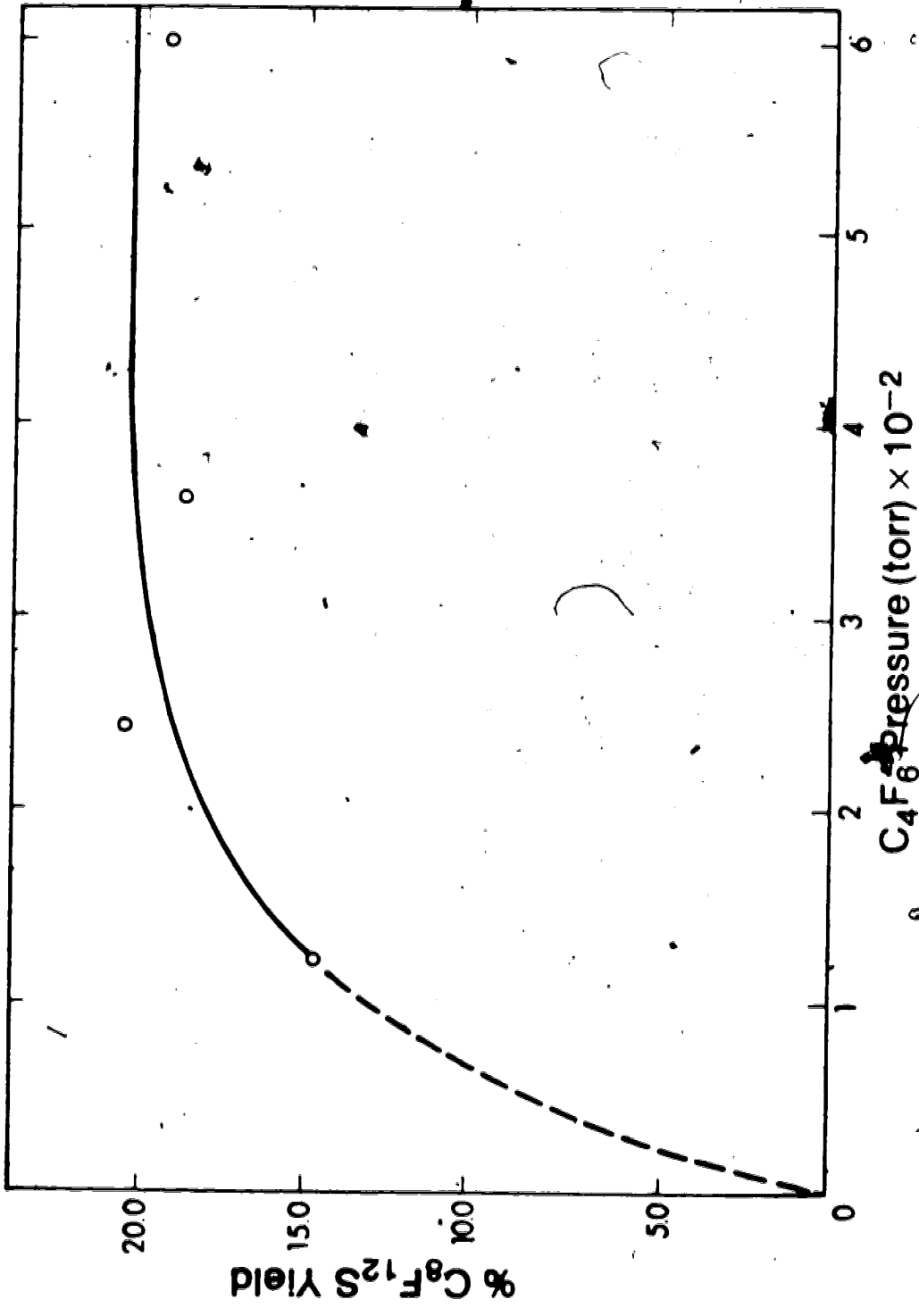
FIGURE V-6. Effect of PFB-2 pressure on the PFTMT yield. $P(CO_2) = 3400$ torr; $P(COS) = 40$ torr.

TABLE V-12.

Effect of temperature on the PFTMT yield from the S($^1D_2$, ^3P) + PFB-2 reaction[a]

Temperature °C	Rates, μmol min⁻¹					
	CO°	CO	PFTMT	$S_{abtr.}$[b]	S_{add}[c]	% PFTMT yield
24	0.336	0.205	0.032	0.039	0.131	24.5
61	0.393	0.257	0.053	0.061	0.136	39.2
82	0.440	0.305	0.079	0.085	0.135	58.6
108	0.518	0.370	0.121	0.111	0.148	81.8
125	0.585	0.432	0.157	0.140	0.153	102.8
160	0.726	0.510	0.221	0.147	0.216	102.3

[a] λ > 240 nm; Photolysis time = 4.0 min.; P(COS) = 80 torr; P(C$_4$F$_6$) = 240 torr.

[b] $S_{abstr.}$ = Rate of sulfur abstraction = $R_{CO} - R_{CO}^0/2$;

[c] $S_{add.}$ = Rate of sulfur addition = $R_{CO}^0 - R_{CO}$.
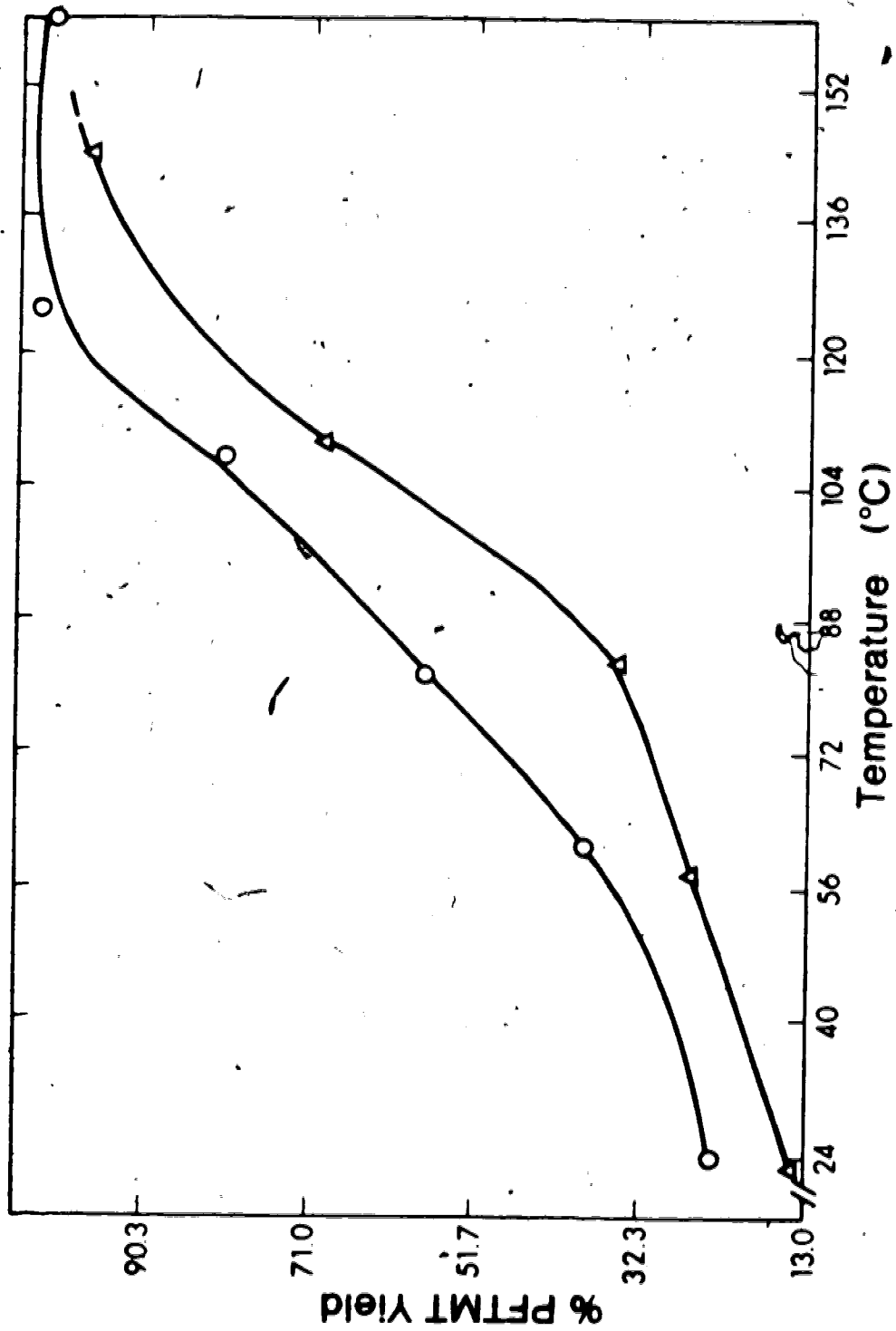
FIGURE V-7. The effect of temperature on the PFTMT yield. O, P(COS) = 80 torr; P(C_4F_6) = 240 torr. Δ, P(COS) = 40 torr; P(C_4F_6) = 120 torr; P(CO_2) = 1400 torr.

The above experiments were also carried out in the presence of a large excess of CO_2 in order to delineate the reactivity of $S(^3P)$ atoms and the results are also illustrated in Figure V-7. As compared to the results in the absence of CO_2, the PFTMT yield approaches 100% at a slightly higher temperature, about 146°C. The pertinent data are given in Table V-13.

6. Effect of added C_2H_2

Sulfur atoms react with mixtures of C_2H_2 and PFB-2 to yield PFTMT and 2,3-bis(trifluoromethyl)thiophene (b-TFMT) as major products, together with traces of a symmetrical bis(trifluoromethyl)thiophene (2,5 or 3,4) and CS_2. Benzene and thiophene were demonstrably absent.

The effects of acetylene pressure and of temperature on the PFTMT and b-TFMT yields are given in Tables V-14 and V-15, respectively.

The addition of small amounts of C_2H_2 leads to a large initial decrease in the PFTMT yield at both temperatures, then with increasing C_2H_2 pressure the PFTMT yield gradually decreases while that of b-TFMT gradually increases. Temperature has a significant effect on the yield of both of these products: at 130°C that of PFTMT increased about three-fold and that of b-TFMT, over ten-fold.

TABLE V-13

Effect of temperature on the yield of PFTMT from the $S(^3P)$ + PFB-2 reaction[a]

Time (min)	Temperature (°C)	Rates, μmol min^{-1}					% PFTMT yield
		CO°	CO	PFTMT	$S_{abstr.}$[b]	S_{add}[c]	
20	23	0.164	0.095	0.009	0.013	0.069	13.6
21	58	0.217	0.131	0.022	0.023	0.086	25.6
15	83	0.244	0.151	0.033	0.029	0.093	35.7
15	111	0.265	0.174	0.063	0.041	0.091	69.1
15	144	0.325	0.225	0.097	0.062	0.101	96.5

[a] λ > 240 nm; P(COS) = 40 torr; P(C_4F_6) = 120 torr; P(CO_2) = 1400 torr.

[b] $S_{abstr.}$ = Rate of sulfur abstraction = $R_{CO} - R_{CO}^0/2$.

[c] $S_{add.}$ = Rate of sulfur addition = $R_{CO}^0 - R_{CO}$.

TABLE V-14

Effect of acetylene pressure on the rates of PFTMT and b-TFMT formation at 25°C[a]

Time (min)	$P_{C_2H_2}$ (torr)	Rates, μmol min^{-1} × 10^3	
		PFTMT	b-TFMT
3.0	0	86.7	–
4.0	25	54.0	trace
4.0	50	46.0	2.3
4.1	100	34.4	5.1
4.0	200	23.0	6.3
3.0	500	6.3	16.7
12.0	500	5.7	16.2

[a] λ > 240 nm; P_{COS} = 80 torr; $P_{C_4F_6}$ = 500 torr; R^0_{CO} = 0.639 μmol min^{-1}.

TABLE V-15

Effect of acetylene pressure on the rates of PFTMT and b-TFMT formation at 132°C[a]

$P_{C_2H_2}$ (torr)	Rates, μmole min^{-1} × 10^3		% Product recovery (Σ PFTMT + b-TFMT)
	PFTMT	b-TFMT	
0	250	-	100
25	162	9.3	68.5
50	141	15.0	62.4
100	106	23.0	51.6
200	70	30.0	40.0

[a] λ > 240 nm; P(COS) = 80 torr; P(C$_4$F$_6$) = 500 torr; R^0_{CO} = 0.640 μmol min^{-1}.

Discussion

1. The primary adduct

MO calculations[32,33] have shown that the primary adduct of the gas phase reaction of $S(^1D_2)$ with acetylene can be $4n-\pi$ antiaromatic thiirene, formed along a spin and orbital symmetry allowed path, i.e.,

$$S(^1D_2) + \equiv \longrightarrow \text{(thiirene)} \quad (S_0), \qquad [1]$$
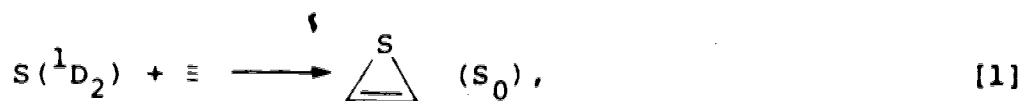
singlet state thioformylmethylene,

$$S(^1D_2) + \equiv \longrightarrow (\overset{\cdot S}{HC=CH} \longleftrightarrow \overset{S}{HC-CH})\,(S_1) \qquad [2]$$
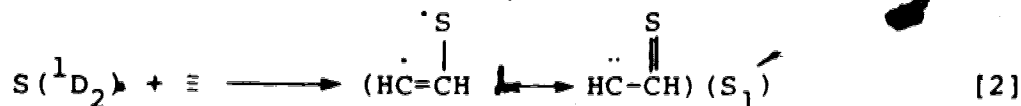
(which may also be formed from opening of the thiirene ring,

$$\text{(thiirene)} \longrightarrow (\overset{\cdot S}{HC=CH} \longleftrightarrow \overset{S}{HC-CH})\,(S_1) \qquad [3])$$
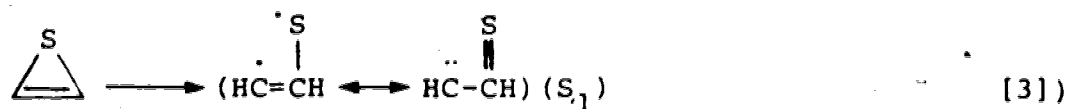
or ethynylthiol, formed by insertion of the $S(^1D_2)$ atom into the acetylenic C-H bond;

$$S(^1D_2) + \equiv \longrightarrow HC\equiv C-SH \qquad [4]$$

In the case of the $S(^3P)$ + acetylene reaction only the formation of ground triplet state thioformylmethylene is a spin and symmetry allowed process:

$$S(^3P) + \equiv \longrightarrow (\overset{\cdot S}{HC=CH} \quad \overset{S}{HC-CH})\,(T_0) \qquad [5]$$
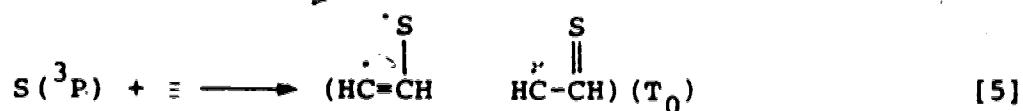
From the calculated relative thermodynamic stabilities (Figure I-5) of these isomers it can be seen that [1]-[5] are exothermic reactions.

Although theoretical calculations are not available for the S + H-C≡C-CF$_3$ and S + CF$_3$C≡CCF$_3$ systems, it will be assumed that the allowed reaction paths and primary adducts are completely analogous.

The transient existence of thiirenes as intermediates in the low temperature matrix photolysis of 1,2,3-thia-diazoles and thioxocarbonates has been well documented[96,102] and it has also been shown that the stability of CF$_3$-substituted thiirene is markedly enhanced. The major mode of decay of thiirene is ring opening to form thioformylmethylene, which subsequently rearranges to thioketene:

$$R_1 \overset{S}{\triangle} R_2 \longrightarrow R_1\overset{S}{\overset{\|}{C}}-\overset{..}{C}R_2 \longrightarrow R_1R_2C=C=S \qquad [6]$$
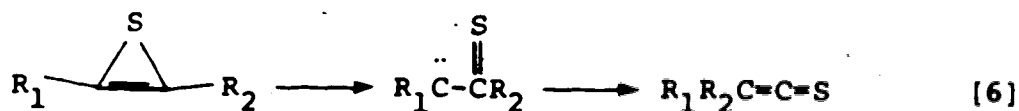
This reaction is however inoperative for $R_1 = R_2 = CF_3$ because of the low migratory aptitude of the CF$_3$ group. In this case, sulfur extrusion has been observed:

$$F_3C \overset{S}{\triangle} CF_3 \longrightarrow CF_3-C≡C-CF_3 + S \qquad [7]$$
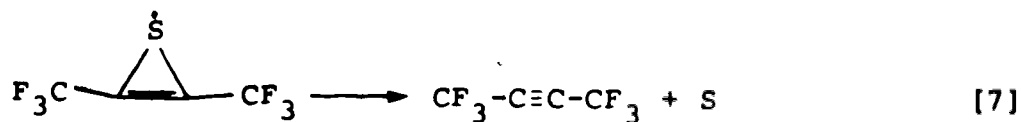
For the case of parent thiirene and methylthiirene rearrangement to ethynylthiol and methylethynylthiol

constitutes an alternative pathway:

$$\triangle \overset{S}{} \longrightarrow RC\equiv C-SH \qquad [8]$$

where R = H, CH_3.

In the presence of alkynes, thiirenes have been shown to undergo concerted addition across the triple bond, preferentially on the less-substituted C-S side, e.g.,

$$\overset{R}{\underset{R}{\underset{|}{\overset{|}{|||}}}} + \triangle\!\!-\!\!R \longrightarrow R\!-\!\underset{S}{\overset{R}{\diagup\!\!\diagdown}}\!\!-\!\!R \qquad [9]$$
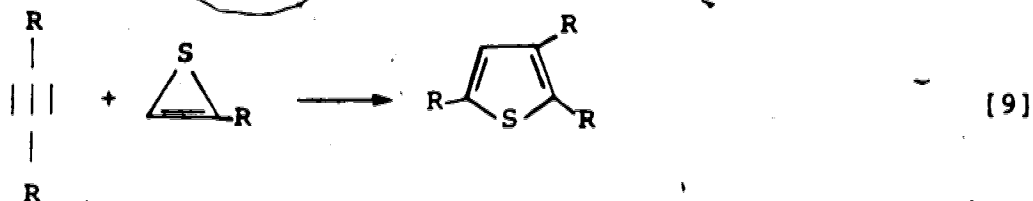
In the $S(^1D_2)$ + alkyne systems steps [1] and [2] may occur in parallel and in competition; alternatively, either one may be predominant but on the other hand both species may be present since the following rearrangement can take place:

$$RC\overset{S}{\overset{||}{C}}R(S_1)^* \longrightarrow RC\overset{\overset{\bullet S}{\diagup\diagdown}}{=\!=\!=}CR \longrightarrow RC\overset{S}{\overset{||}{C}}R(S_1) \qquad [10]$$
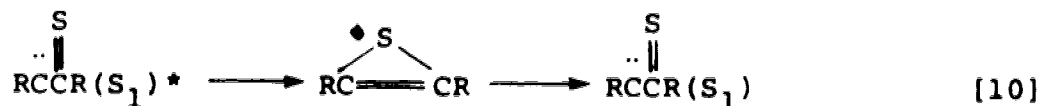
Returning briefly to the photolytic studies carried out on 1,2,3-thiadiazoles + alkyne systems, strong evidence has been presented to the effect that the reactive intermediate in the thiophene-forming reaction [9] is the thiirene and not the thioketocarbene isomer.[95] By

analogy it will therefore be assumed that the reactive intermediate in the $S(^1D_2)$ + alkyne systems is the thiirene structure.

The possible occurrence of direct insertion, step [4], cannot be verified since ethynyl thiols are expected to be thermally and photolytically unstable in the gas phase. Since, however, it has been shown that $S(^1D_2)$ atoms do not insert into the C-H bonds of allene (Chapter IV) it seems even more likely that the greater accessibility of the triple bond in the case of alkynes would favour addition over insertion.

The following brief general comments and predictions can now be made for the $S(^1D_2)$ + C_2H_2, $HC\equiv CCF_3$ and $F_3CC\equiv CCF_3$ adducts:

i) can undergo rearrangement to ethynyl thiol and hence to thioketocarbene, or condensation with C_2H_2 to form thiophene. In fact, small amounts of thiophene were detected along with CS_2, a photolysis product of thioketene. An additional, as yet unknown, mode of decay of C_2H_2S in the presence of acetylene leads to the formation of benzene.

ii) $-CF_3$ can in principle undergo the same reactions as C_2H_2S and should be more stable with respect to polymerization. Accordingly, traces of 3,3,3-tri-fluorothioketene were observed and the corresponding

substituted benzene and thiophene yields were considerably enhanced as compared to the S + C_2H_2 system.

iii) F_3C⟍△⟋CF_3 can only decompose to yield C_4F_6 and S, or undergo addition to the triple bond of C_4F_6. Thus at low conversions PFTMT is the only observable product in 46% yield under optimal conditions. The absence of substituted benzenes may indicate that the benzene-forming ability of C_2H_2S and C_3HF_3S depends on one or more group migrations along the reaction sequence. Alternatively, steric effects may play a decisive role in the formation of benzenes.

Since the S + C_4F_6 reaction has been studied in greatest detail, its kinetic-mechanistic features will now be delineated.

2. Mechanistic details of the S + C_4F_6 reaction

The sole retrievable product from the reactions of sulfur atoms with C_4F_6 is PFTMT, at low conversion, regardless of the spin state of the sulfur atom. This result parallels the S + C_4H_6-1,4 and S + C_3H_4 reactions. (Dithiin 18 and the uncharacterized product 15 appear to be primary products, Figure V-1, but their yields are negligibly small). The yield of PFTMT at room temperature

however is substantially higher, (~30% of the total) for $S(^1D_2)$ atom precursors as compared to $S(^3P)$ atoms (15-18%). Increasing the total pressures has only a marginal effect on the product yields, hence there are no unstable intermediates requiring pressure stabilization.

The many possible primary reactions ensuing from the photolysis of COS in the presence of C_4F_6 can be summarized as follows:

$$COS + h\nu \longrightarrow CO + S(^1D_2) \qquad \sim 67\% \qquad [11a]$$

$$\longrightarrow CO + S(^3P) \qquad \sim 33\% \qquad [11b]$$

$$S(^1D_2): \quad S(^1D_2) + COS \longrightarrow CO + S_2 \qquad [12]$$

$$+ C_4F_6 \longrightarrow F_3C \underset{\triangle}{\overset{S}{\diagup}} CF_3 \quad (S_0) \qquad [13]$$

$$F_3C \underset{\triangle}{\overset{S}{\diagup}} CF_3 + C_4F_6 \longrightarrow \quad (S_0) \qquad [14a]$$

$$F_3C \underset{\triangle}{\overset{S}{\diagup}} CF_3 \xrightarrow{\quad M \quad} F_3C-\overset{S}{\overset{\|}{C}}-\overset{\cdot\cdot}{C}-CF_3 \quad (S_1) \qquad [14b]$$

$$F_3C-\overset{S}{\overset{\|}{C}}-\overset{\cdot\cdot}{C}-CF_3 \quad (S_1) + C_4F_6 \longrightarrow \quad (S_0) \qquad [15a]$$

$$F_3C-\overset{S}{\overset{\|}{C}}-\overset{\cdot\cdot}{C}-CF_3 \quad (S_1) + C_4F_6 \longrightarrow \text{polymer} \qquad [15b]$$

$$2F_3C-\overset{S}{\overset{\|}{C}}-\overset{\cdot\cdot}{C}-CF_3 \quad (S_1) \longrightarrow \qquad [16]$$

$$S(^3P): \quad S(^3P) + C_4F_6 \longrightarrow F_3C-\overset{\overset{\displaystyle S}{\|}}{\ddot{C}}-\overset{..}{C}-CF_3 \ (T_0) \qquad [17]$$

$$+ \ COS \longrightarrow CO + S_2 \qquad [18]$$

$$F_3C-\overset{\overset{\displaystyle S}{\|}}{\ddot{C}}-C-CF_3 \ (T_0) + C_4F_6 \longrightarrow \quad (T_1) \qquad [19a]$$

$$\longrightarrow \ polymer \qquad [19b]$$

$$C_4F_6 \longrightarrow polymer \qquad [20a]$$

$$M \longrightarrow (S_0) \qquad [20b]$$

$$ISC \qquad [20c]$$

$$(T_1) \qquad [20d]$$
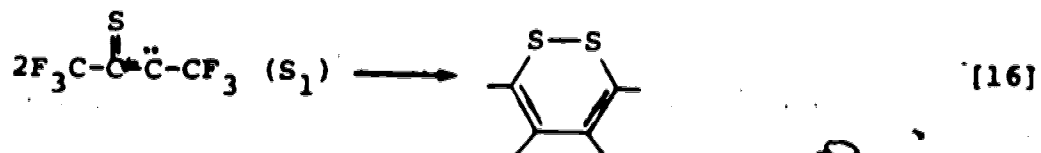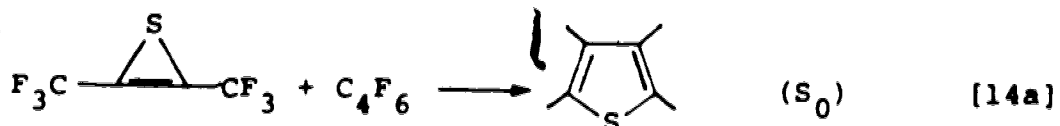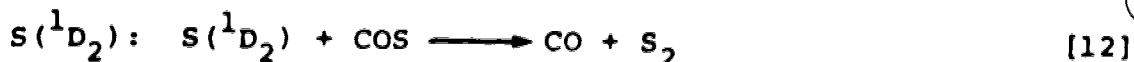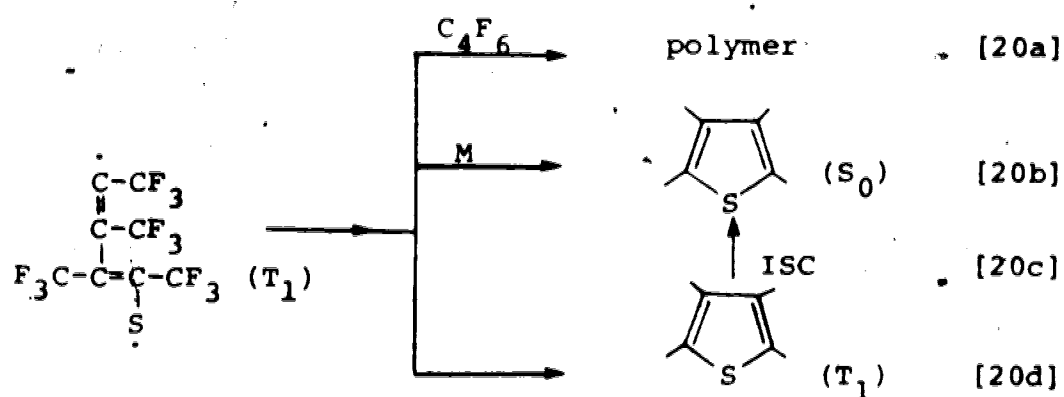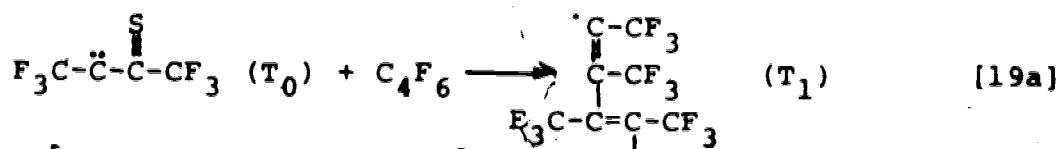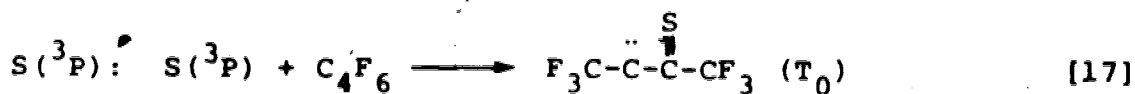
Also intersystem crossing in the carbene

$$F_3C-\overset{..}{C}-\overset{\overset{\displaystyle S}{\|}}{C}-CF_3 \ (T_0) \rightleftharpoons F_3C-\overset{..}{C}-\overset{\overset{\displaystyle S}{\|}}{C}-CF_3 \ (S_1) \qquad [21]$$
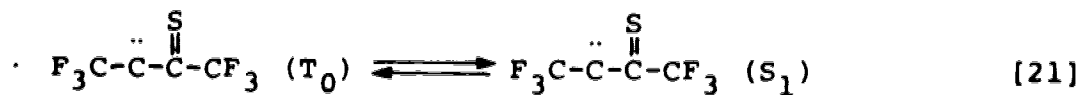
can be expected since the T_0-S_1 energy separation in simple carbenes of the type $RC-\overset{..}{\overset{\displaystyle X}{C}}R$ (X = O, S, NH) is small, of the order of 5-6 kcal mol^{-1}.[102,142]

In the presence of excess CO_2 the relative reactivity of $S(^3P)$ atoms toward COS and C_4F_6 can be estimated from the relationship:

$$\frac{R_{17}}{R_{18}} = \frac{k_{17} [S(^3P)] [C_4F_6]}{k_{18} [S(^3P)] [COS]} = \frac{R_{CO}^0 - R_{CO}}{R_{CO} - R_{CO}^0/2} \qquad \longrightarrow \quad [I]$$

When equation [I], calculated from the data from Table V-13, is plotted in the Arrhenius form, Figure V-8, a good straight line is obtained. From the slope,

$$E_{18} - E_{17} = 2.42 \pm 0.12 \text{ kcal mol}^{-1}$$

and from the intercept,

$$A_{17}/A_{18} = 0.032$$

since $A_{18} = 9.18 \times 10^8$ ℓmol^{-1} s^{-1} and $E_{18} = 3.63 \pm 0.12$ kcal mol^{-1},[83] the rate parameters for the addition of $S(^3P)$ atoms to C_4F_6 are

$$k_{17} = 2.93 \times 10^7 \exp(-1210 \pm 120/RT) \text{ } \ell\text{mol}^{-1} \text{ s}^{-1}.$$

Thus, at room temperature $k_{17} = (3.79 \pm 0.80) \times 10^6$ ℓmol^{-1} s^{-1}, pointing to a relatively inefficient reaction. This low value explains the initial slow decline of the CO yield (Figure V-2) with C_4F_6 pressure since the rate of abstraction by $S(^3P)$ atoms, step [18], is comparable to the rate of addition, step [17].

The rate of addition of $S(^1D_2)$ atoms to C_4F_6, step [13], can now be estimated relative to the abstraction, step [12] with the aid of the data in Table V-7, but first the contribution from $S(^3P)$ atoms must be assessed. The
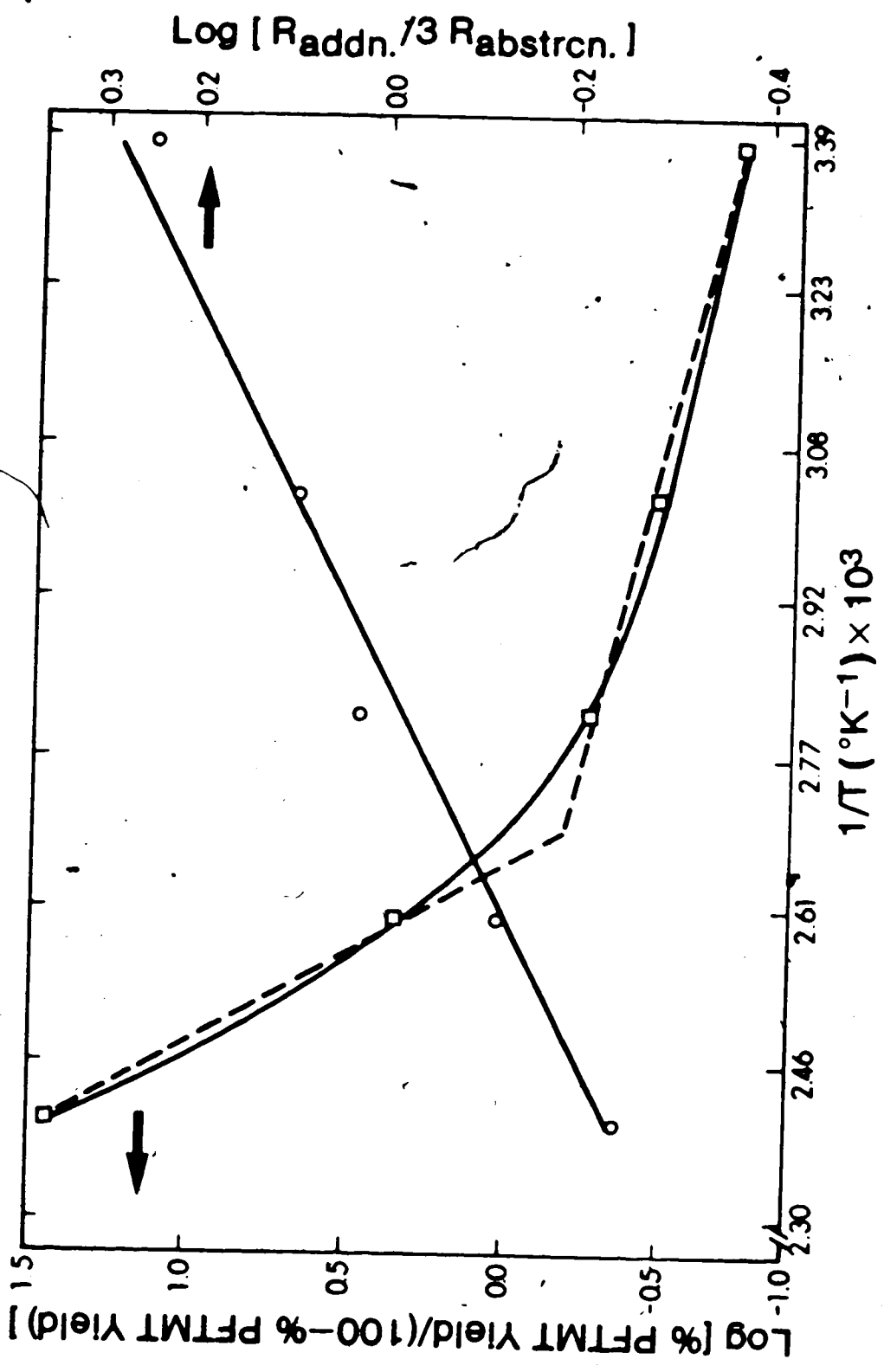
FIGURE V-8. Arrhenius plots for the $S(^3P) + C_4F_6$ system.

rate of initial production of $S(^3P)$ atoms, step [11b], is

$$R_{11b} = R_{17} + R_{18} = 0.33 \times 1.76/2 = 0.29 \ \mu mol \ min^{-1}.$$

Since

$$\frac{k_{18}}{k_{17}} = \frac{2.0 \times 10^6}{3.79 \times 10^6} = 0.53,$$

then

$$R_{17} = \frac{0.29}{(1+0.53\frac{[COS]}{[C_4F_6]})} \quad and \quad R_{18} = 0.29 - R_{17}$$

R_{17} and R_{18} were calculated at each C_4F_6 pressure and the resulting values were subtracted from the experimental data to yield R_{12} and R_{13}. The rate constant ratios $k_{12}\ k_{13}$ are also listed in Table V-7 and the average value, between 40 and 1020 torr C_4F_6, is 1.12. Since $k_{12} \geq 4.3 \times 10^{10} \ \ell mol^{-1} \ s^{-1}$, $k_{13} \geq 3.8 \times 10^{10} \ \ell mol^{-1} \ s^{-1}$. This value is slightly smaller than that estimated for C_2H_4 from computer simulation studies (cf. Chapter III), $4.2 \times 10^{10} \ \ell mol^{-1} \ s^{-1}$, in line with the electrophilic character of S atoms.

PFTMT can be formed by either, (or both), the sequences [19a] + [20b] and [19a] + [20d] + [20c] from the $C_4F_6S(T_0)$ precursor. The less than quantitative yields of PFTMT below 144°C reflects the occurrence of steps [19b] and [20a] and thus the ratio of the product-forming steps to the polymer-forming steps is

$$\frac{R_{PFTMT}}{R_{loss}} = \frac{\% \ PFTMT}{100 - \%PFTMT} \qquad\qquad [II]$$

The RHS of eq. II was calculated from the data in Table V-13 and is plotted in the Arrhenius form in Figure V-8.

It is reasonable to assume that the polymerization reactions, [19b] and [20a], feature activation energies which are negligibly small or even zero: hence the temperature dependence of the plot in Figure V-8 reflects that of the PFTMT-forming reactions. Two fairly distinct regions can be seen: at low temperatures (between approximately 23° and 83°C) the temperature coefficient is small, corresponding to E_a 3 kcal mol^{-1}, and the region above 83°C features a very high coefficient corresponding to E_a ~ 28 kcal mol^{-1}. It is suggested that the PFTMT sequence [19a] + [20b] correspond to the temperature dependence in the low temperature region and the sequence [19a] + [20d] + [20c], to that of the high temperature region. Thus, [20d] should be an endothermic reaction (the T_1 level of parent thiophene lies 82 kcal mol^{-1} above the ground state[143]) and its rate would be expected to be negligibly small at room temperature.

The analogous plot of eq. II for $S(^1D_2)$ atoms, from data in Table V-12, is illustrated in Figure V-9. Here the curvature is more pronounced at low and intermediate temperatures but at high temperatures the slope is very
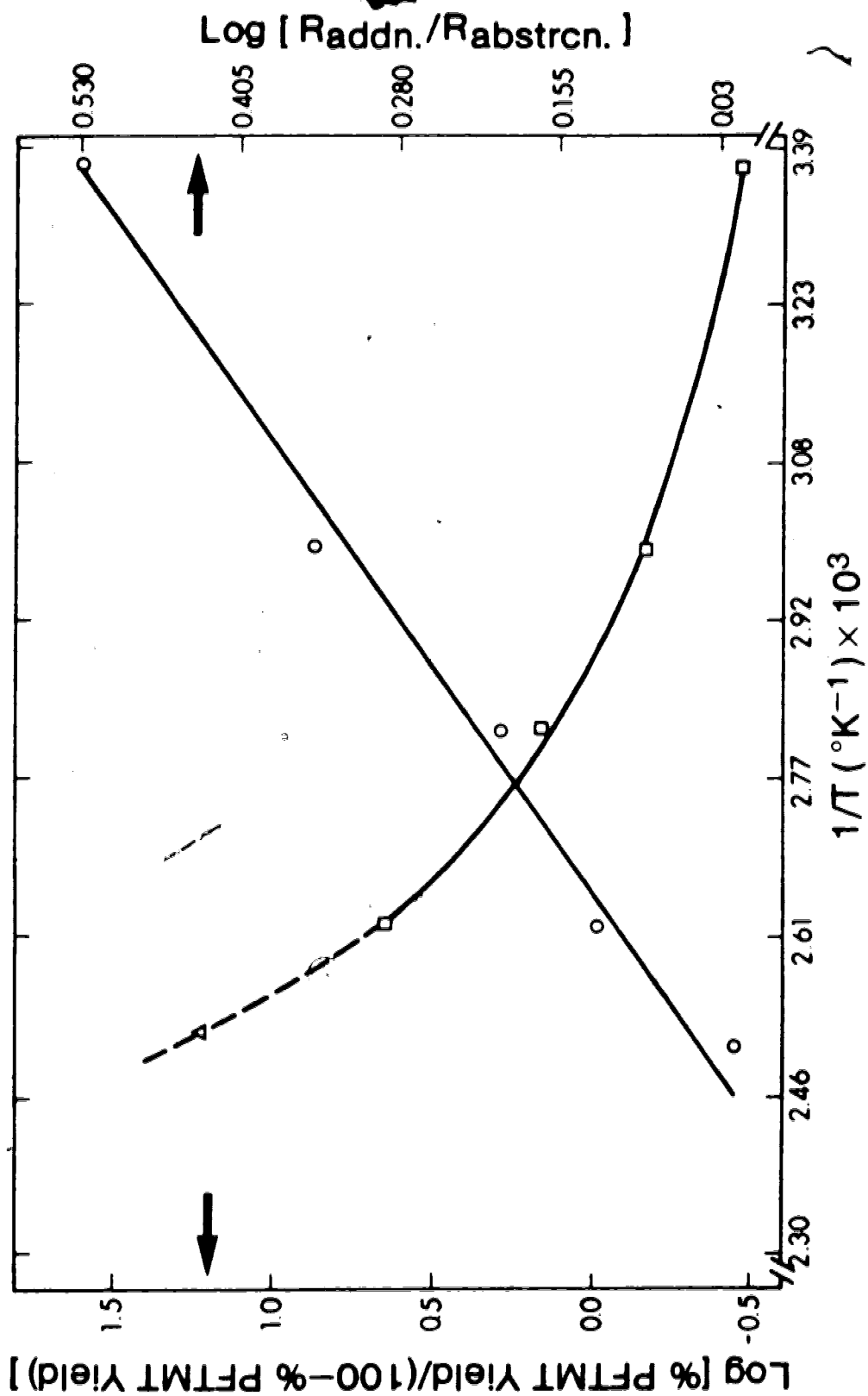
FIGURE V-9. Arrhenius plots of the $S(^1D_2, {}^3P) + C_4F_6$ system.

close to that for the $S(^3P)$ plot, Figure V-8. The latter observation suggests that most, if not all, the PFTMT yields at high temperatures arise from triplet state precursors: $S(^3P)$ atoms (33% yield at 25°C) and $CF_3\overset{\overset{..S}{\|}}{C}CF_3$ (T_0), formed in step [21]. The low temperature region would then correspond to the singlet reactions [14a] and [15a], both of which feature different activation energies.

3. Kinetic study of the $C_2H_2 + C_4F_6 + S$ system.

When C_2H_2 is added gradually to a COS + C_4F_6 mixture the PFTMT yield is rapidly suppressed initially, then declines more slowly with increasing C_2H_2 concentration. The effect is even more pronounced at elevated temperature, as illustrated in Figure V-10. On the other hand, the yields of 2,3-bis(trifluoromethyl)thiophene (b-TFMT) appears to increase monotonically with C_2H_2 pressure (Figure V-11), the rate of increase being much more pronounced at higher temperatures. The competing reactions

$$S(^3P) + C_2H_2 \longrightarrow C_2H_2S \ (T_0) \qquad [5]$$

$$S(^3P) + C_4F_6 \longrightarrow C_4F_6S \ (T_0) \qquad [17]$$
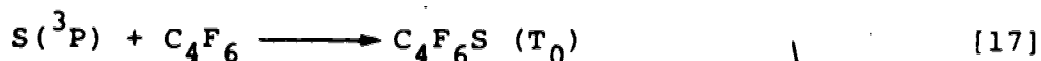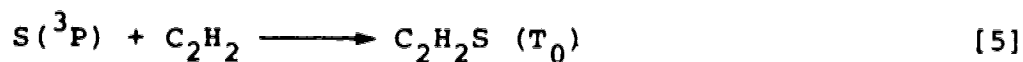
have very different rate constants, i.e., $k_5 = (3.0 \pm 0.4) \times 10^8$ ℓmol^{-1} s^{-1} and $k_{17} = (3.79 \pm 0.80) \times 10^6$ ℓmol^{-1} s^{-1} and hence for $C_2H_2/C_4F_6 \geq 0.2$ it is reasonable to assume
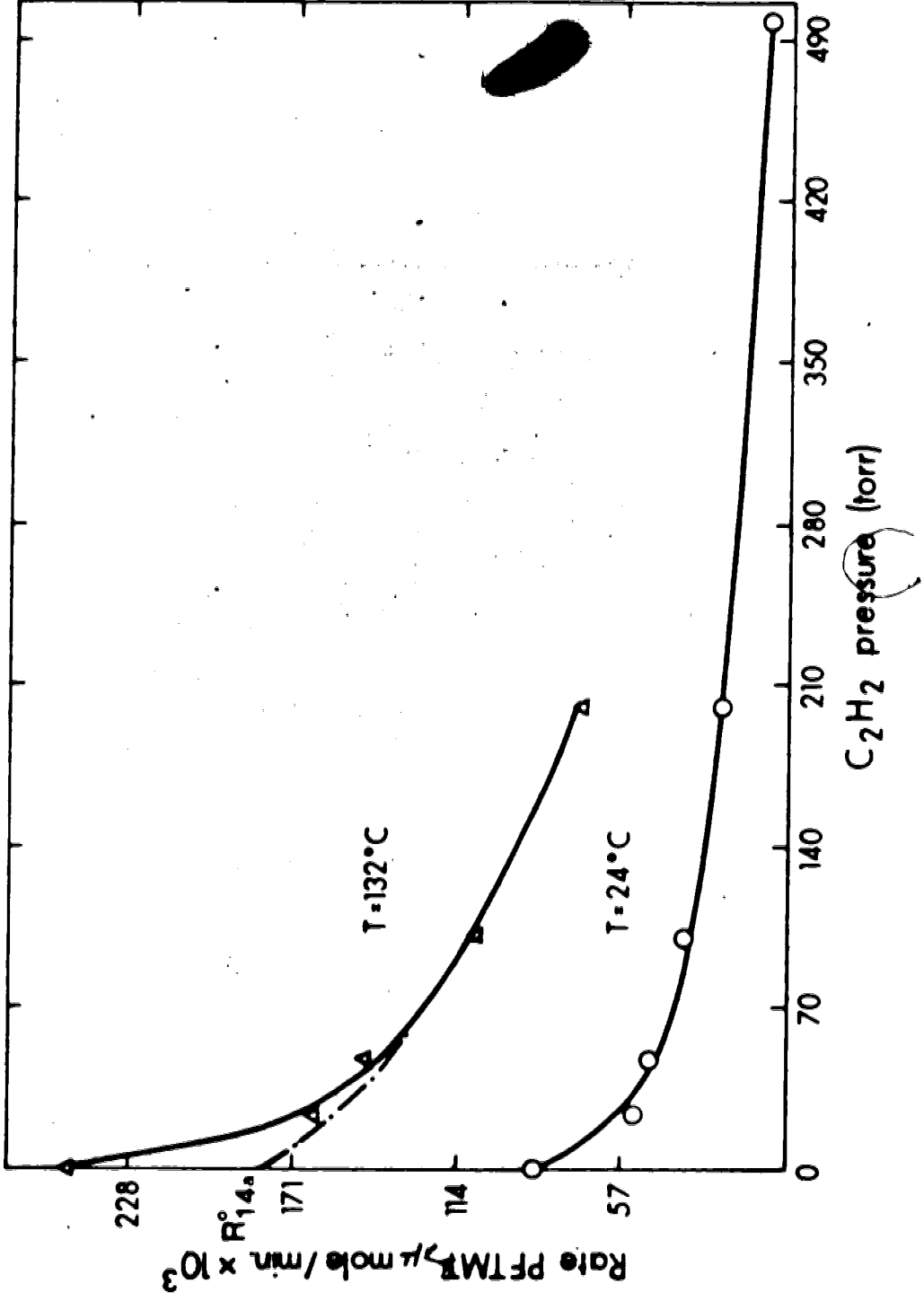
FIGURE V-10. Effects of temperature and acetylene pressure on the PFTMT yields

P(COS) = 80 torr; P(C₄F₆) = 500 torr.
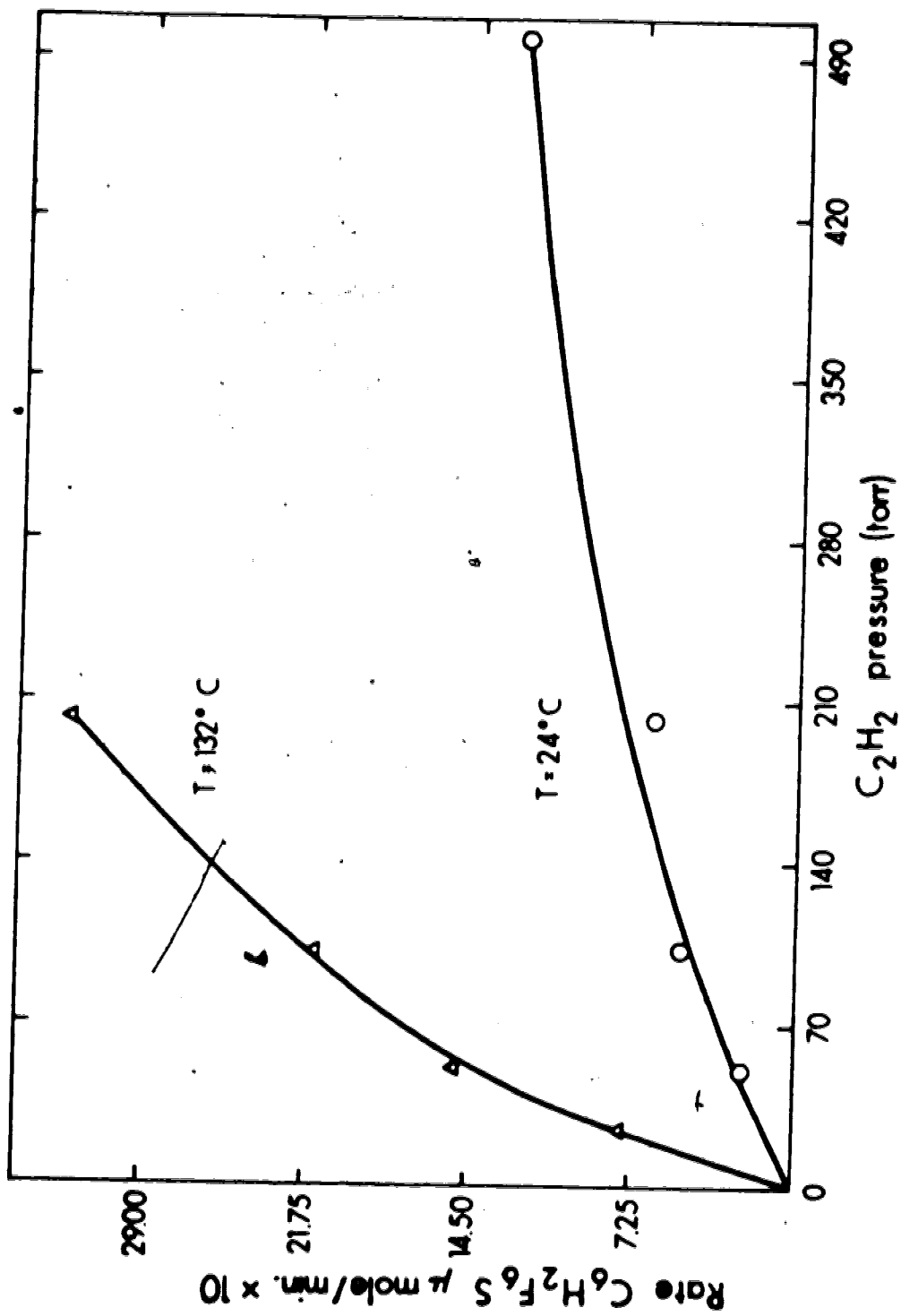
FIGURE V-11. Effects of temperature and acetylene on the b-TFMT yield P(COS) = 80 torr; P(C_4F_6) = 500 torr.

that all the $S(^3P)$ atoms are scavenged by C_2H_2. Also, because the C_2H_2S (T_0) adduct leads to barely detectable product yields, it can also be assumed that under these conditions the product-forming reactions arise solely from $S(^1D_2)$ atom precursors.

When the PFTMT rate data between 25 to 200 torr acetylene pressure at 132°C are corrected for the small contribution from reaction [17] and then extrapolated to zero acetylene pressure one obtains $R^0_{14a} = 0.1824$ μmol min^{-1}, which represents the rate of the $\overset{S}{\triangle}$ + C_4F_6 reaction. The corrected PFTMT yields, along with those of b-TFMT and thiirene, one listed in Table V-16. The following set of elementary reactions will now be considered:

$$S(^1D_2) + C_2H_2 \longrightarrow \overset{S}{\triangle} \qquad [1]$$

$$+ C_4F_6 \longrightarrow \overset{S}{\triangle} \qquad [13]$$

$$\overset{S}{\triangle} + C_4F_6 \longrightarrow \qquad [14a]$$

$$+ C_2H_2 \longrightarrow \qquad [22]$$

$$\overset{S}{\triangle} + C_4F_6 \longrightarrow \qquad [23]$$

$$+ C_2H_2 \longrightarrow \text{polymer} \qquad [24]$$
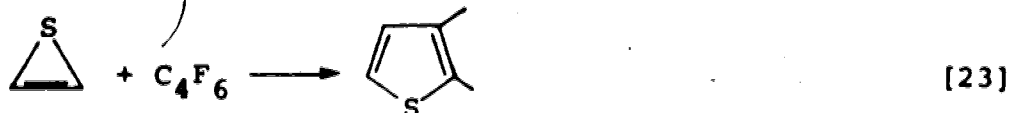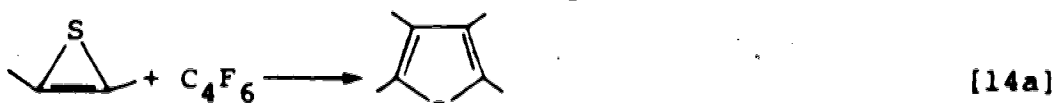
TABLE V-16

Effect of C_2H_2 pressure on the rates of PFTMT and b-TFMT formation at 132°C[a]

P(C_2H_2) (torr)	Rates, μmoles min^{-1} × 10^3		
	PFTMT[b]	b-TFMT[c]	S $\triangle$[d]
0	182.4	-	-
25	157	9.3	16.1
50	137	15.0	30.4
100	105	23.0	54.4
200	70	30.3	82.4

[a] λ > 240 nm; R^0_{CO} = 0.650 μmol min^{-1}; P(COS) = 80 torr; P(C_4F_6) = 500 torr.

[b] Corrected for the triplet contribution, reaction [17].

[c] $R_{22} + R_{23}$.

[d] R_{24}.

Steady state treatment of the above mechanism (derived in Appendix B) leads to the following equations for the rates of formation of PFTMT and b-TFMT:

$$\frac{R_{14a}^0}{R_{14a}} = 1 + \left(\frac{k_1}{k_{13}} + \frac{k_{22}}{k_{14_a}}\right) \frac{[C_2H_2]}{[C_4F_6]} + \left(\frac{k_1}{k_{13}} \times \frac{k_{22}}{k_{14a}}\right)\left\{\frac{[C_2H_2]}{[C_4F_6]}\right\}^2$$

[III]

and

$$\frac{R_{14a}^0}{R_{24}} = 1 + \left(\frac{k_{13}}{k_1} + \frac{k_{23}}{k_{24}}\right) \frac{[C_4F_6]}{[C_2H_2]} + \left(\frac{k_{13}}{k_1} \times \frac{k_{23}}{k_{24}}\right)\left\{\frac{[C_4F_6]}{[C_2H_2]}\right\}^2$$

[IV]

It also can be shown that the following relations hold:

$$R_{22} = R_{14a} \frac{k_{22}}{k_{14a}} \frac{[C_2H_2]}{[C_4F_6]}$$

[V]

$$R_{23} = R_{24} \frac{k_{23}}{k_{24}} \frac{[C_4F_6]}{[C_2H_2]}$$

[VI]

Equations III and IV can be transformed into the following linear forms:

$$\left(\frac{R_{14a}^0}{R_{14a}} - 1\right)\Big/Q = \left(\frac{k_1}{k_{13}} + \frac{k_{22}}{k_{14a}}\right) + \left(\frac{k_1}{k_{13}} \times \frac{k_{22}}{k_{14a}}\right)Q$$

[IIIa]

and

$$\left(\frac{R_{14a}^0}{R_{24}} - 1\right)\Big/Q' = \left(\frac{k_{13}}{k_1} + \frac{k_{23}}{k_{24}}\right) + \left(\frac{k_{13}}{k_1} \times \frac{k_{23}}{k_{24}}\right)Q'$$

[IVa]

where $Q = \dfrac{[C_2H_2]}{[C_4F_6]}$ and $Q' = \dfrac{[C_4F_6]}{[C_2H_2]}$

The input parameters for equations IIIa and IVa are listed
in Tables V-17 and V-18, respectively and the plots are
shown in Figures V-12 and V-13. Least-square methods
were used to calculate the slopes and intercepts, from
which the following constant ratios were derived:
from equation IIIa,

$$\dfrac{k_1}{k_{13}} = 2.3 \quad ; \quad \dfrac{k_{22}}{k_{14a}} = 0.9$$

and from equation IVa,

$$\dfrac{k_1}{k_{13}} = 2.2 \quad ; \quad \dfrac{k_{24}}{k_{23}} = 100$$

From these ratios the rates of reactions [22] and
[23], eqns. V and VI, can be computed. The results are
summarized in Table V-19 along with experimentally observed
values. The reasonably good agreement indicates that the
above mechanism for the $S + C_2H_2 + C_4F_6$ system is probably
a valid one.

The value $k_{13} = 3.8 \times 10^{10}$ ℓ mol^{-1} s^{-1} has been
derived from Table V-7 and thus $k_1 = 8.7 \times 10^{10}$ ℓ mol^{-1} s^{-1}.

From the above rate constant ratios it may be concluded
that b-TFMT is formed mainly by reaction [22] and that only
a small contribution, if any, comes from reaction [23].

TABLE V-17

Input data for equation IIIa

Q^a	$\dfrac{R^0_{14a}}{R_{14a}}$	$\left(\dfrac{R^0_{14a}}{R_{14a}} -1\right)/Q^a$
0.05	1.162	3.24
0.01	1.331	3.31
0.20	1.737	3.69
0.40	2.606	4.02

$a \quad Q = \dfrac{[C_2H_2]}{[C_4F_6]}$

TABLE V-18

Input data for equation IVa

Q'^a	$\dfrac{R^0_{14a}}{R_{24}}$	$\left(\dfrac{R^0_{14a}}{R_{24}} - 1\right) / Q'^a$
2.5	2.21	0.485
5	3.35	0.471
10	6.00	0.500
20	11.33	0.516

$$a \quad Q' = \frac{[C_4F_6]}{[C_2H_2]}$$

T = 132°C

$P_{(COS)}$ = 80 torr

$P_{(C_4F_6)}$ = 500 torr

$P_{(C_2H_2)}/P_{(C_4F_6)}$ = Q

$(R_{14}°/R_{14} - 1)/Q$

Q

4.0 3.5 3.0 2.5

0 0.05 0.10 0.15 0.20 0.25 0.30 0.35 0.40
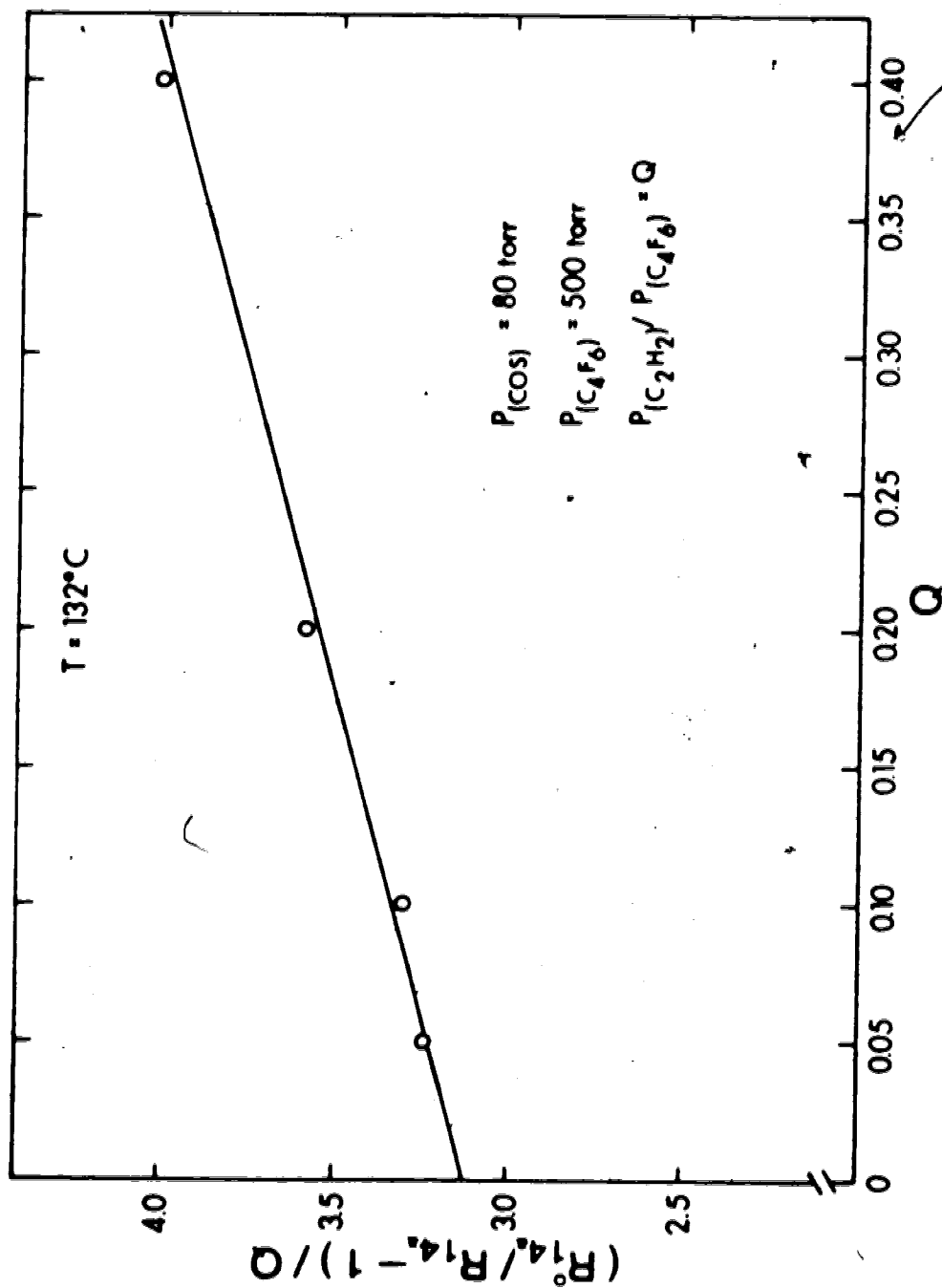
FIGURE V-12. Plot of equation IIIa.

The plot has axes labeled with vertical axis $(R^\circ_{14}/R_{24} - 1)/Q'$ with values 0.7, 0.6, 0.5, 0.4, and horizontal axis Q' with values 2, 4, 6, 8, 10, 12, 14, 16, 18, 20.

Annotations: $T = 132°C$; $P_{(COS)} = 80$ torr; $P_{(C_4F_6)} = 500$ torr; $P_{C_4F_6} / P_{C_2H_2} = Q'$
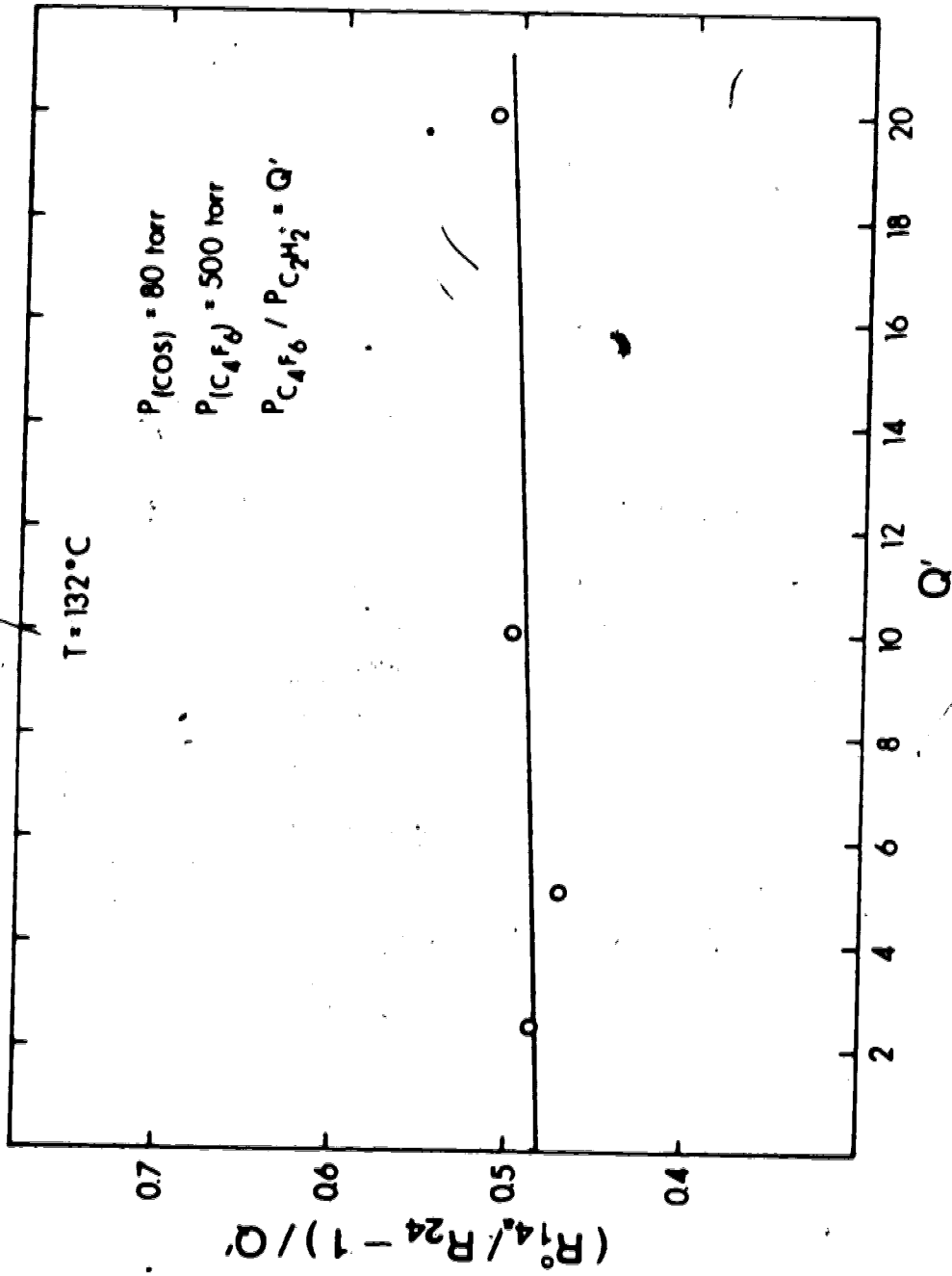
FIGURE V-13. Plot of equation IVa.

TABLE V-19

Experimental and calculated rates[a] of formation of b-TFMT at 132°C

$[C_2H_2]$ (torr)	R_{22} (calc.)	R_{23} (calc.)	$[R_{22}+R_{23}]$ (calc.)	$[R_{22}+R_{23}]^b$ (expt.)
25	7.06	3.22	10.28	9.3
50	12.3	3.04	15.34	15
100	18.9	2.72	21.62	23.0
200	25.2	2.06	27.26	30.0

[a] λ > 240 nm; all rates are in units x 10^{-3} μmoles min^{-1}

[b] From the data in Table V-16.

With increasing C_2H_2 concentrations the product yields gradually decrease from 100 to ~40% (Table V-15). Benzene and thiophene were not detected, even at the highest C_2H_2 pressure employed, and under these conditions only trace amounts of CS_2 were formed. This is in sharp contrast to the $S(^1D_2) + C_2H_2$ system at 160°C, where the CS_2 yield was ~82%. CS_2, as noted above, is a characteristic thermal and photo-product of thioketenes. Although its mode of formation is not well established, the most reasonable pathway is *via* bimolecular disproportionation. In the $S + C_2H_2$ system the following sequence of reactions can thus be envisaged,

$$\overset{S}{\triangle} \ (\text{or } \overset{\overset{S}{\|}}{HCCH}) \longrightarrow HC\equiv C-SH \longrightarrow H_2C=C=S^* \qquad [25]$$

$$2H_2C=C=S^* \longrightarrow CS_2 + C_3H_4 \qquad [26]$$

$$H_2C=C=S^* + M \longrightarrow H_2C=C=S \qquad [27]$$

$$nH_2C=C=S \longrightarrow polymer \qquad [28]$$
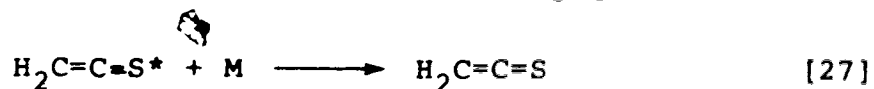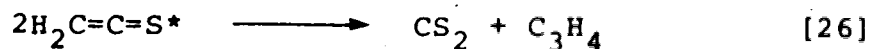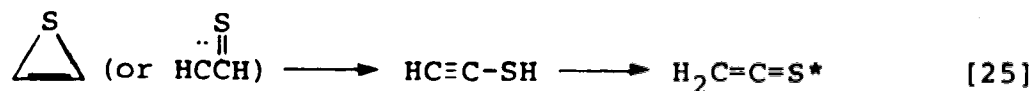
where at 160°C steps [27] and [28] are unimportant. For $M = C_4F_6$, however, it would appear that step [27] is quite efficient, and thus the reduction in the product yields in the $S + C_4F_6 + C_2H_2$ system can be ascribed to the occurrence of step [28].

The value $k_{22}/k_{14} = 0.9$ implies that bis(trifluoro-methyl)thiophene reacts as a nucleophile, in agreement with earlier findings and predictions. The rate constant ratio $k_{24}/k_{23} = 100$ should not be interpreted as correspond-ing directly to the relative rates of reactions [23] and [24] since the kinetic treatment was performed on the strict basis of product yields. Thus thiirene, generated from the photolysis of 1,2,3-thiadiazole, has been found to react with C_4F_6 to yield b-TFMT in only 15-20% yield, under pressure conditions similar to those employed in the present study.[144] The above kinetic treatment, however, ascribes the entire loss of products in reactions [23] and [24] as a result of polymerization solely to reaction [24].

4. Reactions of sulfur atoms with acetylene and
   3,3,3-trifluoropropyne

i) With acetylene

The reactions of sulfur atoms with C_2H_2 lead to the formation of benzene, thiophene and CS_2 in a combined yield of 5% at 25°C. Extensive polymerization was observed. Neither the nature of the products nor their relative distribution was affected by the spin state of the sulfur atom, and this appears to be a general feature of S + alkyne systems. The primary reactions can be summarized

as follows:

$$S(^1D_2) + C_2H_2 \longrightarrow \overset{\displaystyle S}{\triangle} \; (S_0) \tag{1}$$

$$S(^3P) + C_2H_2 \longrightarrow \overset{\displaystyle S}{\underset{\displaystyle HC-\ddot{C}H}{\parallel}} \; (T_0) \tag{5}$$

$$\overset{\displaystyle S}{\triangle} \; (S_0) \longrightarrow \overset{\displaystyle S}{\underset{\displaystyle HC-\ddot{C}H}{\parallel}} \; (S_1) \tag{3}$$

$$\overset{\displaystyle S}{\triangle} \; (S_0) + C_2H_2 \longrightarrow \langle\!\!\langle \rangle\!\!\rangle_S \; (S_0) \tag{29}$$

$$\overset{\displaystyle S}{\underset{\displaystyle HC-\ddot{C}H}{\parallel}} \; (T_0) \longrightarrow \overset{\displaystyle S}{\underset{\displaystyle HC-\ddot{C}H}{\parallel}} \; (S_1) \tag{30}$$

$$\overset{\displaystyle S}{\underset{\displaystyle HC-\ddot{C}H}{\parallel}} \; (S_1) + C_2H_2 \longrightarrow \langle\!\!\langle \rangle\!\!\rangle_S \; (S_0) \tag{31}$$

$$\overset{\displaystyle S}{\underset{\displaystyle HC-\ddot{C}H}{\parallel}} \; (S_1) \xrightarrow{\;[32]\;} H_2C=C=S \; (S_0) + H_2C + CS \tag{33}$$

$$\overset{\displaystyle S}{\underset{\displaystyle HC-\ddot{C}H}{\parallel}} \; (T_0) + C_2H_2 \longrightarrow polymer \tag{34}$$
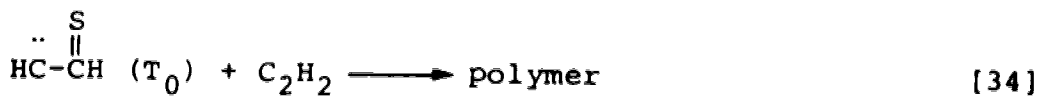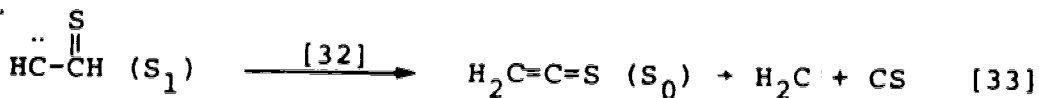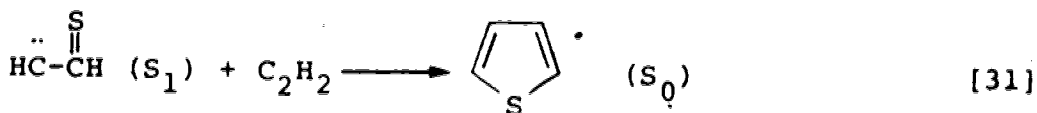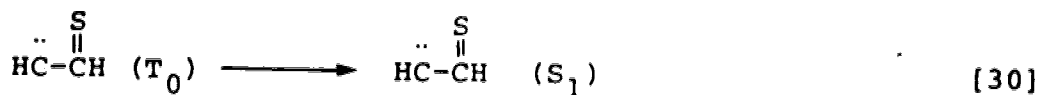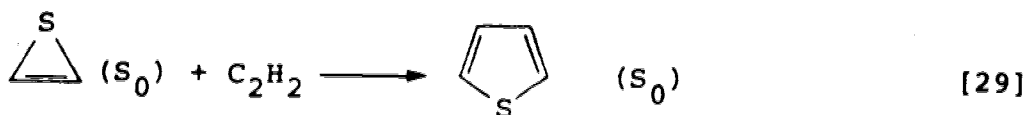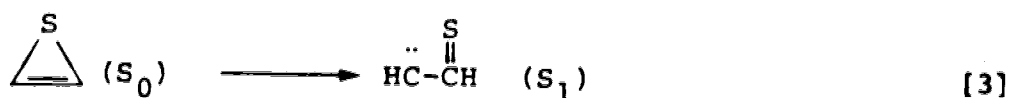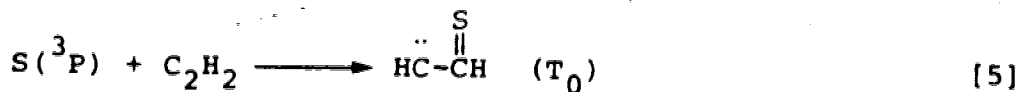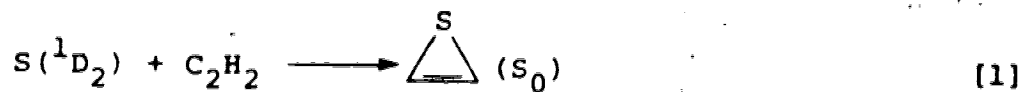
The modes of formation of CS_2 and benzene cannot be elucidated at this time but one possible route to CS_2 is condensation of two hot thioketene molecules:

$$2H_2C=C=S* \longrightarrow CS_2 + C_3H_4 \tag{26}$$
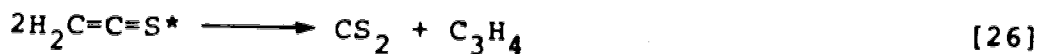
Unfortunately, it was not possible to detect the presence of allene in the present investigation but CS_2 is a characteristic products of the photochemical and thermal

decomposition of thioketenes and moreover at higher temperature, 160°C, its yield corresponds nearly quantitatively to that of $S(^1D_2)$ produced in the photolysis of COS. There is no additional evidence either in favour of, or against, the mechanism originally proposed by Dedio (cf. I Section I,-2-iii) for the mode of formation of benzene.

As observed for the case of the $S(^1D_2) + C_4F_6$ reaction, the CS_2, benzene and thiophene yields from the $S(^1D_2) + C_2H_2$ reaction are quantitative at 160°C (Table V-1); CS_2 is still by far the major product. In contrast, the dominant overall $S(^3P) + C_2H_2$ reaction at 144°C is still polymerization (Table V-2).

ii) With 3,3,3-trifluoropropyne

The $S + C_3HF_3$ system was only briefly investigated. The major products (Table V-3) are 1,3,5-tristrifluoromethylbenzene and 2,4-bis(trifluoromethyl)thiophene, formed in nearly equal yields, and smaller amounts of 2,5-bis(trifluoromethyl)thiophene were detected. Hence of the four possible conformations of the transition state of the trifluoromethylthiirene + C_3HF_3 → bis(trifluoromethyl)thiophene reaction, i.e.,
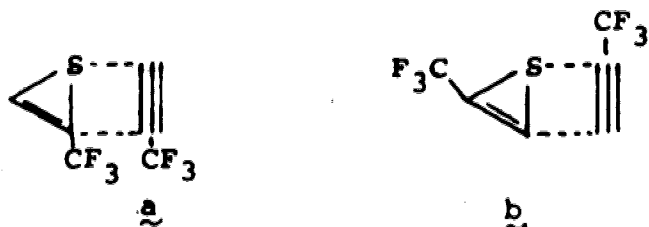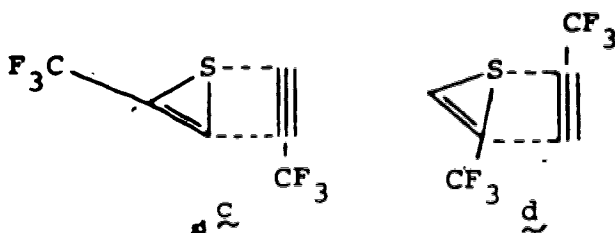
Structures c and d both lead to 2,4-bis(trifluoromethyl)-thiophene. Although steric hindrance is at a minimum in both cases it. is suggested that d more accurately represents the transition state since in this case addition takes place across the weaker, substituted C-S bond of the thiirene. Structures a and b lead to the 3,4- and 2,5-isomers, respectively. In a however the bulky CF_3 groups are expected to destabilize the transition state, thus lending credence to the tentative assignment of product 5 as the 2,5- isomer. Because of the weaker F_3CC-S bond however reaction *via* the transition complex d is favoured five-fold over that involving b.

Although quantitative analyses were not performed the combined benzene and thiophene yields were substantially higher than those observed in the S + C_2H_2 reaction, owing to the higher stability of perfluoro-methylthiirene as compared to parent thiirene.

The detection of $CF_3CH=C=S$ is significant because it constitutes direct evidence for the transient existence of thioketocarbenes in these systems,

Product 8, the Dewar benzene, is a secondary photolysis product of 1,3,5-tris(trifluoromethyl)benzene 4.

Monosubstituted thiophene 7 is formed in significant amounts, as is the uncharacterized product of MW 288 (3).

a) Effect of added C_4F_6

In the presence of C_4F_6 (Table V-4) the only products attributable to the S. + HC≡CCF$_3$ reaction are 6 and 8 and these are only formed in trace amounts. The two major products, formed in equal yields are tri- and tetra-substituted thiophenes from the cross reactions

$$C_3F_3HS + C_4F_6 \longrightarrow \underset{S}{\text{[thiophene ring]}}-(CF_3)_3 \qquad [35]$$

$$C_4F_6S + C_3F_3H \longrightarrow \underset{S}{\text{[thiophene ring]}}-(CF_3)_3 \qquad [36]$$

and

$$C_4F_6S + C_4F_6 \longrightarrow \underset{S}{\text{[thiophene ring]}}-(CF_3)_4 \qquad [37]$$
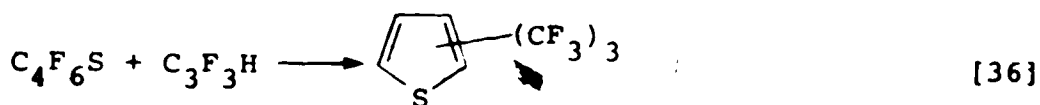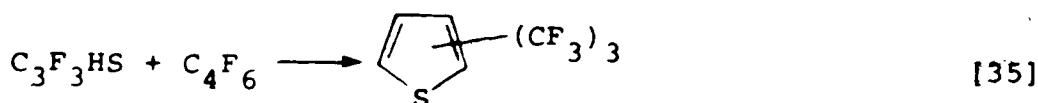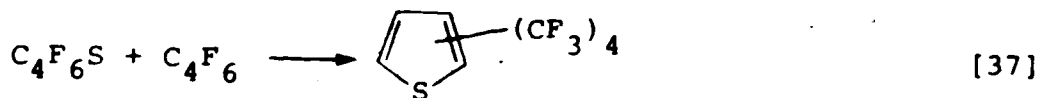
From the above observations, and on the basis of the known stability of bis(trifluoromethyl)thiirene, it is suggested that most of the trisubstituted thiophene product arises from reaction [36]. If so, then C_4F_6S would appear to be equally reactive with all the alkynes investigated here.

b) Effect of temperature and of added C_2H_2

The overall product yields increase with increasing temperature but under the conditions employed their

distribution remained the same.

In the presence of C_2H_2 the yields were suppressed and no additional products were observed.

These results are consistent with previous observations on the S + alkyne systems.

5. High conversion experiments and secondary reactions in the S + C_4F_6 system.

As can be seen from Table V-5, a large variety of products was detected in the high conversion experiments. It was possible, in some cases, to deduce structural assignments for the major products and two of the minor ones on the basis of spectral data and kinetic (vide infra) considerations, but those products formed in trace amounts (15, 16, 19, 20) remained uncharacterized.

The major secondary product is PFTMDT and from the data in Figure V-1 and the results of the photolysis experiments with PFTMT, PFTMDT is clearly formed by photoinduced isomerization of PFTMT:

[38]
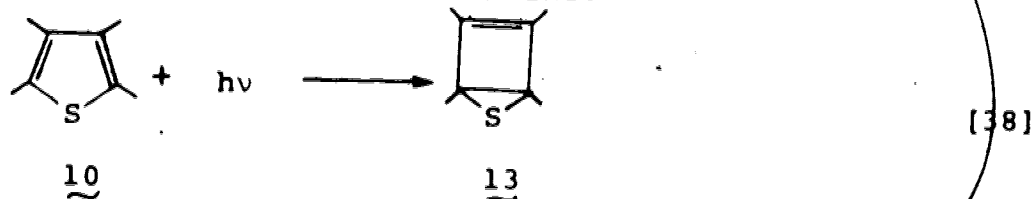
Heicklen et al. were the first to study the gas phase photochemical and mercury sensitized PFTMT-PFTMDT isomerization.[138] They reported C_4F_6 and 13 as the
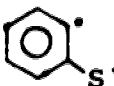
principal gas phase products, and suggested that the formation of valence bond isomers is a general reaction of photoexcited thiophenes.

The yield of dithiin 18 is negligibly small at low conversions but the results shown in Figure V-1 indicate that it is a primary product. It is proposed that 18 is formed *via* recombination of the thioketocarbene isomers formed in step [14b]. This may occur *via* a "head to head" mechanism,

[16]

18

or "head to tail":

[16a]

15
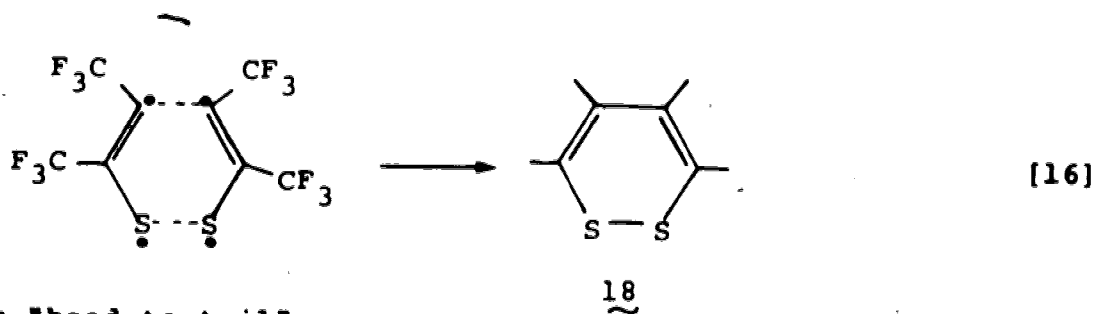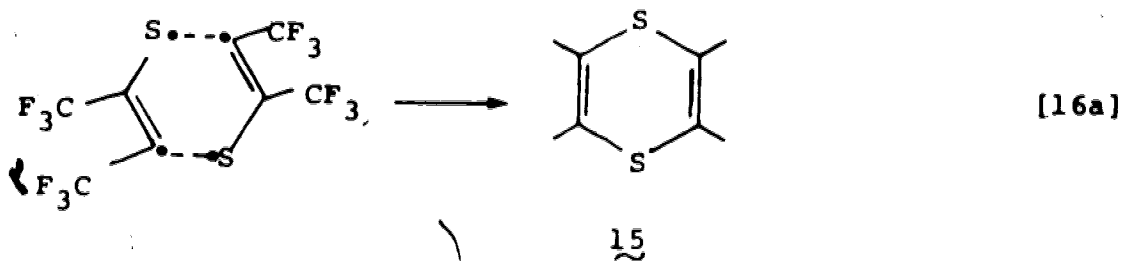
However, the recombination of a variety of $R\overset{\cdot\cdot}{C}=\overset{\cdot}{C}R'$ adducts (R, R' = Ph, H, COOMe, COOEt, PhCO, MeCO, Me) in benzene solution has been studied by Zeller and coworkers,[140,141] and only for the case of was

the analog of step [16a] found to be important: for all the other adducts examined the "head to head" type recombination predominates. The intermediate dithiins examined in this study were unstable and supposedly lose a sulfur atom to yield thiophene:

$$\text{(structure)} \longrightarrow S \;+\; \text{(thiophene structure)} \qquad [39]$$
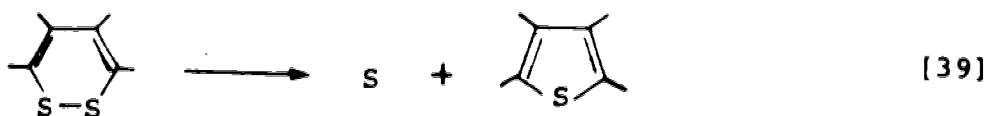
The stability of dithiin $\underline{18}$ is attributed to the presence of the strong electron-withdrawing CF_3 group.·

The uncharacterized dimer product $\underline{15}$ may arise from a small contribution of the "head to tail" recombination, step [16a].

At this point it is necessary to take cognizance of the secondary reactions involving sulfur atoms. The most obvious one is addition to PFTMT:

$$S(^1D_2, \ ^3P) \;+\; \text{(thiophene structure)} \longrightarrow \text{(structure)} \qquad [40]$$
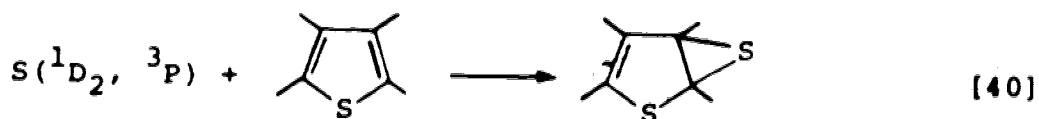
The hypothetical $C_8F_{12}S_2$ species was not detected but it is assumed to be the precursor of $\underline{14}$, $\underline{17a}$ and $\underline{21}$. Thus,

$$S(^1D_2, \ ^3P) \;+\; \text{(structure)} \longrightarrow \underset{\underline{21}}{\text{(structure)}} \qquad [41]$$

$$C_4F_6 \;+\; \text{(structure)} \longrightarrow \underset{\underline{14}}{\text{(structure)}} \qquad [42]$$

$$\overset{\cdot}{C}_4F_6\overset{\cdot}{S} \;+\; \text{(structure)} \longrightarrow \underset{\underline{17a}}{\text{(structure)}} \qquad [43]$$
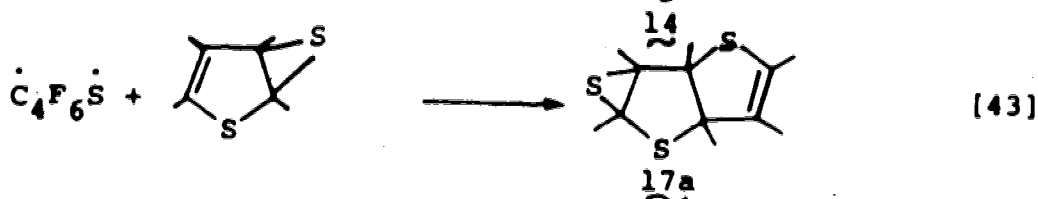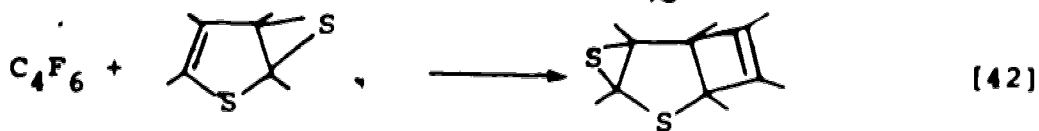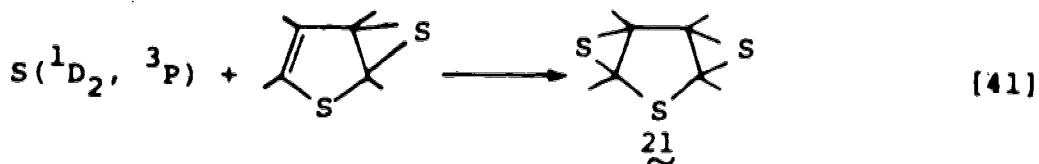
with k_{41} and k_{43} being much greater than k_{42}, as suggested by the experimental results (sections V-2, -3, -5). It should be pointed out that 21 represents the first reported reaction product of sulfur atoms with an aromatic substrate; with benzene, the only observable reaction was polymerization.[144] The dramatic increase in the yield of 21 when PFTMT is already present in the reaction mixture suggests that steps [40] and [41] are quite efficient.

Trimer 17 is a major secondary product and the spectral data did not allow a definitive choice between the possible structures 17a and 17b. The only reasonable pathways for the formation of 17b are

[44]

or

[45]
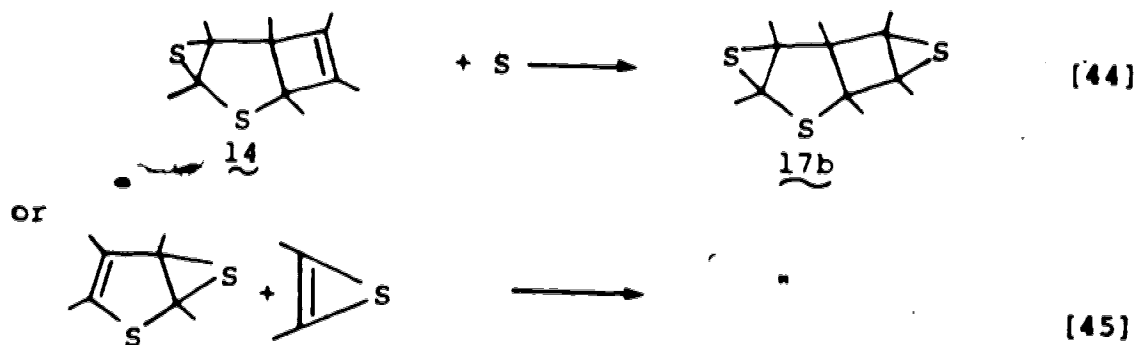
However, product 14 is only formed in low yield and is only marginally time dependent, and for these reasons is unlikely to be a precursor of 17b. Step [45] can also be discounted because the 2+2 cycloaddition reaction of thiirene has not been observed,[102] furthermore, this reaction would feature a higher E_a in comparison to step

[43]. On the other hand, trimer 17 decomposes thermally
to yield PFTMT, and C_4F_6 was demonstrably absent. This
result is significant since elimination of PFTMT can be
readily visualized from isomer a, i.e.,

[46]

17a
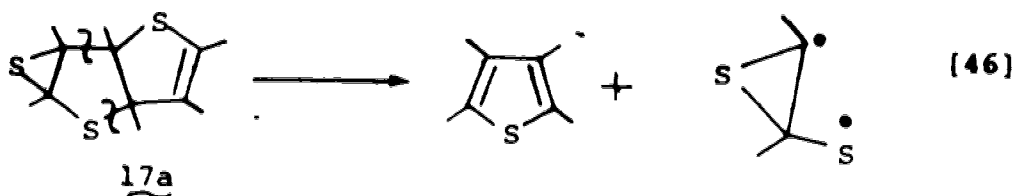
but not from isomer b. This result strongly supports the
assignment of structure a to the trimer 17.

CHAPTER VI

SUMMARY AND CONCLUSIONS

$S(^1D_2)$ atoms react with C_2H_4 to yield vinylthiol (VT) and thiirane (Th). The VT/Th ratio decreases with increasing exposure time and increases with total pressure and COS/C_2H_4 ratio, from which it is concluded that VT forms by a dual mechanism, direct insertion of the $^1D_2$ atom into the C-H bond, and isomerization of the initially formed "hot" thiirane. The overall reaction consists of the following elementary steps:

$$COS + h\nu \longrightarrow CO + S(^1D_2) \qquad (67\%) \qquad [1a]$$

$$\longrightarrow CO + S(^3P) \qquad (33\%) \qquad [1b]$$

$$COS + S(^1D_2) \longrightarrow CO + S_2 \qquad [2a]$$

$$\longrightarrow COS^* + S(^3P) \qquad [2b]$$

$$C_2H_4 + S(^1D_2) \longrightarrow CH_2CHSH \qquad [3a]$$

$$\longrightarrow (\triangle S)^* \qquad [3b]$$

$$(\triangle S)^* \longrightarrow CH_2CH\text{-}SH \qquad [4]$$

$$+ M \longrightarrow \triangle S + M^* \qquad [5]$$

$$C_2H_4 + S(^3P) \longrightarrow \triangle S \quad (T_1) \qquad [6]$$

224
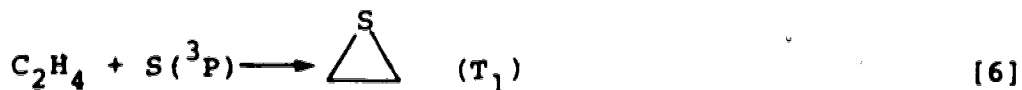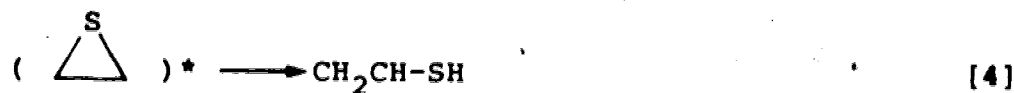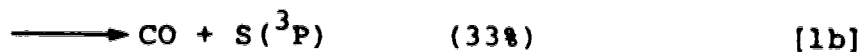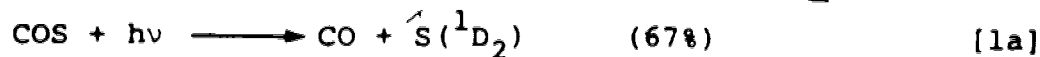
Steady state treatment of this sequence, together with
standard polynomial "best fits" for the pressure dependence
of VT/Th, adequately reproduced the experimentally derived
zero and high pressure extrapolated yields of VT/Th when
the following absolute rate constants were assumed:

$$k_{2a} = 4.3 \times 10^{13} \text{ cm}^3 \text{ mol}^{-1} \text{ s}^{-1}$$
$$k_{2b} = 1.8 \times 10^{13} \text{ cm}^3 \text{ mol}^{-1} \text{ s}^{-1}$$
$$k_{3a} = 4.2 \times 10^{13} \text{ cm}^3 \text{ mol}^{-1} \text{ s}^{-1}$$
$$k_{3b} = 3.8 \times 10^{13} \text{ cm}^3 \text{ mol}^{-1} \text{ s}^{-1}$$
$$k_4 = 5.0 \times 10^{10} \text{ s}^{-1}$$
$$k_5 = 2.3 \times 10^{14} \text{ cm}^3 \text{ mol}^{-1} \text{ s}^{-1}$$

The above results confirm the occurrence of collisional
deactivation of $S(^1D_2)$ atoms by COS, step [2b], since if
this reaction is omitted from the kinetic treatment the
resulting rate equations are in total disagreement with
experiment.

Theoretical calculations employing RRKM theory yield
$k_4 = 7.6 \times 10^{10} \text{ s}^{-1}$ for the unimolecular isomerization
of chemically activated thiirane, in good agreement with
the experimentally derived value of $5.0 \times 10^{10} \text{ s}^{-1}$. In
these calculations it was assumed that the hydrogen migra-
tion proceeds through a bicyclic structure. The set of
frequencies assumed for the internal degrees of freedom
of the activated complex, together with the estimated

activation energy of 55-65 kcal mol^{-1} correspond to a calculated A factor of 1 x 10^{14} s^{-1} and an activation entropy of $\Delta S^{\ddagger} = 3.5$ eu. The low A factor indicates a somewhat rigid structure for the activated complex. In support of these assumptions, *ab initio* MO calculations show that a value of 62 kcal mol^{-1} for the ring distortion potential of thiirane can bring about an increase in the C-C-S bond angle from the 65° equilibrium value to about 120° in the activated complex, thus greatly facilitating intramolecular insertion of the sulfur atom into the C-H bond.

The novel thiirane-vinylthiol isomerization is probably operative in the case of propylene but to a considerably lesser extent, owing to the increased number of internal degrees of freedom in this molecule. For the case of higher alkenes the possible unimolecular isomerization could only be studied at low total pressures, where secondary photolysis and other losses would very likely make quantitative work unreliable.

Both $^1D_2$ and ^3P sulfur atoms react with allene to yield a single product, methylenethiirane (MeTh), in nearly quantitative yields at low conversions. The hypothetical insertion product is expected to be unstable. Furthermore, since S($^1D_2$) atom insertion into the C-H bonds (adjacent to the triple bond) of alkynes has not

been observed, it is possible that the partial triple bond confered to the allene molecule by hyperconjugation will enhance the $S(^1D_2)$ atom addition over the C-H bond insertion. The absence of pressure effects indicates that the initially formed hot MeTh undergoes rapid collisional deactivation.

The room temperature gas phase stability and spectroscopic characterization of MeTh are in excellent agreement with those reported in the literature.

By reference to the measured rate parameters of $O(^3P) + C_3H_4$ reaction[55] and by analogy with the well documented reactivities of $O(^3P)$ and $S(^3P)$ atoms with alkenes it was possible to estimate the following values for the rate constant and activation energy for the $S(^3P) + C_3H_4$ reaction:

$$k = (2-4) \times 10^9 \text{ } \ell\text{mol}^{-1} \text{ s}^{-1} \qquad 0 \leq E_a \leq 1 \text{ kcal mol}^{-1}.$$

While elaborate attempts have been described in the literature for the general synthesis of allene thiiranes, it appears that only the gas phase reactions of sulfur atoms with cummulenes constitute a "clean" and quantitative route.

The reactions of sulfur atoms with alkynes are exceedingly complex because of the high reactivities of the primary S + alkyne adducts. For $S(^1D_2)$ atoms the

formation of S_0 thiirenes is spin and orbital symmetry allowed,

$$S(^1D_2) + RC \equiv CR' \longrightarrow RC \overset{S}{=\!\!=} CR' \quad (S_0)$$

whereas for $S(^3P)$ atoms the formation of ground triplet state thioketocarbene is predicted:

$$S(^3P) + RC \equiv CR' \longrightarrow R\ddot{C} - \overset{S}{\overset{\|}{C}}R' \quad (T_0)$$

In practice, both $S(^1D_2)$ and $S(^3P)$ atoms react with alkynes to yield the same retrievable end products. For the case of thiophene products, which are common to all the S + alkyne reactions studied to date, the following simplified mechanism is proposed:

$$
\begin{array}{c}
\underset{R}{\overset{S}{\triangle}}\underset{R}{} \quad (S_0) \qquad \xrightarrow{C_4F_6} \\[2mm]
R\ddot{C}\overset{S}{\overset{\|}{C}}R \ (T_0) \underset{}{\overset{ISC}{\rightleftharpoons}} R\ddot{C}\overset{S}{\overset{\|}{C}}R \ (S_1) \xrightarrow{C_4F_6} \\[2mm]
\Big\downarrow C_4F_6 \qquad \underset{R \ S \ R}{\overset{R \ R}{\boxtimes}} \ (T_1) \xrightarrow{M} \xrightarrow{ISC}
\end{array}
\Biggr\} \longrightarrow \underset{R \ S \ R}{\overset{R \ R}{\bigcirc}} \ (S_0)
$$
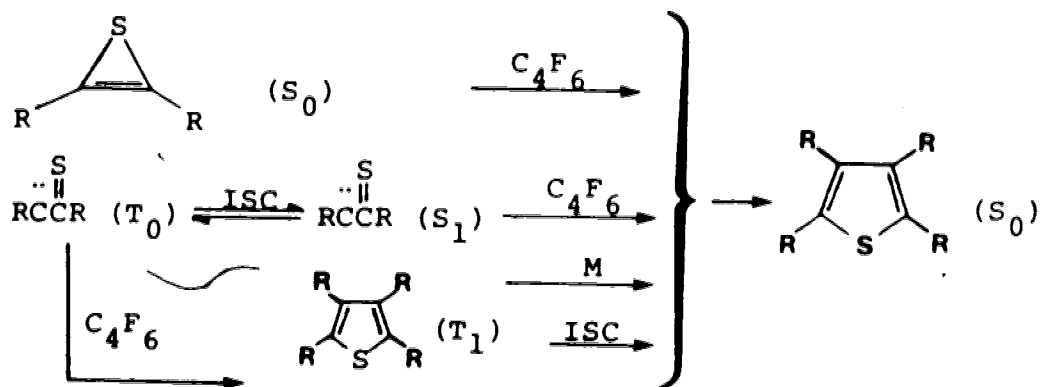
Benzenes were detected only for the cases of C_2H_2 and C_3F_3H. The room temperature $S(^1D_2) + C_2H_2$ reaction afforded only 5% total product recovery (benzene, thiophene, CS_2). At 162°C however the yields are 100% and the major product (~82%) was CS_2. The CS_2 is probably

formed by the interaction of two "hot" thioketene molecules
and thiophene, from the addition of thiirene to acetylene:

It is not known how benzene is formed.

The $S(^3P)$ + C_2H_2 reaction at 162°C on the other hand
led to only 5% total recovery, suggesting that polymer-
ization of the triplet adduct,

$$nC_2H_2S \ (T_0) \longrightarrow polymer$$

features a markedly lower activation energy than the
product-forming reaction.

The reaction with 3,3,3-trifluoropropyne led to the
formation of a variety of products, the major ones being:
1,3,5-tris(trifluoromethyl)benzene, **4**, 2,4-bis(trifluoro-
methyl)thiophene, **6**, 1,3,5-tris(trifluoromethyl)dewar benzene
8, and the minor ones being: 3,3,3-trifluorothioketene,
1, carbon disulfide, **2**, the uncharacterized **3**, 2,5- or
3,4-bis(trifluoromethyl)thiophene, **5**, and 2-trifluoromethyl-
thiophene, **7**. The detection of 3,3,3-trifluorothioketene
from the sequence
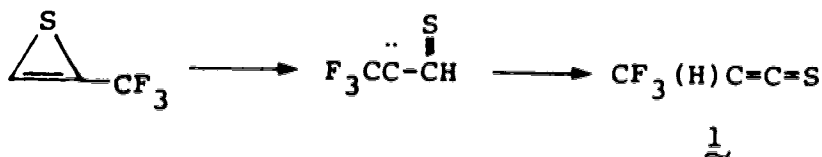
is attributed to the enhanced stability of trifluoromethyl-
thiirene as compared to parent thiirene, as a result of

the electron withdrawing property of the CF_3 group. In the presence of C_4F_6 the yields of the major products 4, 6, 8 were greatly reduced, the minor products 3 and 7 were not detected, and substantial yields of tris-(9) and tetra(trifluoromethyl) 10 thiophenes were detected. The high yield of 9 suggests a lower reactivity for the C_3F_3HS adduct with either substrate as compared to the C_4F_6S species. Although exposure time studies were not carried out, it is likely that 1, 6, 9, perfluorotetra-methylthiophene (PFTMT), tri-substituted dithiin are primary products and that 2, 8 and tetra-substituted benzene 11 are of secondary origin.

The only product detected from the $S(^1D_2, ^3P) + C_4F_6$ reaction at low conversion is PFTMT. From the effects of butyne pressure on the CO yields it was concluded that $S(^3P)$ atoms react very slowly with C_4F_6 and that the rate constant for the reaction

$$S(^1D_2) + C_4F_6 \longrightarrow F_3C-\overset{\overset{\displaystyle S}{\triangle}}{\underline{}}-CF_3$$

is $k \geq 3.8 \times 10^{10} \ \ell \ mol^{-1} \ s^{-1}$. The PFTMT yield gradually increases with increasing C_4F_6/COS ratios reaching 46% for $C_4F_6/COS = 19$, the highest ratio examined. Total pressure only marginally enhances the PFTMT yield.

The PFTMT yield increases with increasing temperature, reaching 100% at -146°C for $S(^3P)$ atoms. From the

Arrhenius plot of the ratios for the reactions

$$S(^3P) + COS \xrightarrow{1} CO + S_2$$

$$+ C_4F_6 \xrightarrow{2} F_3CC\text{-}\overset{\overset{\displaystyle S}{\|}}{C}CF_3 \cdot (T_0)$$
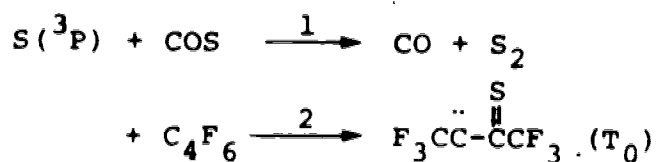
the rate constants and the activation energy for reaction

2 were estimated to be $k_2 = (3.79 \pm 0.80) \times 10^6$ ℓmol^{-1} s^{-1}

and $E_a = 1.21 \pm 0.12$ kcal mol^{-1}. The low A factor,

2.93×10^7 ℓmol^{-1} s^{-1}, points to significant steric

hindrance by the bulky CF_3 groups; dipole interaction

between CF_3 groups and $S(^3P)$ atoms may also be occurring

as suggested by the relatively high activation energy

when compared to the negative activation energy of

$CH_3\text{-}C\equiv C\text{-}CH_3$. The rate of electrophilic attack by the

$S(^3P)$ atom on the triple bond is drastically reduced as

compared to C_2H_2 owing to the inductive effect of the

CF_3 groups.

The corresponding Arrhenius plot of the ratio %PFTMT/

(100-%PFTMT) resulted in a curve which can be resolved

into two nearly linear regions, suggesting that either

two different product-forming reactions are operative

in the system, or more than one loss mechanism for the

C_4F_6S species is operative. The lower temperature region

features $E_a \sim 3$ kcal mol^{-1} and at higher temperatures

$E_a \sim 28$ kcal mol^{-1}. Even though C_4F_6S may decay by more

than one mechanism it is likely that the activation

energies associated with various possible isomerization, polymerization, etc. reactions are close to zero. Hence, it is postulated that the temperature dependence of the ratio refers only to the product-forming reactions and that the low activation energy is associated with the reaction

$$F_3C-\overset{\overset{\displaystyle ..}{S}}{\underset{\displaystyle}{C}}-\overset{\cdot}{C}-CF_3 \;(T_0) + C_4F_6 \longrightarrow \begin{array}{c} \overset{\cdot}{C}-CF_3 \\ \| \\ C-CF_3 \\ | \\ F_3C-C=C-CF_3 \\ | \\ \overset{\cdot}{S} \end{array} \;(T_1) \xrightarrow{M} \underset{S}{\bigtriangleup\!\!\bigtriangledown}\; (S_0)$$
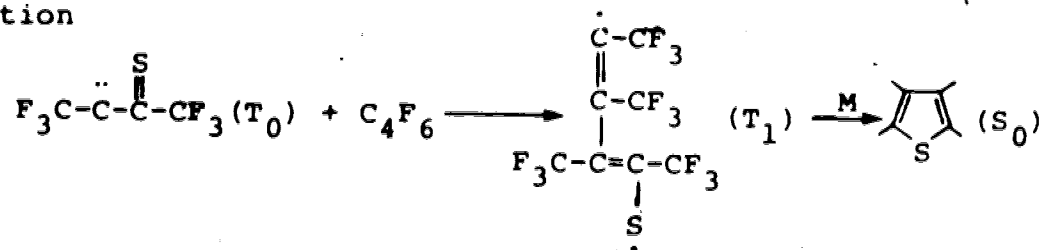
and the high activation energy with the reaction below:

$$\begin{array}{c} \overset{\cdot}{C}-CF_3 \\ \| \\ C-CF_3 \\ | \\ F_3C-C=C-CF_3 \\ | \\ \overset{\cdot}{S} \end{array} \;(T_1) \longrightarrow \underset{S}{\bigtriangleup\!\!\bigtriangledown}\;(T_1) \xrightarrow{ISC} \underset{S}{\bigtriangleup\!\!\bigtriangledown}\;(S_0)$$
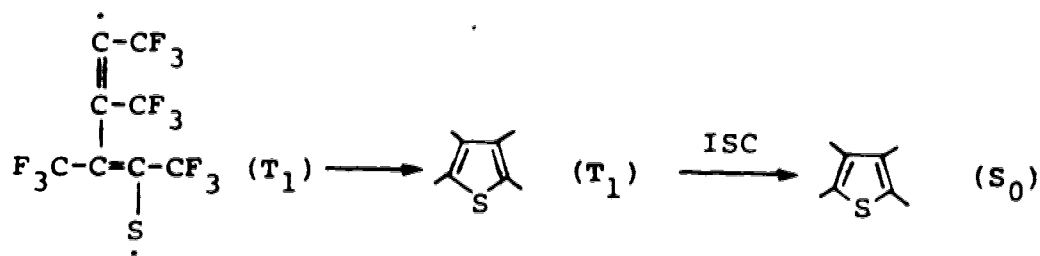
The analogous Arrhenius plot for the $S(^1D_2)$ system resulted in even more pronounced curvature, indicating that an additional reaction is operative in the system, i.e.,

$$CF_3-\overset{S}{\triangle}-CF_3 \;(S_0) + C_4F_6 \longrightarrow \underset{S}{\langle\!\!\rangle}-(CF_3)_4 \;(S_0)$$
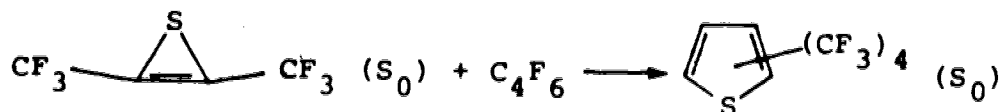
having an activation energy in the region $5 \le E_a \le 10$ kcal mol^{-1}.

The main features of the $S + C_4F_6 + C_2H_2$ system at 142°C can be summarized as follows:.

i) the presence of small amounts of acetylene
drastically reduced the initial PFTMT yield,
but subsequent additions of C_2H_2 had a more
gradual effect. These observations are
consistent with the low reactivity of $S(^3P)$ atoms
with PFB-2 as compared to acetylene.

ii) Benzene and thiophene were not detected even
at the highest concentration of C_2H_2 employed,
and CS_2 appeared in increasing trace amounts
only for $P(C_2H_2) \geq 100$ torr. 2,3-Bis(trifluoro-
methyl)-thiophene was formed in yields proportional
to the C_2H_2 pressure and at the same time the
yields of PFTMT declined.

The major competing reactions in this system were
assumed to be:

$$S(^1D_2) + C_2H_2 \longrightarrow \underset{}{\triangle} \qquad [1]$$

$$+ C_4F_6 \longrightarrow \qquad [13]$$

$$+ \longrightarrow \qquad [14a]$$

$$+ C_2H_2 \longrightarrow \qquad [22]$$

$$+ C_4F_6 \longrightarrow \qquad [23]$$

$$+ C_2H_2 \longrightarrow polymer \qquad [24]$$
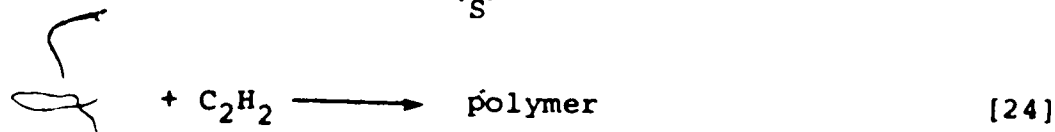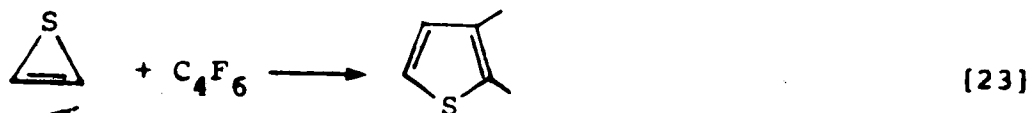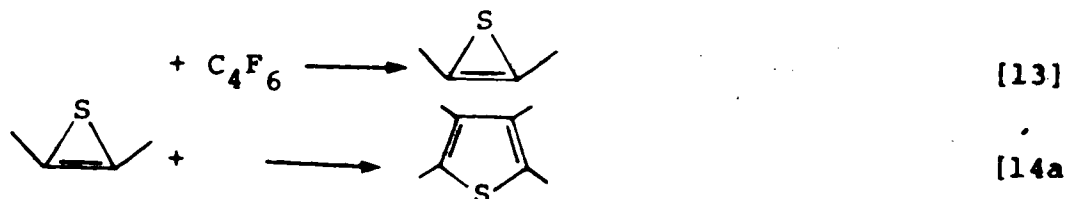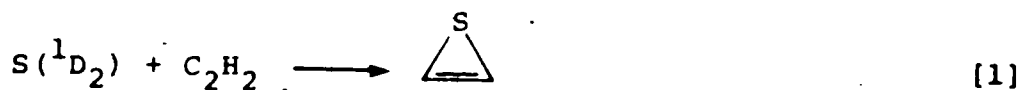
Kinetic analysis of the data led to the following rate constant ratios $\dfrac{k_1}{k_{13}} = 2.3$; $\dfrac{k_{22}}{k_{14a}} = 0.9$; $\dfrac{k_{24}}{k_{23}} = 100$

from which $k_1 = 8.7 \times 10^{10}$ ℓ mol^{-1} s^{-1}. It can further be deduced that 2,3-bis(trifluoromethyl)thiophene is formed mainly by reaction [22] and that only a small contribution, if any, comes from reaction [23]. In the presence of C_2H_2 thiirene is lost via rapid isomerization to ethynylthiol and thioketene.

With the increasing conversion, a large variety of products were detected from the S + C_4F_6 reaction, many of which have not been reported in the literature. The following reactions are proposed to account for the major ones:

$$C_4F_6 \; + \; \left[\text{(thiophene-S structure)} \right] \longrightarrow \text{(product)}$$

14

$$C_4F_6S \; + \; \left[\text{(thiophene-S structure)} \right] \longrightarrow \text{(product)}$$

17a
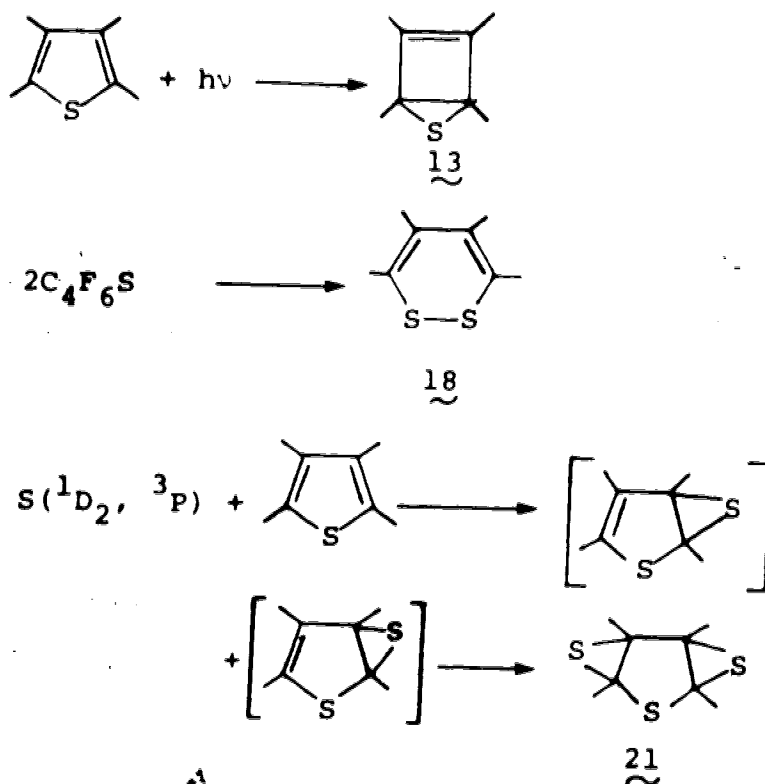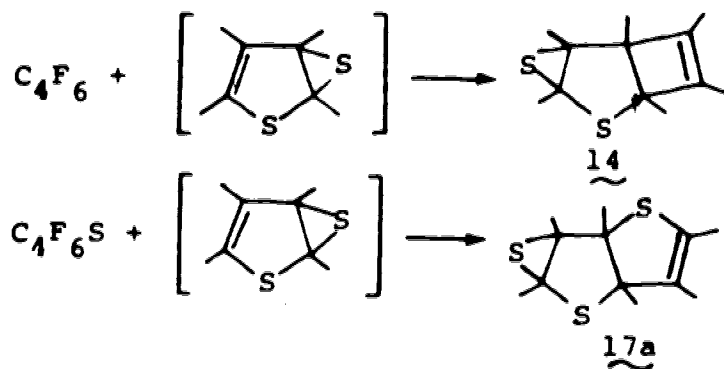
All these products, with the exception of dithiin 18, are secondary in origin.

The reactions of sulfur atoms with PFTMT, leading to product 21, represents the first reported case with an aromatic substrate.

The product recoveries from the S + alkyne systems examined to date parallel the previously reported stabilities for thiirene and trifluoromethyl-substituted thiirenes. It is assumed that the thiophenes are formed from either thiirene or (singlet) thioketocarbene precursors, and that the formation of electronically excited triplet state thiophenes from triplet state thioketocarbenes is energetically unfavourable. The presence or absence of phosphorescence in the photolyzate as a function of temperature, probably would resolve the later point.

The addition reaction with the C_4F_6S adduct is capable of undergoing with 3,3,3-trifluoropropyne leading to the formation of the tris(trifluoromethyl)thiophene merits further studies: along with more detailed and extensive competetive experiments, further insight into

the nature and chemical reactivity of these and other

S + alkyne species, could be deduced.

BIBLIOGRAPHY

1. H.M. Frey, Progr. React. Kinet., $\underline{2}$, 131 (1964).

2. W. Kirmse, "Carbene Chemistry", 2nd ed., Academic Press, New York, N.Y. (1971).

3. R.J. Cvetanovic, J. Chem. Phys., $\underline{23}$, 1203 (1955).

4. R.J. Cvetanovic, Advan. Photochem., $\underline{1}$, 115 (1963).

5. G. Paraskevopoulos and R.J. Cvetanovic, J. Chem. Phys., $\underline{52}$, 5821 (1970) and references therein.

6. O.P. Strausz and H.E. Gunning, J. Am. Chem. Soc., $\underline{84}$, 4080 (1962).

7. K. Sidhu, I.G. Csizmadia, O.P. Strausz and H.E. Gunning, J. Am. Chem. Soc., $\underline{88}$, 2412 (1966).

8. P. Fowles, M. DeSorgo, A.J. Yarwood, O.P. Strausz and H.E. Gunning, J. Am. Chem. Soc., $\underline{89}$, 1352 (1967).

9. K. Gollnick and E. Leppin, J. Am. Chem. Soc., $\underline{92}$, 2217 (1970).

10. W.J.R. Tyerman, W.B. O'Callaghan, P. Kebarle, O.P. Strausz and H.E. Gunning, J. Am. Chem. Soc., $\underline{88}$, 4277 (1966).

11. A.B. Callear and W.J.R. Tyerman, Trans. Farad. Soc., $\underline{61}$, 2395 (1965).

12. J. Connor, G. Greig and O.P. Strausz, J. Am. Chem. Soc., $\underline{91}$, 5695 (1969).

13. C. Candler, Atomic Spectra, Hilger and Watts Ltd. London (1964).

14. M.J. Shaw, M.C. Gower and S. Rolt, Chem. Phys. Lett., 73, 478 (1980).

15. H. Yamazaki and R.J. Cvetanovic, J. Phys. Chem., 41, 3703 (1964).

16. G. Paraskevopoulos and R.J. Cvetanovic, J. Chem. Phys., 50, 590 (1969).

17. P. Michaud, G. Paraskevopoulos and R.J. Cvetanovic, J. Phys. Chem., 76, 1375 (1972).

18. P. Michaud, G. Paraskevopoulos and R.J. Cvetanovic, J. Chem. Phys., 78, 1457 (1974).

19. A.J. Colussi and R.J. Cvetanovic, J. Phys. Chem., 79, 1891 (1975).

20. G. Paraskevopoulos and R.J. Cvetanovic, J. Am. Chem. Soc., 91, 75-72 (1969).

21. C. Lin and W.B. DeMore, J. Phys. Chem., 77, 863 (1973).

22. W.B. DeMore and O.P. Raper, J. Chem. Phys., 46, 2500 (1967); W.B. DeMore and O.P. Raper, J. Phys. Chem., 73, 391 (1969).

23. O. Kajimoto, H. Yamasaki and T. Fueno, Chem. Lett., 349 (1977).

24. A.C. Luntz, J. Chem. Phys., 73, 1143 (1980).

25. S. Sato and R.J. Cvetanovic, Can. J. Chem., 36, 1668 (1958).

26. S. Sato and R.J. Cvetanovic, Can. J. Chem., 36, 970 (1958).

27. K.F. Preston and R.J. Cvetanovic, Ber. Bunseges. Physik. Chem., 72, 177 (1968).

28. O. Kajimato, H. Yamasaki and T. Fueno, Chem. Phys. Lett., 68, 127 (1979).

29. O. Kajimato and T. Fueno, Chem. Phys. Lett., 64, 445 (1979).

30. K. Ogi and O.P. Strausz, to be published.

31. J.K. Stille and D.D. Whitehurst, J. Am. Chem. Soc., 86, 4871 (1964); R.N. McDonald and P.A. Schwab, ibid., 86, 4866 (1964).

32. O.P. Strausz, R.K. Gosavi, A.S. Denes and I.G. Csizmadia, J. Am. Chem. Soc., 98, 4784 (1976).

33. O.P. Strausz, R.K. Gosavi and H.E. Gunning, Chem. Phys. Lett., 54, 510 (1978).

34. O.P. Strausz, T. DoMinh and H.E. Gunning, J. Am. Chem. Soc., 90, 1660 (1968).

35. J. Font, I.G. Csizmadia and O.P. Strausz, J. Am. Chem. Soc., 90, 7360 (1968).

36. J. Fenwick, G. Frater, K. Ogi and O.P. Strausz, J. Am. Chem. Soc., 95, 124 (1973).

37. K.P. Zeller, Tetrahedron Letters, 707 (1977); K.P. Zeller, Chem. Ber., 112, 678 (1979).

38. B. Kim, E. Piotrkwski, H.E. Gunning and O.P. Strausz, unpublished results.

39. See G. Paraskevopoulos and R.J. Cvetanovic, J. Phys. Chem., 81, 2598 (1977) and references therein.

40. P. Andersen and A.C. Luntz, J. Chem. Phys., 72, 5842 (1980).

41. J.T. Herron and R.E. Huie, J. Phys. Chem. Ref. Data 2, 467 (1973).

42. R. Atkinson and J.N. Pitts, Jr., J. Phys. Chem., 78, 1780 (1974).

43. D. Golden and S. Benson, Chem. Rev., 69, 125 (1969).

44. R.J. Cvetanovic, J. Phys. Chem., 74, 2730 (1970).

45. M.D. Scheer and R. Klein, J. Phys. Chem., 74, 2732 (1970).

46. O.P. Strausz, Pure Appl. Chem., 4, 165 (1971).

47. M.D. Scheer and R. Klein, J. Phys. Chem., 73, 597 (1969).

48. R.K. Klein and M.D. Scheer, J. Phys. Chem., 73, 1598 (1969).

49. P.G. Mezey, R.E. Kari, A.S. Denes, I.G. Csizmadia, R.K. Gosavi and O.P. Strausz, Theoret. Chim. Acta, 36, 329 (1975).

50. O.P. Strausz, R.K. Gosavi, G.R. DeMaré and I.G. Csizmadia, Chem. Phys. Lett., 62, 339 (1979).

51. K. Yamaguchi, S. Yabushita, and T. Fueno, Chem. Phys. Lett., 70, 27 (1980).

52. D.L. Singleton and R.J. Cvetanovic, J. Am. Chem. Soc., 98, 6812 (1976).

53. R.J. Cvetanovic, J. Chem. Phys., 30, 19 (1959).

241.

54. R.J. Cvetanovic, J. Chem. Phys., 33, 1063 (1960).

55. W.S. Nip, D.L. Singleton and R.J. Cvetanovic, Can.
    J. Chem., 57, 949 (1979).

56. O.P. Strausz, W.B. O'Callaghan, E.M. Lown and
    H.E. Gunning, J. Am. Chem. Soc., 93, 559 (1971).

57. J. Connor, A. van Roodselaar, R.W. Fair and
    O.P. Strausz, J. Am. Chem. Soc., 93, 560 (1971).

58. A.B. Callear and W.J.R. Tyerman, Trans. Farad.
    Soc., 62, 371 (1966).

59. A.B. Callear and W.J.R. Tyerman, Trans. Farad. Soc.,
    62, 2760 (1966).

60. J.O. Sullivan and P. Warneck, J. Phys. Chem., 69,
    1749 (1965).

61. C.A. Arrington, W. Brennan, G.P. Glass, J.V. Michael
    and N. Niki, J. Chem. Phys., 43, 525 (1965).

62. J.M. Brown and B.A. Thrush, Trans. Faraday Soc.,
    63, 630 (1967).

63. I. Haller and G.C. Pimentel, J. Am. Chem. Soc., 84,
    2855 (1964).

64. D.G. Williamson and K. Bayes, J. Phys. Chem., 73,
    1232 (1969).

65. D.G. Williamson, J. Phys. Chem., 75, 4053 (1971).

66. P. Herbrechtsmeier and H. Gg. Wagner, Ber. Bunseges.
    Phys. Chem., 79, 461 (1975).

67. R.K. Gosavi, private communication.

68. K. Ogi and O.P. Strausz, to be published.

69. H.E. Avery and S.J. Heath, Trans. Faraday Soc.,
    $\underline{68}$, 512 (1972).

70. W.M. Shaub, T.L. Burks and M.C. Lin, Chem. Phys.,
    $\underline{45}$, 455 (1980).

71. C.A. Arrington, Jr., and D.J. Cox, J. Phys. Chem.,
    $\underline{79}$, 2584 (1975).

72. P. Herbrechtsmeier and Gg. Wagner, Ber. Bunsenges.
    Phys. Chem., $\underline{79}$, 673 (1975).

73. A. van Roodselaar, I. Sararik, O.P. Strausz and
    H.E. Gunning, J. Am. Chem. Soc., $\underline{100}$, 4068 (1978).

74. A.B. Callear, Proc. Ray. Soc. Ser. A, $\underline{276}$, 401 (1963).

75. R.J. Donovan, D. Husain, R.W. Fair, O.P. Strausz
    and H.E. Gunning, Trans. Faraday Soc., $\underline{66}$, 1635
    (1970).

76. O.P. Strausz, R.J. Donovan and M. deSorgo, Ber.
    Bunseges. Physik, Chem., $\underline{72}$, 253 (1968).

77. O.P. Strausz and H.E. Gunning in "The Chemistry of
    Sulfides", A.V. Tobolsky, ed., Interscience, New York,
    1968, and references therein.

78. W. Breckenridge and H. Taube, J. Chem. Phys., $\underline{52}$,
    1713 (1970).

79. P.M. Rao and O.P. Strausz, to be published.

80. E.M. Lown, B. O'Callaghan, P.M. Rao and O.P. Strausz,
    "The deactivation of S(^{1}D) atoms by COS + alkanes",
    presented to the 58th Annual Meeting, Chemical
    Institute of Canada, Toronto, Ontario, May 25-28, 1975.

81. R.J. Donovan, L.J. Kirsch and D. Husain, Nature, 222, 1165 (1969).

82. M.C. Addison, C.D. Byrne and R.J. Donovan, Chem. Phys. Lett., 64, 57 (1979).

83. R.B. Klemm and D.D. Davis, J. Phys. Chem., 78, 1137 (1974).

84. H.A. Wiebe, A.R. Knight, O.P. Strausz and H.E. Gunning, J. Am. Chem. Soc., 87, 1443 (1965).

85. A.R. Knight, O.P. Strausz and H.E. Gunning, J. Am. Chem. Soc., 85, 1207 (1963); 85, 2349 (1963).

86. K.S. Sidhu, E.M. Lown, O.P. Strausz and H.E. Gunning, J. Am. Chem. Soc., 82, 2 (1966).

87. R.J. Donovan, Trans. Faraday Soc., 65, 1419 (1969).

88. R.J. Donovan, L.J. Kirsch and D. Husain, Trans. Faraday Soc., 66, 774 (1970).

89. O.J. Dunn, S.V. Filseth and R.A. Young, J. Chem. Phys., 59, 2892 (1973).

90. A.R. Knight, O.P. Strausz, S.M. Malm and H.E. Gunning, J. Am. Chem. Soc., 86, 4243 (1964).

91. H.A. Wiebe, Ph.D. Thesis, University of Alberta, 1967.

92. E.M. Lown, Ph.D. Thesis, University of Alberta, 1966.

93. E.L. Dedio, Ph.D. Thesis, University of Alberta, 1967.

94. O.P. Strausz, J. Font, E.L. Dedio, P. Kebarle and H.E. Gunning, J. Am. Chem. Soc., 89, 4805 (1967).

95. J. Font, M. Torres, H.E. Gunning and O.P. Strausz,
    J. Org. Chem., 43, 2487 (1978).

96. M. Torres, E.M. Lown, H.E. Gunning and O.P. Strausz,
    Pure Appl. Chem., 52, 1623 (1980).

97. M. Torres, A. Clement, J.E. Bertie, H.E. Gunning
    and O.P. Strausz, J. Org. Chem., 43, 2490 (1978).

98. M. Torres, A. Clement, H.E. Gunning and O.P. Strausz,
    Nouv. J. Chim., 3, 149 (1979).

99. M. Torres, I. Safarik, A. Clement, J.E. Bertie and
    O.P. Strausz, Nouv. J. Chim., 3, 365 (1979).

100. A. Krantz and J. Laureni, J. Am. Chem. Soc., 99,
     4842 (1977).

101. A. Krantz and J. Laureni, Ber. Bunseges. Phys. Chem.,
     82, 13 (1978).

102. M. Torres, E.M. Lown and O.P. Strausz, Heterocycles,
     11, 697 (1978).

103. G. Capozzi, V. Lucchini and G. Modena, Rev. Chem.
     Intermediates, 2, 347 (1979).

104. R. Hoffmann, C.C. Wan and V. Neagu, Mol. Phys., 19,
     113 (1970).

105. O.P. Strausz, H.E. Gunning, A.S. Denes and
     I.G. Csizmadia, J. Am. Chem. Soc., 94, 8317 (1972).

106. E.M. Lown, K.S. Sidhu, A.W. Jackson, A. Jodhan,
     M. Green and O.P. Strausz, J. Phys. Chem., in press.

245.

107. G. Black, R.L. Sharpless and T.G. Slanger, J. Chem.
     Phys., 64, 3993 (1976).

108. K.S. Sidhu, unpublished results from this laboratory.

109. C.G. Krespan, J. Am. Chem. Soc., 83, 3434 (1961).

110. R.E. Davis, J. Chem. Soc., 23, 216 (1957).

111. G.B. Guthrie, Jr., D.W. Scott and G. Waddington,
     J. Am. Chem. Soc., 74, 2795 (1951).

112. P. Vitins, Ph.D. Thesis, University of Alberta, (1973).

113. O.P. Strausz, T. Hikida and H.E. Gunning, Can. J.
     Chem., 43, 717 (1965).

114. F.W. Stacey and J.F. Harris, J. Am. Chem. Soc.,
     85, 963 (1963).

115. K.S. Sidhu, E.M. Lown, O.P. Strausz and H.E. Gunning,
     J. Am. Chem. Soc., 88, 254 (1966).

116. O.P. Strausz, R.K. Gosavi, A.S. Denes and
     I.G. Csizmadia, Theoret. Chim. Acta (Berl.) 26, 367
     (1972).

117. R.J. Donovan, L.J. Kirsch and D. Hussain, Nature
     (London), 222, 1164 (1964).

118. The numerical calculations have been performed by
     Dr. I. Safarik, Chemistry Dept., University of Alberta.

119. S.E. Stein and B.S. Rabinovitch, J. Chem. Phys.,
     58, 2438 (1973).

120. "JANAF Thermochemical Tables" Dow Chemical Co.,
     Thermal Laboratories, Midland, Mich., U.S.A.

121. "Selected Values of Chemical Thermodynamic Properties",
     Natnl. Bur. Stand. (U.S.) Tech. Note No. 270-73
     (1968).

122. M. Falk, Ph.D. Thesis, University of Alberta (1975).

123. Mitsutoshi Tanimoto and V. Almond, S.W. Charles,
     J.N. Macdonald, and N.L. Owen, J. of Mol. Spec.,
     78, 95 (1979).

124. Mitsutoshi Tanimoto and J.N. Macdonald, J. of Mol.
     Spec., 78, 106 (1979).

125. J.H. Wotiz and D.E. Mancuso, J. Org. Chem., 22, 207
     (1957).

126. D.R. Taylor, Chem. Rev., 67, 317 (1967).

127. E. Block, R.E. Penn, M.D. Ennis, T.A. Owens,
     Shin-Liang Yu, J. Am. Chem. Soc., 100, 7436 (1978).

128. E. Jongejan, Th. S.V. Buys, H. Steinberg and
     Th. J. deBoer, Recueil Trav. Chim. Pays-Bas, 97,
     214 (1978).

129. F.D. Rossini, K.S. Pitzer, R.L. Arnett, R.M. Braun
     and G.C. Pimentel in "Selected Values of Physical
     and Thermodynamical Properties of Hydrocarbons and
     Related Compounds", Pittsburgh, 1953, p. 62.

130. Y. Hata and M. Watanabe, Tetrahedron Lett., 3827
     (1972); J. Am. Chem. Soc., 97, 2553 (1975).

131. J.J. Havel, J. Am. Chem. Soc., 96, 530 (1974).

132. M.C. Lin, R.G. Shortridge and M.E. Umstead, Chem. Phy. Lett., 37, 279 (1976).

133. M. Green and O.P. Strausz, to be published.

134. W.J. Middleton, J. Org. Chem., 34, 3201 (1969).

135. A.G. Hortmann and A. Bhattacharjya, J. Am. Chem. Soc., 98, 7081 (1976).

136. S. Saito, Chem. Phys. Lett., 42, 399 (1976).

137. M.G. Barlow, R. Haszeldine and R. Hubbard, J. Chem. Soc., (C), 1232 (1970).

138. H.A. Wiebe, S. Braslavsky, and J. Heicklen, Can. J. Chem., 50, 2721 (1972).

139. Y. Kobayashi, I. Kumadaki, A. Oshawa, and Y. Sekine, Tetrahedron Lett., 19, 1639 (1975).

140. K.P. Zeller, H. Meier, and E. Müller, Tetrahedron Lett., 537 (1971).

141. K.P. Zeller, H. Meier, and E. Müller, Justus Liebigs Ann. Chem., 32, 766 (1972).

142. H. Murai, M. Torres and O.P. Strausz, J. Am. Chem. Soc., 102, 1421 (1980); J. Am. Chem. Soc., 101, 3976 (1979).

143. W.F. Flicker, O.A. Mosher and A. Kuppermann, Chem. Phys. Lett., 38, 489 (1976).
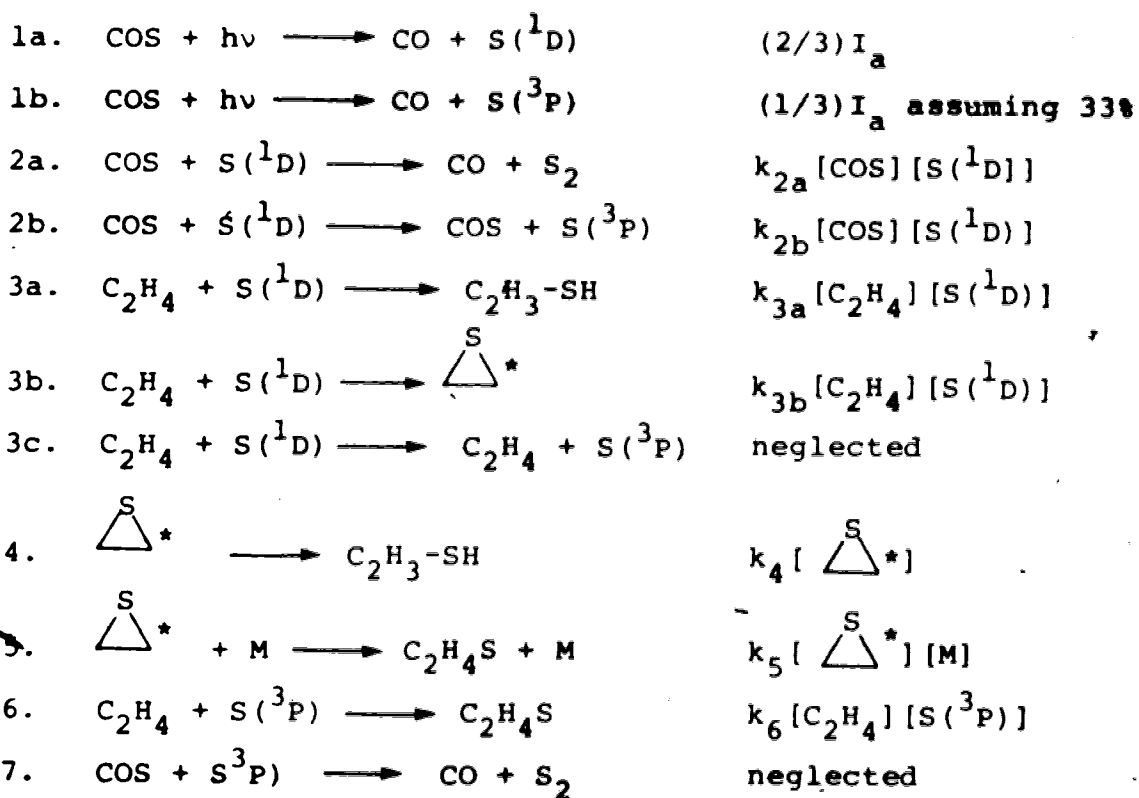
144. O.P. Strausz, private communication.

I. List of polynomial fits of the type $f(y) = at^2+bt+c$ for the data presented in Tables III-2 to III-14, and III-16 to III-20.

Total pressure torr	λ nm	COS/C_2H_4	a $\times 10^4$	b $\times(-10^2)$	c
253	254	0.2	2.00	2.70	1.457
852	254	0.2	1.80	2.50	1.362
1192	254	0.2	2.40	2.60	1.323
1680	254	0.2	1.40	2.00	1.180
100	254	0.7	0.13	1.90	1.136
162	254	0.7	0.62	1.30	1.134
220	254	0.7	7.90	3.30	1.039
336	254	0.7	0.46	0.90	1.028
440	254	0.7	1.40	1.50	1.023
600	254	0.7	1.11	1.40	1.061
660	254	0.7	3.70	2.40	0.991
880	254	0.7	0.46	0.80	0.942
1272	254	0.7	0.48	2.50	0.838
100	214	0.67	0.82	2.40	1.165
200	214	0.67	11.30	4.70	1.280
400	214	0.67	7.80	3.10	1.242
800	214	0.67	0.34	1.00	1.165
843	229	0.2	0.58	1.50	1.586

II. Kinetic analysis.

Steady state treatment of the $S(^3P, \ ^1D_2) + C_2H_4$ system is based on the following proposed mechanism:

1a.	$COS + h\nu \longrightarrow CO + S(^1D)$	$(2/3)I_a$
1b.	$COS + h\nu \longrightarrow CO + S(^3P)$	$(1/3)I_a$ assuming 33%
2a.	$COS + S(^1D) \longrightarrow CO + S_2$	$k_{2a}[COS][S(^1D)]$
2b.	$COS + \acute{S}(^1D) \longrightarrow COS + S(^3P)$	$k_{2b}[COS][S(^1D)]$
3a.	$C_2H_4 + S(^1D) \longrightarrow C_2H_3\text{-SH}$	$k_{3a}[C_2H_4][S(^1D)]$
3b.	$C_2H_4 + S(^1D) \longrightarrow \overset{S}{\triangle}*$	$k_{3b}[C_2H_4][S(^1D)]$
3c.	$C_2H_4 + S(^1D) \longrightarrow C_2H_4 + S(^3P)$	neglected
4.	$\overset{S}{\triangle}* \longrightarrow C_2H_3\text{-SH}$	$k_4[\overset{S}{\triangle}*]$
5.	$\overset{S}{\triangle}* + M \longrightarrow C_2H_4S + M$	$k_5[\overset{S}{\triangle}*][M]$
6.	$C_2H_4 + S(^3P) \longrightarrow C_2H_4S$	$k_6[C_2H_4][S(^3P)]$
7.	$COS + S^3P) \longrightarrow CO + S_2$	neglected

The rates of product formation can be expressed as

$$R_{VT} = \frac{d[VT]}{dt} = k_{3a}[C_2H_4][S(^1D)] + k_4'[\underset{S}{\triangle}^*] = k_{3a}[C_2H_4][S(^1D)] + k_4 \frac{k_{3b}[C_2H_4][S(^1D)]}{k_4 + k_5[M]} \qquad \text{I}$$

$$R_{Th} = \frac{d[\underset{S}{\triangle}]}{dt} = k_5[\underset{S}{\triangle}^*][M] + k_6[C_2H_4][S(^3P)] \qquad \text{II}$$

and the rate of production of S(^{3}P) atoms is

$$\frac{d[S(^3P)]}{dt} = (1/3)I_a + k_{2b}[COS][S(^1D)] - k_6[C_2H_4][S(^3P)] = 0 \qquad \text{III}$$

Hence,

$$k_6[C_2H_4][S(^3P)] = (1/3)I_a + k_{2b}[COS][S(^1D)]$$

The factor $(1/3)I_a$ can be expressed in terms of $[S(^1D)]$ as follows:

$$\frac{2I_a}{3} = (k_{2a} + k_{2b})[COS][S(^1D)] + (k_{3a} + k_{3b})[C_2H_4][S(^1D)]$$

from which

$$\frac{I_a}{3} = \frac{(k_{2a} + k_{2b})[COS][S(^1D)] + (k_{3a} + k_{3b})[C_2H_4][S(^1D)]}{2} \qquad \text{IV}$$

Substituting for equations III and IV in equation II, the rate of formation of Th becomes:

$$R_{Th} = k_5 [\,{}^{S}\!\triangle^*\,][M] + k_{2b}[COS][S(^1D)] + \frac{1}{2}[(k_{2a}+k_{2b})[COS][S(^1D)] + (k_{3a}+k_{3b})[C_2H_4][S(^1D)]]$$

$$= k_5 \frac{k_{3b}[C_2H_4][S(^1D)]}{k_4+k_5[M]}[M]+k_{2b}[COS][S(^1D)]+\frac{1}{2}[(k_{2a}+k_{2b})[COS][S(^1D)]+(k_{3a}+k_{3b})[C_2H_4][S(^1D)]] \qquad V$$

Dividing equation I by equation V, it can be shown that

$$\frac{R_{VT}}{R_{Th}} = \frac{(k_{3a}+k_{3b})k_4 + k_{3a}k_5[M]}{\frac{1}{2}(k_{3a}+k_{3b})k_4+(\frac{1}{2}k_{2a}+\frac{3}{2}k_{2b})k_4\frac{[COS]}{[C_2H_4]}+[(\frac{1}{2}k_{2a}+\frac{3}{2}k_{2b})\frac{[COS]}{[C_2H_4]}+(\frac{1}{2}k_{3a}+\frac{3}{2}k_{3b})]k_5[M]} \qquad VI$$

Equation VI at [M] = 0, reduces to

$$\left[\frac{R_{VT}}{R_{Th}}\right]_{p=0} = \frac{k_{3a}+k_{3b}}{\frac{1}{2}(k_{3a}+k_{3b})+(\frac{1}{2}k_{2a}+\frac{3}{2}k_{2b})\cdot\frac{[COS]}{[C_2H_4]}} \qquad VII$$

and at [M] = ∞ , reduces to

VIII

$$\left[\frac{R_{VT}}{R_{Th}}\right]_{p=\infty} = \frac{k_{3a}}{\frac{1}{2}k_{3a} + \frac{3}{2}k_{3b} + \left(\frac{1}{2}k_{2a} + \frac{3}{2}k_{2b}\right)\frac{[COS]}{[C_2H_4]}}$$

I. Mass Spectral Data

2- or 3-Trifluoromethylthiophene (7)[a]

m/e	relative intensity	m/e	relative intensity
152	100.0	57	16.1
133	78.2	45	49.4
102	32.9	39	18.5

2,4-Bis(trifluoromethyl)thiophene (6)[b]

m/e	relative intensity	m/e	relative intensity
220	98.0	170	35.6
201	100.0	151	20.4
199	12.9	45	43.0

2,5- or 3,4-Bis(trifluoromethyl)thiophene (5)[a]

m/e	relative intensity	m/e	relative intensity
220	100	113	11.2
201	88.1	69	26.5
170	39.9	57	20.8
151	62.5	45	11.1

[a] Compound reference number from Table V-3.

[b] Compound reference number from Table V-4.

2,3,4- or 2,3,5-Tris(trifluoromethyl)thiophene (9)[b]

m/e	relative intensity	m/e	relative intensity
288	100.0	113	13.9
269	91.9	69	28.4
238	41.3	63	12.2
219	62.4		

3,3,3-Trifluorothioketene (1)[a]

m/e	relative intensity	m/e	relative intensity
126	74.4	60	45.1
94	37.2	57	63.1
76	33.7	56	12.6
75	100.0	44	13.5
69	12.3	31	39.5

Perfluoro 3,4,5,6-tetramethyl 1,2-dithiin (18)[c]

m/e	relative intensity	m/e	relative intensity
388	39.5	103	12.1
369	34.7	101	20.0
356	24.3	87	20.2
337	35.6	85	30.8
319	32.2	69	100.0
300	16.2	64	14.9
287	31.8	63	16.4
250	16.8	44	44.4
137	16.8	32	45.1
113	46.9		

[c]Compound reference number from Table V-5.

Dimer, $(C_4F_6S)_2$, (15)^C

m/e	relative intensity	m/e	relative intensity
388	.68.9	250	20.8
369	60.0	199	12.6
356	20.6	157	21.8
337	30.9	113	100.0
319	43.7	93	20.5
300	21.7	69	92.2
287	24.9		

$(C_4F_6)_3S_2$, (14)^C

m/e	relative intensity	m/e	relative intensity
550	7.5	113	20.3
531	13.1	69	37.0
307	100.0		

$(C_4F_6)_3S_2$, (16)^C

m/e	relative intensity	m/e	relative intensity
550	12.5	69	42.3
531	15.0	43	12.0
194	35.4		

Trimer $(C_4F_6S)_3$, (17a)[c]

m/e	relative intensity	m/e	relative intensity
582	9.3	194	2.2
513	8.0	113	27.0
444	7.7	69	23.8
307	100.0		

Trimer $(C_4F_6S)_3$, (19)[c]

m/e	relative intensity	m/e	relative intensity
582	13.5	113	25.9
356	14.0	107	15.3
337	16.6	69	30.4
307	100.0	64	12.5
287	11.5	45	15.3
126	61.7	32	30.8

Trimer $(C_4F_6S)_3$, (20)[c]

m/e	relative intensity	m/e	relative intensity
582	7.9	113	13.4
356	14.3	75	16.2
337	16.7	69	21.7
307	61.2	64	25.1
287	11.8	57	15.9
190	22.8	32	11.5
126	100.0		

$\underline{(C_4F_6)_2S_3}$, $\underline{(21)}^c$
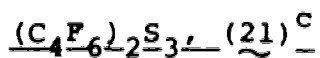
m/e	relative intensity	m/e	relative intensity
420	37.9	287	13.3
356	10.5	69	21.4
337	18.7	64	100.0
307	49.3	32	11.8

$\underline{C_7F_9S_2}$, $\underline{(12)}^b$
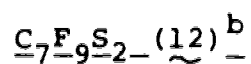
m/e	relative intensity	m/e	relative intensity
320	60.8	219	74.2
301	25.8	207	33.3
300	20.2	113	40.0
288	92.7	69	77.5
269	100.0	63	22.4
251	34.9	45	13.0
238	41.5		

Compound $(3)^a$

m/e	relative intensity	m/e	relative intensity
288	64.1	69	40.1
269	65.1	63	15.4
238	27.8	59	100.0
219	45.1	58	30.8
128	98.4	46	15.0
108	12.5	45	97.2
107	16.5		

1,3,5-Tris(trifluoromethyl)benzene (4)[a]

m/e	relative intensity	m/e	relative intensity
282	87.6	194	15.7
264	25.6	163	41.5
263	88.5	144	25.5
232	80.3	143	25.2
214	13.8	75	27.8
213	100.0	69	26.4
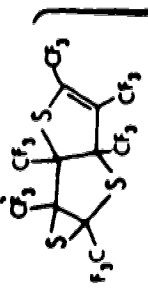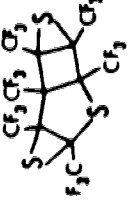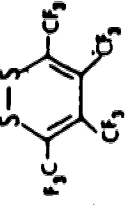
1,3,5-Tris(trifluoromethyl)dewar benzene (8)[a]

m/e	relative intensity	m/e	relative intensity
282	98.1	163	26.7
263	88.2	144	14.6
232	28.6	75	13.4
213	100.0	69	15.6

$\bigcirc$—$(CF_3)_4$ (11)[b]
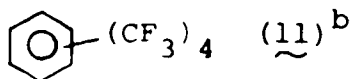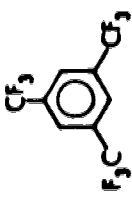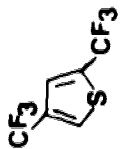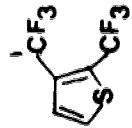
m/e	relative intensity	m/e	relative intensity
350	54.4	262	19.7
331	66.7	152	19.6
306	18.0	133	15.1
288	21.2	69	98.7
·281	88.4		
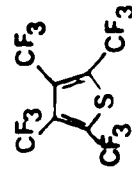
II. ^{19}F-NMR Spectral Data^a

Compound number	Structure	Peak description	Chemical shift(ppm)^b	Integration
14^c		single	109.70	2
		(2 similar)complex	103.19	2
		very complex	99.74	1
		very complex	87.00	1
17a^c		quartet	106.38	1
	OR	quartet	106.04	1
		broad	101.93	1
17b^c		broad	98.61	1
		quartet	97.88	1
		very broad	89.21	1
18^c		complex	108.74	1
		complex	99.45	1

(continued....)
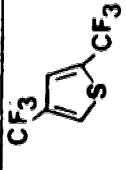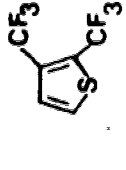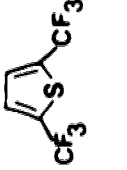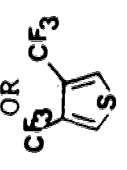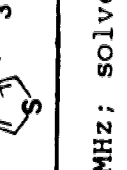
Compound number	Structure	Peak description	Chemical[b] shift (ppm)	Integration
21[c]		very complex	103.50	1
		very complex	101.00	1
4[d]		complex quartet	99.35	1
8[d]		very complex	99.81	2
		broad	96.06	1
7[d]		complex	100.29	1
6[e]		complex doublets	103.65	1
		complex doublets	99.66	1
[f]		quartet	105.51	1
		(complex doublets)		
		quartet	101.80	1
		(complex unresolved)		

(continued....)

Compound number	Structure	Peak description	Chemical[b] shift (ppm)	Integration
9[e]	(CF$_3$)$_3$ thiophene	complex quartet	105.02	1
		quartet	103.26	1
		quartet	101.57	1
10[g]	CF$_3$ substituted thiophene	complex	105.76	1
		complex	103.93	1

a ^{19}F frequency = 376.31 MHz; solvent CDCl$_3$; T = 25°C. ^{b}All chemical shifts are referenced to hexafluorobenzene as external standard. ^{c}Compound reference numbers are from Table V-5. ^{d}Compound reference numbers are from Table V-3. ^{e}Compound reference numbers from Table V-4. ^{f}From reference 93. ^{g}From reference 109.

262.

III. ^{1}H-NMR Spectral Data[a]

Compound number	Structure	Peak description	Chemical shift (ppm)[b]	Integration
6[c]		complex	7.96	1
		complex	7.67	1
—		complex	7.58	1
		complex	7.38	1
5[c]		complex	7.67	1
9		broad	7.66	1

[a] ^{1}H frequency = 400 MHz; solvent, CDCl$_3$; T = 25°C. [b] Referenced to TMS, as internal standard. [c] Reference number from Table V-3. [d] Reference number from Table V-4.

IV. Kinetic analysis.

Steady state treatment of the $CF_3-C\equiv C-CF_3 + C_2H_2$ + $S(^1D_2)$ system is based on the following proposed mechanism where $R = CF_3$, $S = S(^1D_2)$ and R_3^0 is the rate of perfluoro-tetramethylthiophene produced (μmol min^{-1}) in the absence of C_2H_2.
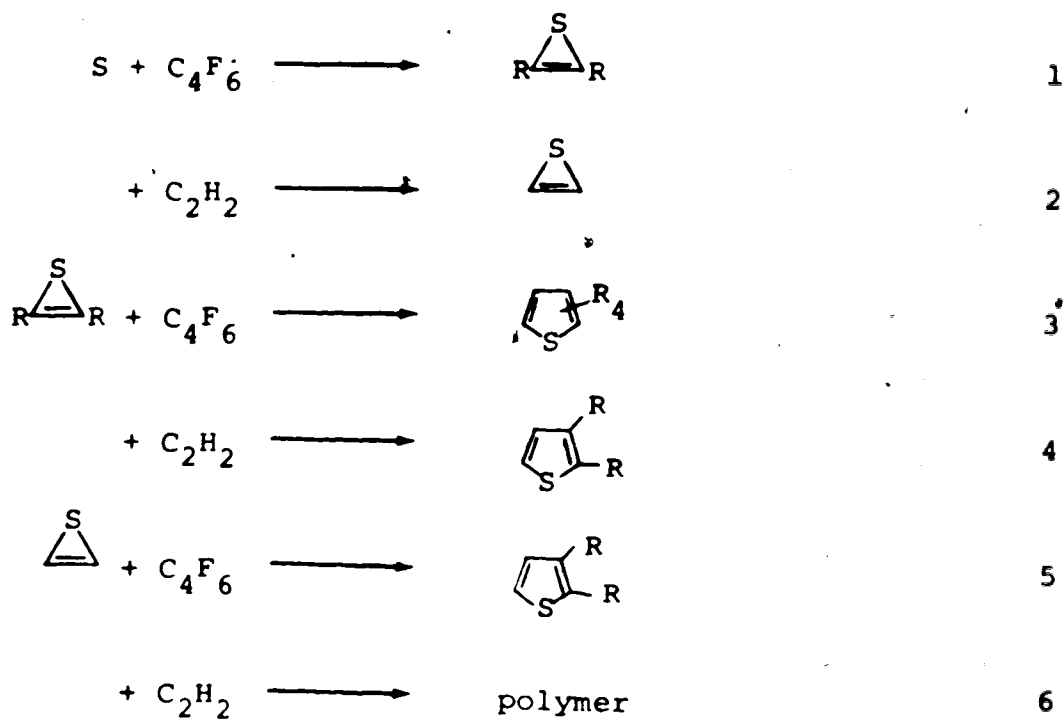
$$\frac{d[S]}{dt} = R_3^0 - k_1[S][C_4F_6] - k_2[S][C_2H_2] = 0$$

$$\therefore [S] = \frac{R_3^0}{k_1[C_4F_6] + k_2[C_2H_2]}$$

and $\dfrac{d[R\triangle R]}{dt} = R_1 - R_3 - R_4 = 0$

or

$$\frac{d[R\overset{S}{\triangle}R]}{dt} = k_1[S][C_4F_6] - k_3[R\overset{S}{\triangle}R][C_4F_6]$$

$$- k_4[R\overset{S}{\triangle}R][C_2H_2] = 0$$

and $[R\overset{S}{\triangle}R] = \dfrac{k_1[S][C_4F_6]}{k_3[C_4F_6]+k_4[C_2H_2]}$

$R_3 = k_3[R\overset{S}{\triangle}R][C_4F_6] = k_3\dfrac{k_1[S][C_4F_6]}{k_3[C_4F_6]+k_4[C_2H_2]}[C_4F_6] =$

$$k_3\frac{\dfrac{R_3^0}{k_1[C_4F_6]+k_2[C_2H_2]}[C_4F_6]}{k_3[C_4F_6]+k_4[C_2H_2]}[C_4F_6]$$

thus $R_3 = \dfrac{k_1k_3R_3^0[C_4F_6]^2}{(k_1[C_4F_6]+k_2[C_2H_2])(k_3[C_4F_6]+k_4[C_2H_2])}$

Dividing R_3 by R_3^0 we obtain

$$\frac{R_3}{R_3^0} = \frac{k_1k_3}{k_1k_3+(k_2k_3+k_1k_4)\dfrac{[C_2H_2]}{[C_4F_6]} + k_2k_4\dfrac{[C_2H_2]^2}{[C_4F_6]^2}}$$

If $\dfrac{[C_2H_2]}{[C_4F_6]} = Q$ the inverse of the above expression is

$$\frac{R_3^0}{R_3} = \frac{k_1k_3 + (k_2k_3 + k_1k_4)Q + k_2k_4Q^2}{k_1k_3} ,$$

which yields the second degree polynomial:

$$\frac{R_3^0}{R_3} = 1 + \left(\frac{k_2}{k_1} + \frac{k_4}{k_3}\right) Q + \left(\frac{k_2}{k_1} \times \frac{k_4}{k_3}\right) Q^2 \qquad [I]$$

Also,

$$\frac{d[\overset{S}{\triangle}]}{dt} = R_2 - R_5 - R_6 = k_2[S][C_2H_2] - k_5[\overset{S}{\triangle}][C_4F_6]$$

$$- k_6[\overset{S}{\triangle}][C_2H_2] = 0$$

and $[\overset{S}{\triangle}] = \dfrac{k_2[S][C_2H_2]}{k_5[C_4F_6] + k_6[C_2H_2]}$

Hence

$$R_6 = k_6[\overset{S}{\triangle}][C_2H_2] = k_6 \frac{k_2[S][C_2H_2]}{k_5[C_4H_6] + k_6[C_2H_2]} [C_2H_2] =$$

$$k_6 \frac{k_2 \dfrac{R_3^0}{k_1[C_4F_6] + k_2[C_2H_2]}[C_2H_2]}{k_5[C_4F_6] + k_6[C_2H_2]} [C_2H_2]$$

$$R_6 = \frac{k_1 k_6 R_3^0 [C_2H_2]^2}{(k_1[C_4F_6] + k_2[C_2H_2])(k_5[C_4F_6] + k_6[C_2H_2])}$$

Dividing the above expression by R_3^0 leads to

$$\frac{R_6}{R_3^0} = \frac{k_2 k_6}{k_1 k_5 \dfrac{[C_4 F_6]^2}{[C_2 H_2]^2} + (k_1 k_6 + k_2 k_5) \dfrac{[C_4 F_6]}{[C_2 H_2]} + k_2 k_6}$$

Again, if we set $\dfrac{[C_4 F_6]}{[C_2 H_2]} = Q'$ the inverse of the above

expression is

$$\frac{R_3^0}{R_6} = \frac{k_1 k_5 Q'^2 + (k_1 k_6 + k_2 k_5) Q' + k_2 k_6}{k_2 k_6}$$

which yields the following second degree polynomial:

$$\frac{R_3^0}{R_6} = 1 + \left(\frac{k_1}{k_2} + \frac{k_5}{k_6}\right) Q' + \left(\frac{k_1}{k_2} \times \frac{k_5}{k_6}\right) Q'^2 \qquad [II]$$

From the coefficients of equations I and II the ratios k_4/k_3 and k_5/k_6 can be expressed as:

$$\frac{R_4}{R_3} = \frac{k_4 [R\overset{S}{\triangle}R] [C_2 H_2]}{k_3 [R\overset{S}{\triangle}R] [C_4 F_6]} \qquad R_4 = R_3 \frac{k_4}{k_3} Q \qquad [III]$$

and

$$\frac{R_5}{R_6} = \frac{k_5 [\overset{S}{\triangle}] [C_4 F_6]}{k_6 [\overset{S}{\triangle}] [C_2 H_2]} \qquad R_5 = R_6 \frac{k_5}{k_6} Q' \qquad [IV]$$